UNIVERSITA' DEGLI STUDI DELL'INSUBRIA

DOTTORATO DI RICERCA IN SCIENZE DELLA VITA E BIOTECNOLOGIE

XXXIII CICLO

Light-based antimicrobial approaches to control the growth of pathogenic microorganisms

Approcci antimicrobici basati sulla luce per controllare la crescita di microrganismi patogeni

Docente guida: Prof.ssa **Flavia Marinelli**
Tutor: Dott.ssa **Viviana Teresa Orlandi**

Tesi di dottorato di:
Eleonora Martegani
Matr. 717632

Dip. Biotecnologie e Scienze della Vita - Università degli Studi dell'Insubria

Anno accademico 2019-2020

Contents

1. Introduction 4

1.1 Clinical relevance of nosocomial pathogens 5

1.1.1 *Pseudomonas aeruginosa*: A Gram-negative model 8

1.1.2 *Staphylococcus aureus*: A Gram-positive model 11

1.1.3 *Candida albicans*: A fungal model 13

1.2 Antibacterial and antifungal compounds 15

1.2.1 Antibiotics to treat *P. aeruginosa* infections 16

1.2.2 Antibiotics to treat *S. aureus* infections 17

1.2.3 Antifungals to treat *C. albicans* infections 17

1.3 Resistance to antimicrobial and antifungal treatments 18

1.3.1 Bacterial and fungal biofilms: tolerance to antimicrobials 21

1.3.2 Targeting microbial biofilms 24

1.4 Light-based antimicrobial approaches 26

1.4.1 Antimicrobial Photodynamic Therapy 27

1.4.2 Antimicrobial Blue Light Therapy 34

2. Aim of the research 36

3. Antimicrobial Photodynamic Therapy 39

A panel of diaryl-porphyrins in antimicrobial photodynamic therapy 40

Abstract 40

1. Introduction 41

2. Materials and methods 43

3. Results 52

4. Discussion 71

5. Conclusions 77

References 78

New BODIPYs as photosensitizers in antimicrobial photodynamic therapy 81

Abstract 81

1. Introduction 82
2. Materials and methods 84
3. Results 92
4. Discussion 113
5. Conclusions 117
References 118
4. Antimicrobial Blue Light Therapy 121
Effect of blue light at 410 and 455 nm on *Pseudomonas aeruginosa* biofilm 122
Abstract 122
1. Introduction 123
2. Materials and methods 125
3. Results 131
4. Discussion 141
References 145
Effect of blue light on *Pseudomonas aeruginosa* biofilms in central venous catheters 149
Abstract 149
1. Introduction 149
2. Materials and methods 150
3. Results and discussion 152
References 153
5. Discussion 154
Conclusions 163
6. Summary 165
7. Bibliography 168
Publications 178
Acknowledgments 179

1.Introduction

1.1 Clinical relevance of nosocomial pathogens

The discovery of antibiotics at the beginning of XX century and their consecutive launch on global market have radically influenced human health. On one hand, the intensive use of antibiotics in medical, industrial and agricultural fields facilitated the development of economic globalization, but, on the other hand, their rapid dissemination contributed to the spread of antimicrobial resistance (AMR) (Pendleton et al., 2013). AMR is a natural phenomenon evolved in microbial cells to defend their ecological niches from other microorganisms. However, the misuse of antibiotics, that increased the selective pressure, and the uncontrolled spread of resistant microorganisms caused the arise of global resistance. In addition, the scarcity of new antimicrobials coming into the market has led to the increasing and fast escalating problem of infections management in healthcare settings (Holmes et al., 2016).

Nowadays, AMR represents an issue not only in clinical field, but it also concerns many industrial and environmental aspects, becoming a threat to public health. The massive use of antibiotics for prophylaxis and treatment of infections in livestock and aquaculture caused high selective pressure on commensal and pathogenic microorganisms, spreading AMR via the food chain. Further, the accumulation of antimicrobial agents, deriving from rivers, farm effluents and sewages from community and hospitals, turned the environment into a huge reservoir of genetic determinants to fight against antimicrobials (i.e. antibiotics, disinfectants, heavy metals and biocides) (Roca et al., 2015).

In medical settings, resistance to antibiotics is increasingly correlated to nosocomial infections, also known as hospital-acquired infections (HAIs), which can be caused by a variety of microorganisms, including bacteria and fungi (Santajit and Indrawattana, 2016). These types of infections occur during healthcare delivery for other diseases, and the population subjected to the highest risk of HAIs are patients in intensive care units, burn units, undergoing to organ transplants, and neonates. Frequently, HAIs are associated with invasive medical devices employed in health care. Indeed, the most recurring infections are central-line associated bloodstream infections (CLABSIs), catheter-associated urinary tract infections (CAUTIs), ventilator-associated pneumonia (VAP), and surgical site infections (SSIs) (Khan et

al., 2017). Pathogenic microorganisms can be acquired by different reservoirs in the hospital environment, including both infected people or contaminated air, water, food, and surfaces. Therefore, possible ways of pathogen transmission are food ingestion, inhalation, breaks in the skin barrier (intravenous lines or surgery), and through mucous membranes, like oral cavity, nose and eyes (Percival et al., 2015).

In recent years, among microbial microorganisms, six clinically relevant bacterial species, acronymically named as "ESKAPE" pathogens, has been outlined for their ability to "escape" from antimicrobials' action. The term "ESKAPE" stands for *Enterococcus faecium, Staphylococcus aureus, Klebsiella pneumoniae, Acinetobacter baumannii, Pseudomonas aeruginosa* and *Enterobacter* spp (Rice and Rice, 2014). These bacterial species are associated with most of nosocomial infections and the highest risk of mortality. All of them have been recently reported by the World Health Organization (WHO) in the list of the 12 bacterial species against which new antibiotics are urgently needed (Mulani et al., 2019).

Not only bacteria cause infections, but also fungal pathogens have emerged as etiological agents of a variety of HAIs, and they are characterised by increasing levels of AMR. Among them, the major threats for hospitalized patients are represented by yeasts belonging to *Candida* spp., such as *C. albicans, C. glabrata, C. parapsilosis,* and *C. tropicalis* that could derive from patient's microflora or by their acquisition from the healthcare environment. Other airborne fungal pathogens are molds belonging to *Aspergillus*, *Zygomycetes* and *Fusarium* genera (Alangaden, 2011).

In contrast to non-pathogenic commensal microorganisms, all pathogens display an arsenal of virulence factors (VFs) aimed at starting and establishing the infection process. These VFs help them in promoting their permanence into the host body and in counteracting the host response.

Firstly, upon the introduction into a niche in the host tissues, pathogens need to remain "*in situ*". Therefore, to prevent their detachment caused by the movement of biological fluids or cell cilia, pathogens use pili or fimbriae to adhere to host cells and form microcolonies (Brannon and Hadjifrangiskou, 2016).

Further, in response to the presence of pathogens, the host body relies on some innate immune system barriers, that can include lysozyme secretion, immunoglobulin A

(IgA), and antimicrobial peptides (AMPs). To counteract this equipment, pathogens could take advantage from their VFs, such as lysozyme inhibitors, specific proteases that cleave IgA, or proteases that degrade AMPs for their use as nutrient sources, respectively. In some cases, certain pathogens could actively manipulate the immune system, such as *Salmonella enterica*, that is able to manipulate the fate of phagolysosomes and decrease the proinflammatory host response, promoting its survival in intracellular environment (Le Negrate et al., 2008; Derbise et al., 2013; Janoff et al., 2014).

Pathogens also need to compete with other microbes for the nutrient acquisition, following the host attempts to starve them. As a consequence, microbes develop strategies to accumulate the necessary provisions, for example through the chelation of nutrient, such as iron, zinc, and manganese (Corbin et al., 2008).

As well as virulence factors owned by individual cells, microorganisms can work together to benefit the entire microbial population. A notable survival strategy is represented by microbial biofilms, which develop on the surface of tissues or medical devices. The term biofilm refers to organised aggregates of microbes, living attached to biotic or inert surfaces, where cells are embedded in a self-produced extracellular polymeric substance (EPS). Biofilms are well-organised communities where microbial cells communicate each other to establish a three-dimensional structure able to protect and preserve the entire microbial population (Percival et al., 2015).

These complex biofilm structures usually involve different microbial species and are considered one of the major virulence factors during chronic infections. Indeed, biofilms favour the increase of tolerance of microorganisms to antimicrobial treatments, representing a challenge in the management of infections (Percival et al., 2015). It is estimated that biofilms are involved in 65% of all bacterial infections, including both device- and non-device-associated ones (Jamal et al., 2018).

In the biofilm scaffold, microbes can be found in different physiological states: high metabolically active cells are present in the outer layers, while nongrowing dormant state cells live in the centre of the structure and are highly difficult to eradicate. Biofilm organization is coordinated by the quorum sensing (QS) system that is a way of communication within individual cells to manage the social behaviour of

microorganisms. QS acts through the release of signalling molecules, called autoinducers, that regulate the expression of specific set of genes. Upon the cell adhesion to a surface, the secretion of the EPS, mainly constituted by exopolysaccharides, proteins, and extracellular DNA, helps microorganisms to firmly attach on it. Therefore, once a low amount of microbes are established, by recruitment of other microbial species or by cell division, QS pathways begin to regulate the phenotypic changes of the biofilm population and the cell differentiation can start, leading to the production of a mature biofilm (Phillips and Schultz, 2012). In addition to planktonic and matrix-embedded sessile populations, a certain number of persister cells can be found in the deepest layers of the biofilm. These cells, characterized by a specific phenotype state and a low rate of metabolism, survive in the presence of high concentrations of antibiotic, about one hundred-fold higher than minimal inhibitory concentration (Beloin et al., 2014). The EPS of microbial biofilms presents a network of signalling pathways very similar to the extracellular matrix of eukaryotic tissues, where a bidirectional and continuous signalling system mediate cell response depending on the surrounding environment (Römling et al., 2014).

Several microbial pathogens are able to form biofilm during infections. In particular, *P. aeruginosa* and *S. aureus* are used as model microorganisms to study bacterial biofilms, while the yeast *C. albicans* represent a fungal model. They are common inhabitants of human microbial flora and they can become opportunistic pathogens. Furthermore, all of them have recently emerged for their increasing resistance to antimicrobial treatments (Taylor et al., 2014; Cavalheiro and Teixeira, 2018; Mohammed et al., 2018). A description of each pathogen is presented herein.

1.1.1 *Pseudomonas aeruginosa*: A Gram-negative model

Pseudomonas aeruginosa is a common Gram-negative bacterium that lives ubiquitously in several environments including soils, waters, sewages, and is a common part of the microflora of different animals. Thanks to its wide genome (5-7 Mbp), this bacterium displays a wide capacity to use various carbon sources and electron acceptors, and to produce a variety of secondary metabolites and polymers. In addition, the highest part of its genome is dedicated to regulatory genes and

networks that are fundamental for the response and adaptation to different and changing environments (Stover et al., 2000). *P. aeruginosa* is known to be a pathogen for a wide range of animals (e.g. nematodes, flies, zebrafish, and various mammals) and plants. In particular, in humans, it causes sever acute or chronic infections in a variety of tissues and body sites, including skin, middle-ear, eyes, and urinary tract, especially in immunocompromised patients. *P. aeruginosa* is a leading cause of nosocomial infections, including device-associated infections, i.e. CAUTIs, CLABSIs and VAP, as well as chronic lung infections in cystic fibrosis (CF) patients (Driscoll et al., 2007; El Zowalaty et al., 2015). Cystic fibrosis is a genetic disease caused by a mutation in the cystic fibrosis transmembrane regulator (CFTR) in pneumocytes, that lead to an excessive presence of mucous in the lungs, making CF patients extremely susceptible to respiratory infections. The recurrence and persistence of these infections are the main cause of morbidity and mortality in CF patients (Winstanley et al., 2016).

The major cause of persistent *P. aeruginosa* infections is the presence of biofilms, formed on tissues or on the surface of surgical implants or medical devices. Biofilm formation of *P. aeruginosa* begins with the reversible attachment on a surface, characterised by twitching motility driven by type IV pili, followed by irreversible attachment to reach the development of a microcolony (figure 1). In microcolonies, bacteria begin to secrete exopolysaccharides, that are Psl, Pel and alginate, and other components of EPS: polypeptides and extracellular DNA. Alginate is produced in large amount during the colonisation of lungs of CF patients and lead to the so-called mucoid conversion of *P. aeruginosa*, worsening the conditions of infection (Rybtke et al., 2015). During biofilm maturation, the community of bacteria acquires its typical three-dimensional structure, covering a wider surface, where EPS serves as highly hydrated scaffold to protect the bacterial population from external insults. The last step of the biofilm lifestyle cycle is characterised by the release of planktonic cells from the biofilm to colonize other surfaces (Rasamiravaka et al., 2015).

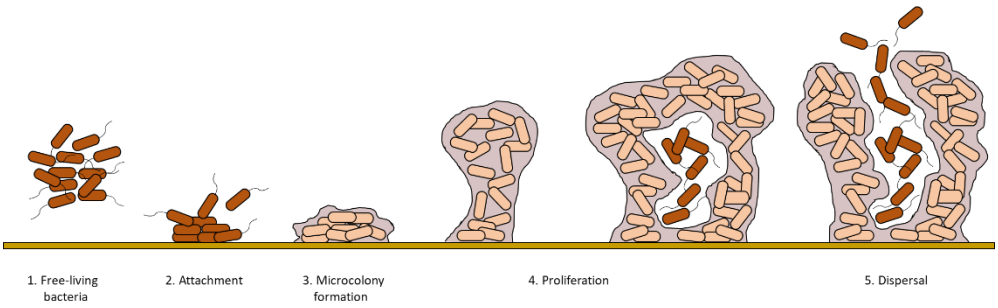

Figure 1. Schematic representation of *P. aeruginosa* biofilm formation.

Biofilm formation and other important bacterial behaviours, including the production of many virulence factors, are controlled by QS systems. In *P. aeruginosa*, four QS signalling pathways have been recognized until now: Las, Rhl, Pqs and IQS systems. The most recently discovered IQS pathway is less understood, and its regulation is not clear yet. Each system consists of at least two main functional elements. Firstly, each autoinducer activates the specific transcriptional factor such as LasR, RhlR, and PqsR, respectively. Therefore, transcriptional factors induce the production of autoinducer synthases (LasI, RhlI, and PqsABCDH, respectively), that lead to the synthesis of specific autoinducers, i.e. 3-oxo-C12-homoserine lactone (HSL), N-butyrylhomoserine lactone (BHL), and 2-heptyl-3-hydroxy-4-quinolone (PQS), respectively. Autoinducers are released outside cells, and then cross the cytoplasmic membrane of other cells to enter again in bacteria. These QS pathways work in a hierarchical way, where LasR is at the top of the cascade. LasR and RhlR mediate the signalling at the early stages of growth, while PQS system is involved in the exponential growth phase. During QS signalling, cell density is a fundamental aspect that directly influences the autoinducers production and triggers the response of the entire population (Moradali et al., 2017).

Starting from the first stages of tissue colonization, *P. aeruginosa* produces several virulence factors, belonging to different chemical categories, and most of them are produced under the control of QS systems. QS-dependent VFs include the following molecules:

- pyocyanin is a secondary metabolite with redox activities that causes oxidative stress and cytotoxicity to the host cells;

- pyoverdine serves as scavenger of iron and other important metals;
- LasA and LasB elastases, characterized by lytic activity, are crucial metalloproteases for tissue invasion and infection;
- alkaline protease can degrade tissue proteins, cause haemorrhagic tissue necrosis and inactivate component of host immune system;
- lectin A is characterized by high rate of cytotoxicity, ability to impair epithelial lung cells and increase permeability of toxins in intestinal epithelium;
- phospholipase C has cytolytic activity important for cell membrane destruction and tissue invasion;
- rhamnolipids are important for motility and maintenance of biofilm architecture and eliminate polymorphonuclear neutrophilic leukocytes;
- exotoxin A is one of the most toxic VF that inhibit protein synthesis in host cells at systemic level, causing immunosuppression and tissue damages.

Other VFs that increase *P. aeruginosa* pathogenicity are represented by cellular appendages like type IV pili and flagella, lipopolysaccharide (LPS) in the outer membrane, type III secretion system (T3SS), and antioxidant defence enzymes, i.e. catalases, superoxide-dismutases, peroxidases (Moradali et al., 2017).

1.1.2 *Staphylococcus aureus*: A Gram-positive model

Staphylococcus aureus is a Gram-positive commensal in human skin flora, that is usually isolated in moist areas like nose and axillae. It can be continuously carried by almost 20% of the population, the so-called health persistent carriers, while 60% of the population are intermittent carriers and harbour *S. aureus* irregularly. However, it can contaminate wounds in the skin or mucous membranes and rapidly infect any other tissue of the body, causing a variety of acute and chronic diseases with increasing severity, such as endocarditis and haemolytic pneumonia (Kwiecinski and Horswill, 2020). Thanks to the production of toxins, *S. aureus* can also cause toxic shock syndrome, scalded skin syndrome, and food poisoning (Kluytmans et al., 1997). The segment of the population exposed to the highest risk of *S. aureus* nosocomial infections are people with compromised immune system or frequently subjected to injections or catheter insertions.

S. aureus genome (2.9 Mbp) is constituted by almost 25% of accessory elements, that consist of bacteriophages, pathogenicity islands, chromosomal cassettes, genomic islands, and transposons. Many of these genomic portions carry genes involved in the production of virulence factors or antimicrobial resistance functions and could be shared among different strains by horizontal gene transfer to rapidly adapt to environmental conditions (Lindsay and Holden, 2004). Indeed, the first evidence of methicillin-resistant *Staphylococcus aureus* (MRSA) was reported in 1960s, and in recent years, in some European countries, MRSA strains have a prevalence of 25–50% within *S. aureus* isolates (Pendleton et al., 2013).

A variety of VFs can help *S. aureus* to establish the infection and avoid the host response. These factors include α and β toxins, enterotoxins, bacteriophage-conferred Panton-Valentine leucocidin, and toxic-shock syndrome toxin (TSST-1). Several adhesins and surface proteins help bacteria in the adhesion to tissues, extracellular matrix of biofilm, and blood components such as platelets, hemin, and haemoglobin. *S. aureus* also takes advantage from proteases, coagulases, collagenases, haemolysins, hyaluronidases, and phospholipase C. Another important segment of VFs helps in the evasion from innate immune system of human body, and include factors involved in neutrophil lysis or migration, resistance to oxidative burst (staphyloxanthin, catalases, alkylhydroxide reductases, thioredoxins), complement inactivation, degradation of immunoglobulins, and resistance to antimicrobial peptides (Zecconi and Scali, 2013).

In clinical history, *S. aureus* was the first microorganism to be shown growing in a biofilm on the surface of an endocardial pacemaker and causing a persistent bacteraemia (Marrie et al., 1982). Biofilm formation by *S. aureus* is still a current problem in infections care, causing prevalently medical devices-associated infections on heart valves, catheters, and joint prosthetics, that are increasingly recalcitrant to host immune response and antibiotic treatments. The initial *S. aureus* attachment on surfaces can take place non-specifically, driven by electrostatic, hydrophobic, and Van der Waals forces. Otherwise, *S. aureus* uses microbial surface components recognizing adhesive matrix molecules (MSCRAMMs) for the anchoring to the host matrix components (fibrinogen, fibronectin, and collagen). Subsequently, biofilm

develops as a mass of confluent cells in a proteinaceous matrix, containing also eDNA. Part of the cells starts to migrate to form three-dimensional microcolonies, and then, a rapid cell division lead to the production of a robust mature biofilm. In the last phase of biofilm life cycle, planktonic cells can be dispersed to initiate the journey for new invasive phases (Moormeier and Bayles, 2017).

S. aureus pathogenicity is subjected to a complex and intricate network of factors that combine physiological processes in response to environmental and host stimuli. The most prominent regulation system of *S. aureus* is the accessory gene regulator (*agr*) QS system. The *agr* system is activated by an autoinducing peptide (AIP) and the following up- and down-regulation of specific genes induced the production of fundamental VFs, as demonstrated in different infections in animal models, including endocarditis, pneumonia, skin, and soft tissue infections, and it also enhances biofilm formation and bacterial colonization of indwelling medical devices. Other two-component regulatory systems, like SaeRS and ArlRS, are linked to VFs and a large number of host-impacting secreted proteins. Finally, to survive in the host environment, this bacterium relies on important cytoplasmic regulators that include the SarA protein family (SarA, Rot, and MgrA) and alternative sigma factors (SigB and SigH) (Le and Otto, 2015; Jenul and Horswill, 2018).

1.1.3 *Candida albicans*: A fungal model

Candida albicans is a yeast naturally living in many natural environments and as a commensal of various animals. In humans, it can be found as part of the skin flora or in gastrointestinal, respiratory, and genitourinary tracts. Generally, *C. albicans* is harmless for the host, but sometimes it becomes an opportunistic pathogen. Indeed, *C. albicans* is the most common cause of superficial vaginal and mucosal oral infections, and it may enter the bloodstream leading to deep-tissue infections, known as systemic invasive candidiasis, that could affect circulatory system, bones and brain, with a mortality rate of almost 40% (Du et al., 2020). Risk factors for *C. albicans* infections are represented by antibiotic therapy, central venous or urinary catheters, surgical procedures, condition of neutropenia, immunocompromised situations (e.g. acquired immunodeficiency syndrome – AIDS), solid cancers, and

other cardiac, neurologic, gastrointestinal, pulmonary and vascular diseases. In clinical settings, *C. albicans* is considered an emergent nosocomial pathogen, and despite other *Candida* species have been isolated in this environment (such as *C. glabrata, C. parapsiolosis, C. tropicalis, C. krusei*), *C. albicans* is the most frequent etiological agent of hospital-acquired yeast infections (Dadar et al., 2018).

C. albicans wide diploid genome (14.4 Mbp) consists of eight chromosomes and is characterised by genetic instability that confers phenotypic and genetic diversity of the yeast and play a major role in pathogenesis. Indeed, in response to some stresses including antifungal drugs, heat shock and host-pathogen interaction, the high plasticity and instability of the genome modulate *C. albicans* behaviour in terms of growth rate, morphology, resistance to antimicrobials, and pathogenicity.

C. albicans is a polymorphic yeast, meaning that it can grow as a unicellular budding yeast or in filamentous forms, known as pseudohyphae and hyphae. In pseudohyphal form, the mother and daughter cells remain attached at the septation point, where a constriction is visible, and cells are more elongated during yeast growth. While, during hyphae formation, a single germ tube evaginates from the mother cell, and during cell division, the migration of the nucleus occurs into the tube. In this case, no constrictions are visible between different cells and the hyphae structure appears thinner and longer than pseudohyphae. The yeast form is usually associated with benign interactions with host cells, while hyphal forms are associated with infections, since they are not well tolerated by host cells and induce a macrophages-mediated immune response by the host (Sudbery, 2011). This change of morphology depends on numerous environmental signals (high pH, starvation, presence of serum or N-acetylglucosamine, temperature, CO_2 concentration) and is considered one of the virulence determinants expressed by this pathogen. Among *Candida* virulence factors, the presence of invasins and adhesins on the cell surface favours the crossing of barrier and the binding to tissues, while the secretion of hydrolytic enzymes and the biofilm formation strengthen the host colonization (Mayer et al., 2013).

C. albicans typically forms a highly structured biofilm in 24-48 hours and is the fourth most frequent cause of bloodstream infections in clinical setting, because once the biofilm is grown on a surface, it seeds fungal cells to colonize other tissues and

organs. Biofilm formation begins with the adherence of spherical yeast cells to a surface (epithelial cells, other microbial cells, or abiotic surfaces) thanks to the presence of adhesins on the cell wall of the yeast. This process is strongly influenced by the nature of the surface on which the biofilm is developing. Thus, the surface influences the adhesion phase and determines the dimension of the mature biofilm. A fast proliferation of yeasts forms a basal layer of anchoring cells that permit the growth of pseudohyphal and hyphal structures and the concomitant production of extracellular matrix. In *C. albicans* biofilm, EPS is mainly composed by proteins and glycosylated proteins (55%), carbohydrates (25%) such as glucose and hexosamine, lipids (15% - not charged or polar glycerolipids and sphingolipids) and non-coding DNA (5%). Also polysaccharides play an important role in biofilm structure and are composed by mannan-glucan complexes (Cavalheiro and Teixeira, 2018).

In *C. albicans*, social behaviour and biofilm lifestyle are regulated by a complex network of master transcriptional regulators and a certain number of autoinducers of QS system. Master regulators (Egf1, Tec1, Bcr1, Ndt80, Brg1, and Rob1) control the synthesis of other regulators, building an intricate pathway that supervise the expression of almost one thousand genes implicated in the main biofilm formation steps (adhesion, matrix production, hyphae formation) (Nobile and Johnson, 2015). QS autoinducers identified in *C. albicans* are farnesol, farnesoic acid, tyrosol, phenylethyl alcohol, tryptophol, and MARS – morphogenic autoregulatory substance. Farnesol is involved in the inhibition of biofilm formation and inhibition of the yeast-mycelium conversion, while tyrosol acts by decreasing the length of lag phase of growth and by stimulating filamentation and biofilm formation. The effect of other QS molecules is not clear yet, but it seems that phenylethyl alcohol, tryptophol and MARS could block filamentation and cell growth (Kruppa, 2009; Albuquerque and Casadevall, 2012).

1.2 Antibacterial and antifungal compounds

Considering the challenging antimicrobial resistance scenario, novel and alternative strategies to treat bacterial and fungal infections are urgently needed. On one hand, possibilities to overcome AMR consist of the improvement of antibiotic

and antifungal agents action, and the discover of new classes of antimicrobial compounds acting via new mechanisms or new cellular targets (Wagner et al., 2016). On the other hand, since biofilm-mediate infections are very difficult to treat with the available therapies, the scientific community is making efforts to find antibiofilm approaches, by targeting the main biofilm components and its regulatory network (Beloin et al., 2014). In the following paragraphs current antimicrobial therapies against the ESKAPE pathogens *P. aeruginosa* and *S. aureus* and the yeast *C. albicans* are described. Furthermore, alternative strategies under investigation to target the biofilm of these pathogens are also depicted.

1.2.1 Antibiotics to treat *P. aeruginosa* infections

In clinical practice, bacterial infections are usually treated with antibiotics acting on different microbial targets: cell wall synthesis, cell membrane integrity, protein synthesis, nucleic acid synthesis, and bacterial specific metabolisms.

Antibiotics adopted to manage *P. aeruginosa* infections can act against cell wall synthesis and belong to the class of β-lactams. This family includes penicillins (piperacillin), cephalosporins (ceftazidime, ceftolozane), and carbapenems (meropenem) and are almost exclusively formulated in combination with β-lactamases inhibitors (avibactam, tazobactam), since all *P. aeruginosa* strains expresses β-lactamase enzymes. Other classes of antibiotics chosen for *P. aeruginosa* treatment are aminoglycosides (tobramycin), a class of antibiotics that acts by binding 30S ribosomal subunit and inhibiting protein synthesis; fluoroquinolones (ciprofloxacin) that inhibits DNA replication targeting DNA gyrase and topoisomerase IV; and polymyxins (colistin) that act on the disruption of outer and inner cell membranes (Gaspar et al., 2013). Recent advances in antibiotic research highlighted the possibility of targeting new cellular elements of *P. aeruginosa*, such as elongation factors in the process of translation, using argyrins; inhibitors of LpxC, an enzyme involved in the biosynthesis of lipid A, essential component of the outer membrane; and topoisomerase inhibitors that bind their target differently from fluoroquinolones (Wagner et al., 2016). Other promising antibiotics are gallium-based drugs, where gallium could replace iron in many enzymes and inhibit redox

processes, siderophore-antibiotic conjugates to facilitate the entrance of the antibiotic in the cytoplasm, and carbon monoxide-releasing molecules to inhibit the respiratory chain of *P. aeruginosa*. For the treatment of sever *P. aeruginosa* infections (e.g. bacteraemia and pneumonia) a combinatorial approach of at least two antibiotics is usually recommended, for example with a β-lactam in addition to an aminoglycoside or fluoroquinolone (Wagner et al., 2016; Bassetti et al., 2018).

1.2.2 Antibiotics to treat *S. aureus* infections

For the treatment of *S. aureus* infections, especially MRSA strains, antibiotics targeting cell wall components are semisynthetic cephalosporins (ceftaraline, ceftobiprole), glycopeptides (vancomycin), and semisynthetic lipoglycopeptides (oritavancin, telavancin and dalbavancin). Daptomycin is used for treating bacteraemia and endocarditis and its target is the bacterial cell membrane. Tetracyclines (tigecycline), aminoglycosides (neomycin, gentamycin), oxazolinidone (linezolid, tedizolid), chloramphenicol, lincomycin, macrolides (erythromycin), fusidic acid, and mupirocin are used in *S. aureus* infections treatments and their target is the protein synthesis machinery. Other antibiotics have nucleic acid biosynthesis as target and the most used to control *S. aureus* infections are rifampicin, fluoroquinolones, and sulphanilamide. A combinatorial approach of these different antibiotics proved to have a synergic effect on MRSA strains (Davis et al., 2015; Purrello et al., 2016; Foster, 2017).

1.2.3 Antifungals to treat *C. albicans* infections

Fungal infections caused by *C. albicans* are treated with antimycotic drugs. The most adopted treatments against candidiasis include azoles (fluconazole, posaconazole) and allylamines that inhibit ergosterol biosynthesis, polyenes (nystatin, amphotericin B) as membrane disruptors, and echinocandins (caspofungin, micafungin) against cell wall biosynthesis. Other therapies involve aureoblastin A that target sphingolipids synthesis, pyrimidines (flucytosine) as inhibitor of nucleic acid biosynthesis, and cispentacin and icofungipen targeting the protein synthesis. Finding new possible cellular target in yeast cells is very important, and recent

advances highlighted the possibility of targeting Hsp90 protein with specific inhibitors (in combination with echinocandins or fluconazole), treholose production, and calcium/calmodulin signalling (Campoy and Adrio, 2017; Nami et al., 2019).

1.3 Resistance to antimicrobial and antifungal treatments

Bacteria and fungi have naturally developed chemical weapons to compete for nutrients and essential elements with other microbial species in their own ecological niches since billions of years. Simultaneously, this secretion of natural antimicrobial products has paved the way toward the development of mechanisms of resistance in microorganisms living in the same local environments. In the last century, this phenomenon of antimicrobial resistance (AMR) has rapidly evolved because of the increasing selective pressure caused by the widespread use of antimicrobial compounds throughout the world. AMR has become an increasing issue especially in medical settings, where multidrug resistant (MDR) strains of a variety of human pathogens represent a threat for hospitalised patients.

Mechanisms of resistance arise in nosocomial pathogens thanks to their high genetic plasticity that allow them to constantly evolve and survive in the presence of antibiotic or antifungal compounds. In general, these mechanisms are based on three strategies: prevent the antimicrobic molecule to reach its target, modify or protect the molecular target of the antimicrobial agent, or directly modify the antimicrobial compound (Blair et al., 2015).

In bacteria, mechanisms of antibiotic resistance can be classified as intrinsic or acquired mechanisms. In the first case, inherent structural and functional cell characteristics confer to all bacteria belonging to the same species the ability to resist to antimicrobial actions of a certain antibiotic. On the other hand, the acquired resistance derives from mutations in chromosomal genes or from horizontal gene transfer. In general, thanks to their cellular structure, Gram-negative bacteria result more intrinsically resistant to antimicrobials than Gram-positive bacteria (Blair et al., 2015).

Antimicrobial resistance in *P. aeruginosa*

P. aeruginosa is characterised by an outer membrane that acts as a selective barrier to prevent the antibiotic entrance, in addition to several non-specific porins that govern membrane permeability. Among these, selective porins such as OprB, OprD, OprE, OprO, and OprP, and non-selective ones, such as OprF that is mainly found as a closed channel, contribute to the reduction of the outer membrane permeability (Hancock and Brinkman, 2002). In addition, a wide variety of efflux pumps (especially MexAB-OprM, MexCD-OprJ, MexEF-OprN, etc.) on cellular envelop are responsible for the transportation of different classes of antibiotic molecules (i.e. β-lactams, quinolones and aminoglycosides) outside the cell (Li and Nikaido, 2009). In the chromosome of *P. aeruginosa,* genetic determinants codify for antibiotic-modifying enzymes. They are resistant to β-lactams because of the production of several β-lactamases or extended-spectrum β-lactamases (ESβL), while their resistance to aminoglycosides depends on the transfer of phosphoryl, acetyl, or adenylyl groups on the antibiotic molecule (Wright, 2005).

Acquired mechanisms of resistance in *P. aeruginosa* are based on mutational changes that can cause overexpression of efflux pumps and antibiotic-inactivating enzymes, reduced antibiotic uptake, and modification of antibiotic target. Moreover, a critical role in dissemination of AMR is played by the acquisition of resistance genes from other strains by means of transformation, transduction, and conjugation processes. Finally, *P. aeruginosa* takes advantage of its adaptability to change its behaviour in response to the environmental conditions, in the mechanisms known as adaptive resistance. This bacterium has very low nutritional requirements and can persist in extremely harsh environments. Indeed, the best characterised mechanism of adaptive resistance is the formation of biofilm with the generation of persister cells (Pang et al., 2019).

Antimicrobial resistance in *S. aureus*

The antibiotic resistance in the Gram-positive *S. aureus* is mediated by acquired mechanisms through the process of random mutation and selection under the pressure of antibiotics, and mainly by horizontal gene transfer of resistance determinants (Pantosti et al., 2007). Among these, plasmid-carrying β-lactamase genes represent a

strategy rapidly evolved to counteract the activity of β-lactams, such as penicillin and methicillin. The attention, nowadays, is focused on MRSA (methicillin resistant *S. aureus*) strains carrying resistance to β-lactam antibiotics, including cephalosporins and carbapenems. As a matter of fact, MRSA strains are more often multidrug resistant microorganisms, being resistant to other classes of antibiotics such as macrolides, aminoglycosides, and fluoroquinolones. Resistance to fluoroquinolones is due to the arising of spontaneous mutations in genes codifying topoisomerase IV and DNA gyrase, implicated in DNA replication processes (Hooper, 2002). Over the last two decades, an emerging issue is represented by vancomycin-resistant *S. aureus* (VRSA) that survive in the presence of glycopeptide antibiotics. In particular, the *vanA* operon is responsible for the synthesis of modified target (D-Ala-D-Lac) on the cell wall, conferring resistance to vancomycin and teicoplanin (Pantosti et al., 2007).

Antifungal resistance in *C. albicans*

The arising of *C. albicans* strains resistant to antifungals is a further issue in clinical environment. Among antifungal agents, azoles inhibit the synthesis of ergosterol, an important component of yeast's cell membrane, and different resistance mechanisms to azoles have been reported. The induction of expression of multidrug efflux pumps operons, such as *CDR* and *MDR* loci, confers resistance to multiple azoles, including fluconazole, by reducing their concentration in the fungal cell cytoplasm (Albertson et al., 1996). In addition, alteration and up-regulation of the target gene, *ERG11* gene encoding for lanosterol 14-α-sterol demethylase, has been found to prevent the binding of azoles to the enzymatic site and to make the azole concentration ineffective (Sanguinetti et al., 2015). Lastly, the substitution of ergosterol with another sterol by means of an alternative pathway, prevents the disruption of the fungal membrane (Kelly et al., 1997). Echinocandins are antifungal molecules blocking the biosynthesis of an important component of cell wall, the β(1,3)D-glucan. The impairment of this pathway due to mutations occurring in genes codifying the target enzymes, induces the increase in chitin biosynthesis as an adaptive stress response. Moreover, a peculiar mechanism of resistance is linked to the loss of heterozygosity at resistance genes, due to genetic recombination and high plasticity of eukaryotic

genome. Finally, chromosomal rearrangements are found to amplify the number of copies of genes associated with antifungal resistance (Sanguinetti et al., 2015).

1.3.1 Bacterial and fungal biofilms: tolerance to antimicrobials

The formation of biofilm communities represents the most widespread lifestyle for microorganisms in natural environments. When dealing with biofilms in clinical environment, another issue needs to be considered: the tolerance of biofilm to antimicrobial treatments. Resistance mechanisms are those implicated in the avoidance of antibiotic-target interaction, while tolerance mechanisms refer to the ability of microorganisms to survive in the presence of a bactericidal/fungicidal agent, without grow nor die (Hall and Mah, 2017).

Bacterial biofilms

In bacterial biofilms, the extracellular matrix represents the first barrier that hinders antibiotic penetration and preserves microbial surviving. However, data available from studies of antibiotic penetration in biofilms are strongly influenced by bacterial strain, biofilm age, growth conditions, and chemical features of antibiotic compounds. Different antibiotics showed opposite rate of penetration through microbial biofilm. Oxacillin, cefotaxime, and vancomycin were found to be limited in their diffusion through biofilms of *S. aureus* and *Staphylococcus epidermidis,* and tobramycin was not able to penetrate in *P. aeruginosa* biofilm. On the contrary, tetracycline and ciprofloxacin effectively penetrate biofilms of *Escherichia coli* and *K. pneumoniae*, respectively. It is important to highlight that EPS components, such as polysaccharides, extracellular DNA and antibiotic-modifying enzymes, could interact with antibiotic molecules and influence their activity (Hall and Mah, 2017). In *P. aeruginosa,* it has been reported the role of polysaccharides Psl and Pel, in interfering with the activity of colistin, tobramycin, polymyxin B, ciprofloxacin and gentamicin. Anionic eDNA chelates cations, such as magnesium ions, and change the extracellular environment. It has also been proposed that charged polysaccharide and eDNA could directly sequester antibiotic molecules by electrostatic interactions. Finally, secreted β-lactamases prevent antibiotic penetration in the deepest layers of

biofilms of *P. aeruginosa* (Bowler et al., 2012; Billings et al., 2013; Chiang et al., 2013).

The biofilm is composed by cells with different physiological features (i.e. gene expression, metabolic activity, antimicrobial tolerance) according to the different region in the 3D structure. This heterogeneity is due to the different concentrations of oxygen and nutrients in the biofilm layers. Metabolically active cells are present in the external layers, while dormant cells are found in the deepest parts of the biofilm. Moreover, a slow growth rate and conditions of hypoxia contribute to a lower sensitivity of cells to antibiotics. Notably, low oxygen conditions were found to upregulate resistance genes like *mexCD-oprJ* locus, codifying for an efflux pump in *P. aeruginosa* biofilm (Hall and Mah, 2017). Usually, bacterial cells have to face the oxidative stress generated by antibiotics generating deleterious reactive oxygen species (ROS), especially hydroxyl radicals, that contribute to cell death. Therefore, hypoxic conditions do not favour the production of ROS (Van Acker et al., 2014). In *P. aeruginosa*, the stringent response, a regulatory mechanism involved in response to nutrient starvation, protects this bacterium from oxidative stress by maintaining high levels of detoxifying enzymes (i.e. catalases and superoxide-dismutases) and by inhibiting production of pro-oxidant molecules, such as 4-hydroxy-2-alkylquinolines (HAQs) (Van Acker et al., 2014). It is well known that Quorum Sensing (QS) signalling is at the basis of biofilm formation. Indeed, QS quenching molecules were found to prevent the formation of mature biofilm and to make more susceptible to antibiotics the biofilms of *P. aeruginosa* and *S. aureus* (Brackman et al., 2011, 2016). The biofilm scaffold could favour the transfer of plasmids among sessile cells entrapped in biofilm matrix, thanks to cells spatial proximity. Moreover, a higher number of plasmid copies, an upregulation of integrase enzymes and a high excision frequency of antibiotic resistance genetic cassettes results in higher levels of resistance in biofilm cells than in planktonic ones. Mutation rates also were found to be increased in biofilm cells and contribute to increase antibiotic resistance (Hall and Mah, 2017).

Lastly, a peculiar subpopulation of cells, called persister cells, could be found in the deepest layer of bacterial biofilms. These cells confer high tolerance to biofilms

thanks to their complex physiology, allowing them to be transiently tolerant to antibiotics. Long persisters are well characterised in planktonic cultures after prolonged exposure to antibiotics in *E. coli* and *P. aeruginosa.* These cells could be metabolically active, but they can not grow. A switch to the growing state can be reached when external stresses, such as antibiotic compounds, are removed guaranteeing the survival of the bacterial population (Fisher et al., 2017).

Yeast biofilms

Similarly to bacterial biofilm, yeast biofilm tolerance to antifungal agents is a complex process. The production of EPS represents a physical barrier to chemical compounds. In *C. albicans*, the presence of eDNA prevents the activity of polyenes and echinocandins, while the predominant carbohydrate component β-1,3 glucan is responsible for azole, pyrimidines, echinocandins and polyenes sequestration, increasing biofilm tolerance to these compounds (Ramage et al., 2012). Although the physiological state (e.g. metabolic activity, dormancy, etc.) of fungal subset of cells can influence antifungal susceptibility, an important role is played by cell density in both yeast and filamentous fungi, where communications within cells is driven by QS systems. Indeed, physical density of cells produces recalcitrance to antifungal agents in *C. albicans*, especially against azoles (Perumal et al., 2007). Furthermore, expression of multidrug efflux pumps operons was shown to be differentially regulate during biofilm development upon exposure to antifungal agents. Indeed, efflux pumps play a primary role in maintaining homeostasis in extracellular environment, but they can contribute to resistance to azoles in the early phases of biofilm formation (Mukherjee and Chandra, 2004). In *C. albicans* biofilm, azoles and polyenes induced changes in the regulation of ergosterol biosynthesis determining tolerance to these antifungals. An upregulation of genes encoding for enzymes involved in ergosterol synthesis, in addition to the changes of sterol components in fungal membranes, were found to decrease susceptibility of fungal cells in biofilms (Ramage et al., 2012). As previously explained for bacterial cells, also fungal cultures could develop phenotypic variants highly tolerant to antimicrobials, called persisters. These cells are responsible of antimicrobial drug failure since they ensure survival after prolonged antifungal treatments (Mukherjee and Chandra, 2004). In *C. albicans* biofilm,

fungicidal agents, such as miconazole, elicit oxidative stress that can be counteracted by upregulation of detoxifying enzymes (superoxide-dismutases) in sessile sub-population of biofilm. Lastly, the response to environmental stress (temperature, pH, osmolarity, and oxidative stress) is shown to be involved biofilm protection and maintenance (Ramage et al., 2012).

1.3.2 Targeting microbial biofilms

As previously reported, biofilm communities rely on complex mechanisms of resistance and tolerance to antimicrobial treatments. Upon the establishment on a surface, biofilm removal become difficult because of the adhesive strength and viscoelastic properties of the structure. Since the current available antimicrobial agents have not been specifically developed to target biofilms, antibiofilm strategies need to be designed, aimed at controlling biofilm-mediated infections. Indeed, many recurrent and persistent infections are caused by the presence of microbes organised in biofilms (Verderosa et al., 2019).

Due to the high complexity of a biofilm, it is clear that a combination of different strategies should be taken into consideration to target microorganisms and the surrounding EPS, to prevent initiation of biofilm formation or to disrupt existing biofilms (Koo et al., 2017; Mulani et al., 2019).

In general, possible antibiofilm strategies could target the biofilm extracellular matrix, through inhibiting its production or disrupting/modifying its main components. In fact, inhibitors of glucan synthesis and adhesin production have been shown to prevent *in vivo* biofilm formation of both bacterial and fungal biofilms (Koo et al., 2017). Matrix-degrading enzymes have also demonstrated their activity by targeting exopolysaccharides, eDNA and bacterial peptidoglycan. These enzymes weaken the biofilm structure and, when used in combination with other antimicrobial agents, a better killing effect was observed. An antibodies-mediated EPS disruption have also been taken into consideration, for example antibodies that bind specific exopolysaccharides (e.g. Psl of *P. aeruginosa*) proved to enhance phagocytic killing of pathogens (Koo et al., 2017).

The complex regulatory network of biofilms could also represent a target for antibiofilm therapies, especially QS signalling pathways. Quorum sensing inhibitors have been found to efficiently compromise the biofilm structure, making microbial cells more susceptible to antibiotic actions (Assis et al., 2017; Richter et al., 2017; Pang et al., 2019). Furthermore, some studies reported the activity of nitric oxide in the dispersion of different bacterial species, that acts by modulating the levels of the secondary messenger cyclic-di-GMP, a key molecule in biofilm life cycle (Koo et al., 2017).

Another important target in biofilm communities is the population of "persister cells". In this case, physical or chemical disrupting approaches (oxidizing agents such as hypochlorite and hydrogen peroxide) should be used, instead of metabolism-interfering molecules. A combination of different antibiotics (rifampicin and acyldepsipeptide antibiotic) showed a great activity on dormant persister cells in infections of *S. aureus* in mouse models (Koo et al., 2017).

Furthermore, a metabolically-independent action was observed in treating biofilm model with antimicrobial peptides (AMPs) or antibiofilm peptides (Chatterjee et al., 2016; Chanda et al., 2017; Magana et al., 2020). Species-specific or broad-spectrum active AMPs could have a therapeutic potential on both bacterial and fungal biofilms. These peptides could also be modified by nanoengineering or immobilised onto solid surfaces to enhance their efficacy or specificity (Belanger et al., 2017; Pang et al., 2019).

Further, the development of attached communities could be penalized by engineered surface of indwelling medical devices, through modification of the surface topography or their chemical modifications. Smart surfaces, containing a reservoir of antibiotic or biocides coating, have also been considered as antibiofilm strategy (Del Pozo and Patel, 2007; Belanger et al., 2017; Koo et al., 2017).

To fight persistent bacterial infections, bacteriophages were also considered as promising alternative strategies to control biofilm development. With their lytic activity, they could act on both active and dormant cells, when the latter return to the metabolically active state. The phage therapy is suggested to be used in combination with other antimicrobial agents, and genetically engineered phages could be designed

to increase their antibiofilm activity (Chatterjee et al., 2016; Pires et al., 2017; Pang et al., 2019).

Recently, organic and inorganic nanoparticles (NPs) have been studied as antimicrobial agents in themselves, or as drug delivery vehicles (nanocarriers) of anti-infective compounds. Conjugation of nanoparticles with other molecules enhance their own antimicrobial properties or help in the transport of the conjugated molecules to the infection site (Koo et al., 2017; Pang et al., 2019). The use of nanofabrication methodologies can provide a promising approach also to reduce biofilm formation on medically relevant surfaces (Natan and Banin, 2017).

Promising sources of antibiofilm agents are natural complexes or molecules extracted by plants or produced by animals or microbes. Examples of naturally active compounds on the biofilm of microbial and fungal pathogens are honey, organic acids (e.g. acetic, citric, oxalic acids), garlic, ginseng, curcumin, chitosan and flavonoids (Belanger et al., 2017).

An interesting therapy developed to control the growth of bacteria and yeasts suggests the use of probiotic microorganisms, such as Lactobacilli. They naturally live in human gut and they secreted important products with antimicrobial activity. When administered to wounds and burns they prevented biofilm formation by *P. aeruginosa,* and helped in managing oral candidiasis (Chatterjee et al., 2016; Chanda et al., 2017).

The irradiation through visible light represents a very interesting antibiofilm strategy. The light alone or in combination with specific drugs, non-toxic dyes or natural compounds, induces an oxidative stress that compromise the viability of biofilm cells, both planktonic and adherent populations (Chanda et al., 2017; Mulani et al., 2019). In depth descriptions of light-based approaches is presented in the next paragraph.

1.4 Light-based antimicrobial approaches

The use of light as anti-infective tool has been known for decades, not only in medical care for the management of infections, but also in environmental (decontamination of waste waters, agriculture) and industrial fields (livestock, aquaculture, food industry) (Yin et al., 2013). Among the spectrum of light, defined

as electromagnetic radiation from 200 to 10000 nm, ultraviolet radiation (UV – 200-400 nm), visible light (400-750 nm), and near infrared light (NIR – 750-1200 nm) showed antimicrobial properties on different microorganisms, including bacteria, fungi, viruses and parasites. UV radiation has a powerful killing effect on almost all known pathogens, but, in clinical field, it presents several side effects, including low penetration through human tissues and the possibility to damage host cells. While visible light, alone or in combination with appropriate molecules, emerged as a safe alternative for host cells, excluding the possible toxicity of the photo-activated compounds. Near infrared light demonstrated good tissue penetration but moderate activity against pathogens (Hamblin and Abrahamse, 2018).

The interest of the scientific community in light-based antimicrobial strategies has significantly arisen in concomitance with the increase and spread of antimicrobial resistance. Indeed, light-induced microbial killing effects are considered a safe method that overcome common AMR mechanisms and do not lead to the production of further pathways of antimicrobial resistance. Furthermore, one of the main advantages of light-based therapies is that most of them have a broad-spectrum activity on many pathogenic microorganisms (Gwynne and Gallagher, 2018).

The main approaches exploiting visible light as anti-infective agents are antimicrobial photodynamic therapy (aPDT) and, more recently, antimicrobial blue light therapy (aBLT), also known as phototherapy (aPT).

1.4.1 Antimicrobial Photodynamic Therapy

Photodynamic therapy was firstly studied as anticancer therapy in 1970s, and only subsequently, in 1990s, its potential anti-infective properties emerged for the treatment of localised infections. In the last five years, PDT have received significant attention, and was reported as promising treatment against ESKAPE pathogens, especially in topical application, and also for the treatment of oral candidiasis caused by *C. albicans* (Chanda et al., 2017; Mulani et al., 2019). Moreover, an increasing number of studies recently highlighted the effect of aPDT in the eradication of biofilms of different pathogens. Indeed, a certain number of preclinical and clinical trials applying aPDT for the treatment of biofilm-associated infections is ongoing.

Human clinical studies concerns wounds and ulcers care, nasal decontamination, dental care, and gastric infections by *Helicobacter pylori* (Hu et al., 2018).

PDT combines the use of harmless visible light, a light-sensitive dye, called photosensitizer (PS), and molecular oxygen. The PS absorbs energy from a light source at appropriate wavelength, and consequently transfer energy or electrons to molecular oxygen, which is abundant in immediate environment, causing the generation of singlet oxygen ($^1O_2$) and reactive oxygen species (ROS), respectively. ROS species includes superoxide anion ($O_2\cdot^-$) which can go on to form hydrogen peroxide (H_2O_2) and hydroxyl radical (·OH). Oxidizing species can interact with microbial macromolecules, including proteins, lipids, nucleic acids, and other cellular structures, leading to strong oxidation and consequent microbial cells death (Wainwright, 1998).

The photochemical generation of oxidizing species start from PS irradiation and absorption of energy (figure 2). Immediately, it passes from the ground (S_0) to the excited singlet state (S_1), through electron transfer from the highest occupied molecular orbital to the lowest unoccupied one. The excited singlet state (S_1) is rather instable and short-lived, and PS may pass to the ground state, emitting fluorescence or releasing heat. Alternatively, PS can undergo to a spin conversion and pass to the excited triplet state (T_1), which is characterized by a lower energy compared to the excited singlet state, and a higher stability. In its excited triplet state, PS can release energy and reach the ground state by emitting phosphorescence or it can start one of the two photodynamic reactions classified as type I and type II mechanisms. Type I reaction involves direct electron or hydrogen transfer to a biomolecule, producing superoxide anion and other ROS. While, in type II reaction, PS transfers energy to molecular oxygen, eliciting the production of singlet oxygen ($^1O_2$), characterized by extremely oxidant power and a very short lifetime. Other than ROS, other oxidizing agents could be produced when interaction between excited PS and nitrogen occurs, that are reactive nitrogen species (RNS), for example nitric oxide (NO·) and peroxide nitrite (ONOO·) (St. Denis et al., 2011).

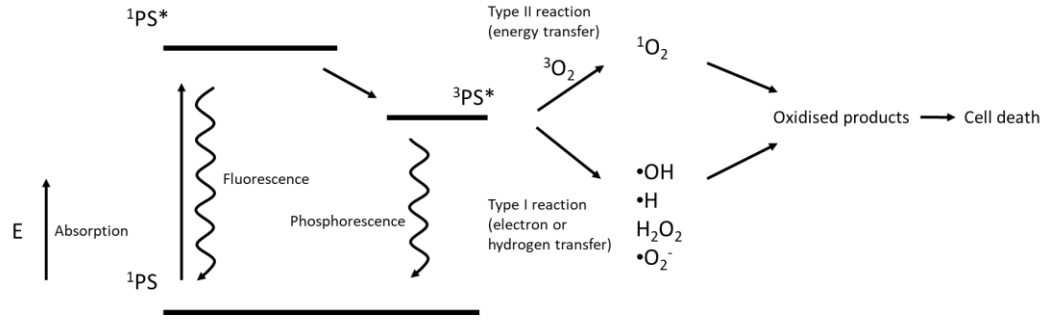

Figure 2. Schematic representation of photodynamic mechanism.

The oxidizing species produced during PDT reactions cause cellular damage by the interaction with biomolecules. The most reactive ROS is hydroxyl radical, that will withdraw electrons to become a hydroxide anion, while the electron-withdrawing effect of superoxide anion leads to the production of hydrogen peroxide. H_2O_2 is not considered so reactive, unless it reacts with ferrous ions, in the Fenton reaction, leading to de production of hydroxyl radical, hydroxide anion and ferric ions. Finally, singlet oxygen, produced via type II photodynamic reaction, is the main reactive agent in PDT responsible for macromolecule modification, by interacting with double bonds, sulphur or aromatic components (St. Denis et al., 2011).

It has been proposed that aPDT-killing effect is mediated by cell membrane or DNA disruption. However, since most oxidizing species are not long-lived, oxidative stress could damage different cellular components according to the cellular localisation of PS molecules. If the PS binds to the external envelops of bacterial or fungal cells, it can affect cell wall, cytoplasmic membrane, or eventually the outer membrane in Gram-negative bacteria. Otherwise, the PS could enter in the cytoplasm, where bacterial chromosome, cytoplasmic structures or organelles in fungal cells could be damaged by the oxidative burst (George et al., 2009).

During the PDT treatment of biofilms, PS molecules are firstly absorbed by the biofilm matrix, and in most of the cases they can partially pass through the EPS and reach microbial cells. Thus, the oxidative damage elicited upon irradiation, could affect matrix components (exopolysaccharides, eDNA, proteins, virulence factors) or directly biofilm-embedded populations of cells (Hu et al., 2018).

Of course, microbial cells possess defence mechanisms against oxidising species, naturally produced in aerobic environment, in both free-living and biofilm state. Indeed, different antioxidant molecules (e.g. sugars, peptides, pigments) could quench hydroxyl radical and singlet oxygen, while $O_2^{\cdot -}$ and H_2O_2 could be detoxified by specific enzymes, that are superoxide-dismutases and catalases, respectively. Although microbial cells could take advantage from this equipped arsenal, in most cases it reveals to be not sufficient in counteract the powerful oxidative burst elicited during PDT process (Maisch, 2015).

In the following paragraphs the main classes of photosensitizers and type of light sources used in PDT treatments are summarised.

Photosensitizers

The ideal photosensitizing compound should have different features to reach a good photoinactivation rate of pathogenic microorganisms. It should be able to interact with cell wall and cell membranes and/or to permeate in the cytoplasm. Therefore, PS chemical features could be different according to the cell envelope characteristics of each microbial species and its uptake abilities. For example, positively charged PSs are suggested to be suitable for the interaction with Gram-negative outer membrane. Moreover, the PS toxicity should be selective for microbial cells upon its photoactivation, and it should be safe for human tissues. No toxicity and mutagenicity in the dark should be presented towards both eukaryotic and prokaryotic cells (Soukos and Goodson, 2011). In addition, a low-molecular weight of PS compound is suggested to facilitate the penetration in microbial biofilms. The production of reactive oxygen species is also an important PS characteristic since a high singlet oxygen quantum yield is preferable in an ideal PS (Cieplik et al., 2018a). Further, absorption coefficient should be appropriate for an effective penetration of light in the infection site. In particular, long wavelengths are preferable since they allow an effective light penetration in human tissues. Finally, the effect of light on the PS molecule, known as photobleaching, should be considered: for therapeutic purposes, the photobleaching effect after the treatment could be suitable to avoid tissue photosensitivity, while for surface disinfection purposes a very low photobleaching

effect is preferable, to reach an extended photosensitizing effect (Wainwright and Giddens, 2003).

The currently available photosensitizers are usually conjugated unsaturated organic molecules of different chemical classes (figure 3). Acridine orange was the first dye used as PS compound, followed by tetrapyrrolic structures that include porphyrins, chlorins, bacteriochlorins and phthalocyanines. Other PSs are phenothiazines (methylene blue – MB, toluidine blue o – TBO), rose bengal, fullerenes, and boron-dipyrromethenes (BODIPYs). Furthermore, many natural substances demonstrated to act as PS molecules, such as curcumin, riboflavin, phenalenone, xanthene, and their derivatives (St. Denis et al., 2011; Maisch, 2020).

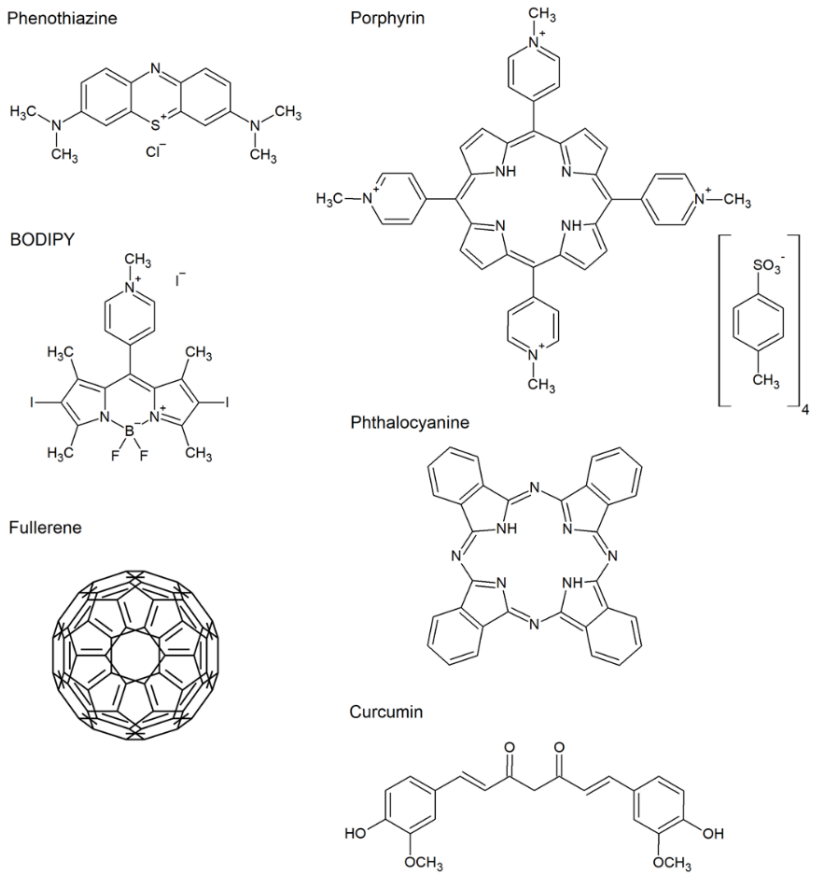

Figure 3. Chemical structure of the main classes of PSs. Phenothiazine (Methylene Blue, MB), BODIPY (2,6-diiodo1,3,5,7-tetramethyl-8-(N-benzyl-4-pyridyl)-4,4′-difluoroboradiazaindacene), fullerenes (C60), porphyrin (5,10,15,20-Tetrakis(1-methyl-4-pyridinio)porphyrin tetra(*p*-toluenesulfonate), TMPyP), phthalocyanine and curcumin.

According to their molecular framework, each class of PS is characterised by a specific absorption in the visible light spectrum, or alternatively in UV or infrared spectrum. Further, PS could react predominantly via one of the two mechanisms of action of PDT process, the type I or type II reactions (Wainwright, 1998).

Porphyrins, chlorins and phthalocyanines compounds, consisting in heterocyclic-macrocyclic structure made of four pyrrolic rings (or three pyrroles and one pyrroline for chlorins), have a specific absorption band centred around 400 nm (Soret band), and smaller peaks between 500 and 600 nm (Q bands), and they mostly produced singlet oxygen (0.5, 0.8 quantum yields), acting by the type II reaction mechanism (Amos-Tautua et al., 2019).

Phenothiazines, such as TBO and MB, are characterised by a quantum yield of singlet oxygen lower than 0.5, and mainly act via type I photodynamic reaction. Their absorption spectrum exhibits a band ranging between 600 and 680 nm in the red region, and smaller bands in the UV region between 200 and 300 mn. Interestingly, MB was the first PS approved for its clinical use in dentistry (Wainwright and Giddens, 2003).

The class of BODIPYs, that more recently has joined the family of antimicrobial photosensitizing compounds, involves molecules that are characterised by high photostability and an excitability around 500-550 nm, in green region. According to their chemical modification they could have different singlet oxygen quantum yields. These compounds are usually employed as dies or fluorescent probes; indeed, their modification is aimed at decreasing fluorescent properties and increasing singlet oxygen production upon photoactivation (Awuah and You, 2012).

Light sources

PDT efficacy strictly depends on PS properties, but also on light parameters, including the spectral emission, the light intensity (fluence) and its delivery mode (direct or by optical fibre).

The principal light sources adopted to photoactivate PSs are lasers (e.g. argon, diode lasers), light-emitting diodes (LEDs) and gas-discharge lamps (e.g. quartz-tungsten-halogen or xenon lamps). Lasers are characterised by monochromatic and coherent

radiation, LEDs deliver a slightly wider emission spectrum, while halogen lamps can be filtered in their wide emission spectrum to match the desired absorption range of each PS. Considering clinical application of aPDT, irradiation from lasers and LEDs can be used directly or easily coupled with optical fibres to efficiently deliver light in non-superficial areas of the body, while halogen lamps present limitation in using optical fibres. Gas-discharge lamps also generate more heating compared to lasers and LEDs, that could have undesired effects for human tissues (Cieplik et al., 2018a).

In general, aPDT approach can offer many advantages and can help in overcoming some limitations of the current antimicrobial agents. Indeed, thanks to its wide-spectrum and a multitarget killing effect, aPDT is suitable compared to the key-hole principle of the majority of antimicrobial treatments. In particular, pathogens seem to be disadvantaged in the development of specific mechanisms of resistance against photooxidation processes, and until now, no aPDT resistant strain has been isolated upon sublethal doses of photoinactivation (Maisch, 2015).

Another important aspect of aPDT concerns the fact that MDR microbes demonstrated to be as susceptible as antibiotic-sensitive strains to photodynamic inactivation (PDI). Thus, PDT could be considered as a valid approach in the management of MDR pathogens-mediated infections (Hamblin, 2016).

Moreover, PDT process allows to selectively acts on a specific region of interest. The light is delivered only in the infected region, for example in the oral cavity or in wounds, and this aspect delineates the photoinactivation process without affecting other tissues where the light is not administered. Thus, after a topical or systemic administration of the PS, the oxidative stress only damages the infected area where a light source activates the PS (Hu et al., 2018).

Possible side-effects in the clinical use of aPDT have been encountered when the PS is administered by systemic route, since it causes a period of skin photosensitivity due to its accumulation. Therefore, topical applications of PS are preferable to systemic administration. Other side-effects of PDT, like pain in the treated area, stomach pain, and, rarely, allergic reaction and change in liver parameters, could arise upon the treatment. Thus, the increase of aPDT efficiency and the improvement of its performances for clinical use are gaining increasing attention (Hu et al., 2018).

However, aPDT represents a promising and alternative approach for the treatment of infections, also where biofilms are involved, as adjuvant of currently available or new antimicrobial agents (Hamblin, 2016).

1.4.2 Antimicrobial Blue Light Therapy

A very recent light-based anti-infective treatment is antimicrobial blue light therapy (aBLT). This approach exploits the ability of visible light alone, particularly in the range of blue light from 400 to 500 nm, in damaging microbial pathogens, and leading to cell death (Wang et al., 2017).

BLT has been recently taken into consideration as a promising method for the treatment of bacterial and fungal infections, including biofilm-mediated ones, regardless of their antimicrobial resistance status (Ferrer-Espada et al., 2019).

Many pathogens demonstrated to be sensitive to blue light treatment, including ESKAPE pathogens, especially *P. aeruginosa*, *S. aureus*, *K. pneumoniae*, and *A. baumannii*, as well as periodontal pathogens such as *Fusobacterium nucleatum* and *Porphyromonas gingivalis*, and otopathogens such as *Moraxella catarrhalis*. Pathogenic yeasts and fungi were also sensitive to blue light, including *C. albicans*, *Saccharomyces cerevisiae*, *Trichophyton rubrum*, and *Aspergillus niger* (Wang et al., 2016, 2017; Zhang et al., 2016; Dai and Hamblin, 2017; Liu et al., 2020).

It has been hypothesised that aBLT mechanism of action is based on the generation of photooxidative stress upon the excitation of endogenous molecules, that behave as photosensitizing agents (Lubart et al., 2011). In different bacterial and fungal species putative endogenous molecules acting as PSs have been recognised, belonging to chemical classes of porphyrins and/or flavins. Indeed, the main types of endogenous compounds found in bacteria and yeasts are protoporphyrin IX, coproporphyrin I and coproporphyrin III (Wang et al., 2016, 2017).

As well as UV radiation, visible light is normally used in dermatology for the treatment of different skin disorders, such as actinic keratoses and acne. However, the photo-toxic effect of UV light for human cells and tissues and its potential carcinogenicity have been extensively studied (Yin et al., 2013). Considering that blue light wavelengths are closely related to UV radiation, it could be hypothesised a

possible damage induced by blue light to host cells and tissues. Studies conducted on the skin of healthy volunteers showed that blue light caused a transient pigmentation, as it happens after UV irradiation, but blue light does not cause DNA damage or early photo-ageing (Kleinpenning et al., 2010). Therefore, blue light is considered harmless and safer than UV irradiation until certain light doses (hundreds of J/cm^2) (Hu et al., 2018).

Interestingly, many studies suggested that no evidences of microbial resistance toward aBLT were found in *P. aeruginosa*, *A. baumanni*, and *C. albicans* after sublethal doses of blue light (Zhang et al., 2014, 2016; Amin et al., 2016). However, a certain degree of tolerance to aBLT was found in *S. aureus* (Rapacka-Zdonczyk et al., 2019).

The use of blue light as antimicrobial tool is not limited to medical care, but could also find interesting applications in agriculture, livestock, and industrial fields, for the treatment of plant and animal pathogens, and for disinfection purposes (Dai and Hamblin, 2017; Wang et al., 2017).

2. Aim of the research

Recently, two issues related to healthcare settings have made the management of clinical infections even more difficult: the arising of multi-resistant strains and the formation of microbial biofilms on tissues and/or clinical devices.

During the last years, light-based techniques have emerged as valid approach to face the spread of MDR strains and the infections caused by microbial biofilms. In particular, two strategies seem very promising:

- "Antimicrobial Photodynamic Therapy" (aPDT) based on the administration of specific drugs (photosensitizers - PSs) and their activation upon irradiation with visible light.
- "Antimicrobial Blue Light Therapy" (aBLT), where irradiation by blue light probably cause photo-oxidative stress by excitation of putative endogenous photoactive compounds that elicit an oxidative burst in microbial cells.

Until now, no standard procedures are available for biofilm studies, making difficult the comparison between each experimental approach. Moreover, in the field of antimicrobial photodynamic therapy, experimental procedures involve a notable number of variables, such as type of light source, fluence rate, PS concentration. Therefore, in this doctoral thesis we considered for the first time two classes of PSs that were compared in their photodynamic action, adopting the same procedures for biofilm inhibition and eradication. PSs belonging to the groups of porphyrins and borondipyrromethens (BODIPYs) were tested on three opportunistic pathogens: two bacterial species, *Pseudomonas aeruginosa* and *Staphylococcus aureus,* and the yeast *Candida albicans*. These microorganisms are included in the list of microbial species that raise concerns in clinical field, since they are involved in a substantial number of hospital-acquired infections and medical devices-associated infections, and increasing attention is focusing on them due to the arise of antimicrobial resistance. Upon the initial screening phase, PSs showing the best photodynamic performances were chosen to target the biofilm of microbial pathogens, which is the main cause of chronic infection and is very difficult to eradicate.

The second aim was to investigate the effect of blue light on *P. aeruginosa* biofilm. Therefore, investigations on *P. aeruginosa* biofilm and its main components were performed with different wavelengths of blue light (410 and 455 nm). Since *P.*

aeruginosa is frequently isolated in devices-associated infections, the potential of aBLT was also applied on catheters colonised by the biofilm of this pathogen.

In the following chapters, two paper drafts report the screening of porphyrins and BODIPYs on the chosen model microorganisms. Studies on blue light and its effects on the biofilm of *P. aeruginosa* are presented as a published paper, and additional data regarding blue light and medical devices are also reported. A schematic representation of the results is presented in Table 1.

Table 1. Scheme of the thesis contents.

Topic	**Published article/paper draft**
Antimicrobial Photodynamic Therapy	
Diaryl-porphyrins as photosensitizers	"A panel of diaryl-porphyrins in antimicrobial photodynamic therapy"
BODIPYs as photosensitizers	"New BODIPYs as photosensitizers in antimicrobial photodynamic therapy"
Antimicrobial Blue Light Therapy	
Targeting *Pseudomonas aeruginosa* biofilm	"Effect blue light at 410 and 455 nm on *Pseudomonas aeruginosa* biofilm"
Targeting *Pseudomonas aeruginosa* biofilm in medical devices	"Effect of blue light on *Pseudomonas aeruginosa* biofilms in central venous catheters"

3. Antimicrobial Photodynamic Therapy

A panel of diaryl-porphyrins in antimicrobial photodynamic therapy

Authors: Eleonora Martegani[1], Fabrizio Bolognese[1], Enrico Caruso[1] and Viviana Teresa Orlandi[1]*

[1]Departement of Biotechnologies and Life Sciences, University of Insubria, Varese, Italy

Abstract

Background. Antimicrobial photodynamic therapy (aPDT) has received great attention in recent years since it is an effective and promising modality for the treatment of human oral and skin infections with the advantage of bypassing pathogens' resistance to antimicrobials. Moreover, aPDT applications demonstrated a certain activity in inhibition and eradication of biofilms, overcoming the well-known tolerance of sessile communities to antimicrobial agents.

Aim. In this study, 13 diaryl-porphyrins (mono-, di-cationic, and non-ionic) were compared in their *in vitro* photo-inactivation efficacies against *Pseudomonas aeruginosa, Staphylococcus aureus* and *Candida albicans*. PDT was also applied as antibiofilm strategy, in preventing the formation of sessile communities and in detaching preformed ones.

Material and methods. In this study, viable count method and photo-spot test were used to compare the effect of PSs on suspended cultures. Crystal-violet staining and confocal analysis highlighted the anti-biofilm activity of porphyrins. ANOVA analysis highlighted the statistical significance of the obtained results.

Results. Among the chosen porphyrins, the dicationic porphyrin P11 was the best PS for *P. aeruginosa*, the non-ionic porphyrin P4 for *S. aureus*, and the monocationic P10 for *C. albicans*, respectively. In all the cases, diaryl-porphyrins were able to inhibit biofilm formation of these pathogens at higher concentrations than that used for suspended cultures. Furthermore, the photo-oxidative stress elicited by these porphyrins significantly impaired the viability of planktonic and adherent cell populations of 24-hour grown biofilms.

Conclusions. Diaryl-porphyrins confirmed their potential to be used as photo-activated antimicrobials to control the growth of bacteria and yeasts and prevent the biofilm formation.

1. Introduction

Photodynamic therapy firstly emerged as an alternative and promising anticancer therapy in the last century and is currently investigated for the treatment of malignant and non-malignant tumours. Only in the last decades of the XX^{th} century this approach was considered as a possible antimicrobial strategy to control the growth of pathogenic microorganisms (Allison and Moghissi, 2013). The photodynamic process is based on the simultaneous presence of three components: a light source, a photosensitive compound, and molecular oxygen. Reactive oxygen species (ROSs), such as hydroxyl radical ($OH^{\cdot}$), hydrogen peroxide (H_2O_2) or superoxide anion (O_2^{-}), and alternatively singlet oxygen ($^1O_2$) are released upon the photoexcitation of a photosensitizer (PS), with an appropriate wavelength of light. As a matter of fact, the antimicrobial effect of aPDT is driven by an oxidative stress that concerns cellular structures and macromolecules, including lipids, proteins, and nucleic acids, that lead to microbial cell death (St. Denis et al., 2011).

In the last decades, the scientific community is facing with the problem of antimicrobial resistance (AMR), that is the ability of microbial pathogens to escape from conventional antibiotic treatments. Therefore, adjuvant multitarget approaches to eradicate infections are urgently required (Jori et al., 2006; Roca et al., 2015). Since antimicrobial PDT is a non-antibiotic-based process, it could contribute to shine a new light among the adjuvant strategies used in clinical settings to treat microbial infections. Indeed, it represents a broad-spectrum multitarget approach with very limited, if any, chances for the development of resistant microorganisms (Maisch, 2015). Interestingly, it was observed that aPDT damages both antibiotic-sensitive and antibiotic-resistant strains of different microbial pathogens (Hamblin, 2016). In addition, very recent studies showed aPDT to be effective also on biofilms of bacterial and fungal origin (Pithan et al., 2016; Hsieh et al., 2018). A disinfection system based on photodynamic treatment could also be applied in other fields, such as in

environmental or industrial areas where light can be easily delivered to the contaminated region (Wainwright et al., 2017a).

Until now, many classes of photosensitizers have been taken into consideration for the inactivation of microbial pathogens, including both natural and synthetic compounds. One of the first classes of dyes used in PDT are porphyrins, consisting in fluorescent coloured pigments characterized by an aromatic tetra-pyrrolic ring (Wainwright, 1998). Interestingly, some porphyrin compounds have already been approved for their clinical use (Allison and Sibata, 2010).

The extensive electron delocalization on the macrocycle ring is responsible for porphyrins' intense absorption spectrum in visible region. The typical porphyrin spectrum is characterised by a higher absorption band around 420 nm, known as Soret band, and weaker bands between 600 and 800 nm (Q bands), making porphyrins suitable PSs to be activated by different light sources, including wide-spectrum emission lamps, sunlight, light-emitting diodes (LEDs) and lasers (Amos-Tautua et al., 2019). Along with this aspect, porphyrins have other advantages for therapeutic purposes, such as a low degree of toxicity in the dark, strong photosensitizing abilities, due to their long-lived triplet state, and notable yield of singlet oxygen production, making these compounds almost ideal photosensitizers (Malatesti et al., 2017). Further, the chemical synthesis of porphyrins is relatively simple and cost-efficient and generally involves the condensation of pyrroles with suitable aldehydes. The resulting tetra-pyrrolic ring is a versatile skeleton bearing different substituents in *meso*-positions, meaning that high number of combinations could lead to the production of different molecules with desired chemico-physical features (Amos-Tautua et al., 2019). In the case of anticancer PDT, specifical PS chemical features are known to affect the interaction with different tumoral cells, while not comparable information is currently available when targeting microbial cells.

Highly ionic compounds are unable to cross mammalian cell membranes, while Gram-negative bacteria are preferably photoinactivated by positively charged molecules that possibly interact with their negatively charged outer membrane (Dai et al., 2009). Moreover, hydrophobic/hydrophilic properties of porphyrins are known to affect the kinetics and the extent of binding to microbial cells (Jori et al., 2006).

Further, the ideal PS for anticancer PDT should absorb in the red region of the visible spectrum to better penetrate in the deeper tissues, while this feature is not strictly necessary for antimicrobial PDT for the treatment of superficial infections on skin or in the oral cavity. However, in odontostomatological field, infections could affect deeper tissues, as in the case of periodontitis, thus a light source with a wavelength between 600–650 nm is suitable for this application (Park et al., 2019).

In the work of Caruso et al., 5,15 *meso*-substituted diaryl-porphyrins were shown to be efficient PS in antitumoral PDT (Caruso et al., 2019b), while PDT antimicrobial activity was observed by Burda and co-workers (Burda et al., 2012) and by our group (Orlandi et al., 2013). In the present study, a panel of 13 diaryl-porphyrins were taken into consideration, having different degrees of amphiphilicity, molecular symmetry and characterised by non-ionic, monocationic or dicationic charge. Porphyrins activity was compared in the photoinactivation of clinically relevant nosocomial bacterial pathogens. In particular, *Pseudomonas aeruginosa* and *Staphylococcus aureus* were taken into consideration as representative models for Gram-negative and Gram-positive strains, respectively. They represent two of the six most life-threatening pathogens in clinical settings, recently named as “ESKAPE” pathogens, due to their ability to escape from antimicrobial treatments and immunity host response (Mulani et al., 2019). The yeast *Candida albicans* was also considered in the study as emerging pathogenic fungus associated with the majority of candidiasis. Diaryl-porphyrins were also tested for their ability to kill or disturb pathogenic microbes organised in highly structured biofilm communities. These microbial aggregations are frequently associated with the emergence of chronic infections as they often display high tolerance to conventional antimicrobial treatments.

2. Materials and methods

2.1 Photosensitizers

A panel of 13 diaryl-porphyrins used in this study is shown in table 1; P1 - P6 porphyrins are non-ionic molecules, P7 - P10 are characterized by monocationic charge and P11 – P13 by dicationic charge. PSs were synthetized as previously described (Orlandi et al., 2013; Caruso et al., 2019a, 2019b), and were dissolved in

DMSO at a concentration of 1 or 0,5 mM, as requested, and stored at 4°C until needed.

Table 1. List of diaryl-porphyrins (P1-P13) used in this study.

	PS	Chemical structure	Chemical denomination	Ref
Non-ionic (ø)	P1	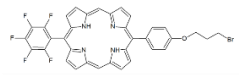	5-Pentafluorophenyl-15-[4-(4-Bromobutoxy)Phenyl]-21H,23H-porphyrin	(Caruso et al., 2019a)
	P2	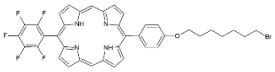	5- Pentafluorophenyl-15-[4-(8-Bromooctaoxy)Phenyl]-21H,23H-porphyrin	(Caruso et al., 2019a)
	P3	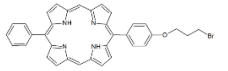	5-Phenyl-15-[4-(4-bromobutoxy)phenyl]-21H,23H-porphyrin	(Caruso et al., 2019b)
	P4	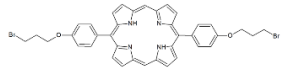	5,15-Di[4-(4-bromobutoxy)phenyl]-21H,23H-porphyrin	(Caruso et al., 2019b)
	P5	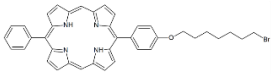	5-Phenyl-15-[4-(8-bromooctanoxy)phenyl]-21H,23H- porphyrin	(Caruso et al., 2019b)
	P6	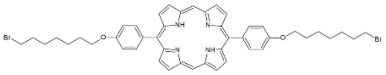	5,15-Di[4-(8-bromooctanoxy)phenyl]-21H,23H- porphyrin	(Caruso et al., 2019b)
Monocationic (+)	P7	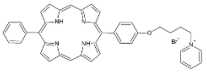	5-Phenyl-15-[4-(4-pyridinobutoxy)phenyl]-21H,23H-porphyrin	(Caruso et al., 2019b)
	P8	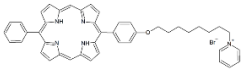	5-Phenyl-15-[4-(4-pyridinooctaoxy)phenyl]-21H,23H-porphyrin	(Caruso et al., 2019b)
	P9	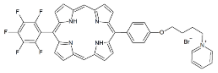	5-Pentafluorophenyl-15-[4-(4-Pyridinobutoxy)Phenyl]-21H,23H-porphyrin	(Caruso et al., 2019a)
	P10	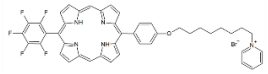	5-Pentafluorophenyl-15-[4-(4-Pyridinooctaoxy)Phenyl]-21H,23H-porphyrin	(Caruso et al., 2019a)
Dicationic (++)	P11	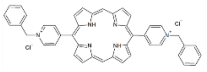	5,15-di(N-benzyl-4-pyridyl)porphyrin	(Orlandi et al., 2013)
	P12	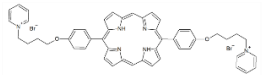	5,15-Di[4-(4-pyridinobutoxy)phenyl]-21H,23H-porphyrin	(Caruso et al., 2019b)
	P13	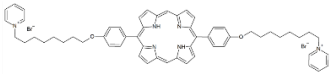	5,15-Di[4-(4-pyridinooctaoxy)phenyl]-21H,23H-porphyrin	(Caruso et al., 2019b)

2.2 Microbial strains and culture conditions

Three microbial species were used in this study: *Pseudomonas aeruginosa, Staphylococcus aureus* and the yeast *Candida albicans*. In table 2 the different strains of each species are listed. Clinical strains UR48 of *P. aeruginosa* derived from a patient with urinary tract catheter-associated infection (CAUTI), and strain BT1 by a cystic fibrosis (CF) patient. *C. albicans* clinical strains were recovered from patients with urinary tract infections.

P. aeruginosa was cultivated in Luria Bertani (LB) medium, *S. aureus* in Tryptic Soy Broth (TSB) medium, and *C. albicans* in YPD medium (Yeast extract 10 g/L, Peptone 20 g/L, and L-Dextrose 20 g/L). All strains where grown overnight in liquid media at 37°C on an orbital shaker at 200 rpm, or in solid media (15 g/L agar) at 37°C.

Table 2. List of bacterial and fungal strains used in this study.

Microbial strains	Ref
Pseudomonas aeruginosa	
PAO1	(Stover et al., 2000)
PAO1_pVOGFP	(Orlandi et al., 2018a)
UR48 (clinical strain)	(Orlandi et al., 2011)
BT1 (clinical strain)	(Bragonzi et al., 2006)
Staphylococcus aureus	
ATCC 6538P (MSSA)	
ATCC 43300 (MRSA)	
Candida albicans	
ATCC 14053	
Ca1 (clinical strain)	(Orlandi et al., 2020)
Ca2 (clinical strain)	(Orlandi et al., 2020)

2.3 Light source

The lighting unit device (LULab) is equipped with a head composed by 25 high power LEDs with maximum emission peak at 410 nm blue light, suitable for the

activation of porphyrins (figure 1) and allows the uniform irradiation of a square area of 75 mm X 75 mm. The system is powered by a specific PC based control system, which allows the setting of irradiation time and irradiance values for a precise evaluation of the radiation fluence rate.

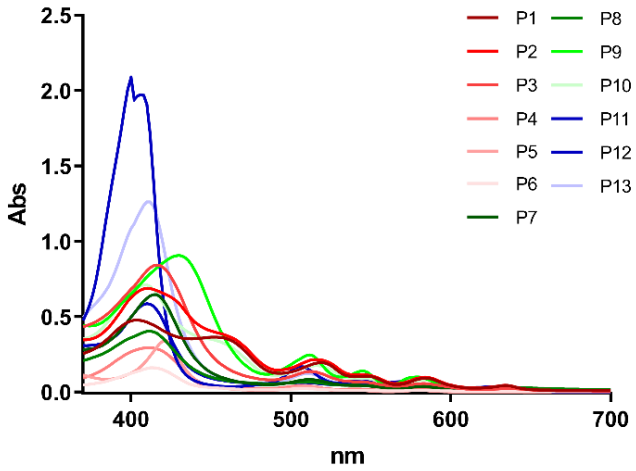

Figure 1. Visible light absorption spectra of diaryl-porphyrins (P1-P13).

The power density of light was kept at 100 mW/cm^2 for all the experimental procedures, while the irradiation time, specified for each protocol, was modified in accordance with the desired final light dose, as presented in table 3.

Table 3. List of light doses employed in this study and the corresponding irradiation time.

Light dose (J/cm^2)	**Irradiation time (s)**
20	200
30	300
40	400
150	1500

2.4 PDT assays

Photo-spot test

The photo-spot test, previously optimized for *P. aeruginosa* and *C. albicans* (Orlandi et al., 2018b, 2020), was adapted also to *S. aureus* as follows. In the case of bacteria,

P. aeruginosa PAO1 and *S. aureus* ATCC6538P were grown overnight, and the cultures were 10-fold serially diluted from ~10^9 to ~10^4 CFU/mL in 96-well plates, in phosphate buffer saline (PBS - KH_2PO_4/K_2HPO_4 10 mM, pH 7.4). Whereas *C. albicans* ATCC14053 overnight culture was centrifuged (5000 x g for 10 min) and the pellet were suspended in 1/10 volume of sterile PBS to a cellular concentration of ~10^8 colony forming unit per millilitre (CFU/mL). Serial 10-fold dilutions were performed in sterile PBS from ~10^8 to ~10^3 CFU/mL.

PSs (10 µM final concentration) were administered to diluted and undiluted samples of bacterial and fungal strains. Untreated samples and DMSO treated samples were included as controls. The final concentration of DMSO control is in accordance with both the stock solution of each PS and the amount of administered PS in each sample. Plates were incubated in the dark to avoid undesired photoactivation of PSs and to permit the interaction between cells and porphyrins. After 10 min, 1 h or 6 h of dark incubation, respectively, volumes of ~ 5 µl of each sample was replica plated on nutrient agar to obtain proportionally spots of decreasing cell density (bacterial strains from ~ 10^7 to ~10^2 CFU/spot; yeast strain from ~ 10^6 to ~10 CFU/spot). A series of plates was irradiated under 410 nm blue light to activate porphyrins. To prevent a possible intrinsic toxicity of blue light alone, the chosen light doses were 20 J/cm^2 for *P. aeruginosa* and *S. aureus*, and 75 J/cm^2 for *C. albicans*, based on preliminary experiments by irradiation at increasing light doses of blue light (data not shown). The LULab system was set at fluence rate of 100 mW/cm^2, and the variation of the irradiation time (200 and 750 s, respectively) permitted to reach the desired light doses. Unirradiated plates were included as a control for the evaluation of potential intrinsic toxicity of porphyrins. After incubation at 37°C, results were recorded as the Log of the maximal cell number at which growth was prevented (a value of 1 would stay for absence of growth for the spot with 10 CFU, a value of 2 for absence of the spot corresponding to 100 CFU etc.). Therefore, a higher Log unit reduction was associated to higher antimicrobial activity. Photo-spot tests were performed at least in triplicate for each strain and each PS, and average data, expressed as Log unit reduction of total cell number, were summarized in tables.

PDT on suspended cells

Upon overnight growth of microbial strains (*P. aeruginosa* PAO1, *S. aureus* ATCC6538P, and *C. albicans* ATCC14053), cells were 1:10 diluted in sterile deionized water, to reach approximate concentrations of 10^8 or 10^6 CFU/mL for bacterial and fungal strains, respectively. Photoinactivation of cells were performed in 12-well plates, each well containing 1 ml of cell suspension and 10 μM porphyrins were added to the samples. Untreated cells, DMSO-treated cells and corresponding dark controls were also included. Samples were irradiated at 20 or 150 J/cm^2 (100 mW/cm^2 for 200 and 1500 s intervals, respectively) for bacterial and fungal cells, respectively. Soon after irradiation, the number of viable cells was evaluated. Briefly, an aliquot of each sample was 10-fold serially diluted and 10 μL of each diluted and undiluted sample were plated. After overnight incubation at 37°C, the colony count was performed, and the corresponding cellular concentration (CFU/mL) was calculated. PDT experiments were performed at least in triplicate for each strain and each PS compound.

2.5 Antibiofilm photodynamic treatment

The effect of diaryl-porphyrins was evaluated on biofilms of *P. aeruginosa, S. aureus* and *C. albicans*, both as inhibition of biofilm formation, and in eradicating mature biofilms. In biofilm inhibition experiments, we evaluated if photodynamic treatment impairs the ability of suspended cells to form the adherent community. In this case, cells were treated with the PS and, upon 1 h of dark incubation at 37°C, irradiated by blue light and subsequently incubated at 37°C for 24 hours. On the other hand, in biofilm eradication experiments, we evaluated the effect of PDT on destroying mature biofilms. Herein, 24-hour mature biofilms were treated with the PS, avoiding any modification of the biofilm environment, except for porphyrin administration, and then, upon 1 hour of dark incubation, irradiated by blue light. In experimental setups, a panel of control biofilm samples were prepared: +PS -light, -PS +light, and -PS -light. In addition, dark and irradiated controls with only DMSO solvent were included in each experiment.

Biofilm preparation and PDT experimental parameters employed for the inactivation of each pathogen are here reported. Biofilms of *P. aeruginosa* PAO1 and clinical strains UR48 and BT1 were obtained in 12-well plates upon 24 h of growth at 37°C in M9 minimal medium added with glucose (10 mM) and casamino acids (0,2% V/V). Overnight inoculum of *P. aeruginosa* was diluted 1:500 in fresh medium, reaching a concentration of about 10^7 CFU/mL. Porphyrins were administered at a final concentration of 30 μM during biofilm inhibition and eradication, and PDT experiments were performed with 410 nm blue light radiation, with a final dose of 30 J/cm^2 (100 mW/cm^2, 300 s).

The same culture conditions used for *P. aeruginosa* were employed for *S. aureus* ATCC6538P and ATCC43300 biofilms. It this case, porphyrins were administered at a concentration of 20 and 30 μM for biofilm inhibition and biofilm eradication, respectively. In each experiment, blue light was used at a final light dose of 40 J/cm^2 (100 mW/cm^2, 400 s).

PDT experiments on the yeast *C. albicans* were performed on ATCC14053 strain and on clinical isolates Ca1 and Ca2 strains to assay biofilm inhibition. Yeast cells from overnight cultures were centrifuged at 5000 X g for 10 min and pellets were 100-fold diluted in sterile deionized water, and a volume of 250 μL was dispensed in 24-well plates. Cells were incubated 1 h in the dark at 37°C with porphyrins (20 μM final concentration), irradiated with 410 nm light (150 J/cm^2 keeping 100 mW/cm^2 for 1500 s). Subsequently, 250 μL of YPD medium were added to each well and plates were incubated at 37°C for 24 h, to allow biofilm formation. *C. albicans* ATCC14053 was submitted to the protocol of biofilm eradication as follows. YPD overnight cultures were 100-fold diluted in fresh YPD. 500 μL of cell suspensions were added to 24-well plates and incubated at 37°C for biofilm growth. Upon 24 hours, planktonic population was removed from each well, to avoid any possible interference of YPD components in PDT treatment. Each well was filled with fresh PBS and porphyrins administered at a final concentration of 40 μM. Upon 1 h of dark incubation at 37°C, samples were irradiated (150 J/cm^2 keeping 100 mW/cm^2 for 1500 s) or dark incubated for the same time. After PDT, biofilms were analysed as detailed in the next paragraph.

In microbial biofilm, two different populations can be distinguished: the planktonic population, which refers to free-floating microbial cells, and the adherent or sessile population, which includes all cells embedded in the extracellular matrix of biofilm, as presented in scheme 1. Moreover, we can refer to the total adherent biomass as the whole of cells and the extracellular matrix.

The detection of adherent biomass was made by staining with crystal violet solution (0,1% W/V for 20 min) upon the removal of planktonic phase and a gentle wash with PBS. Cell viability of planktonic (CFU/mL) and adherent (CFU/well) phases was calculated by the colony count method previously reported. Planktonic population was collected from the supernatant, while adherent population were scraped and resuspended in 1 mL of PBS upon removal of planktonic phase and a single wash with sterile1X PBS.

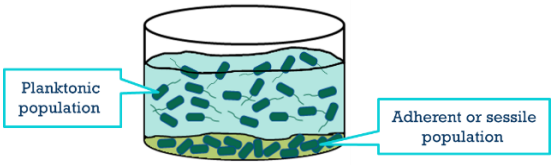

Scheme 1. Schematic representation of a well containing biofilm adherent and planktonic populations.

2.6 Confocal microscopy analyses

P. aeruginosa

Antibiofilm activity of porphyrins on Pseudomonas aeruginosa PAO1 was analysed using PAO1_pVOGFP recombinant strain, in which GFP fluorescent protein is expressed under the control of pBAD arabinose inducible promoter (Orlandi et al., 2018a). PDT protocols of biofilm inhibition and eradication previously described, were applied to PAO1_pVOGFP biofilm. Coverslip glasses positioned in 35 mm Petri dishes, were used as supports for biofilm adhesion and visualization by confocal microscope analysis. Upon photodynamic treatment and biofilm growth, supernatant was removed from the plates and GFP expression was induced for 1 h at 37°C, by the addition of fresh medium containing arabinose 0,1% W/V. Finally, the coverslip was placed on a microscope glass slide for the acquisition of the adherent biofilm images. All microscopic image acquisitions were performed on a Leica TCS SP5 confocal

laser scanning microscope (CLSM; Leica Microsystems, Wetzlar, Germany) equipped for GFP visualization (excitation laser at 488 nm). Images were obtained using a 63X objective lens. When requested, 3X image magnifications were recorded. Simulated 3D images of *P. aeruginosa* biofilm were generated using the free open-source software ImageJ (National Institute of Health, USA).

C. albicans

Yeast cells were visualised by confocal microscopy upon PDT treatment with diaryl-porphyrins in suspension. *C. albicans* ATCC14053 was submitted to PDT protocol explained in paragraph 2.4, and soon after photo-treatment, samples were collected for microscopy analyses as follows. Three replicates of each sample were centrifuged (10000 X g, 5 min) and pellets were pooled and resuspended in 1X sterile PBS. A fluorescent boron-dipyrromethene dye (BODIPY 4,4-difluoro-1,3,5,7-tetramethyl-8-(2-methoxyphenyl)-4-bora-3a,4a-diaza-s-indacene) was added to the suspension (2 µM final concentration) (Sunahara et al., 2007), and cells were incubated with the fluorochrome for 30 min at 37°C on a shaker at 50 rpm. Samples were centrifuged 10000 X g for 10 min and pellets were suspended in 20 µL of 1X PBS. 10 µL of cell suspension were analysed by CLSM using a 63X objective lens (excitation with 488 nm laser) and 5X magnification; editing was performed with the free open-source programme ImageJ. To assess the efficacy of the photodynamic treatment, the cell viability was checked trough viable count technique as previously described.

2.7 Photosensitizer binding assay

All the photosensitizers were tested for their ability to bind bacterial and yeast cells. Upon overnight growth of microbial strains (*P. aeruginosa* PAO1, *S. aureus* ATCC6538P, *C. albicans* ATCC14053), aliquots of each strain were centrifuged at 5000 X g for 10 minutes, and the supernatants were removed. Pellets were resuspended and 10-fold diluted in sterile deionized water. Porphyrins (10 µM for *S. aureus*; 30 µM for *P. aeruginosa* and *C. albicans*) were added to the cells and samples were incubated for 1h at 37°C in the dark. Untreated cells, PSs treated cells, and cells added with DMSO 4% (V/V) were included as controls. To exclude possible toxicity

of PSs, cell viability was assessed for all the samples upon dark incubation by the previously explained colony count method. After dark incubation, samples were centrifuged (10000 X g for 5 min) and the visible spectra of the supernatants were recorded (k = 380 – 700 nm). A calibration plot (μM *vs* OD_x) was obtained for each PS. The amount of PS not bound to bacterial or yeast cells were inferred interpolating the data on the calibration plot. Experimental values were reported as percentage of each PSs bound to *P. aeruginosa, S. aureus* and *C. albicans* cells. The experiments were performed in triplicate.

In table 4, a summary of diaryl-porphyrin concentrations and light doses employed for each microbial strain and each experimental procedure – photo-spot test, binding assay, PDT on suspended cells, biofilm inhibition and biofilm eradication – is illustrated.

Table 4. Summary of diaryl-porphyrins concentration and light doses of blue light employed in this study for each type of experiment.

[PS] (μM) Light dose (J/cm²)	**Photo-spot test**	**Binding assay**	**PDT on suspended cells**	**Biofilm inhibition**	**Biofilm eradication**
P. aeruginosa	10 μM 20 J/cm²	30 μM	10 μM 20 J/cm²	30 μM 30 J/cm²	30 μM 30 J/cm²
S. aureus	10 μM 20 J/cm²	10 μM	10 μM 20 J/cm²	20 μM 40 J/cm²	30 μM 40 J/cm²
C. albicans	10 μM 20 J/cm²	30 μM	10 μM 150 J/cm²	20 μM 150 J/cm²	40 μM 150 J/cm²

2.8 Statistical analyses

Photoinactivation experiments on suspended cells and biofilm formation by each microbial strain were performed at least three times with independent cultures, and statistical analyses were assessed by one-way ANOVA.

3. Results

3.1 Effect of diaryl-porphyrins on microbial cells viability

A group of novel diaryl-porphyrins, previously synthetized by our group, was considered as possible photosensitizers in antimicrobial PDT. Diaryl-porphyrins (P1-

P13) are characterised by two appendages in *meso*-positions of the tetrapyrrole core, featuring a phenyl group or a pyridyl group with different substituents, resulting in symmetrical or asymmetrical molecules. The pyridyl ring bears N-benzyl groups, while the phenyl ring could bear five hydrogen atoms or five fluorine atom or could be featured by alkyl chains (C4 or C8) with bromine atom or pyridine group on the farthest carbon atom. These molecules were grouped in non-ionic (Ø), monocationic (+) and dicationic (++) PSs according to their charge and investigated for the photoinactivation of three microbial pathogens: *P, aeruginosa, S. aureus* and the yeast *C. albicans*.

Since negligible intrinsic toxicity is required for an ideal PS, the effect of diaryl-porphyrins on each microbial species was investigated. The effect of DMSO solvent was also included as a control. The spot-test method allowed to test the same PS concentration (10 μM) at decreasing cell concentrations for bacteria and yeasts and cell viability was detected upon 10 minutes, 1 and 6 hours after dark incubation (figure 2).

The Gram-negative bacterium *P. aeruginosa* was almost insensitive to non-ionic and monocationic porphyrins after 6h incubation, while a certain degree of toxicity was observed for two dicationic PSs. Upon 6 hours of incubation, P12 and P13 showed an antimicrobial effect up to of 3.5 and 1.5 Log_{10} units, respectively.

Diaryl-porphyrins had similar effects on the Gram-positive bacterium *S. aureus*, where a negligible effect was observed for non-ionic and monocationic porphyrins. Nevertheless, all dicationic molecules showed intrinsic toxicity, inhibiting the growth of a population of 10^4 CFU/spot for P11 and P13, and a population of 10^5 CFU/spot for P12.

C. albicans cells showed no basal sensitivity to the non-ionic porphyrins even at the longest dark incubation time. The two monocationic molecules P7 and P8 showed a low degree of toxicity, causing the depletion of the samples with the lowest cellular densities (10 and 10^2 CFU/spot). As reported for bacterial cells, dicationic PS were the most intrinsically toxic molecules for yeast cells, with P12 molecule preventing the growth of 10^4 CFU/spot after 6 h of incubation in the dark.

		P. aeruginosa				*S. aureus*				*C. albicans*			
PS [10 μM]		Log_{10} reduction			Spot test images (6 h incubation)	Log_{10} reduction			Spot test images (6 h incubation)	Log_{10} reduction			Spot test images (6 h incubation)
Incubation time		10′	1 h	6 h	CFU/spot	10′	1 h	6 h	CFU/spot	10′	1 h	6 h	CFU/spot
Untreated		0	0	0		0	0	0		0	0	0	
Solvent ctrl		0	0	0		0	0	0		0	0	0	
ø	P1	0	0	0		0	0	0		0	0	1	
	P2	0	0	0		0	0	0		0	0	0	
	P3	0	0	0		0	0	0		0	0	0	
	P4	0	0	0		0	0	0		0	0	0	
	P5	0	0	0		0	0	0		0	0	0	
	P6	0	0	0		0	0	0		0	0	0	
+	P7	0	0	0		0	0	0.6		0	0.3	2	
	P8	0	0	0		0	0	0		0	0	0.7	
	P9	0	0	0		0	0	0		0	0	0	
	P10	0	0	0		0	0	0		0	0	0	
++	P11	0	0	0		0	2.5	4		0	0	0.3	
	P12	1.5	2	3.5		5	5	5		0.3	2.7	4	
	P13	1	1.5	1.5		0	3.5	4		0	0.3	2.3	

Figure 2. Analysis of intrinsic toxicity of diaryl-porphyrins (P1-P13) administered at a concentration of 10 μM to *P. aeruginosa* PAO1, *S. aureus* ATCC6538P and *C. albicans* ATCC14053 cells, upon 10 min, 1 and 6 hours of dark incubation. Log_{10} reduction values represent the mean of at least three independent experiments. Experimental images reported in the last column of each strain, refer to 6h of dark incubation.

As the optimal interaction between microbial cells and PSs seems to be a crucial step during the photodynamic process, the binding of porphyrins was investigated to test microbial cells after 1 hour of incubation (see figure 3 for details).

Non-ionic diaryl-porphyrins (P1-P6) showed a very low affinity for *P. aeruginosa* cells (less than 10% of binding yield), and same results were obtained for the yeast *C. albicans*. Non-ionic PSs showed a slightly better affinity for the Gram-positive bacterium *S. aureus*, with porphyrin P6 reaching a 40% interaction value (percentage of PS bound to cells). The other not charged porphyrins bound *S. aureus* cells with affinity values ranging from 12 to 28%.

Interestingly, positively charged compounds (P7-P13) were able to interact with Gram-negative, Gram-positive bacteria and yeast cells, independently from the number of charges carried by each PS. Binding yields over 65% were observed in all the strains, and, in some cases, cationic molecules reach almost 100% of binding yield (P7, P9, P10 for *P. aeruginosa*, P10, P12 for *S. aureus*, P9, P10 for *C. albicans*).

In the chosen experimental conditions, non-ionic diaryl-porphyrins showed a general low binding affinity for bacteria and yeasts, while mono- and dicationic PSs reached very high percentages of binding.

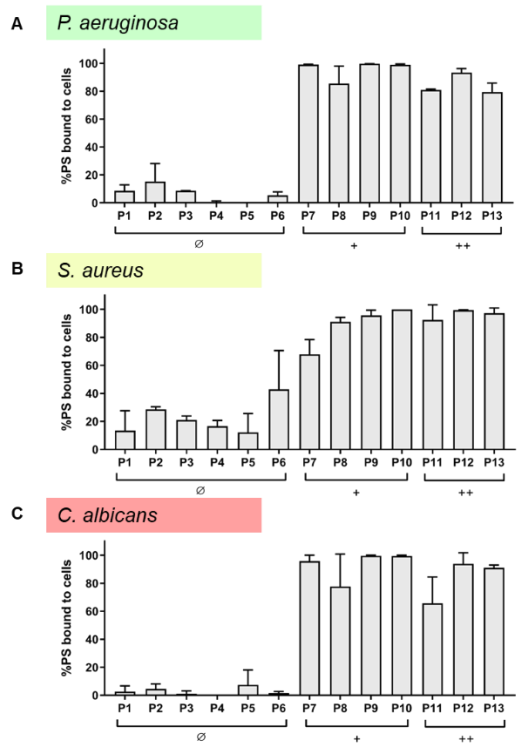

Figure 3. Binding assay of diaryl-porphyrins (P1-P13) on *P. aeruginosa* PAO1 (A), *S. aureus* ATCC6538P (B) and *C. albicans* ATCC14053 (C) cells. Values are presented as a percentage of PS bound to cells upon 1 h of dark incubation. The non-ionic (Ø), monocationic (+), and dicationic (++) porphyrins were administered at a concentration of 30 µM for *P. aeruginosa* and *C. albicans*, and 10 µM for *S. aureus*, respectively.

3.2 Photodynamic activity of diaryl-porphyrins

Diaryl-porphyrins were further investigated for their antimicrobial potential against *P. aeruginosa, S. aureus* and *C. albicans* cells upon photo-activation. Intrinsically toxic PSs (more than 1 Log_{10} reduction of cell viability after incubation in the dark) were excluded from further analyses. A source of blue light at 410 nm was chosen for the activation of diaryl-porphyrins. Since blue light showed an intrinsic antimicrobial effect against different microorganisms, evaluations of light

toxicity at 410 nm were performed on bacteria and yeast cells through the photo-spot test assay. No toxic effect was observed upon irradiation of the strains with 20 J/cm^2 (Figure 4), therefore this light dose was chosen to activate diaryl-porphyrins. Irradiation was performed after 1 h of dark incubation of cells and PSs.

The administration of non-ionic porphyrins to *P. aeruginosa* did not have any effect on cell viability upon activation by blue light, neither at the lowest cell concentration (10^2 CFU/spot) (figure 4A). Activity of P1-P6 was also analyzed with three-fold PS concentration (30 μM), but similar results were obtained, and no antimicrobial effect was observed (data not shown). Among monocationic PSs (10 μM final concentration), only porphyrin P7 caused a Log_{10} reduction of 2.5. The highest activity against *P. aeruginosa* was displayed by the dicationic molecule P11 that showed antimicrobial activity up to 10^5 CFU/spot.

S. aureus seemed to be more sensitive to diaryl-porphyrin-mediated PDT, if compared to the Gram-negative bacterium *P. aeruginosa*. The non-ionic compound P4 caused a clear reduction in cell viability of samples at 10^6 cells/spot, and P8, P9, P10 cationic molecules were able to inactivate samples of bacteria with a density of 10^5 cells/spot. P7 porphyrin showed the best killing rate in the chosen experimental setup with 6.6 Log units reduction (figure 4B).

The yeast *C. albicans* was insensitive to photoinactivation with non-ionic porphyrins (P1, P2, P5 and P6), but a slight antimicrobial activity was found for P3 and P4 with a Log_{10} decrease of 0.5 and 2.5, respectively. Cationic porphyrins were more active on yeast cells, compared to non-ionic ones: P9 - P11 showed an antimycotic activity on populations of 10^4 CFU/spot (figure 4C).

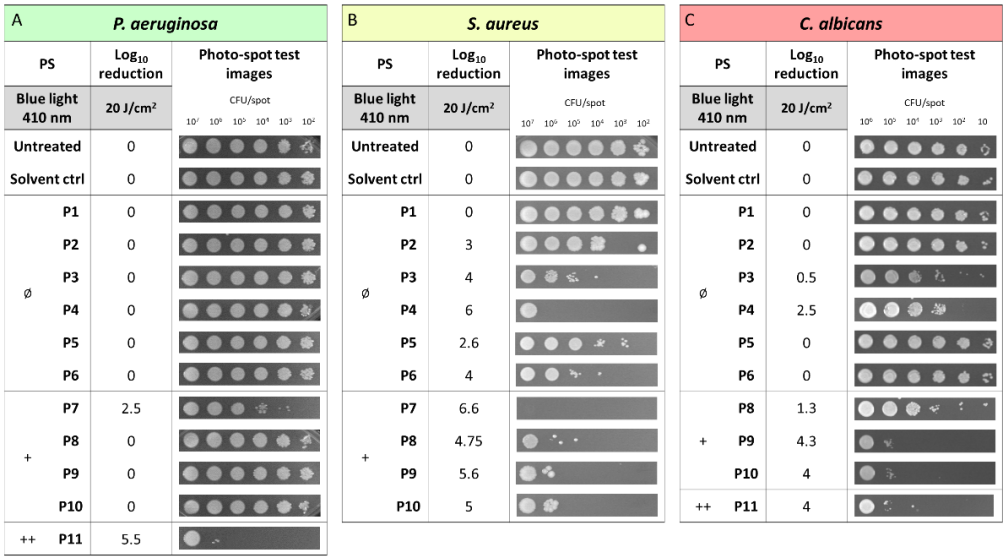

Figure 4. Photodynamic activity of diaryl-porphyrins on *P. aeruginosa* PAO1 (A), *S. aureus* ATCC6538P (B) and *C. albicans* ATCC14053 (C) cells evaluated by the photo-spot test. The non-ionic (Ø), monocationic (+), and dicationic (++) porphyrins were administered at a final concentration of 10 µM. Untreated and solvent-treated samples were also included as controls. Values of Log_{10} reduction were observed after irradiation with 410 nm blue light at radiant exposures of 20 J/cm^2, after 1 h of dark incubation of cells and PS. Data are the mean of at least three independent experiments. Representative experimental results are illustrated in the last columns.

Further investigations on the photodynamic effect of diaryl-porphyrins were performed on suspended cultures of *P. aeruginosa, S. aureus* and *C. albicans*. The preliminary screening ruled out porphyrins with intrinsic toxicity and a low photoactivity for each pathogen. Thus, only porphyrins that showed a strong photoinactivation rate (≥3 and ≥2 Log unit reduction for bacteria and yeasts, respectively) were used in further trials. Experimental conditions were properly designed for each microbial strain according to blue light susceptibility and PS concentrations.

P. aeruginosa resulted as the most tolerant microorganism to photoinactivation by diaryl-porphyrins, and only one dicationic compound (P11) showed significant activity on this pathogen. P11 (10 µM final concentration) was activated by 20 J/cm^2 radiance of 410 nm blue light, that was non-toxic for PAO1 cells. Accordingly, the solvent did not show any toxicity both in the dark and upon irradiation (figure 5A). The administration of P11 and blue light caused a decrease of more than 4 Log units,

reaching 10^4 CFU/mL upon PDT treatment, and no dark toxicity of the PS was observed.

The Gram-positive bacterium *S. aureus* was treated with both non-ionic (P2-P6) and monocationic porphyrins (P7-P10) (10 μM final concentration) and blue light was delivered at 20 J/cm^2 (figure 5B). Non-ionic compounds were non-toxic in dark conditions, while upon irradiation they caused significant reductions in *S. aureus*: P2 and P6 caused a reduction of 2 Log unit in cell viability, while P3 and P4 showed the best PDT effect, causing 5 and 6 Log unit reduction, respectively, reaching the detection limit of the system (10^2 CFU/mL). The two monocationic PSs P7 and P9 showed intrinsic toxicity in the dark and were discarded from further analyses. Upon irradiation, P8 and P10 caused a decrease of 2 and 3 Log units, respectively. From this preliminary screening, non-ionic diaryl-porphyrins P3 and P4 showed the best PDT activity and were further assayed against *S. aureus* biofilms.

C. albicans PDT treatment was performed with 150 J/cm^2 blue light, that did not affect the viability of untreated or 2% DMSO-treated yeast cells in the chosen experimental conditions (Figure 5C). Both non-ionic and positively charged porphyrins (P4, P9, P10 and P11) significantly reduced the yeast viability up to the detection limit of the system (10 CFU/mL), showing a very high inactivation rate.

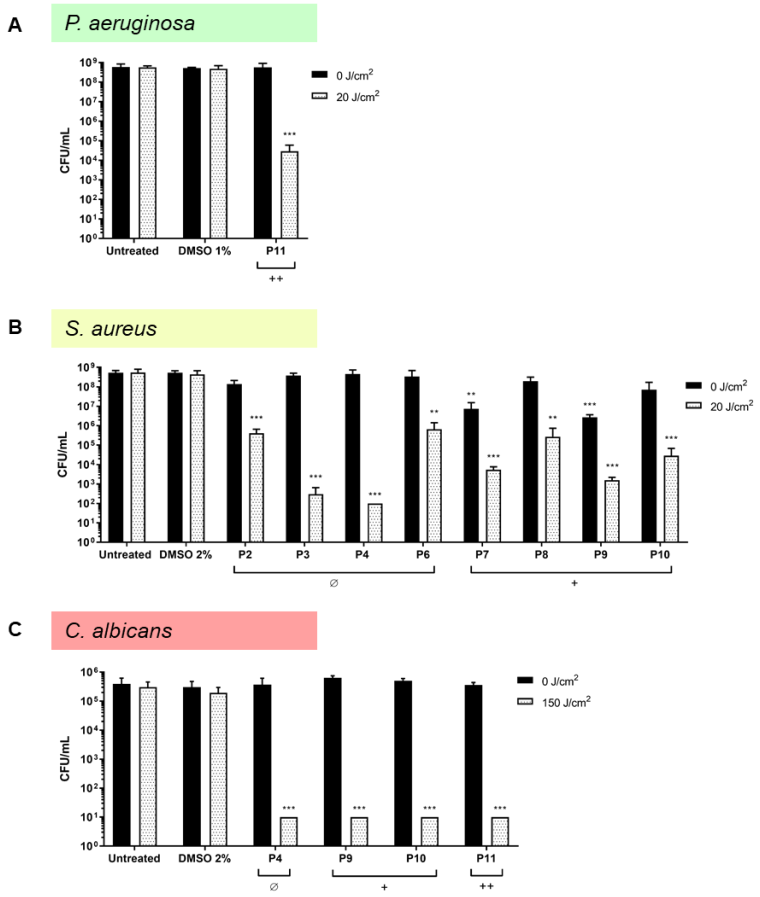

Figure 5. Photodynamic inactivation of *P. aeruginosa* PAO1 (A), *S. aureus* ATCC6538P (B) and *C. albicans* ATCC14053 (C) cells in suspension by diaryl-porphyrins. PS concentration was 10 µM for all the strains, and blue light was delivered as follow: 20 J/cm^2 for bacteria and 150 J/cm^2 for *C. albicans*. Control samples in the dark are presented as black bars, and irradiated samples with dotted bars. Untreated and solvent-treated samples (DMSO) were also included for each pathogen. Values, presented as CFU/mL, are the mean of at least three independent experiments, and the bars represent standard deviations. Statistical analyses were performed by one-way ANOVA (*p < 0.05; **p < 0.01; *** p <0.0001).

To highlight possible more subtle effects of the photodynamic treatment on *C. albicans,* cell morphology of PDT-treated cells was analysed by confocal laser scanning microscopy, using the BODIPY (4,4-difluoro-1,3,5,7-tetramethyl-8-(2-methoxyphenyl)-4-bora-3a,4a-diaza-s-indacene) as a fluorescent tracer (figure 6). *C. albicans* cells showed the typical compartmentalization of eukaryotic cells, with the biggest compartment, compatible with the nucleus, appearing dark and not permeable to the fluorophore. A diffuse fluorescence signal characterized a small but constant

percentage of the cells, where no organelle was clearly identified, a feature that could be explained as a result of non-viability of the cells. The DMSO-treated yeasts kept in the dark were comparable to untreated ones. The dark incubation of non-ionic and monocationic diaryl-porphyrins did not alter the yeast cell architecture compared to the controls (Figure 6e, g, i), except for porphyrin P11. In this sample, a different fluorophore distribution was observed: no organelles were recognizable, and BODIPY was accumulated especially in a central region of the cytoplasm (Figure 6m) still no differences in cellular viability were observed compared to control samples (DMSO and untreated cells). Importantly, no morphological changes could be observed after blue light irradiated samples (Figure 6b) and DMSO-treated samples (Figure 6d). On the other hand, blue light irradiation (150 J/cm^2) in the presence of the non-ionic porphyrin P4 caused an important alteration of yeast cellular structure. As detailed in figure 6f, cell dimensions greatly decreased compared to the dark controls, fluorescent signal was foggy, and the compartmentalization was not so clear as in the corresponding controls. The photoactivation with cationic porphyrins P9 and P10 caused a complete loss of organelle identity, and BODIPY radiated a very bright fluorescent signal. Furthermore, the cellular morphology passed from spherical to an egg-shaped one (Figure 6h, l). A similar impairment of the cell architecture was observed upon irradiation of porphyrin P11 (Figure 6n).

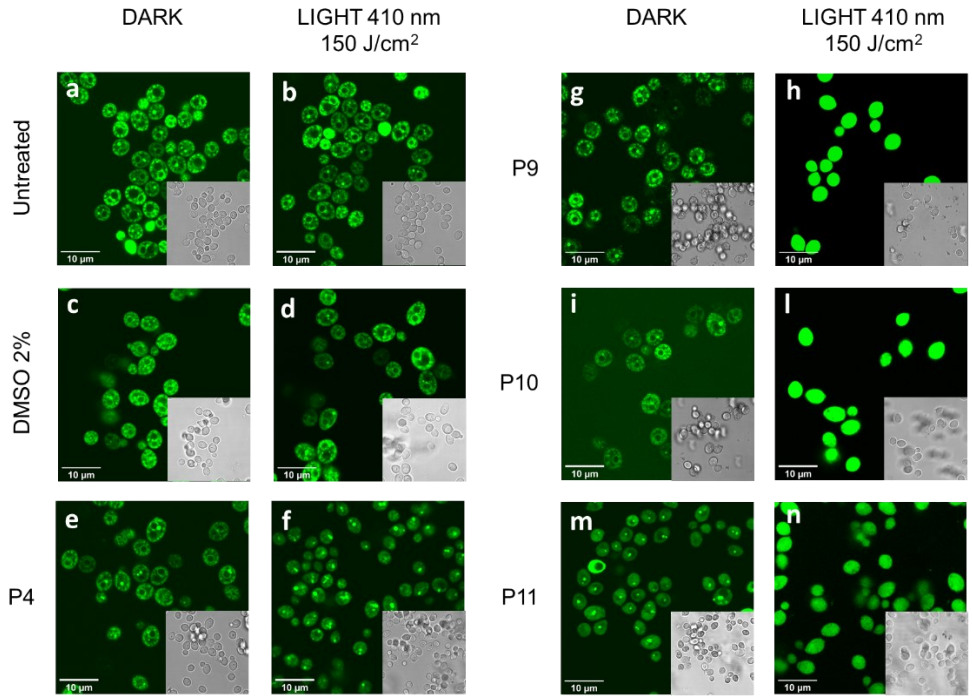

Figure 6. Confocal microscopy analyses of *C. albicans* ATCC14053 cells upon photodynamic treatment with diaryl-porphyrins P4, P9, P10 and P11 (10 µM) activated by blue light (150 J/cm^2). Samples untreated and treated with 2% DMSO are also included. Dark incubated samples are presented in Panels (a), (c), (e), (g), (i), and (m), while light-treated samples are presented in panels (b), (d), (f), (h), (l), and (n). Scale bar = 10 µm.

3.3 Porphyrin-mediated photodynamic treatment of *P. aeruginosa* biofilm

The ability to form structured communities, both on inert surfaces and biological tissues, renders microbial pathogens particularly tolerant to conventional antibiotic therapies. Thus, the potential of PDT in inhibiting and/or eradicating biofilms is a promising strategy to contrast infections. In this work, the potential of diaryl-porphyrins on the biofilm of *P. aeruginosa* was evaluated. For this purpose, the assay was limited to compounds P11, which showed the best results among the tested diaryl-porphyrins against PAO1 strain. In addition to the wild-type, two clinical strains (UR48 and BT1) were included in the study. *P. aeruginosa* UR48 derives from a patient with catheter-associated urinary tract infections (CAUTI), while BT1 strain from the sputum of a cystic fibrosis (CF) patient.

The potential of P11 in inhibiting the biofilm formation of *P. aeruginosa* was firstly evaluate (figure 7). The total biofilm biomass was spectrophotometrically evaluated at OD590 upon crystal violet staining. This parameter is influenced by both matrix and cellular components and its value was around 7, 12 and 27 for PAO1, UR48 and BT1 dark control samples, respectively (figure 7A,D,G). Nevertheless, since comparable cell densities were measured in dark controls of planktonic and adherent populations for all the strains, it seems that UR48 and BT1 are able to produce higher amount of biofilm matrix compared to the wild-type strain PAO1. In the case of PAO1 and UR48, the administration of DMSO solvent caused a notable increase in the biofilm total biomass, but no changes in adherent and planktonic cell concentrations were observed, suggesting that DMSO could stimulate biofilm matrix production. In all the strains, blue light radiation did not cause any toxicity in control samples (untreated and DMSO-treated samples), as witnessed by both OD590 value and cell viability assay of the two subpopulations. The treatment of *P. aeruginosa* PAO1 cells with porphyrin P11 showed no toxicity in the dark, but a significant decrease in adherent biomass production was observed upon irradiation, with inherent decrease of OD590 absorbance value from ~27 to ~1. The antibiofilm effect was confirmed by cell viability assays of planktonic and adherent phases, where values of treated cultures were significantly lower than those of the control samples, reaching the lower detection limit of the system (10^2 CFU/mL or CFU/well). The same effect of P11-mediated PDT was observed in inhibiting the biofilm formation of clinical strains UR48 and BT1, where biomass decreases of about 95%, and cell population-densities were greatly lowered (figure 7D-I).

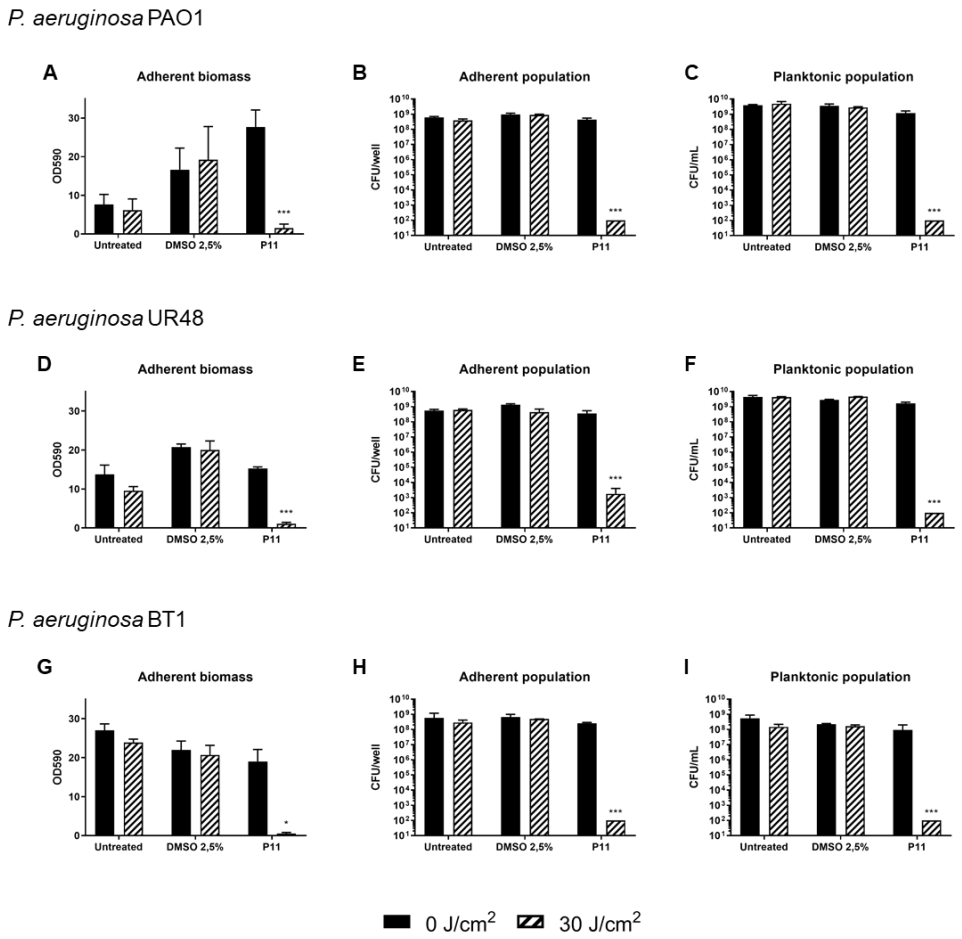

Figure 7. Inhibition of biofilm formation of *P. aeruginosa* PAO1 (A,B,C), UR48 (D,E,F) and BT1 (G,H,I) upon photodynamic treatment with diaryl-porphyrins. Porphyrin P11 was activated by 410 nm blue light radiation at 30 J/cm^2. The graphs report values of the absorbance at 590 nm (OD 590) of biofilm staining with crystal violet (A,D,G), values of adherent population viability (CFU/well) (B,E,H), and planktonic population viability (CFU/mL) (C,F,I). Dark control samples are presented as black bars and light-treated samples as striped bars. Data represent the mean of at least three independent experiments ± the standard deviation. Statistical analyses were performed by one-way ANOVA (*$p < 0.05$; **$p < 0.01$; ***$p < 0.0001$).

Porphyrins activity against *P. aeruginosa* biofilm was also investigated by confocal microscopy analyses with PAO1_pVOGFP. This inducible GFP tagged strain was exposed to PDT with porphyrin P11 and biofilm was grown on microscopy glasses. GFP expression was induced by arabinose administration and pictures of the adherent populations were acquired by CLSM (figure 8). Images of dark control samples showed adherent cells expressing GFP, and no toxicity was observed in sample

treated with P11 in dark condition, confirming our previous results on cell viability. Light irradiation of untreated and DMSO-treated samples did not impair fluorescence emission, since a good GFP signal was visible in the pictures (figure 8b, d) comparable to that of dark controls. PDT treatment of PAO1_pVOGFP cells with porphyrin P11 caused a dramatic decrease in GFP emission, meaning that very few cells could express the fluorescent protein (figure 8f). This experimental result could be related to absence of a structured biofilm. These considerations are in agreement with the previous results on biofilm biomass and cell viability upon photodynamic treatment.

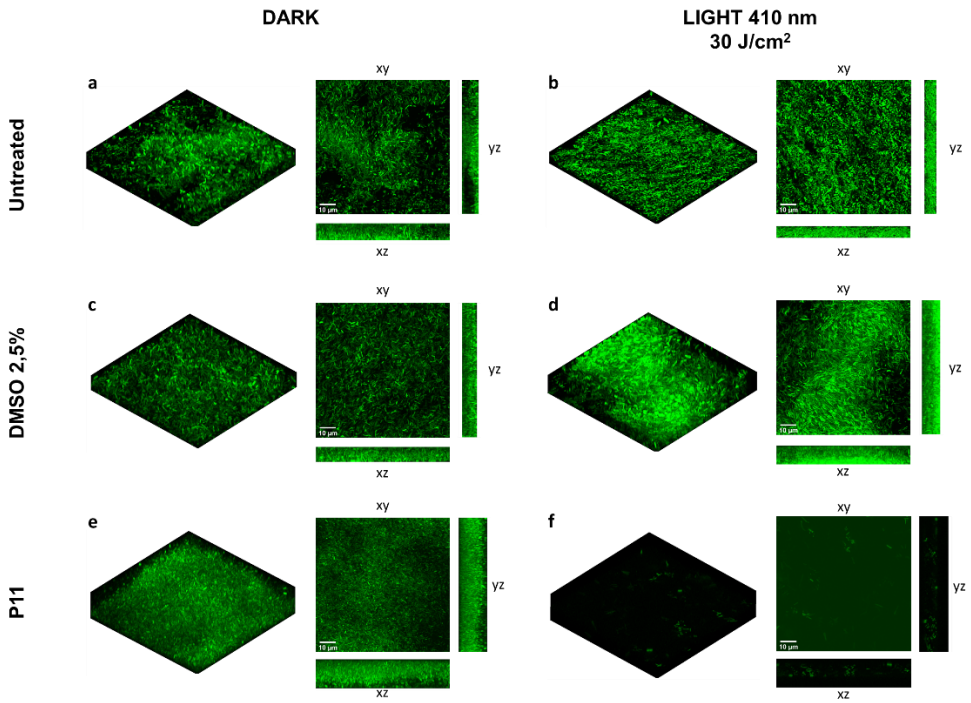

Figure 8. Inhibition of biofilm formation by *P. aeruginosa* PAO1_pVOGFP by dicationic diaryl-porphyrin P11. PAO1_pVOGFP cells were treated with P11 (30 µM final concentration) and irradiated with 410 nm blue light at 30 J/cm^2. Biofilms (24h incubation) of untreated and DMSO-treated samples were included in the experiment. Dark controls are shown in panels a,c,e, while irradiated samples are shown in panels b,d,f. Images of biofilms are shown in volume view, and in xy, xz and yz projections. Scale bar = 10 µM.

If biofilm inhibition is a promising step in antimicrobial therapy, eradication of mature biofilms remains the most arduous challenge for conventional and emerging

antimicrobial strategies. Therefore, the effect of porphyrin-mediated photodynamic treatment was evaluated on 24h-old PAO1 biofilms (figure 9). PDT experimental conditions were set as follows: upon 24 hours of biofilm growth, porphyrin P11 (30 µM final concentration) was gently administered to the samples, without modifying the biofilm environment and, after one hour of dark incubation, samples were irradiated with blue light (30 J/cm^2). Dark controls and DMSO-treated samples were included in each experiment. As shown in figure 9A, the total adherent biomass did not significantly change upon DMSO or P11 administration, in both light and dark conditions, compared to the untreated dark sample. Interestingly, activation of P11 by blue light caused the decrease of 2 Log units in both adherent and planktonic populations (figure 9B,C). These results suggested a potential antibiofilm effect of the dicationic diaryl-poprhyrin P11 on PAO1 cells, while no effect of photodynamic treatment was observed on the biofilm matrix.

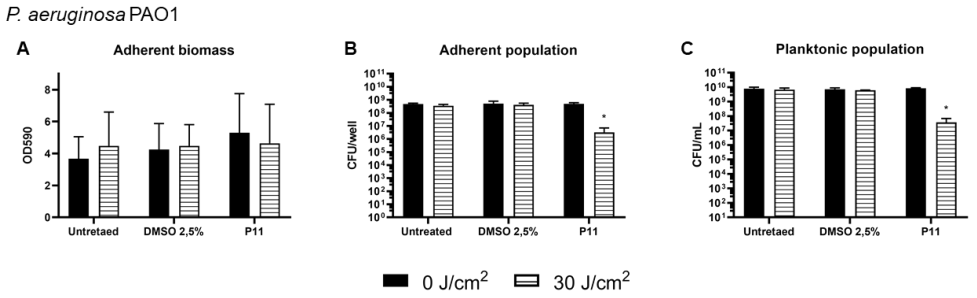

Figure 9. Assay of eradication of *P. aeruginosa* PAO1 biofilm by porphyrin P11 (30 µM) PDT. Adherent biomass of biofilm upon PDT is represented as OD590 (A) and cell viability is expressed as CFU/well for adherent population (B) and as CFU/mL for planktonic biomass (C). Error bars represent standard deviations. Statistical analyses were performed by one-way ANOVA (*p < 0,05).

Biofilm eradication was also evaluated by CLSM analyses. PAO1_pVOGFP biofilm was treated with 30 µM P11 and irradiated with blue light at 30 J/cm^2. Upon irradiation, GFP expression was induced with arabinose and images were acquired by confocal microscope analysis (figure 10). A comparable fluorescent signal was detected in control samples kept in the dark (untreated and DMSO-treated samples), as well as in irradiated ones. The treatment of biofilm with the porphyrin P11 slightly decreased the green signal in the samples kept in the dark, but a notable number of

cells were still alive and could express the GFP. The PDT-treated sample showed a remarkable decrease in fluorescent signal compared to the dark control, suggesting that the treatment possibly impaired cell functions, including the activity of the cellular synthetic machinery. These results suggest that most of the cells are damaged immediately after PDT treatment, and these cells could be more susceptible to antibiotic administration. Together with the decrease of 2 Log units in the viable population, such a result is promising for future development of antibiofilm PDT.

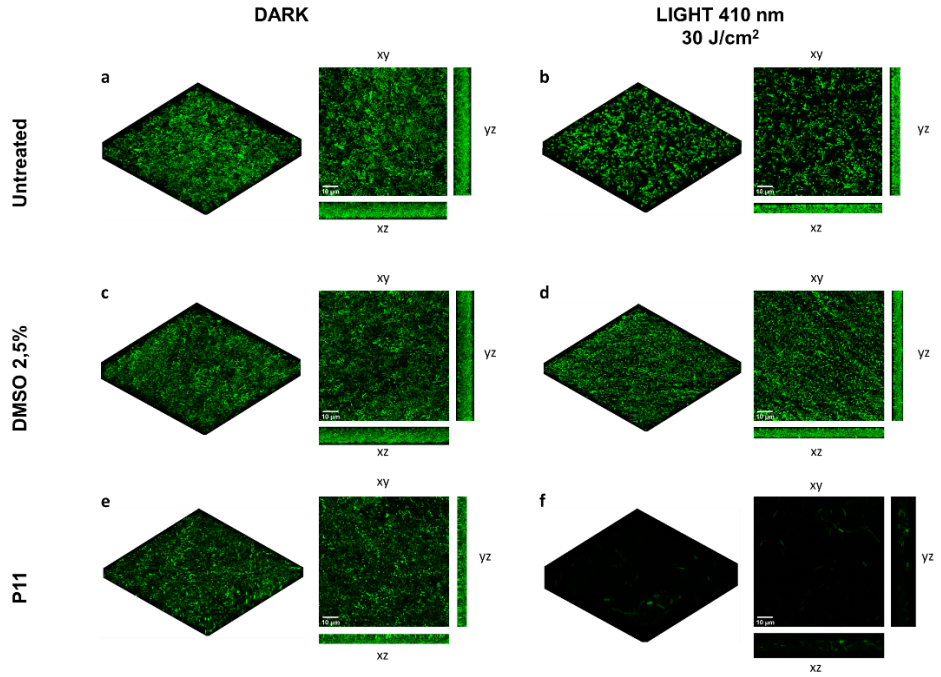

Figure 10. Assay of *P. aeruginosa* PAO1_pVOGFP biofilm eradication with dicationic diaryl-porphyrin P11. 24h-old PAO1_pVOGFP biofilm was treated with P11 (30 µM final concentration) and irradiated with 410 nm blue light at 30 J/cm^2. Biofilms (24h) of untreated and DMSO-treated samples were included in the experiment. Dark controls are shown in panels a,c,e, while irradiated samples are depicted in panels b,d,f. Images of biofilms are shown in volume view, and in xy, xz and yz projections. Scale bar = 10 µM.

3.4 Antibiofilm activity of porphyrins against *S. aureus*

The preliminary screening of diaryl-porphyrins activity on *S. aureus* cells revealed that two non-ionic molecules – P3 and P4 – had the best antimicrobial effect as compared to other PSs. These compounds were chosen to be tested on *S. aureus*

biofilms formed by the MSSA strain ATCC6538P, and the MRSA strain ATCC43300 which is resistant to β-lactam antibiotics.

Firstly, MSSA strain was treated separately with blue light at 40 J/cm^2 or with P3 and P4 PS (20 μM) to assess any possible toxicity of light or PSs. After 24 hours of biofilm growth, OD590 values and cell viability were determined (figure 11A,B,C). The total biomass (OD590) and the viability of adherent and planktonic phases did not change significantly upon treatment with DMSO alone, blue light alone and DMSO irradiated under blue light. In the dark, P3 had no toxic effect on the biofilm, but P4 caused a slightly decrease in OD590 values. Nevertheless, cell viability was unaffected, inferring that the presence of P4 could influence the biofilm matrix production by MSSA. Interestingly, both PSs caused a great decrease of total biomass upon light activation, but P3 and P4 PSs showed great differences on cell populations vitality. P3 was unable to kill MSSA cells in both planktonic and adherent phases, except for a slight decrease of ~1 Log unit compared to the dark control. On the contrary, P4 reduced the bacterial population of about 6 Log units compared to the dark control, inhibiting the biofilm formation. To sum up, porphyrin P3 seemed to have an inhibitory effect on biofilm matrix production, but not on cell viability, while porphyrin P4 showed the best antibiofilm performances on MSSA strain. Thus, P4 was considered for further analyses on MRSA biofilm (figure 11D,E,F). The amount of biofilm produced by MRSA strain was comparable to that of MSSA in terms of OD590 values and cell density. The administration of porphyrin P4 together with blue light showed a great decrease in total biomass of MRSA, and a killing effect of 6 Log units both on adherent and planktonic cells.

Thus, the diaryl-porphyrin P4 could be considered as a promising PS against *S. aureus*, independently from its antibiotic susceptibility profile.

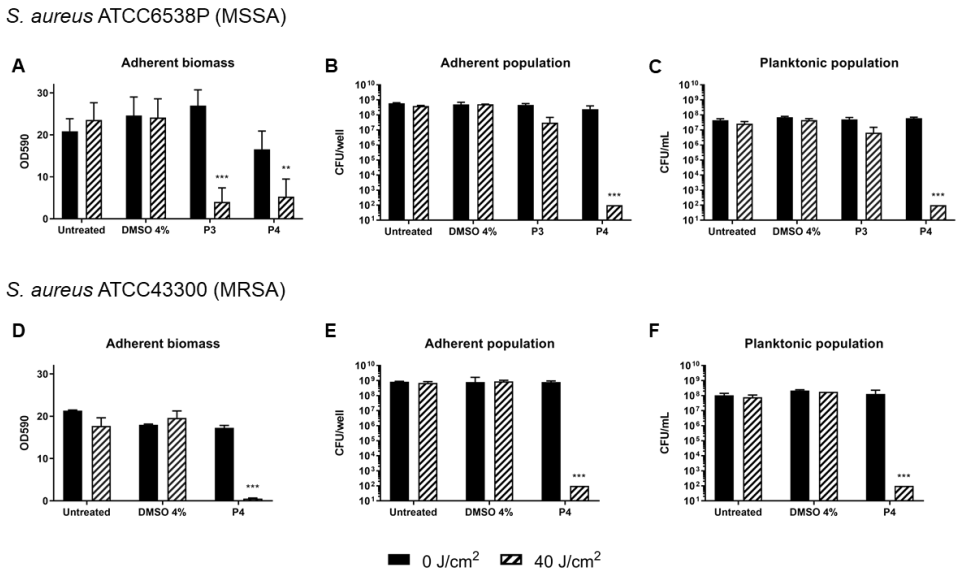

Figure 11. Assay of inhibition of biofilm formation for *S. aureus* ATCC6538P (A,B,C) and ATCC43300 (D,E,F) upon photodynamic treatment with diaryl-porphyrins. Porphyrin P3 and P4 (20 μM) were activated by 410 nm blue light at 40 J/cm^2. The graphs report values of the absorbance at 590 nm (OD 590) after biofilm staining with crystal violet (A,D), values of adherent population viability (CFU/well) (B,E), and planktonic population viability (CFU/mL) (C,F). Dark control samples are presented as black bars and light-treated samples as striped bars. Data represent the mean of at least three independent experiments ± the standard deviation. Statistical analyses were performed by one-way ANOVA (*$p < 0.05$; **$p < 0.01$; ***$p < 0.0001$).

Eradication of 24h *S. aureus* biofilm by P4 porphyrin (30 μM) PDT treatment was also assayed (figure 12). The administration of light alone (40 J/cm^2), DMSO 6% V/V and DMSO in combination with light did not affect neither the total biomass, nor cell viability. Also, P4 administration in dark or light conditions did not affect the total biomass of biofilm, suggesting that no impairment of biofilm matrix happened during PDT. However, antimicrobial effects were observed when cell viability was measured upon porphyrin and light exposure: a significant reduction of about 5 and 4 Log units was observed for adherent and planktonic populations, respectively (figure 12B,C).

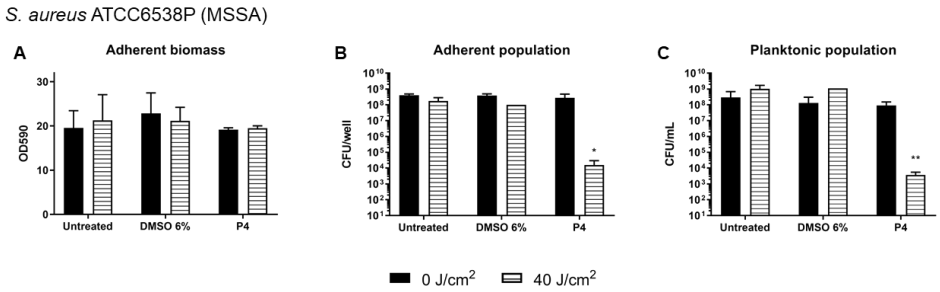

Figure 12. Eradication of *S. aureus* ATCC6538P biofilm by porphyrin P4 (30 μM). Adherent biomass of biofilm upon PDT is represented as OD590 (A) and cell viability is expressed as CFU/well for adherent population (B) and as CFU/mL for planktonic biomass (C). Error bars represent standard deviations. Statistical analyses were performed by one-way ANOVA (*p < 0,05; **p < 0.01).

3.5 Photodynamic activity of porphyrins on *C. albicans* biofilm

The potential of diaryl-porphyrins in inhibiting the biofilm formation of the yeast *C. albicans* was analysed by aPDT experiments. For this purpose, the assay was limited to compounds P9 and P10, which showed the best results among the tested diaryl-porphyrins during the preliminary screening phase. The experiments were performed on *C. albicans* ATCC14053 strain and on two clinical isolates Ca1 and Ca2 deriving from patients with urinary tract infections (figure 13). The clinical strains formed a biofilm comparable to that of the type strain, with comparable values for adherent biomass and adherent phase cell density (~10^7 CFU/well). The administration of 4% DMSO did not alter the biofilm formation of any of the studied strains. The irradiation with light at 410 nm of all the fungal strains treated with P9 and P10 impaired significantly their ability to form biofilm compared to the control samples (−PS, −Light; −PS, +Light; +PS, −Light) (figure 13A,D,G). On the other hand, when the cellular populations of planktonic and adherent phases were considered, some differences between the two monocationic diaryl-porphyrins were observed. Compound P10 was more active than P9 in impairing the viability of biofilm cells in the ATCC and Ca1 strains, while PSs had the same antimicrobial effects on *C. albicans* Ca2 strain. However, a significant depletion of adherent and planktonic populations was observed for all *C. albicans* strains considered in this study.

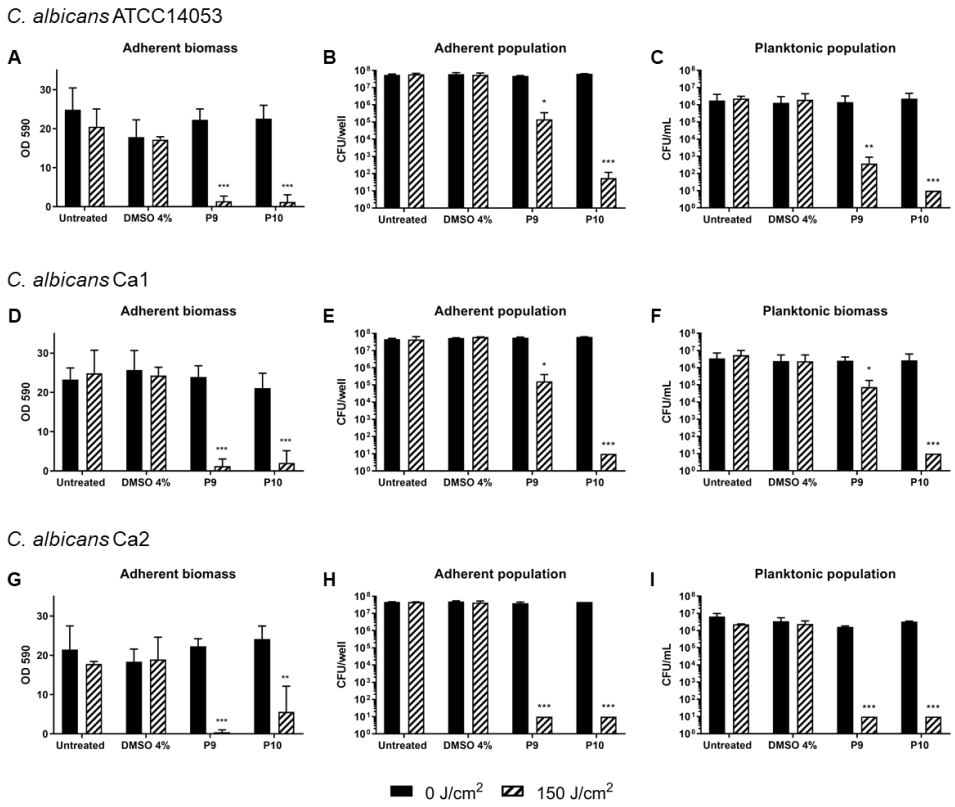

Figure 13. Inhibition of biofilm formation of *C. albicans* ATCC14053 (A,B,C), Ca1 (D,E,F), and Ca2 (G,H,I) upon photodynamic treatment with diaryl-porphyrins. Porphyrin P9 and P10 (20 μM) were activated by 410 nm blue light at 150 J/cm^2. The graphs report values of the absorbance at 590 nm (OD 590) after biofilm staining with crystal violet (A,D,G), values of adherent population viability (CFU/well) (B,E,H), and planktonic population viability (CFU/mL) (C,F,I). Dark control samples are presented as black bars and light-treated samples as striped bars. Data represent the mean of at least three independent experiments ± the standard deviation. Statistical analyses were performed by one-way ANOVA (*$p < 0.05$; **$p < 0.01$; ***$p < 0.0001$).

The eradication of 24-hour biofilms of *C. albicans*, was assayed after treatment with the diaryl-porphyrin P10 (figure 14). The growth in rich YPD medium is optimal to maximize biofilm biomass, but the organic matter could interfere with light penetration during subsequent PDT treatment. Thus, planktonic biomass was removed and replaced with phosphate buffer and cell viability of this population was not considered in these experiments. The adherent biomass (OD590) did not significantly change upon light irradiation, solvent treatment, and PDT treatment with P10 porphyrin. Nevertheless, a certain killing effect of almost 2 Log units was observed in adherent population upon light activation of P10 (figure 14B). If a certain

effect was observed on cell viability, the biofilm matrix was insensitive to PDT treatment with porphyrin P10.

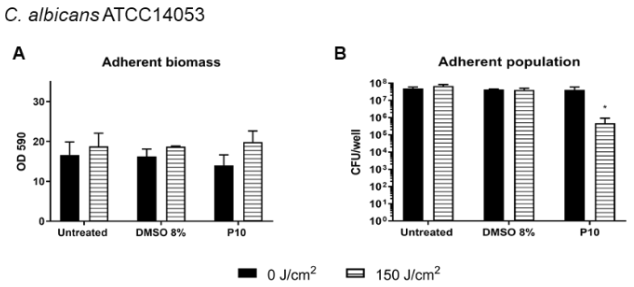

Figure 14. Eradication of *C. albicans* ATCC14053 biofilm by porphyrin P10 (40 µM). Adherent biomass of biofilm upon PDT is represented as OD590 (A) and adherent cell viability is expressed as CFU/well (B). Error bars represent standard deviations. Statistical analyses were performed by one-way ANOVA (*p < 0,05).

4. Discussion

Porphyrins are widely distributed in nature in both prokaryotic and eukaryotic organisms as components of cytochromes, eme groups, and chlorophylls, and are involved in many biological processes, such as photosynthesis and oxygen or electron transport. Recently, the versatility of these compounds has been reported in both diagnostic and therapeutic approaches. Among the therapeutic options, porphyrins demonstrated to be optimal photosensitizing drugs to be used in anticancer photodynamic therapy (Tsolekile et al., 2019). Along with this aspect, porphyrin compounds were found to be effective in the photodynamic treatment of microbial cells, and they present many chemico-physical characteristics to be considered good photo-antimicrobials for their applications in clinical field (Amos-Tautua et al., 2019). However, since aPDT is a versatile and wide-spectrum antimicrobial strategy, it can also find many applications as promising sanitising tool in other fields, such as industry, agriculture, and food-processing.

The tetrapyrrolic skeleton of porphyrins can be chemically modified to obtain a wide variety of PSs featuring different substituents in the four available *meso*-positions to enhance their phototherapeutic effects. If tetraaryl-porphyrins, differently substituted in *meso*-positions, have been widely investigated in aPDT (Philippova et al., 2003; Collins et al., 2010; Taslı et al., 2018), few papers report the potential of 5,15-

substituted diaryl-porphyrins. These PSs were previously reported to be more active than their tetraaryl counterparts in anticancer PDT on human cancer cell lines (Banfi et al., 2006b). Concerning antimicrobial PDT, Burda and colleagues found that diaryl-porphyrins had enhanced potency in the inactivation of *S. aureus* compared to the respective tetra-*meso*-substituted compounds (Burda et al., 2012). In addition, photodynamic inactivation of *C. albicans* yielded better results with a dicationic diaryl-porphyrin compared to the commercial 5,10,15,20-tetrakis(1-methyl-4-pyridyl)-21H,23H-porphine tetra-p-tosylate salt (TMPyP) (Gonzales et al., 2013).

In this study, a panel of 13 diaryl-porphyrins were considered as potential PSs in antimicrobial PDT against pathogenic bacteria belonging to Gram-negative (*P. aeruginosa*) and Gram-positive (*S. aureus*) microorganisms, and the pathogenic yeast *C. albicans*. Diaryl-porphyrins employed in this work have a different degree of amphiphilicity, with ionic and hydrophobic groups differently disposed on the two appendages in 5 and 15 positions, building a panel of symmetric or asymmetric compounds with non-ionic or positive total charges. Non-ionic molecules (P1-P6) bear in *meso*-positions a pentafluorophenyl group, associated with a C4 or C8 *para*-bromoalkyloxy-phenyl group (P1 and P2 respectively). Otherwise, in compounds P3 and P5, the C4 or C8 bromoalkyloxy-phenyl chain is associated with a phenyl group in position 5. P4 and P6 are symmetrical compounds bearing two phenyl groups with *para*-bromobutoxy and two *para*-bromooctanoxy chains, respectively. In positively charged compounds, the charge derives from a pyridyl group. All monocationic PSs are asymmetrical molecules bearing a phenyl (P7, P8) or a pentafluorophenyl group (P9, P10) in position 5 and a pyridinobutoxy-phenyl (P7, P9) or pyridinooctaoxy-phenyl group (P8, P10) in position 15. The three dicationic symmetric porphyrins are characterised by benzyl group as alkylating group of the pyridyl substituent (P11), or alkoxy-linked pyridinium at the end of 4C (P12) or 8C (P13) carbon chains.

Essential for the efficacy of microbial photoinactivation process is the PS accumulation in microbial structures. Thus, an initial screening phase was aimed at understanding porphyrin interaction with bacterial and fungal cells. From our results, we can infer that the charge of diaryl-porphyrins strongly influences their binding to microbial cells. Non-ionic molecules poorly interact with the envelope of the Gram-

negative bacterium *P. aeruginosa* with less than 8% of PS binding for all the non-ionic molecules, except for porphyrin P2 with a binding yield of 15%. The envelope of *P. aeruginosa* forms an effective permeability barrier between the cell and its environment and tends to restrict the binding and penetration of several PSs. Along with the fact that non-ionic PS did not interact with *P. aeruginosa*, these compounds neither affect its viability upon photo treatment. On the contrary, cationic PSs better interact by electrostatic force with Gram-negative bacteria, with binding percentage between 80 and 100%, since they exhibit negative-charged lipopolysaccharides (LPS) on the outer layer of the outer membrane. As previously reported by other authors, one or more positive charges are required on the PS structure for a good interaction with Gram-negative bacteria (Sobotta et al., 2019). The mechanism of binding of cationic PSs with bacteria is the so-called "self-promoted uptake" pathway. This pathway involves the binding of the cationic molecules to LPS in Gram-negative bacteria, that results in the progressive displacement of divalent cations (Ca^{2+}, Mg^{2+}) electrostatically bound to the LPS, thereby weakening the outer membrane. The destabilization of the LPS coat results in the formation of "cracks" in the permeability barrier, and divalent cations neutralize the negative character of cell membrane and eliminate electrostatic repulsion between PS and the bacterial envelope (George et al., 2009).

On the other hand, the Gram-positive bacterium *S. aureus* showed a certain degree of interaction (12-40% of PS binding) with non-ionic diaryl-porphyrins. This is probably due to the cell anatomy of Gram-positive bacteria that are surrounded by a porous cell wall composed of peptidoglycan and lipoteichoic acid that allows the passage of PSs. On the other hand, binding yield between 68 and 100% were found for cationic molecules, probably explainable by the previously cited "self-promoted uptake" pathway. In the case of Gram-positive bacteria, cationic PSs interact with the carboxylate groups of proteins, peptidoglycans, phosphate groups of lipoteichoic and teichoic acids, with consequent increase in the permeability of Gram-positive envelope (Sobotta et al., 2019). Despite the still limited interaction between *S. aureus* cells and non-ionic PSs, compared to positively charged ones, a certain antimicrobial activity was observed upon PDT, and almost all the non-ionic molecules showed a

rate of photoinactivation. These results suggest that, in this experimental setup, a high degree of interaction is not strictly necessary for *S. aureus* inactivation. Thus, the designed binding assay seems to be not predictable of PS activity on this pathogen. As a matter of fact, the best PDT performances were ascribable to the non-ionic porphyrin P4 with just 16.6% of PS binding with *S. aureus* cells.

Non-ionic diaryl-porphyrins hardly interact also with the yeast *C. albicans*. Fungal cells seem to have an intermediate permeability rate between Gram-positive and Gram-negative bacteria (Dai et al., 2009). The cell wall has a complex molecular architecture that confers a negative charge to *C. albicans* cells. The structure is formed by a relatively thick layer of polysaccharide fibrils formed by β-(1,3)-glucan covalently linked to β-(1,6)-glucan and chitin. Further, an external protein layer is formed by mannoproteins and a smaller amount of chitin. These proteins are highly glycosylated by N-linked and O-linked mannosyl and phosphomannosyl residues conferring the overall negative charge of the cell wall (Kapteyn et al., 1995). Thus, a good interaction is driven by electrostatic bonds between cationic diaryl-porphyrins and yeast cells, better than in the case of non-ionic molecules (Wainwright and Giddens, 2003; Donnelly et al., 2008; Cormick et al., 2009). However, despite low binding values, a good photoinactivation rate was observed also for non-ionic molecules, in particular porphyrin P2, P3, P4 and P6.

Even if a good rate of interaction between PSs and microbial cells is crucial for PDT efficacy, a possible PS intrinsic toxicity should be avoided. In dark conditions, dicationic diaryl-porphyrins were the most toxic for all microbial pathogens. P12 and P13 caused a certain inhibition rate in *P. aeruginosa, S. aureus* and *C. albicans* populations, while P11 was toxic only for the Gram-positive bacterium *S. aureus*. Monocationic compounds were not as toxic as dicationic molecules, except for P7 that impaired *C. albicans* viability. In all the cases, PSs toxicity was directly dependent on dark incubation time and inversely proportional to microbial cell concentration. Non-ionic diaryl-porphyrins did not show any intrinsic toxicity in all the tested microorganisms.

A source of blue light, with maximum emission peak at 410 nm, was used to photoactivate diaryl-porphyrins, and the preliminary photo-spot assay allowed to choose the best PSs for the inactivation of each pathogen.

P. aeruginosa was the less susceptible microorganism to porphyrin-mediated PDT. Monocationic porphyrins, despite a good rate of interaction, did not show any photo-toxicity. Only the symmetric dicationic compound P11 was able to cause a 4 Log reduction in PAO1 populations. P11 was previously discovered by our group as versatile PS with a wide-spectrum antimicrobial activity on *P. aeruginosa*, *E. coli*, *S. aureus*, and *E. faecalis* (Orlandi et al., 2013).

The adhesion and growth of highly structured biofilm communities is considered a major problem in the progression of infections. Thus, increasing attention in antimicrobial field is devoted to preventing and/or detach microbial biofilms. Administered at relatively low concentration (30 μM), P11 was able to inhibit *in vitro* biofilm development by the wild-type strain PAO1 and two biofilm hyperproducers isolated in clinical context (UR48 and BT1).

Eradication of mature biofilm is the most challenging goal to achieve in antimicrobial field, in both clinical, industrial, and environmental settings. Antimicrobial agents hardly penetrate within the complex exopolysaccharide (EPS) matrix of biofilms, making cell inactivation very difficult. Usually, a successful eradication of bacteria in biofilms requires 100-1000 times higher concentrations of specific antibiotic or disinfectant (Maisch, 2015). However, PDT treatment proved to be effective on *P. aeruginosa* biofilms by means of PS belonging to the class of phenothiazinium dyes and tetraaryl-porphyrins. The tetracationic tetraaryl-porphyrin TMP was found by two research groups to cause a substantial killing in *P. aeruginosa* biofilm, reaching the disruption of biofilm matrix only at high PS concentrations (225 μM) (Collins et al., 2010; Beirao et al., 2014). Moreover, Mamone and colleagues found that the non-ionic tetraaryl-porphyrin TAPP was able to decrease the viability (3 Log units) of *P. aeruginosa* cells organised in biofilms (Mamone et al., 2016). However, it has been recently hypothesized that the presence of negative charges in the EPS matrix could protect bacteria from the interaction with positively charged PSs. Furthermore, larger molecules are disadvantaged in the penetration through the biofilm matrix if

compared to smaller ones (Maisch, 2015). Since no standard procedures are available for biofilm studies, comparisons can not be made between each experimental approach (Maisch, 2015). In our case, stringent conditions were applied in antibiofilm PDT and no changes in biofilm environment were made upon biofilm growth. The diaryl-porphyrin P11 (30 μM) caused a 2-Log-unit depletion of both adherent and planktonic population of PAO1 biofilm. In addition, confocal analyses allowed to observe the biofilm adherent population immediately upon photo-treatment. PDT provoked a certain damage to embedded PAO1 cells, suggesting that they could be more sensitive to other antimicrobial agents delivered upon photodynamic treatment. These results could pave the way through the development of combined antibiofilm strategies where P11-mediated PDT in addition to other antimicrobial therapies could successfully eradicate *P. aeruginosa* biofilm.

The Gram-positive bacterium *S. aureus* was more susceptible to PDT with diaryl-porphyrins as compared to the Gram-negative bacterium *P. aeruginosa*. In general, monocationic compounds were less active than non-ionic porphyrins in MSSA photoinactivation. Indeed, the best PDT killing rate was obtained with two non-ionic porphyrins – P3 and P4 – that only differ for a C4 bromoalkyl chain in *meso*-position. However, when tested on biofilm, P3 was not as prone as P4 in the inhibition of biofilm formation by *S. aureus*. Further, P4 successfully impaired biofilm development ability of MRSA strain ATCC43300.

Biofilm eradication by photodynamic treatment was previously achieved by Beirao and colleagues by means of 20 μM tetracationic porphyrin TMP (Beirao et al., 2014). Moreover, TAPP porphyrin (20 μM) was active on *S. aureus* biofilm, causing a biomass depletion of 3 Log units (Mamone et al., 2016). In our case, the chosen stringent conditions of biofilm eradication allowed to reach a good killing effect in adherent and planktonic population of *S. aureus* biofilm with 20 μM P4 porphyrin.

The initial screening of diaryl-porphyrins in antifungal PDT found that *C. albicans* was greatly inactivated by compounds P4, P9, P10 and P11. From a morphological analysis upon photo-treatment, monocationic porphyrins P9 and P10 revealed to impaired yeast cells better than other PSs with a complete loose of cellular identity. From these analyses, structural alterations were prevalently associated with the

cytoplasmic environment, therefore it could be hypothesized that, upon irradiation, the main damage occurred inside the cell and not at the cell wall level.

Further, both cationic porphyrins inhibited the formation of an adherent biomass. However, P10, with a C8 pyridyl chain in 15 *meso*-position, had a greater effect on cell viability compared to P9 (C4 pyridyl chain in the same position) on planktonic and sessile cellular populations of the biofilm of *C. albicans* ATCC14053 and two *C. albicans* clinical strains. Eradication of fungal biofilm performed by porphyrin P10 had a slight effect on adherent population viability.

5. Conclusions

In conclusion, diaryl-porphyrins showed to be suitable PSs for the inactivation of all microbial pathogens considered in this study. In general, non-ionic molecules appeared to be optimal for *S. aureus* inactivation, while monocationic and dicationic porphyrins emerged as best PSs for the treatment of *C. albicans* and *P. aeruginosa*, respectively.

In all the cases, porphyrins with best photoinactivation performances negatively influenced the biofilm formation by microbial species, making PDT appropriate as a preventive disinfection approach on inert surfaces of medical devices, where biofilms are prone to develop on. Furthermore, aPDT could be also applicable to localized superficial infections in oral cavity or on the skin, to avoid the beginning of chronic infections and the spread of microbial pathogens in other body districts.

Interestingly, a certain effect of diaryl-porphyrin PDT on cell population viability living in biofilm environment was observed for all the pathogens. This aspect could suggest that the photodynamic treatment could be regarded as a complementary approach that may increase the efficiency of antimicrobial drugs or new properly designed antibiofilm strategies in the management of biofilm-mediated infections.

These types of screening studies could pave the way through the identification of new compounds to be tested on superficial infections in animal models to investigate their effect *in vivo*, and to highlight possible toxic effects. In addition, PSs could be modified to improve their delivery in *in vivo* environments by conjugation to nanoparticles, peptides, or biopolymers.

References

Allison, R. R., and Moghissi, K. (2013). Photodynamic therapy (PDT): PDT mechanisms. Clin. Endosc. 46, 24–29. doi:10.5946/ce.2013.46.1.24.

Allison, R. R., and Sibata, C. H. (2010). Oncologic photodynamic therapy photosensitizers: A clinical review. Photodiagnosis Photodyn. Ther. 7, 61–75. doi:10.1016/j.pdpdt.2010.02.001.

Amos-Tautua, B. M., Songca, S. P., and Oluwafemi, O. S. (2019). Application of porphyrins in antibacterial photodynamic therapy. Molecules 24. doi:10.3390/molecules24132456.

Banfi, S., Caruso, E., Buccafurni, L., Murano, R., Monti, E., Gariboldi, M., et al. (2006). Comparison between 5,10,15,20-tetraaryl- and 5,15-diarylporphyrins as photosensitizers: Synthesis, photodynamic activity, and quantitative structure-activity relationship modeling. J. Med. Chem. 49, 3293–3304. doi:10.1021/jm050997m.

Beirao, S., Fernandes, S., Coelho, J., Faustino, M. A. F., Tom, P. C., Neves, M. G. P. M. S., et al. (2014). Photodynamic Inactivation of Bacterial and Yeast Biofilms With a Cationic Porphyrin. 1387–1396. doi:10.1111/php.12331.

Bragonzi, A., Wiehlmann, L., Klockgether, J., Cramer, N., Worlitzsch, D., Döning, G., et al. (2006). Sequence diversity of the mucABD locus in Pseudomonas aeruginosa isolates from patients with cystic fibrosis. Microbiology 152, 3261–3269. doi:10.1099/mic.0.29175-0.

Burda, W. N., Fields, K. B., Gill, J. B., Burt, R., Shepherd, M., Zhang, X. P., et al. (2012). Neutral metallated and meso-substituted porphyrins as antimicrobial agents against Gram-positive pathogens. Eur. J. Clin. Microbiol. Infect. Dis. 31, 327–335. doi:10.1007/s10096-011-1314-y.

Caruso, E., Cerbara, M., Malacarne, M. C., Marras, E., Monti, E., and Gariboldi, M. B. (2019a). Synthesis and photodynamic activity of novel non-symmetrical diaryl porphyrins against cancer cell lines. J. Photochem. Photobiol. B Biol. 195, 39–50. doi:10.1016/j.jphotobiol.2019.04.010.

Caruso, E., Malacarne, M. C., Banfi, S., Gariboldi, M. B., and Orlandi, V. T. (2019b). Cationic diarylporphyrins: In vitro versatile anticancer and antibacterial photosensitizers. J. Photochem. Photobiol. B Biol. 197, 111548. doi:10.1016/j.jphotobiol.2019.111548.

Collins, T. L., Markus, E. A., Hassett, D. J., and Robinson, J. B. (2010). The Effect of a Cationic Porphyrin on Pseudomonas aeruginosa Biofilms. 411–416. doi:10.1007/s00284-010-9629-y.

Cormick, M. P., Alvarez, M. G., Rovera, M., and Durantini, E. N. (2009). Photodynamic inactivation of Candida albicans sensitized by tri- and tetra-cationic porphyrin derivatives. Eur. J. Med. Chem. 44, 1592–1599. doi:10.1016/j.ejmech.2008.07.026.

Dai, T., Huang, Y. Y., and Hamblin, M. R. (2009). Photodynamic therapy for localized infections-State of the art. Photodiagnosis Photodyn. Ther. 6, 170–188. doi:10.1016/j.pdpdt.2009.10.008.

Donnelly, R. F., McCarron, P. A., and Tunney, M. M. (2008). Antifungal photodynamic therapy. Microbiol. Res. 163, 1–12. doi:10.1016/j.micres.2007.08.001.

George, S., Hamblin, M. R., and Kishen, A. (2009). Uptake pathways of anionic and cationic photosensitizers into bacteria. Photochem. Photobiol. Sci. 8, 788–795. doi:10.1039/b809624d.

Gonzales, F. P., Felgenträger, A., Bäumler, W., and Maisch, T. (2013). Fungicidal photodynamic effect of a twofold positively charged porphyrin against Candida albicans planktonic cells and biofilms. Futur. Med. 8, 785–797.

Hamblin, M. R. (2016). Antimicrobial photodynamic inactivation : a bright new technique to kill resistant microbes. Curr. Opin. Microbiol. 33, 67–73. doi:10.1016/j.mib.2016.06.008.

Hsieh, Y. H., Zhang, J. H., Chuang, W. C., Yu, K. H., Huang, X. Bin, Lee, Y. C., et al. (2018). An in vitro study on the effect of combined treatment with photodynamic and chemical therapies on Candida albicans. Int. J. Mol. Sci. 19. doi:10.3390/ijms19020337.

Jori, G., Fabris, C., Soncin, M., Ferro, S., Coppellotti, O., Dei, D., et al. (2006). Photodynamic therapy in the treatment of microbial infections: Basic principles and perspective applications. Lasers Surg. Med. 38, 468–481. doi:10.1002/lsm.20361.

Kapteyn, J. C., Montijn, R. C., Dijkgraaf, G. J. P., Van den Ende, H., and Klis, F. M. (1995). Covalent association of β-1,3-glucan with β-1,6-glucosylated mannoproteins in cell walls of Candida albicans. J. Bacteriol. 177, 3788–3792. doi:10.1128/jb.177.13.3788-3792.1995.

Maisch, T. (2015). Resistance in antimicrobial photodynamic inactivation of bacteria. Photochem. Photobiol. Sci. 14, 1518–1526. doi:10.1039/c5pp00037h.

Malatesti, N., Munitic, I., and Jurak, I. (2017). Porphyrin-based cationic amphiphilic photosensitisers as potential anticancer, antimicrobial and immunosuppressive agents. Biophys. Rev. 9, 149–168. doi:10.1007/s12551-017-0257-7.

Mamone, L., Ferreyra, D. D., Gándara, L., Di Venosa, G., Vallecorsa, P., Sáenz, D., et al. (2016). Photodynamic inactivation of planktonic and biofilm growing bacteria mediated by a meso-substituted porphyrin bearing four basic amino groups. J. Photochem. Photobiol. B Biol. 161, 222–229. doi:10.1016/j.jphotobiol.2016.05.026.

Mulani, M. S., Kamble, E. E., Kumkar, S. N., Tawre, M. S., and Pardesi, K. R. (2019). Emerging strategies to combat ESKAPE pathogens in the era of antimicrobial resistance: A review. Front. Microbiol. 10. doi:10.3389/fmicb.2019.00539.

Orlandi, V. T., Bolognese, F., Rolando, B., Guglielmo, S., Lazzarato, L., and Fruttero, R. (2018a). Anti-pseudomonas activity of 3-nitro-4-phenylfuroxan. Microbiol. (United Kingdom) 164, 1557–1566. doi:10.1099/mic.0.000730.

Orlandi, V. T., Caruso, E., Tettamanti, G., Banfi, S., and Barbieri, P. (2013). Photoinduced antibacterial activity of two dicationic 5,15-diarylporphyrins. J. Photochem. Photobiol. B Biol. 127, 123–132. doi:10.1016/j.jphotobiol.2013.08.011.

Orlandi, V. T., Martegani, E., and Bolognese, F. (2018b). Catalase A is involved in the response to photooxidative stress in Pseudomonas aeruginosa. Photodiagnosis Photodyn. Ther. 22, 233–240. doi:10.1016/j.pdpdt.2018.04.016.

Orlandi, V. T., Martegani, E., Bolognese, F., Trivellin, N., Maťátková, O., Paldrychová, M., et al. (2020). Photodynamic therapy by diaryl-porphyrins to control the growth of Candida albicans. Cosmetics 7, 1–19. doi:10.3390/COSMETICS7020031.

Orlandi, V. T., Villa, F., Cavallari, S., Barbieri, P., Banfi, S., Caruso, E., et al. (2011). Photodynamic therapy for the eradication of biofilms formed by catheter associated Pseudomonas aeruginosa strains. 26, 129–133.

Park, D., Choi, E. J., Weon, K. Y., Lee, W., Lee, S. H., Choi, J. S., et al. (2019). Non-Invasive Photodynamic Therapy against -Periodontitis-causing Bacteria. Sci. Rep. 9, 1–12. doi:10.1038/s41598-019-44498-4.

Philippova, T. O., Galkin, B. N., Zinchenko, O. Y., Rusakova, M. Y., Ivanitsa, V. A., Zhilina, Z. I., et al. (2003). The antimicrobial properties of new synthetic porphyrins. J. Porphyr. Phthalocyanines 7, 755–760. doi:10.1142/s1088424603000926.

Pithan, E., Righi, M., Bruno, C., Christ, R., Antonio, M., and Zanini, K. (2016). Photodiagnosis and Photodynamic Therapy Antimicrobial photodynamic effect of phenothiazinic photosensitizers in formulations with ethanol on Pseudomonas aeruginosa biofilms. Photodiagnosis Photodyn. Ther. 13, 291–296. doi:10.1016/j.pdpdt.2015.08.008.

Roca, I., Akova, M., Baquero, F., Carlet, J., Cavaleri, M., Coenen, S., et al. (2015). The global threat of antimicrobial resistance: Science for intervention. New Microbes New Infect. 6, 22–29. doi:10.1016/j.nmni.2015.02.007.

Sobotta, L., Skupin-Mrugalska, P., Piskorz, J., and Mielcarek, J. (2019). Porphyrinoid photosensitizers mediated photodynamic inactivation against bacteria. Eur. J. Med. Chem. 175, 72–106. doi:10.1016/j.ejmech.2019.04.057.

St. Denis, T. G., Dai, T., Izikson, L., Astrakas, C., Anderson, R. R., Hamblin, M. R., et al. (2011). All you need is light, antimicrobial photoinactivation as an evolving and emerging discovery strategy against infectious disease. Virulence 2, 509–520. doi:10.4161/viru.2.6.17889.

Stover, C. K., Pham, X. Q., Erwin, A. L., Mizoguchi, S. D., Warrener, P., Hickey, M. J., et al. (2000). Complete genome sequence of {Pseudomonas} aeruginosa {PAO}1, an opportunistic pathogen. Nature 406, 959–964. doi:10.1038/35023079.

Sunahara, H., Urano, Y., Kojima, H., and Nagano, T. (2007). Design and synthesis of a library of BODIPY-based environmental polarity sensors utilizing photoinduced electron-transfer-controlled fluorescence ON/OFF switching. J. Am. Chem. Soc. 129, 5597–5604. doi:10.1021/ja068551y.

Taslı, H., Akbıyık, A., Topaloğlu, N., Alptüzün, V., and Parlar, S. (2018). Photodynamic antimicrobial activity of new porphyrin derivatives against methicillin resistant Staphylococcus aureus. J. Microbiol. 56, 828–837. doi:10.1007/s12275-018-8244-7.

Tsolekile, N., Nelana, S., and Oluwafemi, O. S. (2019). Porphyrin as diagnostic and therapeutic agent. Molecules 24. doi:10.3390/molecules24142669.

Wainwright, M. (1998). Photodynamic Antimicrobial Chemotherapy. J. Antimicrob. Chemother. 42, 13–28. doi:10.1002/9783527676132.ch10.

Wainwright, M., and Giddens, R. M. (2003). Phenothiazinium photosensitisers: Choices in synthesis and application. Dye. Pigment. 57, 245–257. doi:10.1016/S0143-7208(03)00021-4.

Wainwright, M., Maisch, T., Nonell, S., Plaetzer, K., Almeida, A., Tegos, G. P., et al. (2017). Photoantimicrobials—are we afraid of the light? Lancet Infect. Dis. 17, e49–e55. doi:10.1016/S1473-3099(16)30268-7.

New BODIPYs as photosensitizers in antimicrobial photodynamic therapy

Authors: Eleonora Martegani[1], Fabrizio Bolognese[1], Enrico Caruso[1] and Viviana Teresa Orlandi[1]*

[1]Departement of Biotechnologies and Life Sciences, University of Insubria, Varese, Italy

Abstract

Background. Widespread drug resistance of common pathogenic microorganisms urgently requires alternative strategies to conventional antibiotic therapies. In recent years, antimicrobial photodynamic therapy (aPDT) gained increasing attention for its potential to inhibit the growth and spread of bacteria and fungi, both as free-living cells and/or in biofilm communities. A new class of compounds, the boron-dipyrromethenes (BODIPYs), were recently identified as promising photosensitizers to be applied in the antimicrobial field.

Aim. In this study 15 BODIPYs, prevalently characterised by non-ionic charge and synthesised for antitumoral PDT, were evaluated in antimicrobial field for the inactivation of the Gram-positive bacterium *Staphylococcus aureus*. Further, two other clinically relevant pathogens, *Pseudomonas aeruginosa,* and *Candida albicans,* were included in the study. Since the development of microbial biofilms in infected areas worsens patients' conditions, the best BODIPYs were investigate for their potential in inhibiting/eradicating microbial biofilm.

Material and methods. In this study, viable count method and photo-spot test were used to compare the effect of PSs on suspended cultures. Crystal-violet staining and confocal analysis highlighted the anti-biofilm activity of BODIPYs. ANOVA analysis highlighted the statistical significance of the obtained results.

Results. *S. aureus* was successfully inactivated by non-ionic BODIPYs B2 and B5, and unexpectedly *P. aeruginosa* was sensitive to the non-ionic compound B9. Encouraging results against yeast cells were obtained by the positively charged PS B13. Furthermore, BODIPYs revealed to be efficient in inhibiting the development

of microbial biofilms when administered at relatively low concentrations, and were also active in biofilm eradication, showing activity against both planktonic and sessile populations, while biofilm matrix seemed to be insensitive to induced photo-oxidative stress.

Conclusions. BODIPYs demonstrated to be suitable photosensitisers for the inactivation of microbial pathogens.

1. Introduction

In recent years, the scientific community is facing with the widespread, rising, and severe phenomenon of antimicrobial resistance (AMR). As a result of intensive and sometimes excessive use of antibiotics and biocides, microorganisms evolved resistance mechanisms that rapidly spread through the environment (Pendleton et al., 2013; Roca et al., 2015). As well as the improvement of existent antibiotic and antimycotic therapies, nowadays many efforts have been made to find adjuvant strategies to overcome the problem of AMR (Mulani et al., 2019). Photodynamic therapy (PDT), initially proposed as antitumoral approach, has recently found interesting applications also in the antimicrobial field. The reason is that microbial killing happens by means of a rapid photo-oxidative stress generated during photodynamic treatment, regardless from the drug susceptibility profile of each microbial strain (Cieplik et al., 2018b). The photodynamic process exploits the power of a light source to activate a specific photosensitizer (PS), that undergoes chemico-physical reactions and generates highly reactive oxygen species (ROS) or singlet oxygen ($^1O_2$) in aerobic environments. If the PS is strictly associated or enters microbial cells, oxidising species rapidly attack different cellular structures or macromolecules including lipids, proteins, and nucleic acids, leading to the death of microorganisms (St. Denis et al., 2011).

Until now, no resistance mechanisms able to counteract the oxidative stress induced by photodynamic process have been found in microbes (Maisch, 2015). Thus, antimicrobial PDT should be considered as a promising and adjuvant strategy in controlling microbial growth. This technique has a wide-spectrum activity against many pathogen species and easily finds clinical applications for the treatment of

superficial skin and oral cavity infections or as anti-infective tool in industrial and agricultural fields (Hamblin, 2016).

Different classes of natural or synthetic compounds have been considered as suitable PSs in the antimicrobial and antitumoral fields: phenothiazinium salts, acridines, porphyrins, chlorins, phthalocyanines, fullerenes, curcumin, riboflavin, xanthene, (Cieplik et al., 2018a). In 2005, Gallagher et al. identified boron-dipyrromethenes (BODIPYs) as a class of chemicals with suitable features for anticancer PDT and cationic BODIPYs were further highlighted as active PSs against microbial pathogens, such as bacteria and fungi (Frimannsson et al., 2010; Caruso et al., 2012). BOPIPYs have a typical skeleton based on difluoro-boradiazaindacene, whose synthetic pathway is relatively flexible and easy, starting from commercial pyrroles and acid chlorides, anhydrides, aldehydes, or ketones. The core of BODIPY presents a great reactivity and chemical versatility that allows the incorporation of different functional groups and the generation of new compounds with diverse properties (Agazzi et al., 2019). These molecules are widely applied as fluorophores for fluorescent labelling of biomolecules (e.g. fatty acids, nucleotides, proteins, etc.), as chemosensors for the detection of ionic species, or as light-harvesting antennas to improve the absorption of different chromophores (Benstead et al., 2011; Gayathri et al., 2014). In PDT application, fluorescence emission is considered a negative aspect, since absorbed energy upon light activation is directed to the singlet excited PS form. Thus, possible chemical modifications aimed at decreasing fluorescence have been taken into account to increase PS triplet excited state and quantum yield singlet oxygen production. BODIPY dyes are characterised by an excitability around 500 nm of the visible light spectrum, however, compounds absorbing at longer wavelength could be developed by appropriate chemical modifications (Awuah and You, 2012).

In this work, a group of 15 BODIPYs was investigated for their photodynamic activity in the antimicrobial field. All compounds are characterised by a 4,4-difluoro-1,3,5,7-tetramethyl-4-bora-3a,4a-diaza-s-incacene core, modified by the insertion of two iodine atoms in position 2 and 6 by electrophilic aromatic substitution. The iodination converts the highly fluorescent molecule into a potent PS, causing a bathochromic shift of maximum absorption peak in ~30 nm, decreasing fluorescence

properties, and improving singlet oxygen generation (Yogo et al., 2005; Awuah and You, 2012). BODIPYs differ from each other for the substituent in the *meso*-position (position 8), which can be an aromatic ring with an activating or deactivating substituent, holding non-ionic groups or positive charges.

The efficacy of photodynamic treatment through these BODIPYs was assessed on the Gram-positive bacterium *Staphylococcus aureus*, a model microorganism that has recently risen concerns due to its increased resistance to conventional antimicrobial treatments. Furthermore, even if most of the compounds are non-ionic molecules, two other microbial pathogens were included in the study: the Gram-negative bacterium *Pseudomonas aeruginosa*, and the fungal pathogen *Candida albicans* (Alangaden, 2011; Mulani et al., 2019).

In this work, BODIPYs were screened for their ability to bind pathogen cells in view of efficient performance against cell suspensions and, hopefully, microbial biofilms. These structured communities are characterized by intercellular communication and share of "public goods", and behave like a pseudo-multicellular organism (Verderosa et al., 2019). In clinical environments, biofilms are one of the major virulence factors associated with chronic infections, and are very difficult to eradicate (Jamal et al., 2018). Since antimicrobial PDT has been recently reported as a potential antibiofilm strategy (Chanda et al., 2017; Mulani et al., 2019), the effect of PDT with BODIPYs was assessed to target the biofilm of the chosen model pathogens.

2. Materials and methods

2.1 Photosensitizers

A panel of 15 borondipyrromethens (BODIPYs) was employed in this study (table 1). Compounds B1-B9 are characterised by an alkyloxy group on the phenyl ring in 8 position of the BODIPY core, B10-B12 bears halogen atoms on the phenyl ring, and B13-B15 are positively charged. PSs were synthetized as previously described (Caruso et al., 2012, 2017, 2020; Banfi et al., 2013; Zagami et al., 2018; Rugiero et al., 2019), and were dissolved in DMSO at final concentration of 1 mM, and stored at 4°C until needed.

Table 1. List of BODIPYs (B1-B15) used in this study.

BODIPY core		PS	Substituents	Chemical denomination	Ref
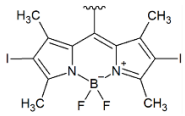	Activated aromatic ring	B1		4,4-Difluoro-2,6-Diiodo-1,3,5,7-Tetramethyl-8-(3'-Methoxyphenyl) -4-Bora-3a,4adiaza-s-Indacene	(Banfi et al., 2013)
		B2		4,4-Difluoro-2,6-Diiodo-1,3,5,7-Tetramethyl-8-(2'-Methoxyphenyl) -4-Bora-3a,4adiaza-s-Indacene	(Caruso et al., 2017)
		B3	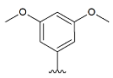	4,4-Difluoro-2,6-Diiodo-1,3,5,7-Tetramethyl-8-(3',5'-Dimethoxyphenyl)-4-Bora-3a,4adiaza-s-Indacene	(Caruso et al., 2017)
		B4	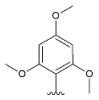	.4,4-Difluoro-2,6-Diiodo-1,3,5,7-Tetramethyl-8-(2',4',6'-Trimethoxyphenyl)-4-Bora-3a,4adiaza-s-Indacene	(Caruso et al., 2017)
		B5	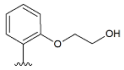	4,4-Difluoro2,6-Diiodo-1,3,5,7-Tetramethyl-8-[2'-(2''-Hydroxyethoxy)Phenyl)]-4-Bora-3a,4adiaza-s-Indacene	(Caruso et al., 2017)
		B6		4,4-Difluoro-2,6-Diiodo-1,3,5,7-Tetramethyl-8-[4'-(4''-Chlorobuthoxy)Phenyl)]-4-Bora-3a,4adiaza-s-Indacene	(Caruso et al., 2017)
		B7		4,4-Difluoro-2,6-Diiodo-1,3,5,7-Tetramethyl-8-{4-[(4-Bromobutyl) oxy]phenyl}-4-Bora-3a,4adiaza-s-Indacene	(Caruso et al., 2020)
		B8	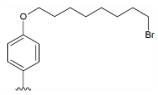	4,4-Difluoro-2,6-Diiodo-1,3,5,7-Tetramethyl-8-{4-[(4-Bromooctyl) oxy]phenyl}-4-Bora-3a,4adiaza-s-Indacene	(Zagami et al., 2018)
		B9		4,4-Difluoro-2,6-Diiodo-1,3,5,7-Tetramethyl-8-(4'-Methoxynaphthalene)-4-Bora-3a,4a-diaza-s-Indacene	(Banfi et al., 2013)
	Deactivated aromatic ring	B10		4,4-Difluoro-2,6-Diiodo-1,3,5,7-Tetramethyl-8-(2',5'-Dibromophenyl)-4-Bora-3a,4a-diaza-s-Indacene	(Caruso et al., 2017)
		B11		4,4-Difluoro-2,6-Diiodo-1,3,5,7-Tetramethyl-8-(2',6'-Dichlorophenyl)-4-Bora-3a,4a-diaza-s-Indacene	(Banfi et al., 2013)
		B12		4,4-Difluoro-2,6-Diiodo-1,3,5,7-Tetramethyl-8-(2',6'-Dichloro-4'-Nitrophenyl)-4-Bora-3a,4adiaza-s-Indacene	(Caruso et al., 2017)
	Monocationic	B13		4,4-Difluoro-2,6-Diiodo-1,3,5,7-Tetramethyl-8-(N-methyl-4-Pyridyl)-4-Bora-3a,4adiaza-s-Indacene	(Caruso et al., 2012)
		B14	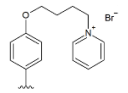	4,4-Difluoro-2,6-Diiodio-1,3,5,7-Tetrametil-8-(4-(4-pyridinobutoxy)phenyl)-4-Bora-3a,4adiaza-s-Indacene	(Rugiero et al., 2019)
		B15	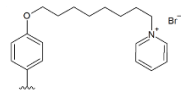	4,4-Difluoro-2,6-Diiodio-1,3,5,7-Tetrametil-8-(4-(4-pyridinooctanoxy)phenyl)-4-Bora-3a,4adiaza-s-Indacene	(Rugiero et al., 2019)

2.2 Microbial strains and culture conditions

Three microbial species were used in this study: *Pseudomonas aeruginosa, Staphylococcus aureus* and the yeast *Candida albicans* (Table 2). The clinical strains of *P. aeruginosa* UR48 and BT1 derived from patients with catheter-associated urinary tract infection (CAUTI and cystic fibrosis (CF), respectively, while *C. albicans* clinical strains were recovered from patients with urinary tract infections. *P. aeruginosa* was cultivated in Luria Bertani (LB) medium, *S. aureus* in Tryptic Soy Broth (TSB) medium, and *C. albicans* in YPD medium (Yeast extract 10 g/L, Peptone 20 g/L, and L-Dextrose 20 g/L). All microbial strains were grown overnight in liquid or solid media (15 g/l agar) at 37°C on an orbital shaker at 200 rpm.

Table 2. List of bacterial and fungal strains used in this study.

Microbial strains	Ref
Pseudomonas aeruginosa	
PAO1	(Stover et al., 2000)
PAO1_pVOGFP	(Orlandi et al., 2018a)
UR48 (clinical strain)	(Orlandi et al., 2011)
BT1 (clinical strain)	(Bragonzi et al., 2006)
Staphylococcus aureus	
ATCC 6538P (MSSA)	
ATCC 43300 (MRSA)	
Candida albicans	
ATCC 14053	
Ca1 (clinical strain)	(Orlandi et al., 2020)
Ca2 (clinical strain)	(Orlandi et al., 2020)

2.3 Light source

The lighting unit employed for the photoactivation of BODIPYs is a Light Emitting Diode (LED) apparatus composed by 12 diodes distributed on a 11 cm diameter disk equipped with a heat sinker. LEDs have a maximum emission peak at

520 nm in the green region of the visible spectrum, suitable for the activation of BODIPYs (figure 1). The system is powered by a 50 W current transformer and the lamp was positioned 35 cm over the samples with a fluence rate of 2,4 mW/cm^2.

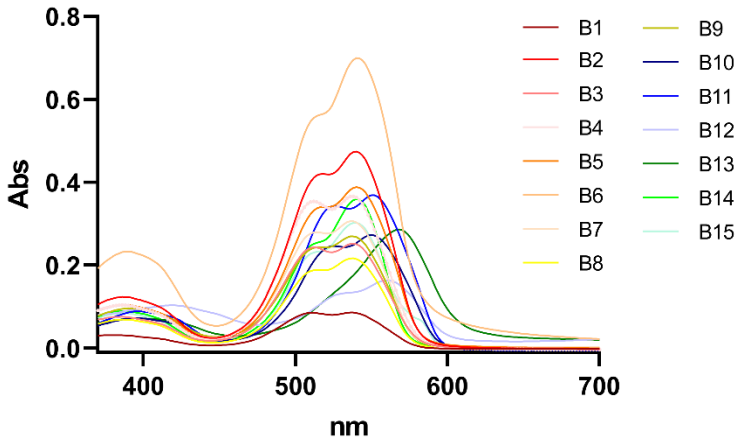

Figure 1. Visible light absorption spectra of BODIPYs (B1-B15).

The irradiation time, specified for each protocol, was modified in accordance with the desired final light dose, as presented in table 3.

Table 3. List of light doses employed in this study and the corresponding irradiation time.

Light dose (J/cm^2)	**Irradiation time (min)**
20	138
30	207

2.4 PDT assays

Photo-spot test

The photo-spot test, previously optimized for *P. aeruginosa* (Orlandi et al., 2018b), was adapted to *S. aureus* and *C. albicans* as follows. In the case of bacteria, *P. aeruginosa* PAO1 and *S. aureus* ATCC6538P were grown overnight, and the cultures were 10-fold serially diluted from ~10^9 to ~10^4 CFU/mL in 96-well plates, in phosphate buffer saline (PBS - KH_2PO_4/K_2HPO_4 10 mM, pH 7.4). *C. albicans* ATCC14053 overnight cultures were centrifuged (4000 rpm for 10 min) and cells were suspended in 1/10 volume of sterile 1X PBS to reach a cellular concentration of

~10^8 colony forming unit per millilitre (CFU/mL). The obtained yeast suspensions were 10-fold serially diluted in 1X PBS to obtain samples with decreasing concentrations, from ~10^8 to ~10^3 CFU/mL.

PSs (10 µM for *P. aeruginosa* and *C. albicans,* and 1 µM for *S. aureus*) were added to diluted and undiluted samples of bacterial and fungal strains. Untreated and DMSO treated samples were included as controls. The final concentration of DMSO control is in accordance with both the stock solution of each PS and the amount of administered PS in each sample. Plates were incubated in the dark to avoid photoactivation of PSs and to allow the interaction between cells and BODIPYs. After 10 min, 1 h or 6 h of dark incubation, a volume of 5 µl of each sample was spotted on agar plates by replica plating, to obtain samples with decreasing cell density (bacterial strains from ~ 10^7 to ~10^2 CFU/spot; yeast strain from ~ 10^6 to ~10 CFU/spot).

Samples were irradiated under 520 nm green light to activate PSs with a light dose of 20 J/cm^2 for 138 min and a corresponding set of plates was kept in the dark to evaluate the intrinsic toxicity of BODIPYs. After incubation at 37°C, results were recorded as Log values of the highest cell concentration at which growth was inhibited (i.e: a Log value of 1 corresponds to inhibition of 10 CFU/spot etc.). High Log values were assopciated with efficient antimicrobial activity. Photo-spot tests were performed at least in triplicate for all the microbial strains and PSs, and the average values of growth inhibition were expressed as Log units and summarized in the corresponding tables.

PDT on suspended cells

Upon overnight growth of microbial strains (*P. aeruginosa* PAO1, *S. aureus* ATCC6538P, and *C. albicans* ATCC14053), cells were tenfold diluted in sterile water, to reach concentrations of 10^8 or 10^6 CFU/mL for bacterial and fungal strains, respectively. PDT experiments were performed in 12-well plates, with 1 mL of cellular suspension per well, in the presence of the corresponding BODIPYs (10 µM for *P. aeruginosa* and *C. albicans,* and 1 µM for *S. aureus,* respectively). Untreated cells, DMSO-treated cells and corresponding dark controls were also included. Soon

after irradiation with green light at 20 J/cm^2 for 138 min, samples were assayed for cell viability with the viable count technique. Agar plates were incubated at 37°C and the cellular concentration (CFU/mL) was calculated accordingly. PDT experiments were performed at least in triplicate for each strain and PS.

2.5 Antibiofilm photodynamic treatment

The activity of the different BODIPYs in inhibiting and/or eradicating biofilms was assayed for the model pathogens *P. aeruginosa, S. aureus* and *C. albicans*. In inhibition experiments, cells were treated with the PS and, upon 1 h of dark incubation at 37°C, were irradiated with green light and subsequently incubated at 37°C for 24 hours. In the latter case, 24-hour mature biofilms were treated with the PS, avoiding any modification of the biofilm environment, except for PS administration and, upon 1 hour of dark incubation, irradiated with green light. The following control samples were included: +PS -light, -PS +light, and -PS -light. To exclude any interference of the solvent, dark and irradiated controls with DMSO were included in each experiment.

Biofilms of *P. aeruginosa* PAO1 and clinical strains UR48 and BT1 were obtained in 12-well plates upon 24 h of growth at 37°C in M9 minimal medium added with glucose (10 mM) and casamino acids (0.2% V/V) as carbon sources. Overnight inoculum of *P. aeruginosa* was diluted 1:500 in fresh medium, reaching a concentration of 10^7 CFU/mL. BODIPYs were added at a final concentration of 40 μM, and biofilm photoinactivation was performed with 520 nm green light with a fluence of 30 J/cm^2 (2,4 mW/cm^2, 207 min).

The same growth conditions were used for *S. aureus* ATCC6538P and ATCC43300. BODIPYs were used at a final concentration of 0,5 μM and green light was delivered at a final light dose of 20 J/cm^2 (2,4 mW/cm^2, 138 min).

C. albicans ATCC14053 and Ca1, Ca2 clinical strains were grown ON at 37°C in YPD medium. After centrifugation at 4000 rpm for 10 min, cells were 100-fold diluted in sterile water, and 250 μL samples were aliquoted in 24-well plates. Cells were treated 1 h in the dark at 37°C with BODIPYs (20 μM) and incubated in the dark or irradiated with 520 nm light (30 J/cm^2, 207 min). After addition of 250 μL of

YPD medium, samples were incubated at 37°C for 24 h, to allow biofilm formation. The following experimental setup was used to assay the eradication activity on *C. albicans* ATCC14053 biofilms: overnight cultures were 100-fold diluted in fresh YPD medium. A volume of 500 µL of yeast suspensions were placed in 24-well plates and incubated for 24h at 37°C for biofilm growth. Planktonic population was removed with exhausted medium to avoid any possible interference of the organic matter during PDT assay. After filling with a suitable volume of sterile 1X PBS, BODIPYs were added at a final concentration of 40 µM. Upon 1 h of dark incubation with at 37°C, samples were irradiated (30 J/cm^2 for 207 min) or dark incubated. Experimental results were analysed as detailed in the following paragraph.

Total biomass production was quantified after staining with crystal violet solution (0,1% W/V for 20 min) upon removal of planktonic phase and a gentle wash with 1X PBS. Cell viability of planktonic (CFU/mL) and adherent (CFU/well) phases were calculated by the viable count method. After collection of the planktonic phase and gentle rinsing with 1 ml of 1X PBS, adherent biomass was collected by scraping.

2.6 Confocal microscope analyses

P. aeruginosa

Antibiofilm activity of BODIPYs was analysed by confocal microscopy using PAO1_pVOGFP strain, which espresses GFP recombinant protein ubder the control of pBAD arabinose inducible promoter. PDT protocols for biofilm inhibition and eradication, previously explained in paragraph 2.5, were applied to PAO1_pVOGFP biofilms. Coverslip glasses positioned in 35 mm Petri dishes, were used as supports for biofilm adhesion and visualization at the microscope. Upon photodynamic treatment and biofilm growth, supernatant was removed from the plates and GFP expression was induced for 1 h at 37°C, by the addition of fresh medium containing 0,1% W/V arabinose. The coverslip was placed on a microscope glass slide for the acquisition of the adherent biofilm images. All microscope analyses were performed on a Leica TCS SP5 confocal laser scanning microscope (CLSM; Leica Microsystems, Wetzlar, Germany) with 488 nm laser excitation. Images were obtained using a 63x objective lens with 3x magnification if required. Simulated 3D

images of *P. aeruginosa* biofilm were generated using the free open-source software ImageJ (National Institute of Health, USA).

C. albicans

BODIPYs affinity to *C. albicans* was also exploited for yeast cell fluorescence imaging in confocal microscope analyses after PDT. After treatment as detailed in paragraph 2.4, *C. albicans* ATCC14053 cells were centrifuged (10000 rpm, 5 min); pellets were pooled and resuspended in sterile 1X PBS. A fluorescent BODIPY dye (4,4-difluoro-1,3,5,7-tetramethyl-8-(2-methoxyphenyl)-4-bora-3a,4a-diaza-s-indacene) was added to the yeast suspension (2 μM) (Sunahara et al., 2007), and cells were incubated with the fluorochrome for 30 min at 37°C on a shaker at 50 rpm. Afterwards, samples were centrifuged 10000 rpm for 10 min and pellets suspended in 20 μL of 1X PBS. Samples of 10 μL were analysed with CLSM. Experiments were performed at least in triplicate. Images were recorded using a 63x objective lens (488 nm laser) with 5x magnification when required. Editing was performed with the free open-source programme ImageJ. To assess the efficacy of the photodynamic treatment, cell viability was checked trough the viable count technique described previously.

2.7 Binding assay

All the photosensitizers were tested for their ability to bind to bacterial and yeast cells. Upon overnight growth of microbial strains (*P. aeruginosa* PAO1, *S. aureus* ATCC6538P, *C. albicans* ATCC14053), appropriate volumes of cell cultures were centrifuged at 5000 rpm for 10 minutes. After supernatant removal, pellets were resuspended in sterile water and 10-fold diluted and BODIPYs (10 μM) were added to the cell suspensions. Control samples were included as follows: untreated cells, PSs alone, and cells added with DMSO 4% (V/V). All the samples were incubated in the dark at 37°C for 1 h, to allow the interaction between PS and cells. To exclude any possible toxicity of PSs, cell viability was assessed upon dark incubation colony count method. After dark incubation, samples were centrifuged (10000 rpm for 5 min) and the visible spectra of the supernatants were recorded (k = 380 – 700 nm). A

calibration plot (μM concentration *vs* OD_x) was obtained for each PS. The amount of free PS was calculated by interpolating the data on the calibration plot. Experiments were performed in triplicate for *P. aeruginosa, S. aureus* and *C. albicans* and percentage values of bound PSs were calculated accordingly.

In table 4, a summary of BODIPY concentrations and light doses employed for each microbial strain and each experimental procedure – photo-spot test, binding assay, PDT on suspended cells, biofilm inhibition and biofilm eradication – is illustrated.

Table 4. Summary of BODIPY concentrations and light doses of green light employed in this study for each type of experiment.

[PS] (μM) Light dose (J/cm^2)	**Photo-spot test**	**Binding assay**	**PDT on suspended cells**	**Biofilm inhibition**	**Biofilm eradication**
P. aeruginosa	10 μM 20 J/cm^2	10 μM	10 μM 20 J/cm^2	40 μM 30 J/cm^2	40 μM 30 J/cm^2
S. aureus	1 μM 20 J/cm^2	10 μM	1 μM 20 J/cm^2	0.5 μM 20 J/cm^2	0.5 μM 20 J/cm^2
C. albicans	10 μM 20 J/cm^2	10 μM	10 μM 150 J/cm^2	20 μM 30 J/cm^2	40 μM 30 J/cm^2

2.8 Statistical analyses

Photoinactivation experiments on suspended cells and biofilms were performed at least in triplicate with independent microbial cultures. Statistical analyses were assessed by one-way ANOVA.

3. Results

3.1 Effect of BODIPYs on microbial cells viability

Fifteen novel BODIPYs, synthetized by our group, were assayed against three model microbial species: the Gram-negative bacterium *P. aeruginosa*, the Gram-positive bacterium *S. aureus* and the pathogenic yeast *C. albicans*.

BODIPYs (B1-B15) employed in the study have the typical indacene core characterised by four methyl groups in position 1,3,5,7, and two iodine atoms in positions 2,6 aimed at decreasing fluorescence and increasing quantum yield production of singlet oxygen. A phenyl group, in *meso*-position, carries different

substituents that characterize each molecule. PSs were firstly divided according to their total charge: B1-B12 are non-ionic molecules, while B13-B15 are monocationic compounds. Non-ionic PSs were also grouped according to the type of substituents on the aromatic ring in *meso*-position. B1-B9 are molecules with activating groups, while B10-B12 carry deactivating substituents on the benzyl group. The first group (B1-B9) includes compounds with alkyloxy-phenyl substituents. Methoxy groups are present in position 3' and 2' for B1 and B2 respectively, while in position 3',5' in B3, and 2',4',6' in compound B4. B5 holds a 2″-hydroxyethoxy group in position 2'. Compound B6 carries a 4''-chlorobutoxy group in position 4, while B7 holds the same alkyloxy chain with bromine at the end of the carbon chain. B8 is similar to compound B7 but has a C8 chain instead of C4 chain. BODIPY B9 differs from all the other compounds since presents a 4'-methoxynaphtalene in *meso*-position. PSs with deactivating groups on the aromatic ring are characterized by bromine atoms in 2',5' positions (B10) or chlorin atoms in 2',6' positions (B11). Compound B12 differs from B11 only for the presence of a nitro group in 4' position. Monocationic BODIPYs carry a pyridyl group that confer the positive charge. B13 has a N-methyl-4'-pyridiyl substituent in *meso*-position, while in B14 and B15 the pyridyl group is positioned at the end of a C4 (B14) or C8 (B15) alkyloxy chain.

During the photodynamic process, the PS should demonstrate the desired photo-toxicity upon light treatment, but an intrinsic toxicity of PS in the dark should be avoided. Therefore, an initial screening survey was aimed at highlighting possible toxic compounds. The same PS concentration (10 μM for *P. aeruginosa* and *C. albicans* and 1 μM for *S. aureus*) was tested at decreasing cell concentrations of bacteria and yeasts, and cell viability was detected upon 10 minutes, 1 and 6 hours of dark incubation (figure 2).

The Gram-negative bacterium *P. aeruginosa* was almost insensitive to non-ionic BODIPYs even after the highest incubation time (6 h), while a certain degree of toxicity was observed for two cationic PSs. Upon 6 hours of incubation, B13 and B14 showed an inhibitory effect of 3 and 1.6 Log_{10} units, respectively.

The Gram-positive bacterium *S. aureus* was sensitive to BODIPYs administered at 10 μM (data not shown), therefore a concentration of 1 μM was chosen. A reduction

of about two Log Unit was observed only for non-ionic PSs B1, B5, B7, B8 and B12 at the highest incubation time, and a stronger inactivation was observed for compound B9 at the highest incubation time (10^4 CFU/spot). Among cationic compounds, B14 showed an average value of 2.3 Log_{10} reduction upon 6 hours of incubation.

The majority of non-ionic BODIPYs did not display any intrinsic toxicity against yeast cells, even at the longest incubation time in the dark, except for B1, B2 and B9 compounds that inhibited cell growth at very low concentrations (between 10 and 10^2 CFU/spot). On the contrary, all monocationic molecules displayed a certain degree of toxicity. B13 and B15 inhibited the growth of cell populations with 10 and 10^2 CFU/spot respectively upon 6 hours of incubation. A higher toxicity was observed in the presence of B14 that showed a certain degree of inhibition upon 10 minutes of incubation. Upon 6 hours of dark incubation, B14 prevented the growth of population with more than 10^3 CFU/spot.

		P. aeruginosa PS [10 µM]				*S. aureus* PS [1 µM]				*C. albicans* PS [10 µM]			
PS		Log_{10} reduction			Spot test images (6 h incubation) CFU/spot	Log_{10} reduction			Spot test images (6 h incubation) CFU/spot	Log_{10} reduction			Spot test images (6 h incubation) CFU/spot
Incubation time		10′	1 h	6 h	10^7 10^6 10^5 10^4 10^3 10^2	10′	1 h	6 h	10^7 10^6 10^5 10^4 10^3 10^2	10′	1 h	6 h	10^6 10^5 10^4 10^3 10^2 10
	Untreated	0	0	0		0	0	0		0	0	0	
	Solvent ctrl	0	0	0		0	0	0		0	0	0	
Activated aromatic ring	**B1**	0	0	0		0	0.6	2.5		0	0.3	1.5	
	B2	0	0	0		0	0	0		0	0	1	
	B3	0	0	0		0	0	0		0	0	0	
	B4	0	0	0		0	0	0		0	0	0	
	B5	0	0	0		0	0	1.3		0	0	0	
	B6	0	0	0		0	0	0		0	0	0	
	B7	0	0	0		0	0.6	2.3		0	0	0	
	B8	0	0	0		0	0	2		0	0	0	
	B9	0	0	0		2	3	4		0	1.6	2	
Deactivated aromatic ring	**B10**	0	0	0		0	0	0		0	0	0	
	B11	0	0	0		0	0	0		0	0	0	
	B12	0	0	0		0.5	0.5	1.3		0	0	0	
Monocationic	**B13**	0.6	0.6	3		0	0	0		0	0	1	
	B14	0	0	1.6		1.3	2	2.3		1.3	3	3.3	
	B15	0	0	0		0	0	0		0	0	2	

Figure 2. Intrinsic toxicity of BODIPYs (B1-B15) at 10 µM against *P. aeruginosa* PAO1 and *C. albicans* ATCC14053, and 1 µM against *S. aureus* ATCC6538P cells, upon 10 min, 1 and 6 hours of dark incubation. Log_{10} reduction values represent the average of at least three independent experiments. Every third column represents spot test images upon 6 h of dark incubation for each microbial strain.

The interaction between microbial cells and PSs, essential for photo-oxidative damage, was investigated by a binding assay upon 1 hour of incubation in the presence of 10 µM BODIPYs (figure 3).

The majority of non-ionic BODIPYs (B1-B12) showed a low biding performance with *P. aeruginosa* cells (less than 20%), except for B5 and B6 with a binding yield around 35%. Similar outcomes were obtained in the case of *C. albicans* yeast, where higher binding values are shown by B2 and B5 BODIPYs (27 and 35% respectively). The interaction of non-ionic PSs with the Gram-positive bacterium *S. aureus* showed a binding yield higher than 60%, except for B12 with an interaction around 25% (figure 3B).

Positively charged compounds (B13-B15) were more prone to interact with Gram-negative and yeast cells than non-ionic ones. When considering *P. aeruginosa*, compounds B14 and B15 reached values of interaction around 72%, while 78% and 56% binding yields were obtained in *C. albicans* for B14 and B15, respectively. The cationic molecule B13 showed lower values of interaction if compared to B14 and B15. With *S. aureus*, the same outcomes emerged from the binding assays of cationic compounds. B14 and B15 displayed binding affinities higher than, while B13 interacted with a considerably lower yield of about 50%.

In general, non-ionic BODIPYs seemed to be less prone to interact with Gram-negative bacteria and yeasts, while cationic PSs reached very high percentages of binding in these experimental conditions. A good degree of interaction was reached by BODIPYs and the Gram-positive bacterium *S. aureus,* independently of their total charge.

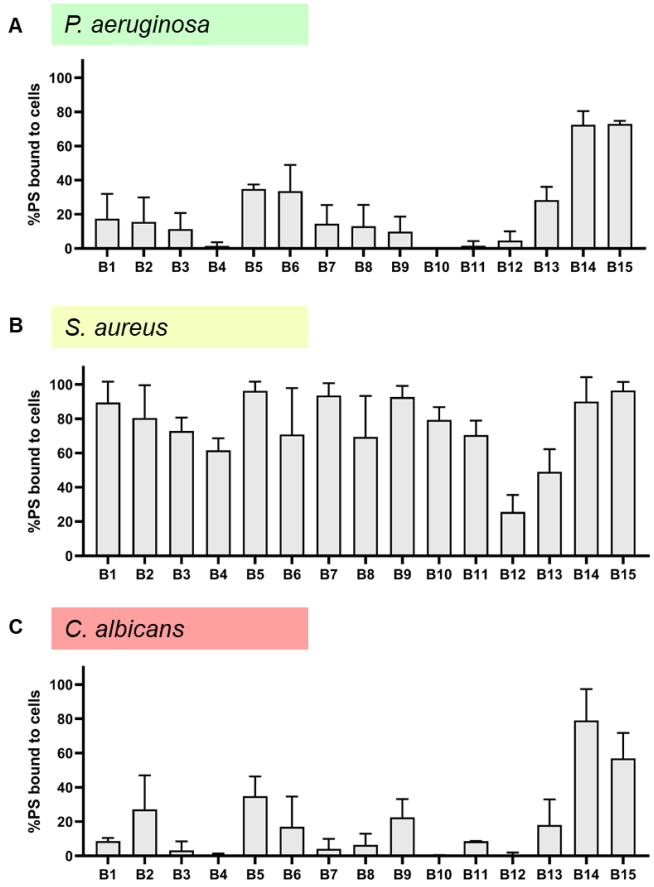

Figure 3. Binding assay of BODIPYs (B1-B15) to *P. aeruginosa* PAO1 (A), *S. aureus* ATCC6538P (B) and *C. albicans* ATCC14053 (C) cells. Untreated and solvent-treated samples were also included in the experiments. Values are presented as a percentage of PS bound to cells upon 1 h of dark incubation of BODIPYs and microbial cells. PSs were administered at a concentration of 10 μM.

3.2 Photodynamic activity of BODIPYs

BODIPYs were further investigated for their potential of inducing photo-damage on *P. aeruginosa, S. aureus* and *C. albicans* cells upon light activation; PSs characterized by any intrinsic toxicity (more than 1 Log_{10} reduction) were discarded from following analyses. A source of green light at 520 nm (20 J/cm^2) was chosen for the activation of BODIPYs, that are characterized by a maximum absorption peak in the green region of the visible light spectrum, and irradiation was performed after 1 h of dark incubation of cells and PSs. Control samples with separate light or DMSO treatments were included for each microbial strain (figure 4).

Non-ionic BODIPYs B2, B5, B7 and B9 administered to *P. aeruginosa* had a certain effect on cell viability upon activation by green light (figure 4A). In fact, the most active compound was B2 that inhibited the growth of a population of almost 10^6 CFU/spot, while 4.3 Log unit reduction were observed in the case of B5 and B9. A slight effect was ascribable to BODIPY B7 that had a mean value of 1 Log_{10} reduction. Non-ionic BODIPYs with deactivated aromatic ring as substituent in *meso*-position (B10-B12) did not have any photodynamic effect on *P. aeruginosa* cells. Finally, the only non-toxic cationic compound B15 caused a reduction of population vitality of about 2.6 Log units.

The Gram-positive bacterium *S. aureus* showed a higher sensitivity to BODIPYs and good rates of inhibition were obtained with one tenth concentration (1 μM) of PSs if compared to the Gram-negative species *P. aeruginosa*. Indeed, all non-ionic compounds had an anti-Staphylococcal activity since they were able to inhibit the growth of at least 10^4 CFU/spot, and the best performances were obtained with B5 compound, characterized by an activated aromatic ring as substituent, with a Log reduction mean value of 7 units, reaching the maximum detection limit of the system. The two positively charged PSs B13 and B15 showed different behaviours. The first appeared to be almost inactive (1.3 Log_{10} reduction), while the latter had a good rate of killing of populations with more than 10^5 CFU/spot.

Non-ionic PSs showed a different degree of photoinactivation of *C. albicans* cells. The yeast was almost insensitive to B3, B4 and B6 compounds (1 Log unit reduction), and completely insensitive to B11 (figure 4C). Better rates of inactivation were obtained with B2, B5 (5 Log units reduction) and B7 (6.3 Log_{10} reduction). A certain activity was displayed by the other non-ionic molecules (B8, B10 and B12), and also by the cationic compound B13 (4.6 Log_{10} reduction).

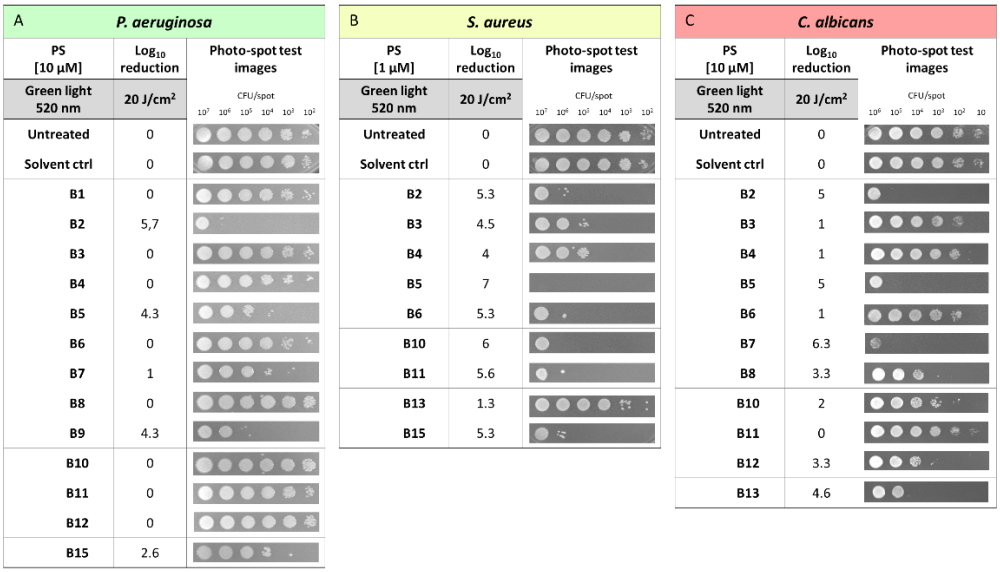

Figure 4. Photodynamic activity of BODIPYs on *P. aeruginosa* PAO1 (A), *S. aureus* ATCC6538P (B) and *C. albicans* ATCC14053 (C) cells evaluated by the photo-spot test method. BODIPYs (B1-B15) were administered at a concentration of 10 µM for *P. aeruginosa* and *C. albicans* and 1 µM for *S. aureus*. Untreated and solvent-treated samples were also included in the figure as controls. Values of Log_{10} reduction were observed after irradiation with 520 nm light at radiant exposures of 20 J/cm^2, after 1 h of dark incubation of cells and PS. Data are the mean of at least three independent experiments. Representative photo-spot test pictures are illustrated in every third column.

Further investigations on the photodynamic effect of BODIPYs were performed on suspended cultures of *P. aeruginosa, S. aureus* and *C. albicans*. The preliminary screening ruled out PSs with intrinsic toxicity and a low photoactivity for each pathogen. Thus, only BODIPYs that showed strong photoinactivation rates (>2 Log_{10} for P. *aeruginosa* and *C. albicans,* and >5 Log units for *S. aureus*) were used in further trials with suspended cells. Experimental conditions were identical to those of the previous photo-spot test, with a final light dose of 20 J/cm^2 and a PS concentration of 10 µM for *P. aeruginosa* and *C. albicans* and 1 µM for *S. aureus.* As illustrated in figure 5, all the strains were insensitive to green light irradiation, and DMSO solvent concentration did not show toxic effects neither in the dark, nor upon light irradiation. *P. aeruginosa* resulted the most resistant microorganism to photoinactivation by BODIPYs, and only one compound (B9) was active against this pathogen. P9 caused a significant decrease of 4 Log units in PAO1 population, reaching 10^4 CFU/mL upon PDT treatment, and no dark toxicity of the PS was observed. The other non-ionic PSs

B2 and B5 did not show any photodynamic effect on suspended cultures, as well as the treatment with the monocationic compound B15 (figure 5A).

The Gram-positive bacterium *S. aureus* was treated with both non-ionic (B2, B5, B6, B10, B11) and monocationic BODIPYs (B15). None of the tested compounds was toxic in dark conditions, while all of them caused a significant Log reduction in *S. aureus* cultures upon irradiation. B2 and B5 caused the highest reduction rate in cell vitality (6 Log units) reaching the lowest detection limit of the system (10^2 CFU/mL). B6, B10, B11 and B15 caused the depletion of *S. aureus* populations of about 4 Log units. Thus, from this preliminary screening, non-ionic BODIPYs B2 and B5 were considered for subsequent analyses on *S. aureus* biofilm.

C. albicans PDT treatment with both non-ionic (B2, B5, B7, B8, B12) and positively charged (B13) BODIPYs significantly reduced the yeast viability up to the detection limit of the system (10 CFU/mL), showing a very high inactivation rate (figure 5C).

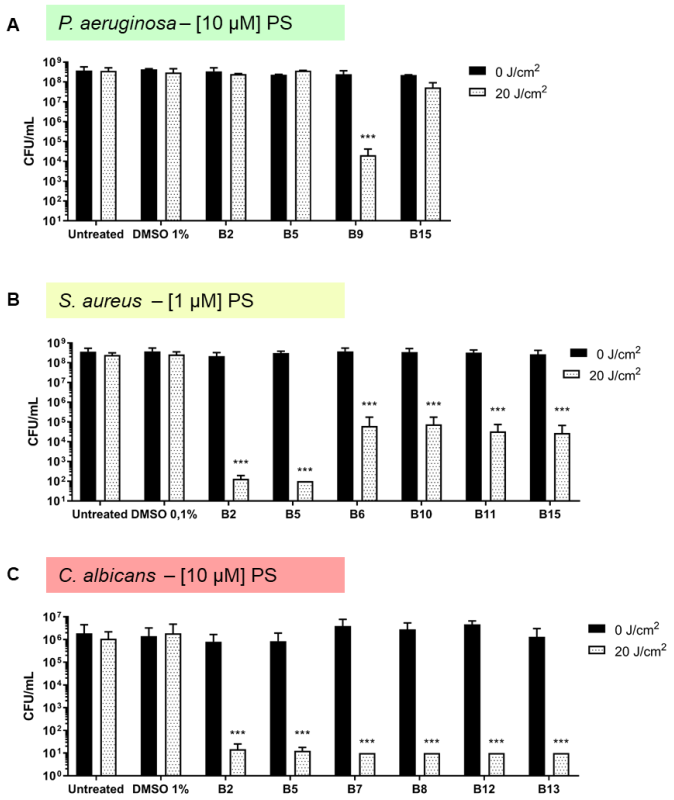

Figure 5. Photodynamic inactivation of *P. aeruginosa* PAO1 (A), *S. aureus* ATCC6538P (B) and *C. albicans* ATCC14053 (C) cells in suspension by BODIPYs. PS concentration was 10 µM *P. aeruginosa* and *C. albicans* and 1 µM for *S. aureus*. Experimental samples were irradiated by 20 J/cm^2 of green light. Values referring to control samples are presented as black bars, and irradiated samples with dotted bars. Untreated and solvent-treated samples (DMSO) were also included for each pathogen. Values, presented as CFU/mL, are the mean of at least three independent experiments, and the bars represent standard deviations. Statistical analyses were performed by one-way ANOVA (*** p <0.0001).

To highlight the effects of the photodynamic treatment with BODIPYs on *C. albicans* cell morphology, PDT-treated yeast cells were analysed by confocal laser scanning microscopy (figure 6). *C. albicans* cells showed the typical compartmentalization of eukaryotic cells, with the largest compartment, compatible with the nucleus, appearing dark and not permeable to the fluorophore. The irradiation of yeasts with green light in the absence of PSs and the treatment with DMSO in the dark and upon irradiation did not impair cell integrity, since samples were comparable to untreated ones. Notably, also the dark incubation of non-ionic and monocationic BODIPYs did not alter the yeast architecture (Figure 6 e,g,i,m,o,q). A visible change in probe distribution was observed after PDT treatment with all the tested BODIPYs. No

organelles were recognizable in fungal cells since a foggy signal of the fluorescent probe was equally distributed in all the cell volume, and a peculiar accumulation of the tracer was clearly visible in a central region of the cytoplasm. Moreover, cells appeared to be egg-shaped and not spherical as in the controls, and cell dimensions seemed to decrease upon photodynamic treatment if compared to control samples. This evident alteration of cell structure as a possible result of PDT treatment PDT is compatible with the loss of cell viability previously outlined by the viable count.

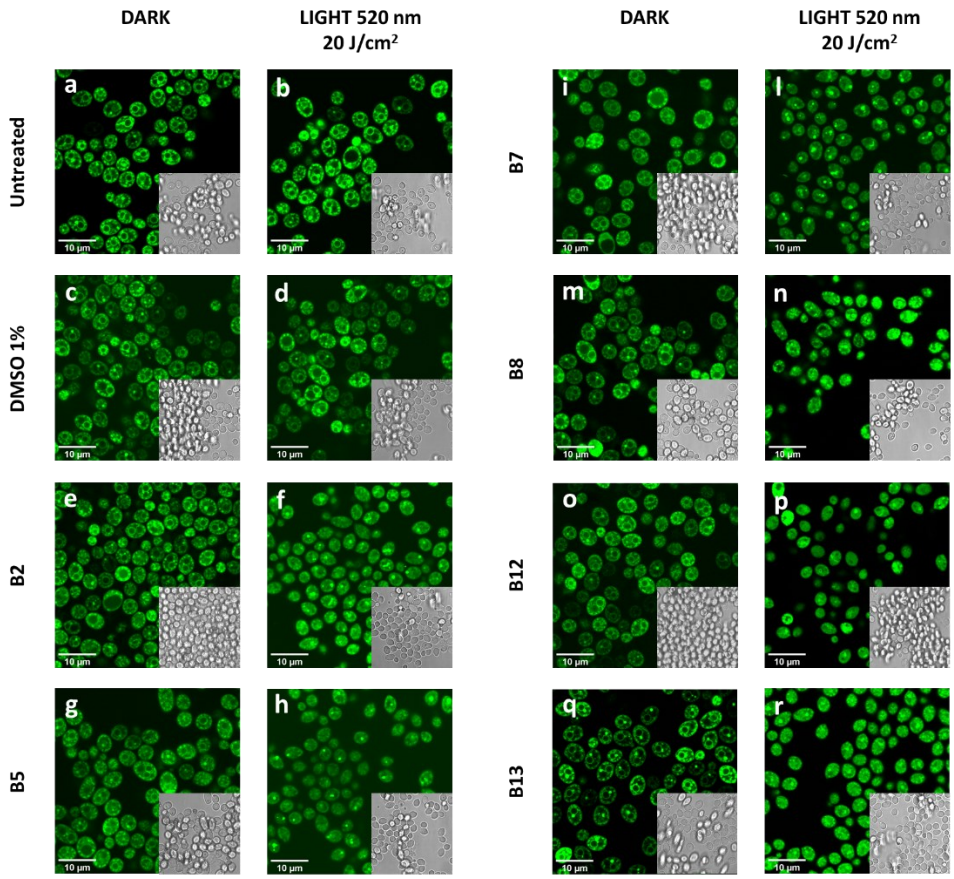

Figure 6. Confocal microscopy analyses of *C. albicans* ATCC14053 cells upon photodynamic treatment with BODIPYs B2, B5, B7, B8, B12, and B13 (10 µM) activated by green light (20 J/cm^2). Untreated samples and cells treated with 1% DMSO are also included. Dark incubated samples are presented in panels (a), (c), (e), (g), (i), (m), (o), and (q), while light-treated samples are presented in panels (b), (d), (f), (h), (l), (n), (p) and (r). Scale bar = 10 µm.

3.3 BODIPYs photodynamic treatment of *P. aeruginosa* biofilms

Photodynamic therapy driven by BODIPYs was considered as a possible strategy to target pathogen microbial communities. The inhibition of biofilm formation by the Gram-negative bacterium *P. aeruginosa* was firstly examined (figure 7). For this purpose, the assay was limited to compounds B9, which showed good outcomes on PAO1 suspended cultures. In addition to the wild-type strain, two clinical strains (UR48 and BT1), known to be biofilm hyperproducers, were included in the study. *P. aeruginosa* UR48 derives from a CAUTI patient, while BT1 strain was isolated from the sputum of a CF patient.

Total biomass production, quantified as OD 590 nm after crystal violet staining for untreated samples was about 6, 10 and 22 for PAO1, UR48 and BT1 strains, respectively (figure 7A,D,G). Nevertheless, comparable cell densities of planktonic and adherent populations of these samples were detected. The administration of DMSO solvent caused a notable increase in total biomass production for PAO1 and UR48 strains, but no changes in suspended (CFU/mL) and adherent cells (CFU/well) were observed, suggesting that DMSO could specifically affect biofilm matrix production. For all the tested strains, irradiation under green light did not cause any toxicity in control samples (untreated and DMSO-treated samples). The treatment of *P. aeruginosa* PAO1 with BODIPY B9 40 μM did not alter biofilm formation in the dark, but a significant decrease in adherent biomass production was observed upon light treatment. Indeed, OD590 values were reduced of 96% compared to B9 dark control. Good rates of biomass inhibition were reached also in the case of clinical isolates, where B9 caused a depletion of biofilm production of about 86 and 92% for UR48 and BT1, respectively.

The adherent and planktonic phases of biofilm were impaired by photodynamic treatment with B9 since a significant difference in cell count was detected in PDT-treated samples as compared to controls. A decrease of at least 5 Log units was detected in adherent (CFU/well) and planktonic (CFU/mL) populations of PAO1 and UR48 strains. Interestingly, BT1 populations were the most sensitive to photodynamic treatment, since the reduction in cell viability reached the detection limit of the experimental set up (10^2 CFU/well or CFU/mL) (figure 7H,I).

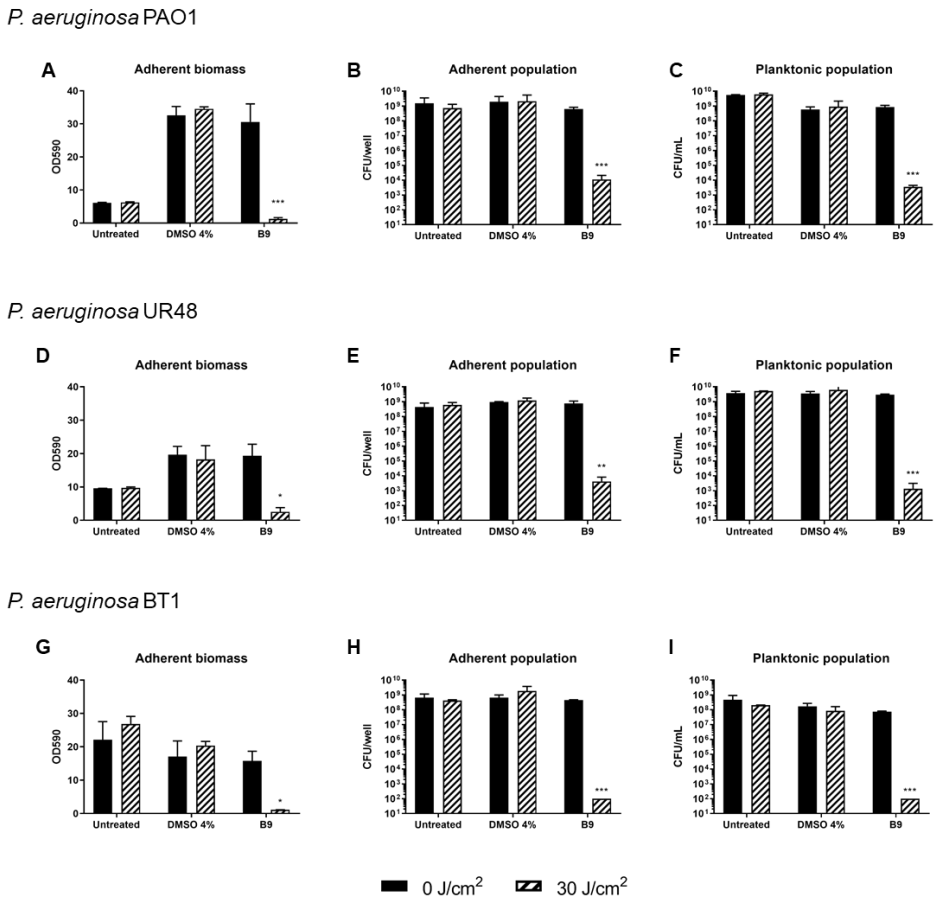

Figure 7. Inhibition of biofilm formation by *P. aeruginosa* PAO1 (A,B,C), UR48 (D,E,F) and BT1 (G,H,I) upon photodynamic treatment with BODIPYs. B9 (40 μM) was activated by green light at 30 J/cm^2. The graphs report values of the absorbance at 590 nm (OD 590) of biofilm after staining with crystal violet (A,D,G), values of adherent population viability (CFU/well) (B,E,H), and planktonic population viability (CFU/mL) (C,F,I). Dark control samples are presented as black bars and light-treated samples as striped bars. Data represent the mean of at least three independent experiments ± standard deviation. Statistical analyses were performed by one-way ANOVA (*$p < 0.05$; **$p < 0.01$; ***$p < 0.0001$).

BODIPYs activity on *P. aeruginosa* biofilms was also investigated by confocal microscopy analyses. A PAO1_pVOGFP strain was exposed to PDT with B9 and biofilm was grown on microscopy glasses. Subsequently, GFP expression was induced and pictures of the adherent populations were acquired by CLSM (figure 8). Images of dark control samples show adherent cells expressing GFP with a volume thickness of 8 μm, while no toxicity was observed in samples exposed to green light

alone, where a comparable adherent biomass is present. DMSO (4% V/V) did not impair cells physiology in both dark and light exposed samples since a clearly detectable GFP fluorescence is visible in the pictures (figure 8 b, d). However, elongated cells could be observed in the sample exposed to light and DMSO, suggesting a certain degree of suffering of PAO1 cells. Still, no decrease in cell viability was observed in these samples compared to control ones. Interestingly, DMSO treated samples in both dark and light conditions show a biofilm thickness of 15 µm, higher than that measured for untreated samples. This outcome could agree with previous observations of probable DMSO enhancement of biofilm matrix production. Incubation with B9 PS in the dark, induced comparable levels of biofilm production as DMSO treatment, but a higher fluorescent signal was visible instead (figure 8e). This effect could be due to a possible residual intrinsic fluorescence of the B9 BODIPY molecule, that can be detected by the 488 nm laser during confocal images acquisition. Upon photodynamic treatment of PAO1 cells, a much lower GFP fluorescent signal was visible (figure 8f). This could be explained either by a significant impairment in the structure of existing biofilms or with the survival of a few living cells, still expressing a functional GFP protein.

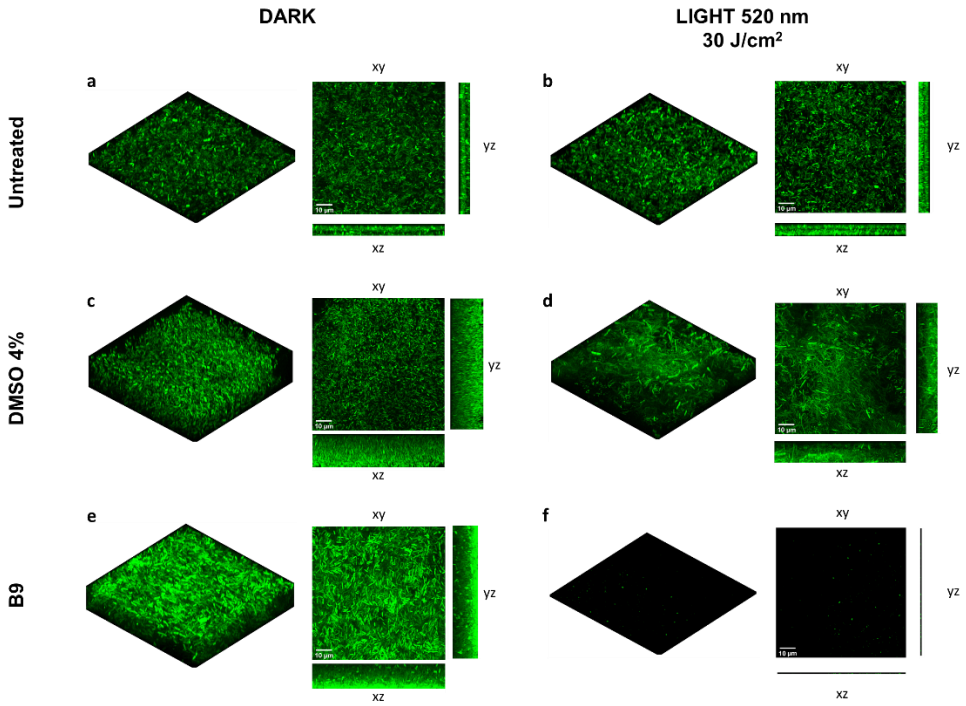

Figure 8. Inhibitory effect on biofilm formation by *P. aeruginosa* PAO1_pVOGFP by BODIPY B9. PAO1_pVOGFP cells were treated with B9 (40 µM) and irradiated by 520 nm light at 30 J/cm^2. Biofilms (24h) of untreated and DMSO-treated samples were included in the experiment. Dark controls are shown in panels a,c,e, while irradiated samples in panels b,d,f. Images of biofilms are shown in volume view, and in xy, xz and yz projections. Scale bar = 10 µM.

Eradication of mature biofilms is the most arduous challenge in the antimicrobial field, therefore, the effect of photodynamic treatment with non-ionic BODIPY B9 was evaluated on 24h-old PAO1 biofilms (figure 9). PDT experimental conditions were set as follows: upon 24 hours of biofilm growth, B9 (40 µM) was gently administered to the samples, without modifying the biofilm environment, and upon one hour of dark incubation, samples were irradiated with 520 nm green light (30 J/cm^2). Dark and DMSO-treated controls were included in each experiment. As shown in figure 9A, the total adherent biomass did not significantly change upon DMSO or B9 administration, in both light and dark conditions, as compared to the untreated dark samples. It seemed that, upon photodynamic treatment, the total biomass slightly increased, but not in a statistically significant way. However, the activation of B9 by green light caused a significant depletion of 5 and 4 Log units in

adherent and planktonic populations, respectively (figure 9B,C). These results suggested a potential antibiofilm effect of the non-ionic BODIPY B9 on PAO1 cells, but no effect of PDT was observed on the amount of biofilm matrix.

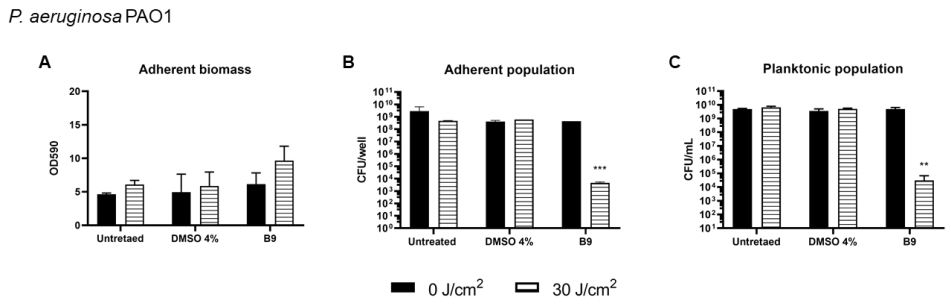

Figure 9. Eradication of *P. aeruginosa* PAO1 biofilm by BODIPY B9 (40 μM). Adherent biomass of biofilm upon PDT is represented as OD590 (A) and cell viability is expressed as CFU/well for adherent population (B) and as CFU/mL for planktonic biomass (C). Bars represent standard deviations. Statistical analyses were performed by one-way ANOVA (**$p < 0.01$; ***$p < 0.0001$).

Biofilm eradication was also evaluated by confocal microscope analyses. *P. aeruginosa* PAO1-pVOGFP biofilm was grown on microscope glasses, treated with 40 μM B9 and irradiated by 30 J/cm^2 of green light. Upon irradiation, GFP expression was induced and images were acquired at CLSM (figure 10). Similar fluorescent signals and biofilm thickness were observed in control samples kept in the dark (untreated and DMSO-treated samples), as well as in irradiated ones. The treatment of biofilm with the BODIPY B9 in the dark slightly decreased biofilm volume, but a notable number of cells were still alive and could express functional GFP protein. PDT-treated samples showed a very thin layer of biofilm with a remarkable less fluorescent signal than dark controls. This observation could be ascribable to an impairment in cell functions, such as the expression of a functional recombinant protein, and is consistent with the decrease in cell viability previously reported. This outcome suggests that most of the cells were damaged immediately after PDT treatment, and they could be possibly more susceptible to antibiotic or biocide administration.

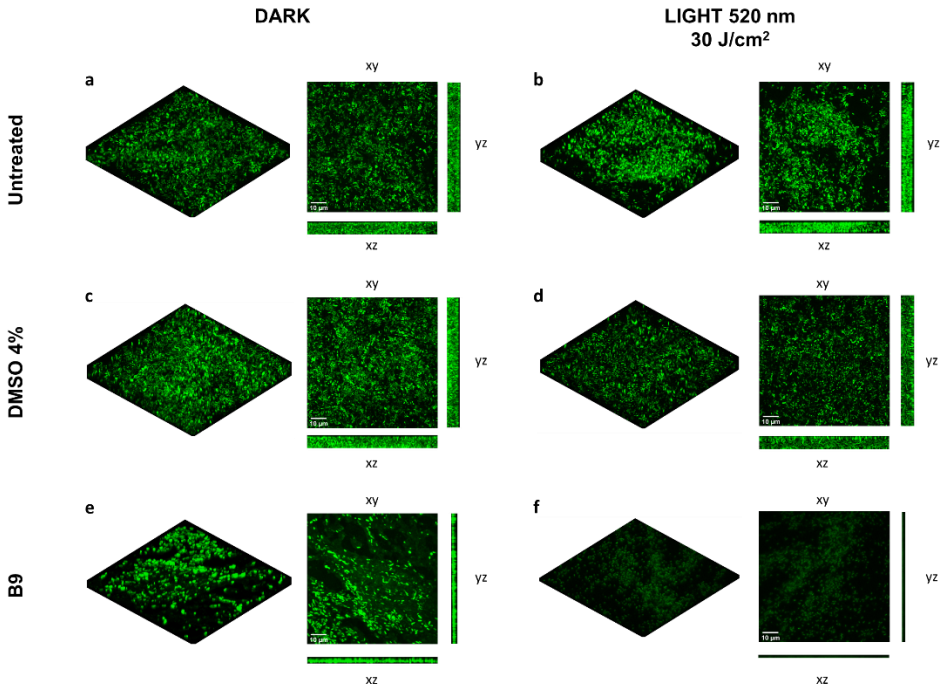

Figure 10. Eradication of *P. aeruginosa* PAO1_pVOGFP biofilm with B9 BODIPY. 24h-old PAO1_pVOGFP biofilms were treated with B9 (40 µM) and irradiated with 520 nm green light at 30 J/cm^2. Biofilms of untreated and DMSO-treated samples were included in the experiment. Dark controls are shown in panels a,c,e, while irradiated samples in panels b,d,f. Images of biofilms are shown in volume view, and in xy, xz and yz projections. Scale bar = 10 µM.

3.4 Activity of BODIPYs on *S. aureus* biofilms

The preliminary screening of BODIPYs on *S. aureus* cells revealed that two non-ionic molecules – B2 and B5 – had the best antimicrobial effect if compared to other PSs. These compounds were tested on *S. aureus* biofilms formed by the MSSA strain ATCC6538P, and the MRSA strain ATCC43300 which is resistant to β-lactam antibiotics.

B2 and B5 (0,5 µM) were administered to MSSA strain and activated by green light radiation at a fluence rate of 20 J/cm^2. After sample incubation at 37°C for 24 hours, adherent biomass (OD590) and cell viability were evaluated (figure 11A,B,C). The total biomass and the viability of adherent and planktonic phases did not change significantly upon treatment with DMSO alone, green light alone, and DMSO upon irradiation. In the dark, BODIPYs had no toxic effects on both biofilm production and cell viability. On the other hand, *S. aureus* cells were strongly inactivated by PDT

treatment, given that cell viability reached the lowest detection limit of the system (10^2 CFU/well or CFU/mL). No structured biofilms were formed, in agreement with a total biomass reduction up to about 90% following PDT treatment with both B2 and B5 molecules.

In the same experimental conditions, a strong photoinactivation rate was observed also with MRSA strain (figure 11D,E,F), where a comparable depletion of total biomass was observed (90%). MRSA planktonic population was as sensitive as for the MSSA strain, and the adherent population reached very low values of density with a decrease of 6 Log units as compared to the samples kept in the dark. Therefore, B2 and B5 could be considered as promising PSs against *S. aureus*, independently from its antibiotic susceptibility profile.

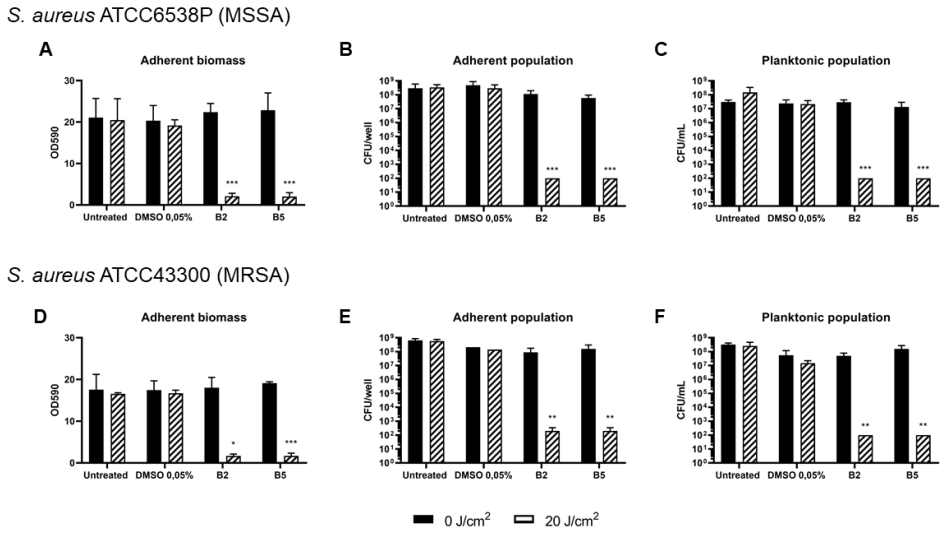

Figure 11. Inhibition of biofilm formation by *S. aureus* ATCC6538P (A,B,C) and ATCC43300 (D,E,F) upon photodynamic treatment with BODIPYs B2 and B5. PSs (0,5 µM) were activated by green light at 20 J/cm^2. The graphs report values of the absorbance at 590 nm (OD 590) of biofilms after staining with crystal violet (A,D), values of adherent population viability (CFU/well) (B,E), and planktonic population viability (CFU/mL) (C,F). Dark control samples are presented as black bars and light-treated samples as striped bars. Error bars represent standard deviation. Statistical analyses were performed by one-way ANOVA (*$p < 0.05$; **$p < 0.01$; ***$p < 0.0001$).

BODIPYs (0,5 µM) were used, as well, in experiments of eradication of 24h *S. aureus* biofilms (figure 12). The administration of light alone (20 J/cm^2), DMSO and DMSO in combination with light did not affect neither the total biomass, nor cell viability.

Also, B2 and B5 administration in dark or light conditions did not affect the total biomass of biofilm, suggesting that no impairment of biofilm matrix happened during PDT. However, immediately after PDT, antimicrobial effects were obtained on MSSA cells, where a significant reduction of about 6 Log units was observed for both adherent and planktonic populations (figure 12B,C).

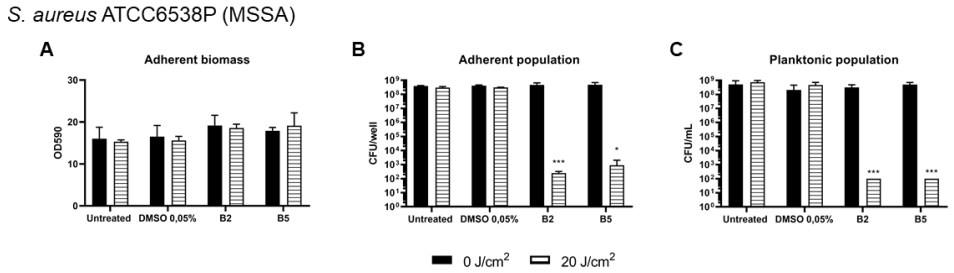

Figure 12. Eradication of *S. aureus* ATCC6538P biofilms by BODIPYs B2 and B5 (0,5 µM). Adherent biomass of biofilm upon PDT is represented as OD590 (A) and cell viability is expressed as CFU/well for adherent cell population (B) and as CFU/mL for planktonic biomass (C). Bars represent standard deviations. Statistical analyses were performed by one-way ANOVA (*p < 0,05; **p < 0.01).

3.5 Photodynamic activity of BODIPYs on *C. albicans* biofilms

The potential of aPDT with BODIPYs as PSs was assayed on biofilms of the pathogen yeast *C. albicans*. Five non-ionic PSs (B2, B5, B7, B8, B12) and one positively charged compound (B13) were previously found to have a good photoinactivation activity on fungal cells. Thus, all of them were assessed in biofilm inhibition assays on *C. albicans* ATCC14053 (figure 13). This strain formed a biofilm biomass with an OD 590 value around 18, that did not change upon light treatment (figure 13A). A slight increase of biomass was observed in samples treated with DMSO in both dark and light conditions. The administration of all PSs without irradiation did not significantly change the amount of biofilm formed by the yeast, while photodynamic treatment with all BODIPYs caused a 50% reduction in biofilm formation.

Cell viability of adherent population was unchanged upon light treatment and DMSO administration if compared to untreated controls kept in the dark. Also, PSs administration in the dark did not change the CFU/well of the adherent phase. When

activated by light, non-ionic BODIPYs B5 and B8 caused a depletion of 2 Log unit on yeast viability, while B2 and B12 caused a decrease of 3 Log units. The best PDT performances were obtained with the non-ionic PS B7 and the monocationic PS B13 that inhibited the growth of an adherent population of *C. albicans*, reaching the detection limit of the set up (10^2 CFU/well), with more than 5 Log units reduction. Planktonic populations were more sensitive to PDT treatment since a statistically significant reduction of CFU/mL was observed in all the cases. B7 and B13 had the best PDT effects since they inhibited the growth of the planktonic population reaching the lowest limit of the system (10^2 CFU/mL).

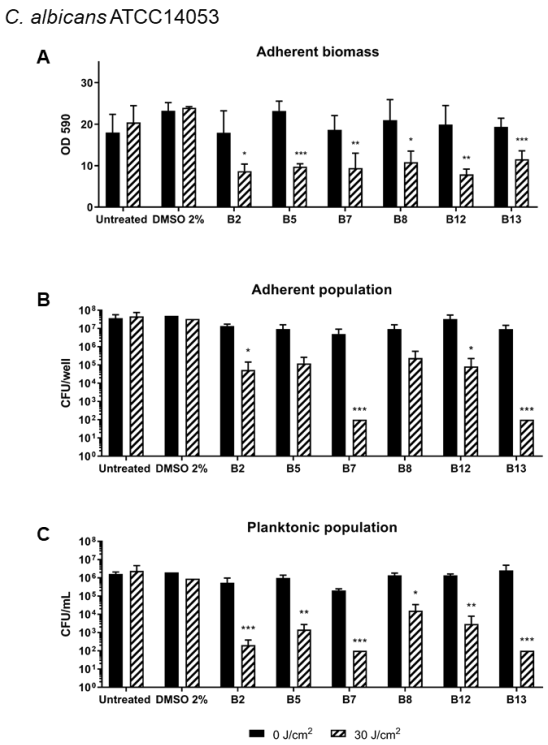

Figure 13. Inhibition of biofilm formation by *C. albicans* ATCC14053 upon photodynamic treatment with BODIPYs B2, B5, B7, B8, B12, B13. PSs (20 μM) were activated by green light radiation at 30 J/cm^2. The graphs report values of the absorbance at 590 nm (OD 590) of biofilms after staining with crystal violet (A), values of adherent population viability (CFU/well) (B), and planktonic population viability (CFU/mL) (C). Dark control samples are presented as black bars and light-treated samples as striped bars. Data represent the mean of at least three independent experiments ± the standard deviation. Statistical analyses were performed by one-way ANOVA (*p < 0.05; **p < 0.01; ***p < 0.0001).

In addition to the ATCC strain, biofilm assays were also performed on Ca1 and Ca2 clinical strains, deriving from patients with urinary tract infections (figure 14). These strains were treated with BODIPYs B7 and B13 that showed the best outcome with *C. albicans* ATCC14053 reference strain.

The clinical strains formed a comparable amount of adherent biofilm with OD590 values around 28, adherent biomass and adherent phase cell density of about 10^7 CFU/well and 10^6 CFU/mL, respectively. The administration of 2% DMSO as a control did not alter the biofilm formation of Ca1, but a slight decrease in adherent biomass was observed in the case of *C. albicans* Ca2 strain. If no toxicity in the dark was observed for B7 and B13 on OD590 values, the irradiation with green light impaired significantly yeast ability to form biofilm compared to the control samples (−PS, −Light; −PS, +Light; +PS, −Light), with an OD590 reduction of about 65% in both strains (figure 14A,D). When the cellular populations of planktonic and adherent phases were evaluated, some differences between the two PSs were observed. In dark conditions, compound B7 had a certain toxic effect on adherent and planktonic populations of Ca1 and Ca2, causing a reduction of 1 Log unit if compared to control samples. On the contrary, the monocationic PS B13 did not show any dark toxicity on yeast populations. However, both BODIPYs significantly impaired the viability of both embedded and free-living cells, reaching the lowest detection limit of the system.

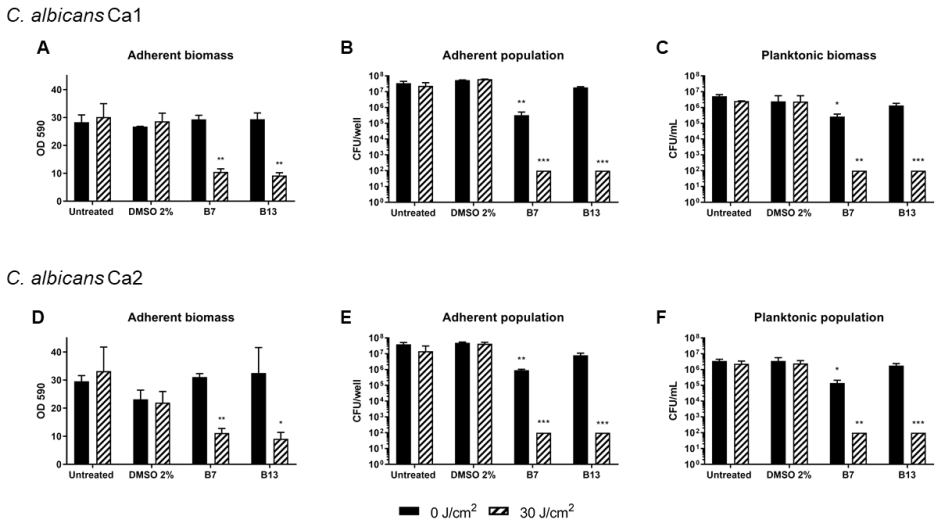

Figure 14. Inhibition of biofilm formation by *C. albicans* clinical isolates Ca1 and Ca2 upon photodynamic treatment with BODIPYs B7 and B13. PSs (20 μM) were activated by green light at 30 J/cm^2. The graphs report values of the absorbance at 590 nm (OD 590) of biofilm staining with crystal violet (A,D), values of adherent population viability (CFU/well) (B,E), and planktonic population viability (CFU/mL) (C,F). Dark control samples are presented as black bars and light-treated samples as striped bars. Error bare represent standard deviations. Statistical analyses were performed by one-way ANOVA (*$p < 0.05$; **$p < 0.01$; ***$p < 0.0001$).

Twenty-four hours *C. albicans* biofilms were grown in optimal YPD medium and subjected to the protocol of biofilm eradication by BODIPYs B7 and B13 (figure 15). In order to avoid any possible interference of organic components in PDT experiments, planktonic biomass was removed, and a suitable volume of PBS was added. Adherent biomass (OD590) did not significantly change upon light treatment, DMSO administration, and single treatments with B7 and B13 both in dark and light conditions. On the contrary, a slight killing effect of 1 Log units was observed in adherent population upon light activation of B7, while BODIPY B13 did not cause any decrease in yeast viability (figure 15B).

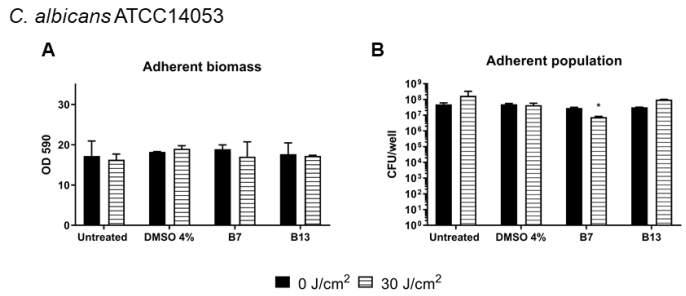

Figure 15. Assay for the eradication of *C. albicans* ATCC14053 biofilms by B7 and B13 (40 μM). Adherent biomass of biofilms upon PDT is represented as OD590 (A) and adherent cell viability is expressed as CFU/well (B). Error bars represent standard deviations. Statistical analyses were performed by one-way ANOVA (*p < 0,05).

4. Discussion

In the photodynamic process, a key role is played by the photosensitizing compounds that need to interact with microbial cells to cause the oxidative stress when activated by a light source. Chemical compounds belonging to the class of boron-dipyrromethenes have recently found interesting applications as photosensitizers in the field of photodynamic therapy. Proposed in the early 2000s for anticancer PDT, BODIPYs were immediately appreciated for their high chemical versatility, good photo- and chemo-stability, high molar absorption coefficient, and high singlet oxygen quantum yield (Gallagher et al., 2005). Suitable modifications of the BODIPY core allow to obtain a wide range of molecules bearing different substituents to obtain PSs with suitable chemical features and photoactivity (Awuah and You, 2012).

If BODIPYs have been investigated and properly designed as antitumoral photosensitizers (Agazzi et al., 2019), few papers report the potential of these compounds in antimicrobial PDT. Indeed, Durantini *et al*. recently reported that only a dozen BODIPYs with different chemical complexity and charge have been applied in the antimicrobial field (Durantini et al., 2018). The cationic compound 4,4-difluoro-2,6-diiodo-1,3,5,7-tetramethyl-8-(N-methyl-4-Pyridyl)-4-bora-3a,4adiaza-s-indacene (here named as B13) was the most investigated PS. Our group outlined its photodynamic activity on *Escherichia coli*, *Staphylococcus xylosus*, and *Pseudomonas aeruginosa*, at relatively low concentrations (5, 0,5 and 2,5 μM, respectively) (Caruso et al., 2012; Orlandi et al., 2014). Further, a broad-spectrum

activity of this compound was also observed in the work of Carpenter and colleagues, where six bacterial pathogens, three fungal species, and three types of human viruses were successfully photoinactivated by B13 at nanomolar concentrations with short irradiation times (Carpenter et al., 2015).

Herein, we reported an antimicrobial PDT study, where 15 BODIPYs (B1-B15), characterized by a relatively simple chemical structure, were screened for their ability to photoinactivate clinically relevant microbial pathogens: *P. aeruginosa*, *S. aureus*, and *C. albicans*. The panel of PSs used in this study is based on a 4,4-difluoro-1,3,5,7-tetramethyl-4-bora-3a,4a-diaza-s-incacene core bearing two iodine atoms in positions 2 and 6, that exert the heavy atom effect, resulting in decreasing of fluorescence and increasing of quantum yield singlet oxygen production (Gorman et al., 2004; Yogo et al., 2005). Each compound differs from the others for its aromatic substituent in *meso*-position that could be non-ionic (B1-B12) or positively charged (B13-B15). Furthermore, PSs have a maximum absorption peak around 540-550 nm of the visible spectrum, that fits with the phototherapeutic window to treat *in vivo* superficial infections in skin and oral cavity wounds, in addition to their potential application on contaminated inert surfaces or medical devices.

The initial screening phase of this study was aimed at outlining possible undesired intrinsic toxicity of the BODIPYs on the three considered pathogens. As expected, the Gram-positive bacterium *S. aureus* was more sensitive than the Gram-negative *P. aeruginosa* to BODIPYs interaction in the dark, thus, it was necessary to reduce the concentration of PS at 1 μM. *P. aeruginosa* was almost insensitive to BODIPY administration, indeed its intrinsic resistance to antimicrobial agents is well-known (Breidenstein et al., 2011). The yeast *C. albicans* showed a certain degree of sensitivity to 10 μM BODIPYs with both non-ionic and cationic charge. However, BODIPY compounds seemed to be selective for the Gram-positive bacterium *S. aureus*.

These differences in sensitivity between each pathogen could be explained by a different interaction between PSs and microbial cells (Jori et al., 2006). Upon one hour of incubation, the Gram-negative bacterium *P. aeruginosa* poorly interacted with the majority of non-ionic PSs (less than 20% of binding), while the monocationic

BODIPYs had a greater interaction with PAO1 cells. These outcomes are consistent with the fact that Gram-negative bacteria display negatively charged lipopolysaccharides (LPS) on the external layer of the outer membrane, and their envelope forms a very effective permeability barrier (Durantini et al., 2018). On the contrary, Gram-positive bacteria have a porous and thick peptidoglycan layer outside the cell membrane, thus a better interaction between BODIPY and *S. aureus* was reached. Non-ionic BODIPYs hardly interact also with the yeast *C. albicans,* compared to cationic ones. Fungal cell envelopes seem to have an intermediate degree of permeability between Gram-positive and Gram-negative bacteria, however the yeast cell wall has a complex molecular architecture that confers a negative charge to the cells and allows an electrostatic interaction with cationic molecules (Dai et al., 2009).

BODIPYs were screened for their photodynamic activity after irradiation with a low energy LED device with a maximum emission peak at 520 nm. *P. aeruginosa* was the less susceptible microorganism to BODIPY-mediated PDT. When suspended cultures of PAO1 were treated with BODIPYs and green light, only one compound (B9), administered at 10 μM concentration, showed a certain antimicrobial efficacy (4 Log units reduction). Unexpectedly, a non-ionic compound was active on *P. aeruginosa*, indeed B9 bears a 4'-methoxynaphtalene group in *meso*-position. The only difference of this PS could be the peculiar three-dimensional configuration if compare to the others that hold one aromatic ring. However, other PSs similar to B9 should be tested to infer further hypotheses on structure-activity relationship.

Since biofilm development is considered a major virulence factors during the infection process and could worsen patients' health conditions, the antibiofilm activity of B9 on *P. aeruginosa* biofilm was evaluated. This compound at 40 μM was able to inhibit the formation of a structured biofilm by the wild-type PAO1 and by two *P. aeruginosa* strains isolated in clinical settings. When dealing with biofilm eradication, usually high concentrations of antimicrobial compounds are needed to reach a significant impairment of the biofilm structure (Maisch, 2015). Herein, a certain antibiofilm activity was displayed by 40 μM B9 on a 24h PAO1 biofilm, where planktonic and adherent populations were subjected to a significant depletion

in viability. Moreover, analyses by confocal microscopy confirmed the impairment of adherent PAO1_pVOGFP cells in their metabolic functions upon biofilm eradication by PDT. The matrix production was greatly impaired in biofilm inhibition, since the cell machinery and the quorum sensing (QS) systems of *P. aeruginosa* could be damaged by the oxidative stress generated during PDT. On the contrary, when the biofilm matrix produced during biofilm growth undergoes photodynamic treatment, it seemed to be not susceptible to photo-oxidative stress.

The Gram-positive bacterium *S. aureus* demonstrated high susceptibility to PDT treatment with BODIPYs if compared to the Gram-negative species *P. aeruginosa*, in accordance with findings obtained with other classes of PSs (Banfi et al., 2006a; Hsieh et al., 2014). A low PS concentration (1 μM), independently from the charge, showed good photoinactivation rates on suspended cultures. However, non-ionic BODIPYs (B2, B5) showed the best photo-killing effects. Both PSs hold a 2'-substituted aromatic ring in *meso*-position, where B2 bears a methoxy group, while B5 has a 2''-hydroxyethoxy group. Thus, it could be inferred that a better interaction and PDT activity was ascribable to non-ionic BODIPYs with a mono substitution on the aromatic ring. B2 and B5 also inhibited the formation of biofilms, preventing the development of an adherent biomass and were active against cells in both planktonic and sessile populations. BODIPYs impaired the formation of structured bacterial communities of both sensitive and resistant *S. aureus* strains (MSSA, MRSA). Notably, aPDT demonstrated its antimicrobial and antibiofilm effects regardless from the antibiotic susceptibility profile, as previously reported by other authors by means of different PSs (García et al., 2015; Freitas et al., 2019). A great eradication effect of B2 and B5 was detected in 24h MSSA biofilms. If the biofilm matrix seemed to be not susceptible to photo-oxidative stress induced by BODIPYs, the adherent and planktonic populations were highly affected by photodynamic treatment, as observed in the case of *P. aeruginosa*.

The screening of BODIPYs in antifungal PDT showed that *C. albicans* was greatly inactivated by non-ionic compounds B2, B5, B7 B8 and B12, and by the cationic PS B13. From a morphological analysis upon photo-treatment, all BODIPYs revealed to

impaire yeast cell morphology since structural alterations were visible by the fluorophore arrangement inside the cells upon PDT.

Two BODIPYs – B7 and B13 – better inhibited the formation of an adherent biomass by *C. albicans* ATCC strain if compared to the other compounds. B7 is a non-ionic compound characterised by a 4''-bromobutoxyphenyl group in *meso*-position, while B13 holds a 4-methylpyridyl group in the same position that confers a positive charge to the PS. When applied to clinical strains, B7 showed a certain toxicity in the dark for planktonic and sessile populations, while B13 greatly impaired cell viability and matrix production only upon photo-treatment. Eradication of yeast biofilm by BODIPYs was not as successful as for bacterial eradication, as only a slight decrease of sessile population viability was observed.

5. Conclusions

This screening work considered a panel of BODIPYs for the photoinactivation of three microbial pathogens. This class of compounds proved to be a suitable reservoir of antimicrobial PSs, even if an ideal compound active on all the pathogens has not emerged yet. Unexpectedly, *P. aeruginosa* was successfully inactivated by the non-ionic compound B9, while *S. aureus* by B2 and B5 at low concentrations. Among the tested molecules, the best antifungal PS was found to be B13 compound.

In all the cases, BODIPYs with best photoinactivation performances negatively influenced the biofilm formation by microbial species, making PDT appropriate as a preventive disinfection approach for inert surfaces of medical devices, or on localized infections in oral cavity or on the skin. Importantly, biofilm inhibition activity of BODIBYs, could avoid the beginning of chronic infections and the spread of microbial pathogens in other body districts.

Interestingly, a certain effect of BODIPYs administered at low concentrations was observed on pathogens living in biofilms. This aspect could suggest that the photodynamic treatment, in combination with other antibiofilm strategies, could help the management of biofilm-mediated infections.

This work could help in shedding a new light on a novel class of versatile compounds that demonstrated to be promising photosensitizers in antimicrobial photodynamic

therapy. BODIPYs should be taken into consideration for *in vivo* experimental trials and in chemical studies to improve their delivery efficiency.

References

Agazzi, M. L., Ballatore, M. B., Durantini, A. M., Durantini, E. N., and Tomé, A. C. (2019). BODIPYs in antitumoral and antimicrobial photodynamic therapy: An integrating review. J. Photochem. Photobiol. C Photochem. Rev. 40, 21–48. doi:10.1016/j.jphotochemrev.2019.04.001.

Alangaden, G. J. (2011). Nosocomial Fungal Infections: Epidemiology, Infection Control, and Prevention. Infect. Dis. Clin. North Am. 25, 201–225. doi:10.1016/j.idc.2010.11.003.

Awuah, S. G., and You, Y. (2012). Boron dipyrromethene (BODIPY)-based photosensitizers for photodynamic therapy. RSC Adv. 2, 11169–11183. doi:10.1039/c2ra21404k.

Banfi, S., Caruso, E., Buccafurni, L., Battini, V., Zazzaron, S., Barbieri, P., et al. (2006). Antibacterial activity of tetraaryl-porphyrin photosensitizers: An in vitro study on Gram negative and Gram positive bacteria. J. Photochem. Photobiol. B Biol. 85, 28–38. doi:10.1016/j.jphotobiol.2006.04.003.

Banfi, S., Nasini, G., Zaza, S., and Caruso, E. (2013). Synthesis and photo-physical properties of a series of BODIPY dyes. Tetrahedron 69, 4845–4856. doi:10.1016/j.tet.2013.04.064.

Benstead, M., Mehl, G. H., and Boyle, R. W. (2011). 4,4'-Difluoro-4-bora-3a,4a-diaza-s-indacenes (BODIPYs) as components of novel light active materials. Tetrahedron 67, 3573–3601. doi:10.1016/j.tet.2011.03.028.

Bragonzi, A., Wiehlmann, L., Klockgether, J., Cramer, N., Worlitzsch, D., Döning, G., et al. (2006). Sequence diversity of the mucABD locus in Pseudomonas aeruginosa isolates from patients with cystic fibrosis. Microbiology 152, 3261–3269. doi:10.1099/mic.0.29175-0.

Breidenstein, E. B. M., de la Fuente-Núñez, C., and Hancock, R. E. W. (2011). Pseudomonas aeruginosa: All roads lead to resistance. Trends Microbiol. 19, 419–426. doi:10.1016/j.tim.2011.04.005.

Carpenter, B. L., Situ, X., Scholle, F., Bartelmess, J., Weare, W. W., and Ghiladi, R. A. (2015). Antiviral, antifungal and antibacterial activities of a BODIPY-based photosensitizer. Molecules 20, 10604–10621. doi:10.3390/molecules200610604.

Caruso, E., Banfi, S., Barbieri, P., Leva, B., and Orlandi, V. T. (2012). Synthesis and antibacterial activity of novel cationic BODIPY photosensitizers. J. Photochem. Photobiol. B Biol. 114, 44–51. doi:10.1016/j.jphotobiol.2012.05.007.

Caruso, E., Gariboldi, M., Sangion, A., Gramatica, P., and Banfi, S. (2017). Synthesis, photodynamic activity, and quantitative structure-activity relationship modelling of a series of BODIPYs. J. Photochem. Photobiol. B Biol. 167, 269–281. doi:10.1016/j.jphotobiol.2017.01.012.

Caruso, E., Malacarne, M. C., Marras, E., Papa, E., Bertato, L., Banfi, S., et al. (2020). New BODIPYs for photodynamic therapy (PDT): Synthesis and activity on human cancer cell lines. Bioorganic Med. Chem. 28, 115737. doi:10.1016/j.bmc.2020.115737.

Chanda, W., Joseph, T. P., Wang, W., Padhiar, A. A., and Zhong, M. (2017). The potential management of oral candidiasis using anti-biofilm therapies. Med. Hypotheses 106, 15–18. doi:10.1016/j.mehy.2017.06.029.

Cieplik, F., Deng, D., Crielaard, W., Buchalla, W., Hellwig, E., Al-Ahmad, A., et al. (2018a). Antimicrobial photodynamic therapy – what we know and what we don't. Crit. Rev. Microbiol. 44, 571–589. doi:10.1080/1040841X.2018.1467876.

Cieplik, F., Deng, D., Crielaard, W., Buchalla, W., Hellwig, E., Al-Ahmad, A., et al. (2018b). Antimicrobial photodynamic therapy – what we know and what we don't. Crit. Rev. Microbiol. 44, 571–589. doi:10.1080/1040841X.2018.1467876.

Dai, T., Huang, Y. Y., and Hamblin, M. R. (2009). Photodynamic therapy for localized infections-State of the art. Photodiagnosis Photodyn. Ther. 6, 170–188. doi:10.1016/j.pdpdt.2009.10.008.

Durantini, A. M., Heredia, D. A., Durantini, J. E., and Durantini, E. N. (2018). BODIPYs to the rescue: Potential applications in photodynamic inactivation. Eur. J. Med. Chem. 144, 651–661. doi:10.1016/j.ejmech.2017.12.068.

Freitas, M. A. A., Pereira, A. H. C., Pinto, J. G., Casas, A., and Ferreira-Strixino, J. (2019). Bacterial

viability after antimicrobial photodynamic therapy with curcumin on multiresistant Staphylococcus aureus. Future Microbiol. 14, 739–748. doi:10.2217/fmb-2019-0042.
Frimannsson, D. O., Grossi, M., Murtagh, J., Paradisi, F., and Oshea, D. F. (2010). Light induced antimicrobial properties of a brominated boron difluoride (BF2) chelated tetraarylazadipyrromethene photosensitizer. J. Med. Chem. 53, 7337–7343. doi:10.1021/jm100585j.
Gallagher, W. M., Allen, L. T., O'Shea, C., Kenna, T., Hall, M., Gorman, A., et al. (2005). A potent nonporphyrin class of photodynamic therapeutic agent: Cellular localisation, cytotoxic potential and influence of hypoxia. Br. J. Cancer 92, 1702–1710. doi:10.1038/sj.bjc.6602527.
García, I., Ballesta, S., Gilaberte, Y., Rezusta, A., and Pascual, Á. (2015). Antimicrobial photodynamic activity of hypericin against methicillin-susceptible and resistant Staphylococcus aureus biofilms. Future Microbiol. 10, 347–356. doi:10.2217/FMB.14.114.
Gayathri, T., Barui, A. K., Prashanthi, S., Patra, C. R., and Singh, S. P. (2014). Meso-Substituted BODIPY fluorescent probes for cellular bio-imaging and anticancer activity. RSC Adv. 4, 47409–47413. doi:10.1039/c4ra07424f.
Gorman, A., Killoran, J., O'Shea, C., Kenna, T., Gallagher, W. M., and O'Shea, D. F. (2004). In vitro demonstration of the heavy-atom effect for photodynamic therapy. J. Am. Chem. Soc. 126, 10619–10631. doi:10.1021/ja047649e.
Hamblin, M. R. (2016). Antimicrobial photodynamic inactivation : a bright new technique to kill resistant microbes. Curr. Opin. Microbiol. 33, 67–73. doi:10.1016/j.mib.2016.06.008.
Hsieh, C. M., Huang, Y. H., Chen, C. P., Hsieh, B. C., and Tsai, T. (2014). 5-Aminolevulinic acid induced photodynamic inactivation on Staphylococcus aureus and Pseudomonas aeruginosa. J. Food Drug Anal. 22, 350–355. doi:10.1016/j.jfda.2013.09.051.
Jamal, M., Ahmad, W., Andleeb, S., Jalil, F., Imran, M., Nawaz, M. A., et al. (2018). Bacterial biofilm and associated infections. J. Chinese Med. Assoc. 81, 7–11. doi:10.1016/j.jcma.2017.07.012.
Jori, G., Fabris, C., Soncin, M., Ferro, S., Coppellotti, O., Dei, D., et al. (2006). Photodynamic therapy in the treatment of microbial infections: Basic principles and perspective applications. Lasers Surg. Med. 38, 468–481. doi:10.1002/lsm.20361.
Maisch, T. (2015). Resistance in antimicrobial photodynamic inactivation of bacteria. Photochem. Photobiol. Sci. 14, 1518–1526. doi:10.1039/c5pp00037h.
Mulani, M. S., Kamble, E. E., Kumkar, S. N., Tawre, M. S., and Pardesi, K. R. (2019). Emerging strategies to combat ESKAPE pathogens in the era of antimicrobial resistance: A review. Front. Microbiol. 10. doi:10.3389/fmicb.2019.00539.
Orlandi, V. T., Bolognese, F., Rolando, B., Guglielmo, S., Lazzarato, L., and Fruttero, R. (2018a). Anti-pseudomonas activity of 3-nitro-4-phenylfuroxan. Microbiol. (United Kingdom) 164, 1557–1566. doi:10.1099/mic.0.000730.
Orlandi, V. T., Martegani, E., and Bolognese, F. (2018b). Catalase A is involved in the response to photooxidative stress in Pseudomonas aeruginosa. Photodiagnosis Photodyn. Ther. 22, 233–240. doi:10.1016/j.pdpdt.2018.04.016.
Orlandi, V. T., Martegani, E., Bolognese, F., Trivellin, N., Maťátková, O., Paldrychová, M., et al. (2020). Photodynamic therapy by diaryl-porphyrins to control the growth of Candida albicans. Cosmetics 7, 1–19. doi:10.3390/COSMETICS7020031.
Orlandi, V. T., Rybtke, M., Caruso, E., Banfi, S., Tolker-Nielsen, T., and Barbieri, P. (2014). Antimicrobial and anti-biofilm effect of a novel BODIPY photosensitizer against Pseudomonas aeruginosa PAO1. Biofouling 30, 883–891. doi:10.1080/08927014.2014.940921.
Orlandi, V. T., Villa, F., Cavallari, S., Barbieri, P., Banfi, S., Caruso, E., et al. (2011). Photodynamic therapy for the eradication of biofilms formed by catheter associated Pseudomonas aeruginosa strains. 26, 129–133.
Pendleton, J. N., Gorman, S. P., and Gilmore, B. F. (2013). Clinical relevance of the ESKAPE pathogens. 11, 297–308.
Roca, I., Akova, M., Baquero, F., Carlet, J., Cavaleri, M., Coenen, S., et al. (2015). The global threat of antimicrobial resistance: Science for intervention. New Microbes New Infect. 6, 22–29. doi:10.1016/j.nmni.2015.02.007.
Rugiero, M., Orlandi, V. T., and Caruso, E. (2019). Effetto di due nuovi BODIPY in terapia fotodinamica antimicrobica. doi:10.1017/CBO9781107415324.004.
St. Denis, T. G., Dai, T., Izikson, L., Astrakas, C., Anderson, R. R., Hamblin, M. R., et al. (2011). All

you need is light, antimicrobial photoinactivation as an evolving and emerging discovery strategy against infectious disease. Virulence 2, 509–520. doi:10.4161/viru.2.6.17889.
Stover, C. K., Pham, X. Q., Erwin, A. L., Mizoguchi, S. D., Warrener, P., Hickey, M. J., et al. (2000). Complete genome sequence of {Pseudomonas} aeruginosa {PAO}1, an opportunistic pathogen. Nature 406, 959–964. doi:10.1038/35023079.
Sunahara, H., Urano, Y., Kojima, H., and Nagano, T. (2007). Design and synthesis of a library of BODIPY-based environmental polarity sensors utilizing photoinduced electron-transfer-controlled fluorescence ON/OFF switching. J. Am. Chem. Soc. 129, 5597–5604. doi:10.1021/ja068551y.
Verderosa, A. D., Totsika, M., and Fairfull-Smith, K. E. (2019). Bacterial Biofilm Eradication Agents: A Current Review. Front. Chem. 7, 1–17. doi:10.3389/fchem.2019.00824.
Yogo, T., Urano, Y., Ishitsuka, Y., Maniwa, F., and Nagano, T. (2005). Highly efficient and photostable photosensitizer based on BODIPY chromophore. J. Am. Chem. Soc. 127, 12162–12163. doi:10.1021/ja0528533
Zagami, R., Sortino, G., Caruso, E., Malacarne, M. C., Banfi, S., Patanè, S., et al. (2018). Tailored-BODIPY/Amphiphilic Cyclodextrin Nanoassemblies with PDT Effectiveness. *Langmuir* 34, 8639–8651. doi:10.1021/acs.langmuir.8b01049.

4. Antimicrobial Blue Light Therapy

Effect of blue light at 410 and 455 nm on *Pseudomonas aeruginosa* biofilm

Authors: Eleonora Martegani[1], Fabrizio Bolognese[1], Nicola Trivellin[2] and Viviana Teresa Orlandi[1]*

[1]Departement of Biotechnologies and Life Sciences, University of Insubria, Varese, Italy
[2]Department of Industrial engineering, University of Padua, Italy

Journal of Photochemistry & Photobiology, B: Biology 204 (2020) 111790

Abstract

Background. *Pseudomonas aeruginosa* is an opportunistic pathogen resistant to many antibiotics, is able to form biofilm and causes serious nosocomial infections. Among anti-*Pseudomonas* light-based approaches, the recent antimicrobial Blue Light (aBL) treatment seems very promising.

Aim. The aim of this study was to evaluate and compare the efficiency of blue light at 410 and 455 nm in inhibiting and/or eradicating *P. aeruginosa* biofilm.

Material and methods. In this study, photo-spot tests, viable count method, crystal-violet staining and confocal analysis were used to evaluate the effect of blue light on *P. aeruginosa* cells. Enzymatic assays were performed to evaluate the effect of blue light on biological molecules chosen as representative targets. ANOVA analysis highlighted the statistical significance of the obtained results.

Results. Light at 410 nm has been identified as successful in inhibiting biofilm formation not only of the model strain PAO1, but also of CAUTI (catheter-associated urinary tract infection) isolates characterized by their ability to form biofilm. Light at 410 nm light showed that: i) the lowest tested radiant exposure (75 J cm^{-2}) prevents matrix formation; ii) higher radiant exposures (225 and 450 J cm^{-2}) light impairs the cellular components of biofilm, adherent and planktonic ones; iii) eradicates with a good rate young and older biofilm in a light dose dependent manner; iv) it is also efficient in inactivating catalase A, a virulence factor playing an important role in pathogenic mechanisms. Furthermore, light at 410 nm caused detrimental effects on

enzyme activity of β-galactosidase, modifications of plasmid DNA conformation and changes in *ortho*-nitrophenyl-β-D-galactopyranoside structure.

Light at 455 nm, even if at a lower extent than 410 nm, showed a certain anti-*Pseudomonas* activity.

Conclusions. This study supports the potential of blue light for anti-infective and disinfection applications.

1. Introduction

Pseudomonas aeruginosa is an opportunistic pathogen responsible for nosocomial infections such as pneumonia, bacteraemia and infections in wounds, corneas, gastrointestinal and urinary tracts. Moreover, it worsens the health of immunocompromised individuals, Cystic Fibrosis (CF) patients, individuals carrying HIV (Human Immunodeficiency Virus) and cancer patients [1]. The presence of a semi-permeable outer membrane together with the production of periplasmic β-lactamases and the expression of efflux pump systems lead *P. aeruginosa* to be intrinsically resistant to many antibiotics. Furthermore, the virulence of *P. aeruginosa* increases in biofilm communities, where cells produce extracellular matrix favouring the adhesion to biotic or abiotic surfaces, making difficult its eradication [2]. Sessile bacteria are physiologically different from their free-living planktonic counterparts; they are tolerant to immune system and antibiotics, rendering biofilm a source of chronic and persistent infections [3]. The exopolysaccharide matrix prevents antibiotic diffusion, and the presence of anionic extracellular DNA reduces the activity of positively charged antibiotics (e.g. polymyxins and aminoglycosides). Moreover, in the deepest anoxic biofilm layers, populations of persistent cells, with reduced metabolic activity and low rate of cell division, can survive to antibiotic treatment and are considered the main contributor of resilience in biofilm-mediated infections [4]. Biofilms of *P. aeruginosa* have been identified on tissues, wounds, organ transplants, and on medical devices such as catheters and prostheses [5,6]. Since the spread of *P. aeruginosa* represents an important issue in clinical context, international research is focused on novel anti-*Pseudomonas* strategies to combine with traditional antibiotics [7].

Among new approaches, a tool based on visible light seems very promising: violet-blue light from 380 to 480 nm showed a broad-spectrum activity against many microorganisms among Gram-negative and Gram-positive bacteria, yeasts, fungi [8]. The term aBL (antimicrobial blue light) Therapy has been specifically created to indicate this novel approach [9]. In particular, *P. aeruginosa* PAO1 and clinical strains in suspended cultures showed their sensitivity to 400 nm blue light in a dose dependent manner, and biofilm formation was also impaired [10]. Furthermore, no arise of *P. aeruginosa* resistant strains has been observed after repeated cycle of sub-lethal blue light doses [11]. Interestingly, aBL approach showed to be selective for microbial pathogen: *P. aeruginosa* cells from mouse-infected wounds were sensitive to blue light, while host cells were insensitive [12]. Since aBL is not dangerous to the host tissues, in contrast to UV irradiation, and does not require external drug administration, it could be used to control *P. aeruginosa* growth in wounds and in mouth and upper respiratory tract of CF patients. Furthermore, the aBL could be exploited for environmental applications such as decontamination purposes and food disinfection.

The mechanism of blue light toxicity is under investigation. It has been hypothesized that blue light may activate endogenous photosensitizers, such as metal-free porphyrins or flavins, which generate reactive oxygen species (ROS) causing oxidative stress of cellular structures, lipids, nucleic acids and proteins, leading microbial cells to death [9]. Indeed, protoporphyrin IX like compounds were isolated from *P. aeruginosa,* supporting the presence of putative endogenous photosensitizers that could be activated by blue light [13]. Upon irradiation of suspended *P. aeruginosa* cells with 411 nm light, hydroxyl radical and singlet oxygen were detected [14]. Moreover, the photooxidative stress induced by a blue light with longer wavelength, 464 nm, induced the arising of hydrogen peroxide: a catalase A (KatA) knockout mutant of PAO1, showed increased sensitivity upon irradiation compared to wild type strain [15].

To the best of our knowledge, few papers reported the inhibitory effect of blue light between 400 and 420 nm in biofilm formation of *P. aeruginosa* [10,13,16]. Indeed, additional research is required to evaluate the great potential of this

technology as antibiofilm strategy both in clinical and environmental fields. Thus, in this study, we examined the effect of blue light at 410 nm to inhibit biofilm formation and/or eradicate formed biofilm of *P. aeruginosa* PAO1 chosen as model microorganism. The attention was focused on the effect on viability of adherent and planktonic cells of biofilm. The comparison with blue light at 455 nm has also been included to get a bigger picture.

2. Materials and methods

2.1 Bacterial strains and culture conditions

Pseudomonas aeruginosa PAO1 [17] was used as model microorganism to perform biofilm photoinactivation. Confocal analyses were performed with *P. aeruginosa* PAO1_pVOGFP [18]. Fifteen *P. aeruginosa* strains, isolated from catheter-associated urinary tract infections (CAUTIs), were also used in this study [19]. *Escherichia coli* MG1655 and *E. coli* JM109 were used to produce recombinant β-galactosidase. All the strains were grown in Luria-Bertani broth in liquid or solid form (1,5% agar). When needed, ampicillin was added as a selection antibiotic at a final concentration of 100 μg/mL.

2.2 Light sources

The lighting unit for the antibiofilm tests (LULab) was designed by University of Padua (Italy) in order to allow a uniform irradiation of an area of 75x75 mm^2 (figure 1). The LULab was equipped with an interchangeable head with 25 high power LEDs, each LED equipped with a specific optic in order to allow the maximum collimation of the light on the target. The interchangeable head allows the irradiation with different wavelengths (410 nm and 455 nm). The system is powered with a specific PC based power controller which allows the set of desired irradiances on the target and the duration of the experiment. The irradiance on the target was measured by means of an absolute calibrated ocean optics USB4000 spectrometer equipped with a cosine corrector. The software allows the execution of specific routines in order to automatize the irradiation protocol. Irradiance and exposure times can be selected thus allowing a precise control of the light dose.

At the maximum irradiance the electrical power of the lamp is 50W (2 watt per each LED, 25 LEDs in total). The total radiated optical power is in excess of 15W, so the residual thermal power dissipated by the LED lamp heatsink is less than 35W. The designed heatsink has a thermal resistance of 1K/W and considering a controlled environmental temperature of 24°C the temperature of the LED devices can be estimated at 60°C. Considering that there is no thermal connection between the sample and the lamp, the thermal contribution of the LED lamp to the sample is therefore negligible.

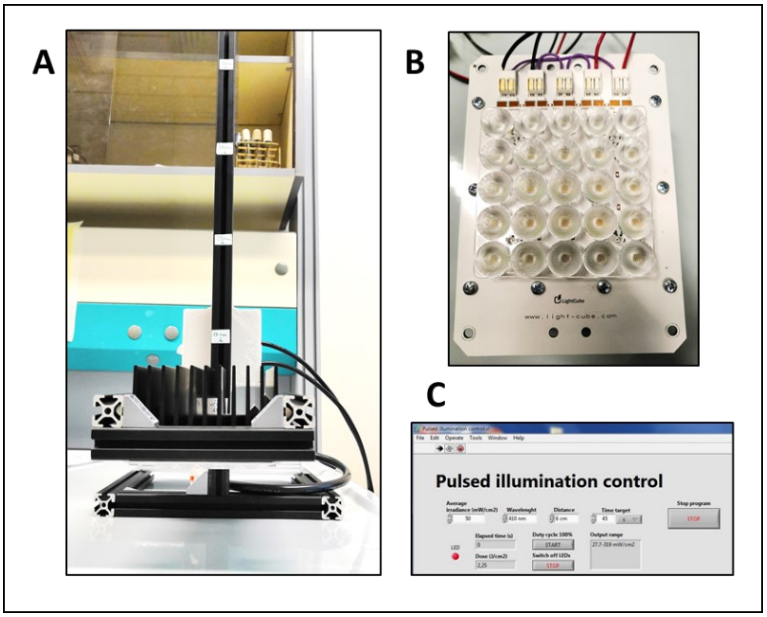

Figure 1. A) LULab apparatus; B) LED device; C) LightCube Pulsed illuminator control programme.

The power density of 410 and 455 nm blue light was kept at 100 mW/cm^2 for all the experimental procedures, while the irradiation time, specified for each protocol, was modified in accordance with the desired final light dose, as presented in table 3.

Table 3. List of light doses employed in this study and the corresponding irradiation time.

Light dose (J/cm^2)	Irradiation time (s)
5	50
25	250
50	500
75	750
100	1000
225	2250
450	4500

2.3 Biofilm photoinactivation assay

P. aeruginosa PAO1 and clinical strains were grown in LB medium at 37°C under agitation (200 rpm). Overnight cultures were diluted 1: 200-fold in M9 medium supplemented with glucose 10 mM and 0.2% W/V casamino acid, used as carbon and nitrogen sources, respectively. One millilitre of the diluted culture (approx. 10^7 CFU/mL) was added to each well of a 12-well polystyrene plate. One plate was kept in the dark as control and the other one was irradiated as follow. To investigate the effect on inhibition of biofilm formation, the cells were irradiated under blue light (100 mW/cm^2) at 410 or 455 nm at increasing radiant fluences 75, 225 and 450 J/cm^2. Upon irradiation, the cells were incubated at 37°C under 200 r.p.m shaking for 6 h. The biofilm dispersal effect of increasing radiant fluences (75, 225 and 450 J/cm^2) of blue light at 410 and 455 nm was observed upon 6 hour of biofilm growth [20].

To assess the amount of adherent biomass the crystal violet staining was performed as follow. Planktonic phase of biofilm grown on each well was removed, and adherent biomass was gently washed with phosphate buffer solution (KH_2PO_4 /K_2HPO_4 10mM pH 7.4). Biofilm was stained with 1 mL of 0,1% W/V crystal violet solution for 20 minutes and then wells were washed twice with deionized water and dried overnight at room temperature. Spectrophotometric quantification of adherent biomass was performed upon solubilisation of crystal violet by 33% V/V acetic acid solution for 10 minutes. Samples were 1:50 diluted with deionized water and measured at 590 nm wavelength.

To evaluate the effect of different treatments on cellular viability of suspended and adherent populations, the planktonic phase was axenically collected and adherent

cells were recovered by scraping and suspended in 1 ml of phosphate buffer. Viable counts - expressed as colony forming units per mL (CFU/mL) in cell suspensions and as CFU per well in adherent biomass – were estimated using a plate count technique; a volume (0.01 mL) of undiluted or serially diluted samples was plated onto LB agar plates and incubated for 24 h at 37 °C. All experiments were independently repeated at least three times.

2.4 Photo-spot test

P. aeruginosa PAO1 overnight cultures were 10-fold serially diluted from 10^8 to 10^3 CFU/well in sterile phosphate buffer, in a 96 well microplate. Bacterial suspensions (5 µL) were replicated on LB agar plates and irradiated under blue LED devices, at increasing light doses. Control plates were incubated in the dark. After irradiation, agar plates were incubated overnight at 37°C. Experiments were performed at least in triplicate.

2.5 Confocal analysis

Overnight GFP-tagged PAO1 cultures [18] were 1: 200-fold diluted in M9 medium supplemented with glucose 10 mM and 0.2% W/V casamino acid. Five millilitres of the diluted culture were added to a glass coverslip and placed in a well of a 6-well polystyrene plate. After 48h of incubation at 37°C, cells were irradiated with blue light at 410 or 455 nm (450 J/cm^2) and induced with arabinose 1 mM to express green fluorescent protein. The coverslip was placed on a microscope glass slide for the acquisition of the adherent biofilm image. All microscopic observations and image acquisitions were performed on a Leica TCS SP5 confocal laser scanning microscope (CLSM; Leica Microsystems, Wetzlar, Germany) equipped with a detector and filter set for GFP monitoring. Images were obtained using a 63x objective lens. Simulated 3D images were generated using the free open-source software ImageJ (National Institute of Health, USA).

2.6 Effect of blue light on plasmidic DNA and ONPG

To evaluate the sensitivity of DNA to blue light the plasmid degradation upon irradiation at 410 and 455 nm, was evaluated. A 2500 bp plasmid (pMB plasmid) [21] was added to wells of a 96-well polystyrene plate at a final concentration of 100 ng/µl. Upon irradiation at 450 J/cm^2 (100 mW/cm^2 irradiance for 75), samples were lyophilized for 30 minutes, suspended in 10 µL of deionized water and analysed by electrophoresis in 1% agarose gel added with ethidium bromide dye at final concentration of 0.5 µg/mL. Power supply was set at a value of 10 V/cm (of electrophoretic chamber Biorad) and images were acquired with Biorad Gel Doc 2000 imaging system.

To evaluate the effect of blue light on sugar, *ortho*-nitrophenyl-β-D-galactopyranoside (ONPG) was chosen as saccharide model. ONPG was suspended in different solvent to reach the concentration of 0,8 mg/mL: deionized water, fresh M9 medium, overnight spent broth and heat treated (95°C for 15 min) overnight spent broth of PAO1 cultures cells. The samples added to wells of 96-well microplate were irradiated with blue LEDs at 410 and 455 nm at increasing light doses 75, 225 and 450 J/cm^2, respectively. Upon irradiation, the presence of *ortho*-nitrophenol, derived by ONPG, was spectrophotometrically quantified at 420 nm.

2.7 Effect of blue light on recombinant β-galactosidase and catalase A

Recombinant protein purification

To evaluate the effect of light on proteins, β-galactosidase was chosen as model enzyme to spectrophotometrically follow the catalytic activity. Catalase A from *P. aeruginosa* was chosen as virulence factor to photoinactivate, owing to its detoxifying activity against hydrogen peroxide and its protective role in stressful conditions. To express and purify recombinant β-galactosidase and catalase A the following procedure was performed. *LacZ* gene from *E. coli* MG1655 and *KatA* from *P. aeruginosa* were PCR amplified and cloned in pVO6His plasmid, containing pBAD promoter and 6His-Tag [22]. *E. coli* JM109 competent cells were transformed by heat-shock with the two obtained plasmids: pVO6His-LacZ and pVO6His-KatA plasmids. Transforming clones were selected on LB agar plates added with 100

μg/mL ampicillin. Overnight cultures of *E. coli* carrying pVO6His-LacZ or pVO6His-KatA were 1: 50 diluted in 400 mL of fresh LB medium and grown at 37°C at 200 rpm up OD_{600} 0,6. Arabinose 0,01% W/V was added to the cultures to induce the expression of recombinant proteins (three-hour incubation). Cells were centrifuged at 7000 rpm at 4°C for 10 minutes. Supernatant was discarded, and pellets were suspended in 20 mL of protein buffer (10 mM HEPES, 40 mM imidazole, 100 mM KCl, 10% V/V glycerol, 0,05% V/V tryton, pH 7,5). Cell suspensions were exposed to 7 cycles of sonication (30 seconds of sonication at 80% power and 1 minute of rest in ice). The clarified lysate obtained upon centrifugation at 18000 rpm at 4°C for 40 minutes, was purified through a nickel-sepharose resin column. Resin was equilibrated with ten volumes of protein buffer and clear lysate was allowed to pass by gravity flow for three times. The flow through fraction was kept for further SDS-PAGE analysis. Then, two washing with ten volumes of protein buffer were performed. Ten volumes of elution buffer (10 mM HEPES, 400 mM imidazole, 100 mM KCl, 10% V/V glycerol) were used to collect protein fractions. The protein content and size of purified samples was determined by Bradford method and SDS PAGE, respectively [22].

β-galactosidase photoinactivation

Recombinant β-galactosidase (final concentration 10 μg/mL) was suspended in deionized water, fresh M9 medium, overnight spent broth and heat treated (95°C for 15 min) overnight spent broth of PAO1 cultures grown in M9 medium (added with 10 mM glucose). The samples were added to wells of 96-well polystyrene microplate and irradiated with light at 410 and 455 nm, at increasing light doses 75, 225 and 450 J/cm^2. Upon irradiation, the β-gal assay was performed as follow. β-galactosidase activity was assessed quantifying the arise of ortho-nitrophenol using ONPG as substrate. A volume of 50 μL of irradiated or dark incubated sample were added in a tube containing 250 μL of Z buffer and 200 μL of ONPG solution (4 mg/mL). The solution was incubated at 37°C for 1 minute and then, the reaction was blocked adding 250 μL of 1 M Na_2CO_3. The amount of ortho-nitrophenol was measured by spectrophotometric analysis at 420 nm.

Catalase A photoinactivation

Recombinant Catalase A was diluted in deionized water until final concentration of 100 µg/mL. The protein solution was irradiated with 410 and 455 nm blue lights at increasing light doses from 5 to 450 J/cm^2, keeping the irradiance at 100 mW/cm^2, and the control was kept in the dark. Upon irradiation, the detection of KatA activity was performed using the method taken from Hadwan *et. al* and modified as follow [23]. The twentieth part of each sample was resuspended in 500 µL of 50 mM H_2O_2 and the enzymatic reaction was incubated at 37°C for 1 minute. Afterwards, 500 µL of ammonium molybdate solution (32,4 mM) were added to each reaction. This compound is able to react with the residual hydrogen peroxide producing a yellow substance easily detectable by spectrophotometer at 405 nm. As positive control, ammonium molybdate was added to 50 mM hydrogen peroxide reaching values of Abs_{405nm} around 2.

2.8 Statistical analyses

P. aeruginosa PAO1 biofilm photoinactivation experiments were performed at least three times with different cultures, and statistical significance was assessed by one-way ANOVA. β-galactosidase, catalase A and ONPG photoinactivation experiments were performed three times for each light dose, and data were analysed by one-way ANOVA.

3. Results

3.1 Effect of blue light on the inhibition of *Pseudomonas aeruginosa* biofilm formation

The effect of blue light at 410 nm in preventing *Pseudomonas aeruginosa* PAO1 biofilm formation was evaluated at increasing radiant exposures (75, 225 and 450 J/cm^2). All the tested energy doses caused a similar and statistically significant reduction of adherent biomass with respect to the dark incubated sample (Figure 2a). The concomitant decrease of adherent cell concentration was dose-light dependent: at the lowest tested radiant exposure 2-log unit decrease was observed compared to dark control, while the lowest cellular concentration (detection limit of the procedure)

was reached with the two highest radiant exposures 225 and 450 J/cm^2 (figure 2a). The bacterial concentration of the planktonic phase of biofilm significantly decreased in a light dose dependent manner (Figure 2b).

Blue light at 455 nm was less efficient than blue light at 410 nm. Although no antibiofilm effect upon 75 J/cm^2 irradiation was observed, a significant decrease of adherent biomass, as well as cell viability, were detected at higher light energies (figure 2c). Under 225 J/cm^2, a 3-fold decrease of adherent biomass with respect to the control kept in the dark was observed; and adherent cell concentration decreased from 10^9 to 10^8 CFU/well. Under the highest tested light dose (450 J/cm^2) adherent biomass was almost undetectable, and four log unit decrease of adherent cell concentration was observed (figure 2c). Similarly, the cellular concentration of planktonic phase of the biofilm decreased in a light dose-dependent manner (figure 2d).

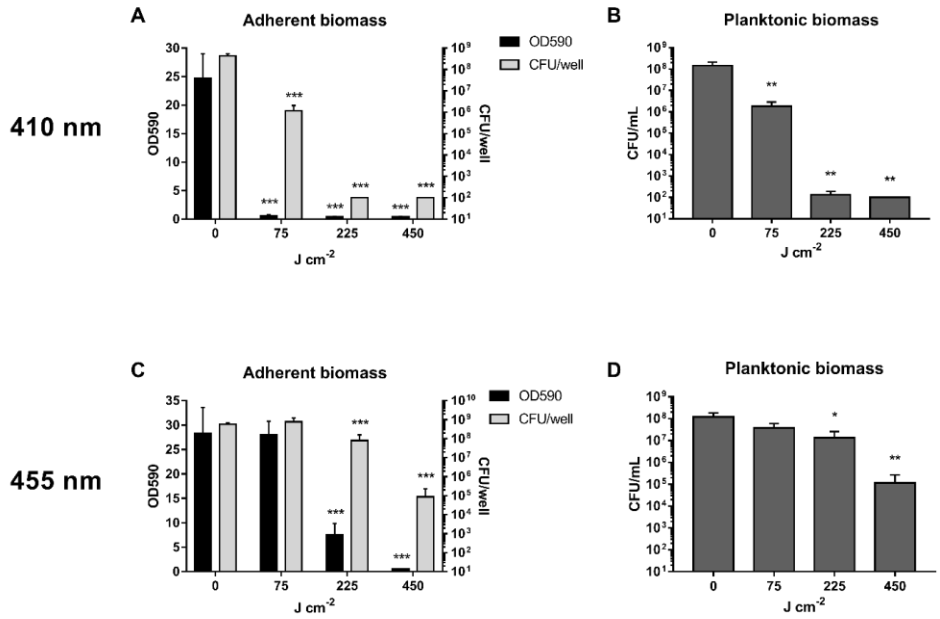

Figure 2. Inhibition of *P. aeruginosa* PAO1 biofilm formation by 410 and 455 nm blue LEDs at increasing light doses. a) adherent biomass of biofilm upon irradiation at 410 nm represented as OD590 and cell viability expressed as CFU/well; b) planktonic biomass (CFU/mL) after irradiation with 410 nm LED; c) adherent biomass of biofilm upon 455 nm irradiation; d) planktonic cell counts after 455 nm light treatments. The values are the means of at least three independent experiments and the bars represent standard deviations. Statistical analyses were performed by one-way ANOVA (*p < 0,05; **p < 0,01; ***p < 0,0001).

The effect of blue light at 410 nm and 455 nm in inhibiting biofilm formation was also tested on 15 isolates of *P. aeruginosa* from urinary catheter-associated infection. The clinical isolates showed a different ability to form biofilm: the majority of them produced less biofilm than PAO1, two strains (UR10 and UR45) produced a biofilm similar to that of PAO1 strain and UR46 and UR48 were biofilm hyperproducer (figure 3a). For each wavelength, the lowest energy dose that showed an inhibitory effect on *P. aeruginosa* PAO1 strain was chosen: 75 J/cm^2 for 410 nm and 225 J/cm^2 for 455 nm. Although the irradiation caused an inhibitory effect of biofilm formation in all the tested strains, independently of the wavelength, the rate of inhibition by 75 J/cm^2 of 410 nm light (figure 3c) was higher than that obtained by 225 J/cm^2 of 455 nm light (figure 3b).

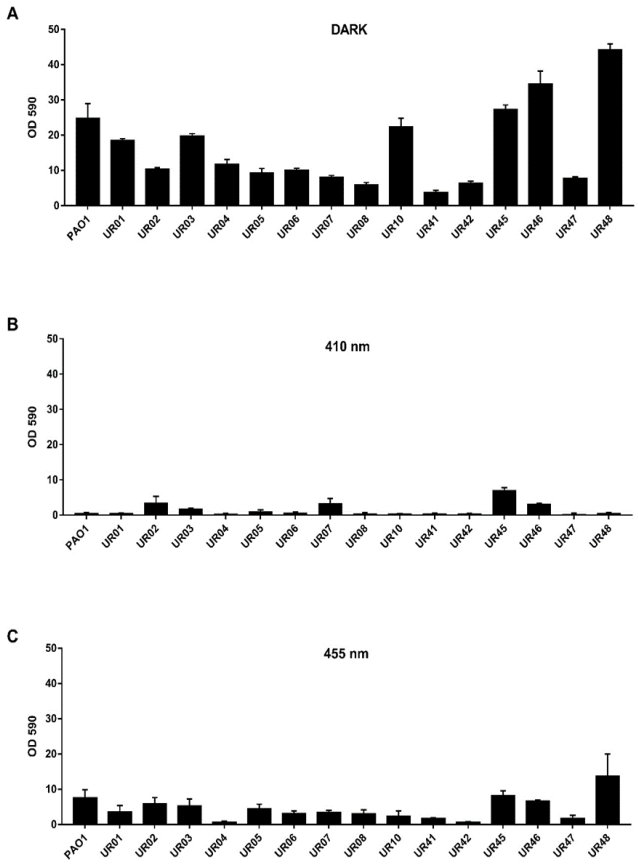

Figure 3. Inhibition of biofilm formation by blue lights of *P. aeruginosa* clinical isolates. A) control samples kept in the dark; B) samples irradiated by 410 nm blue light at 75 J/cm^2 (100 mW/cm^2 for 12.5 minutes); C) irradiation by 455 nm LED at 225 J/cm^2 (100 mW/cm^2 for 37.5 minutes). The bars represent standard deviations.

3.2 Effect of blue light on *Pseudomonas aeruginosa* biofilm eradication

As the eradication of biofilm is the most difficult goal to reach, the effect of blue light at 410 nm in eradicating 6 hour grown *P. aeruginosa* PAO1 biofilm was evaluated. Upon irradiation, the amount of adherent biomass of PAO1 biofilm decreased in a dose-light dependent manner with respect to the dark control (figure 4a). Furthermore, the amount of adherent cells decreased with increasing light energies, reaching a reduction of 6 log units upon 450 J/cm^2 (figure 4a). In all the experiments, the amount of adherent cell reduction was found to be statistically significant with respect to the dark control. Similarly, the planktonic phase of the biofilm showed a significant reduction under the highest radiant fluences (figure 4b).

The eradicating activity of light at 455 nm was not comparable to that of light at 410 nm. Interestingly, light at 455 nm did not affect cell viability of sessile and planktonic subpopulations, however, a significant depletion of matrix was observed (figure 4c).

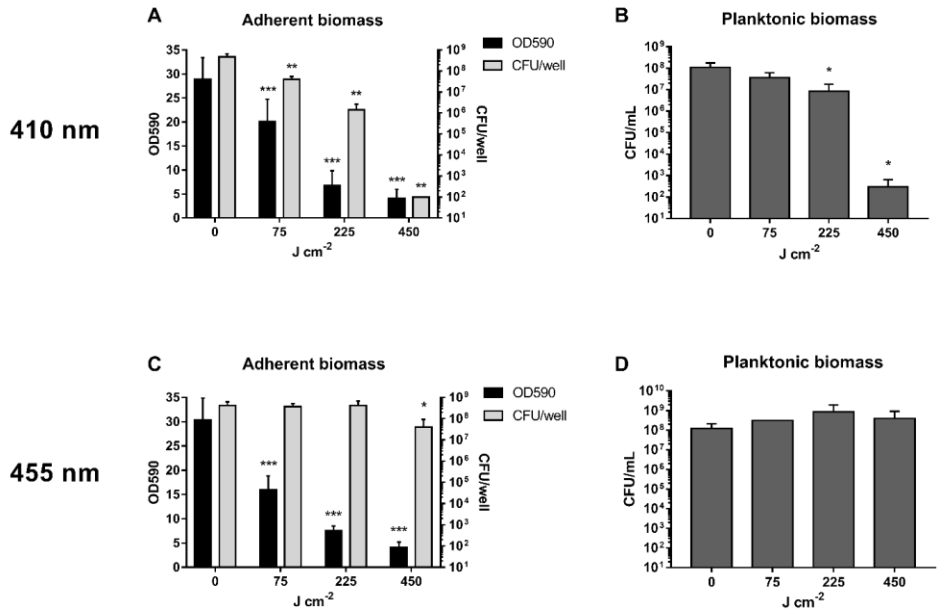

Figure 4. Eradication of *P. aeruginosa* PAO1 biofilm by 410 and 455 nm blue LEDs at increasing light doses. A) adherent biomass of biofilm upon irradiation at 410 nm represented as OD590 and cell viability expressed as CFU/well; B) planktonic biomass (CFU/mL) after irradiation with 410 nm LED; C) adherent biomass of biofilm upon 455 nm irradiation; D) planktonic cell counts after 455 nm light treatments. The values are the mean of at least three independent experiments and the bars represent standard deviations. Statistical analyses were performed by one-way ANOVA (*p < 0,05; **p < 0,01; ***p < 0,0001).

To further study the efficiency of light at 410 nm in eradicating older biofilm, a PAO1 GFP-tagged strain was let to grow on glass as biofilm for 48 hours. The blue irradiation demonstrated its efficacy in eradicating biofilm as shown from confocal analysis (figure 5). Cells from untreated biofilm were able, upon arabinose induction, to produce the green fluorescent protein (figure 5a). On the other hand, cells from irradiated biofilm did not show a fluorescent GFP signal comparable to the dark control, suggesting that 410 nm blue light impaired the main cell functionalities, including their biosynthetic machineries (figure 5b). *P. aeruginosa* biofilm irradiated with 455 nm light showed, in accordance with previous results, a higher amount of fluorescent cells compared to 410 nm (figure 5c).

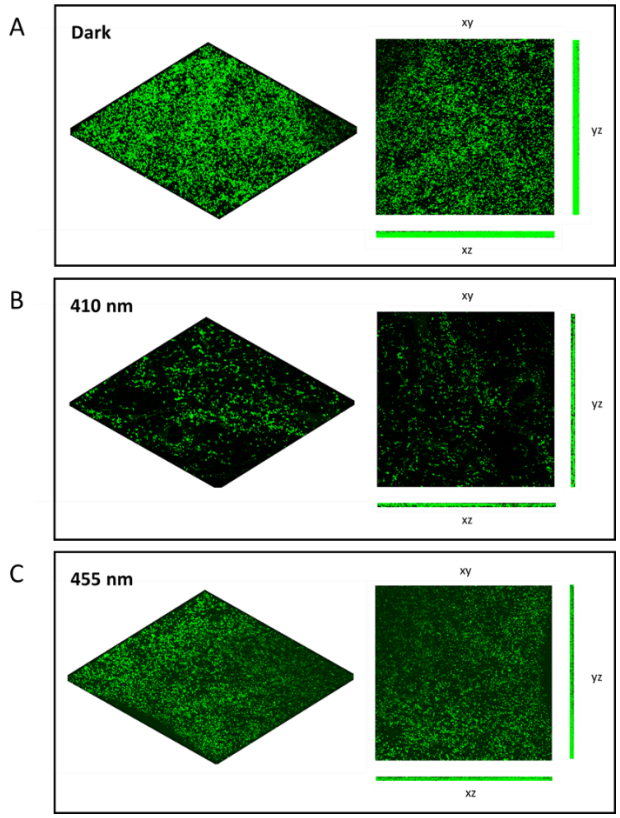

Figure 5. Eradication of 48 hours old biofilm of *P. aeruginosa* PAO1_pVOGFP by blue lights. A) control sample kept in the dark; B) irradiated biofilm by 410 nm light, 450 J/cm^2 (100 mW/cm^2 for 75 minutes); C) biofilm irradiated by 455 nm blue light, 450 J/cm^2 (100 mW/cm^2 for 75 minutes).
Images are shown in volume view and in xy, yz and xz projections.

3.3 Effects of blue light on different targets

The photo-oxidative stress elicited by blue light could damage cells and/or macromolecular component of formed matrix. In order to compare the effect of the two different wavelengths on these targets, preliminary investigations were performed as follows.

Suspended cells

The effect of blue light at two different wavelengths was tested on suspended cells through photo-spot tests: 100 J/cm^2 was the light dose from 410 nm light able to determine a 7 Log_{10} unit reduction, while 450 nm J/cm^2 was the light dose by 455 nm light able to reach the same photoinactivation rate (figure 6).

Since *P. aeruginosa* produces an extracellular matrix composed by polysaccharides, nucleic acids and proteins [24], aBL treatment was performed on different chemical targets belonging to these family compounds.

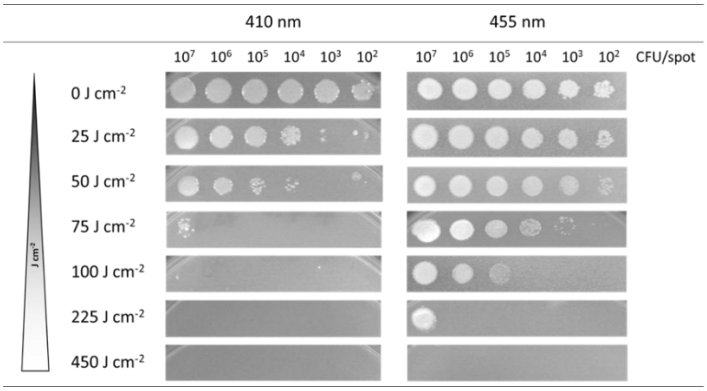

Figure 6. Representative images of photo-spot test on *P. aeruginosa* PAO1 with 410 and 455 nm blue lights. Diluted bacterial suspensions were plated on LB agar plates (from 10^7 to 10^2 CFU/spot) and irradiated at increasing light doses, keeping 100 mW/cm^2 of irradiance and increasing irradiation time.

β-galactosidase

At first, the recombinant β-galactosidase was chosen as protein target to irradiate since its enzymatic activity, that is easily detectable, reveals its structural integrity. The irradiation of β-galactosidase was performed under different conditions: in fresh minimal medium and exhausted minimal medium from PAO1 overnight culture. Interestingly, the irradiation at 410 nm at increasing radiant fluence, caused a significant decrease of the enzymatic activity only of the enzyme suspended in spent medium (figure 7). A further sample was included to evaluate if compounds from spent medium, possibly involved in sensitization by blue light, were heat sensitive. The impairment of β-galactosidase activity from both samples, heat (at 95°C for 15 minutes) and not heat-treated, was comparable. The decrease of β-galactosidase activity upon irradiation was not ascribable to alteration in primary structure (i.e. polypeptide chain break), as supported by SDS-PAGE analyses (data not shown). On the other hand, light at 455 nm (450 J/cm^2) did not show any effect on β-gal activity in all the tested conditions (fresh, spent and heat treated spent medium) (data not shown).

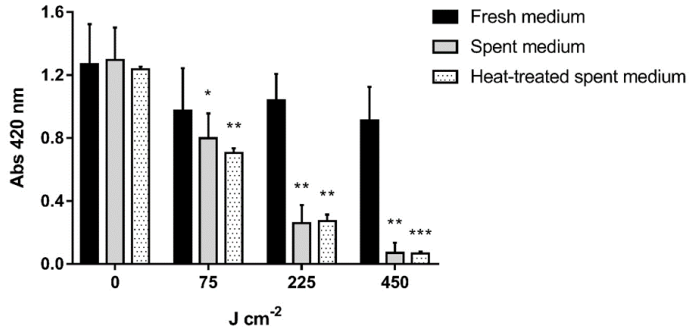

Figure 7. Irradiation of β-galactosidase by 410 nm light. Enzymatic activity was assessed by absorbance at 420 nm, measured upon 75, 225 and 450 J/cm^2 irradiation at 100 mW/cm^2 for 12.5, 37.5 and 75 minutes respectively. The values are the mean of three independent experiments and the bars represent standard deviations. Statistical analyses were performed by one-way ANOVA (*p < 0,05; **p < 0,01; ***p < 0,0001).

Plasmid DNA

In order to evaluate the effect of blue light on nucleic acid, plasmid DNA was irradiated. DNA preparations were suspended both in fresh and spent medium, heat and not heat-treated, as previously described. Plasmid DNA suspended in fresh minimal medium and irradiated at 410 nm (450 J/cm^2) did not show any change in agarose gel mobility with respect to dark control. On the other hand, the mobility of irradiated DNA suspended in spent medium was greatly slowed down compared to dark incubated DNA. Since a similar shift was observed upon irradiation of DNA suspended in heat-treated spent minimal medium, proteins seem to be not involved in blue-light photosensitization. Furthermore, an evident smear, compatible with DNA degradation, occurred when plasmid suspended in spent medium (heat and not heat treated) were irradiated (figure 8). However, blue light at 455 nm did not showed any effect on DNA mobility (data not shown).

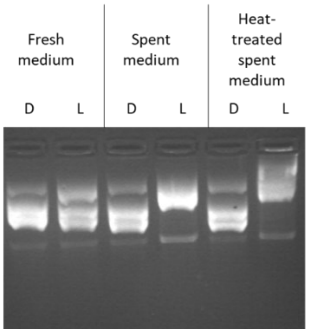

Figure 8. Irradiation of plasmid DNA by 410 and 455 nm blue lights at 450 J/cm^2 (100 mW/cm^2 for 12.5 minutes); D = samples kept in the dark; L = irradiated samples.

ONPG

As *ortho*-nitrophenyl-β-D-galactopyranoside (ONPG) mimics disaccharide lactose and it is colourless, it was chosen as sugar model. Usually, the release of yellow *ortho*-nitrophenol from ONPG shows that a break occurred in the substrate. As can be observed in figure 9, the irradiation with light at 410 nm caused an energy-dose dependent release of a yellow-orange compound, not observable under dark incubation. Similarly to previous investigations, ONPG was suspended in different medium, but no difference between the tested condition was observed. No effect was visible upon irradiation at 455 nm (data not shown).

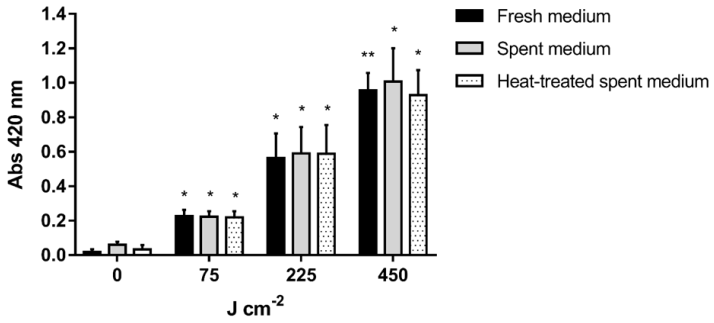

Figure 9. Irradiation of *ortho*-nitrophenyl-β-D-galactopyranoside (ONPG) by 410 nm blue light. Absorbance at 420 nm was measured upon 75, 225 and 450 J/cm^2 irradiation at 100 mW/cm^2 for 12.5, 37.5 and 75 minutes respectively. Irradiation was performed in three different condition: fresh medium, spent medium and heat-treated spent medium. The values are the mean of three independent experiments and the bars represent standard deviations. Statistical analyses were performed by one-way ANOVA (*p < 0,05; **p < 0,01; ***p < 0,0001).

Catalase A

Biofilm matrix also plays the role of reservoir of virulence factors increasing the pathogenicity of *P. aeruginosa*. Among these factors, catalase A (KatA) from PAO1 strain was chosen as macromolecule to photoinactivate. KatA is a metalloprotein containing heme as prosthetic group, that could behave as a possible photosensitizer during blue light irradiation. To evaluate the sensitivity of KatA upon irradiation, enzymatic activity was determined by reaction of undecomposed hydrogen peroxide with ammonium molybdate to form a yellowish complex which was measured spectrophotometrically at 405 nm. Blue light was delivered at increasing light doses up to 450 J/cm^2. Catalase A activity, upon incubation in the dark, reaches a mean value of Absorbance at 405 nm of 0,6 (figure 10). Upon irradiation with 5 J/cm^2 of 410 nm blue light, catalase activity significantly decreased, since the amount of remaining H_2O_2 is higher than the control kept in the dark. Light doses from 10 to 450 J/cm^2 of 410 nm blue LED caused a significant reduction in enzymatic activity reaching values around 2, which represent the value of Abs at 405 nm of hydrogen peroxide incubated alone (highlighted by the horizontal line in the graph). Interestingly, also 455 nm blue light was efficient in catalase A photoinactivation, and a complete enzymatic inactivation was observed upon 225 J/cm^2.

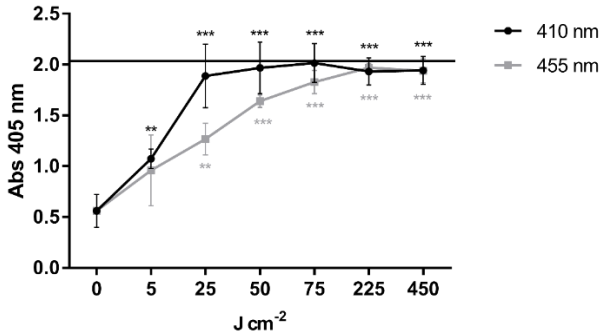

Figure 10. Photoinactivation of recombinant catalase A by 410 and 455 nm blue lights. Absorbance at 405 nm was measured upon irradiation at increasing light doses and incubation of protein solution with hydrogen peroxide and the subsequent addition of ammonium molybdate. Horizontal line approx. at A_{405nm} = 2 represents the positive control with hydrogen peroxide in complex with ammonium molybdate. The data are the means of three independent experiments ± standard deviation.

4. Discussion

Pseudomonas aeruginosa biofilms are tolerant to traditional antibiotics. It is urgent to find new techniques that prevent biofilm formation and/or eradicate formed biofilms. Among alternative approaches, EDTA and EGTA [25], surfactants such as SDS [26], D-amino acids [27] and more recently, photo-antimicrobials [28] have been proposed as eradicating treatments. Since recently, blue light alone showed interesting anti-*Pseudomonas* activity, in this study the effect of blue light on *P. aeruginosa* biofilm was investigated. The chosen wavelengths, 410 and 455 nm, showed different activity on PAO1 strain.

Blue light at 410 nm prevented PAO1 suspended cells from forming an adherent community. A decrease of ~98 % of adherent biomass, obtained for all the tested radiant fluence, represents a very good inhibition rate. Under the tested conditions, the amount of recovered sessile and suspended cells decreased in a light-dose dependent manner, while the decrease of extracellular matrix was independent of the radiant exposure. Thus, it seems that low energy doses are sufficient to impair matrix formation, while higher doses are necessary to impair cell growth. It seems that light at 410 nm affects *P. aeruginosa* machinery involved in the production of biofilm matrix that is induced by Quorum Sensing (QS) mediators. Fila et al. reported that among QS mediators mainly involved in biofilm formation, C4-HSLs (Rhl) and 3-oxo-C12-HSL (Las) showed a certain degree of sensitivity to light at 410 nm, while PQS was not affected [14]. Moreover, the effect of blue light on autoinducers is an add-value influencing not only the biofilm formation, but also the production of virulence factors controlled by QS, such as pyoverdine, phenazine, protease, lipase, toxins [29, 14].

Furthermore, in this study, 410 nm light at a low radiant fluence (5 J/cm^2) impaired the activity of catalase A, an enzyme constitutively expressed and not regulated by QS system, involved in counteracting hydrogen peroxide production. This detoxifying enzyme, usually released in the extracellular environment [30], contributes to counteract the oxidative burst induced by immune cells such as polymorphonuclear neutrophils and stress induced by some antimicrobials, supporting the bacterial survival. The inactivation of katA renders indeed *P.*

aeruginosa more sensitive to immunity system attack and H_2O_2 releasing antibiotics [31].

Light at 455 nm inhibited the biofilm formation, even if to a lower extent than 410 nm source. The blue light at 455 nm compromised the ability to form matrix and successfully impaired catalase A activity, but at higher radiant exposure compared to 410 nm light source.

Both wavelengths, 410 and 455 nm, were efficient in inhibiting the biofilm formation of *P. aeruginosa* CAUTIs strains. Among the tested clinical strains, few isolates were strong and other were weak biofilm formers, compared to PAO1 strain chosen as biofilm former. Blue light inhibited not only biofilm formation of PAO1, but also of all the tested clinical isolates. It was necessary to increase the radiant exposure of light at 455 nm to get inhibition rates comparable to that of 410 nm light. This study supports the potential of blue light irradiation in disinfection and/or preventing pathogen dissemination in hospital environment.

Although it is very important to prevent the biofilm formation on medical devices and human tissues, the eradication of formed biofilm is a difficult goal and represents a purpose that nowadays most of the current antimicrobials fail to reach. Indeed, light doses necessary to eradicate biofilm were higher than those used to inhibit the biofilm formation. This is in accordance with the well-known tolerance of biofilm to antimicrobials: it is more difficult to kill adherent cells than the planktonic ones [32].

The irradiation of formed biofilms with blue light damaged both the cellular (adherent and planktonic populations) and the matrix components. In particular, irradiation with 410 nm was successful in eradicating young and older biofilms. Under the tested conditions, both biofilm matrix and adherent cells decreased with increasing light doses. Blue light irradiation demonstrated not only detach and spread sessile cells, but also to kill them. In particular, 455 nm wavelength was active in decreasing the amount of biomass, and not active in killing cells from planktonic and/or adherent phases. It should be considered that common antibiofilm approaches permit the detachment of adherent bacteria and a further antibiotic/antimicrobial treatment is needed to prevent further dispersion [33]. Thus, 455 nm blue light could have a possible application in combination with other antimicrobial agents.

To investigate the effect of blue light on biofilm components, cellular and matrix components were considered. *P. aeruginosa* PAO1 suspended cells showed a different sensitivity to blue light depending on wavelength and cellular concentration. Tomb et al. reported that the effect of blue light at increasing wavelengths on *P. aeruginosa* was similar [8]. In contrast, under the tested conditions, light at 410 and 455 nm showed different rates of photoinactivation: 455 nm light was less efficient than 410 nm in killing suspended cells. It was necessary to increase threefold the radiant exposure of 455 nm light to obtain the anti-*Pseudomonas* effect obtained at 410 nm. This observation is in accordance with the analysis performed by Hessling et al., in 2017, aimed at comparing the antimicrobial activity of 470 and 405 nm light sources on different microbial species: the former was less effective than the latter by a factor between 2 and 5 [34].

In the present study, the efficiency of blue light treatment on suspended *P. aeruginosa* PAO1 cells showed to be proportionally dependent on bacterial density and light dose: it was necessary to increase the light dose to photoinactivate samples at high cellular concentration. These results are in accordance with Bumah et al. that reported that wavelength and bacterial density influenced the bactericidal effect of 405 and 470 nm blue light [35].

It is well-known that in antimicrobial photodynamic treatment, is essential to administer exogenous PS that interact with microbial cell wall and/or enter the cytoplasmic environment, and upon irradiation with visible light induce a photo-oxidative stress via type I and II reactions [36]. In blue light treatment, it is not necessary to administer exogenous PS, different compounds were proposed as endogenous photosensitizers, presumably belonging to porphyrin family such as coproporphyrin III, flavins, and cytochromes [37]. In addition to porphyrin derivatives, *in P. aeruginosa*, other compounds could be activated by blue light. Sabino suggested that such high sensitivity of *P. aeruginosa* to blue light might be linked to high yield production of pyoverdine, a naturally occurring fluorescent pigment that strongly absorbs light at 415 nm and may undergo photodynamic reactions [38]. Among pyocyanin derivatives, phenazine-1-carboxylic acid (absorbance peak at 415 nm) could be activated by blue light and play the role of

endogenous photosensitizer [39]. Lipovski reported that, despite the fact that pyocyanin generates ROS upon irradiation, *P. aeruginosa* 1316 was tolerant to broadband visible light-induced toxicity. Nevertheless, irradiation of *E. coli* 1313 in the presence of pyocyanin, decreased significantly their viability in comparison to light alone. In this case, pyocyanin could play the role of photosensitizer [40]. Furthermore, Reszka observed that, despite a substantial bleaching of pyocyanin upon photodynamic inactivation, the capacity for generation of superoxide diminished by only 50%, suggesting that the pyocyanin-derived oxidation product(s) still possesses significant reactivity [41]. On the other side, Hendiani et al., and our group reported the possible protective role of pyocyanin in oxidative stress induced by photodynamic treatment [42, 39]. Until now, researchers focused their attention on protoporphyrin derivative as putative endogenous photosensitizers. The role of pigments in photosensitization induced by blue light or PDT could depend *in vivo* by a complex and dynamic balance between their pro-oxidant and antioxidant activities. However, further investigations are necessary to evaluate if pyocyanin, pyoverdine, other pigments and catabolites could contribute to bacterial photosensitization.

As previously introduced, this study also considered the effect of blue light on biofilm matrix. For this aim, molecules representative of matrix compounds were irradiated under different experimental conditions. The enzyme β-galactosidase, chosen as representative protein, was suspended in fresh medium, irradiated with blue light at 410 nm and its catalytic activity did not change. By contrast, suspending the enzyme in spent medium from overnight cultures of *P. aeruginosa* PAO1, made β-galactosidase sensitive to blue light. Interestingly, this sensitivity was also maintained upon heat treatment of the supernatant, suggesting that a cellular component insensitive to heat stress could play the role of photosensitizer for the photoinactivation by blue light. Moreover, 410 nm blue light impaired the plasmid DNA migration when combined with *P. aeruginosa* spent medium (heat-treated and not) supporting the involvement of a putative extracellular PS activated by blue light. The disaccharide ONPG, chosen as sugar target, was sensitive to 410 nm blue light irradiation in a dose dependent way, independently from the presence or absence of overnight spent medium.

The mechanism of blue light in the antimicrobial field seems linked to the involvement of endogenous photosensitizers. This study supports further considerations to take into account, such as the possible involvement of extracellular photosensitizers. Light at 410 nm showed a great inactivation effect when combined with *P. aeruginosa* released substances in overnight-spent media. Our findings support the possible presence of non-heat-sensitive extracellular photosensitizers that could be activated by blue light and damage extracellular macromolecules. This is in accordance with the hypothesis formulated by Hamblin, that the light-induced bacterial killing is a result of endogenous bacterial photosensitizers and of various photosensitizing metabolites produced and secreted by bacteria [43]. Furthermore, it can be also hypothesized that bacterial overcrowding, different metabolic pathways, oxygen tension, environmental stresses, and other conditions influence the physiological state of bacterial cell, and can change the pool of endogenous and/or released PSs, and favor or not the sensitivity to blue light.

In conclusion, the irradiation of a target surface or a tissue with light at 410 nm could be a technique aimed to prevent the growth and the biofilm formation and/or to eradicate formed biofilm of *Pseudomonas aeruginosa*. A certain degree of anti-*Pseudomonas* activity was also displayed by light at 455 nm, even if at a lower extent. This study supports the validity and the great potential of blue light in controlling the dissemination of an opportunistic pathogen such as *P. aeruginosa*. A simple technique, such aBL, in combination with other strategies could contribute to the reduction of the infection incidence by *P. aeruginosa* in clinical context.

References

[1] Y. Morita, J. Tomida, Y. Kawamura, Responses of Pseudomonas aeruginosa to antimicrobials, Front. Microbiol. 4 (2013) 1–8. doi:10.3389/fmicb.2013.00422.

[2] M.W. Azam, A.U. Khan, Updates on the pathogenicity status of Pseudomonas aeruginosa, Drug Discov. Today. 00 (2018) 1–10. doi:10.1016/j.drudis.2018.07.003.

[3] Q. Wei, L.Z. Ma, Biofilm matrix and its regulation in Pseudomonas aeruginosa, Int. J. Mol. Sci. 14 (2013) 20983–21005. doi:10.3390/ijms141020983.

[4] P.K. Taylor, A.T.Y. Yeung, R.E.W. Hancock, Antibiotic resistance in Pseudomonas aeruginosa biofilms: Towards the development of novel anti-biofilm therapies, J. Biotechnol. 191 (2014) 121–130. doi:10.1016/j.jbiotec.2014.09.003.

[5] C. Chenoweth, S. Saint, Preventing Catheter-Associated Urinary Tract Infections in the Intensive Care Unit, Crit. Care Clin. 29 (2013) 19–32. doi:10.1016/j.ccc.2012.10.005.

[6] E.B.M. Breidenstein, C. de la Fuente-Núñez, R.E.W. Hancock, Pseudomonas aeruginosa: All roads lead to resistance, Trends Microbiol. 19 (2011) 419–426. doi:10.1016/j.tim.2011.04.005.
[7] K. Bush, P. Courvalin, G. Dantas, J. Davies, B. Eisenstein, P. Huovinen, G.A. Jacoby, R. Kishony, B.N. Kreiswirth, E. Kutter, S.A. Lerner, S. Levy, K. Lewis, O. Lomovskaya, J.H. Miller, S. Mobashery, L.J.V. Piddock, S. Projan, C.M. Thomas, A. Tomasz, P.M. Tulkens, T.R. Walsh, J.D. Watson, J. Witkowski, W. Witte, G. Wright, P. Yeh, H.I. Zgurskaya, Tackling antibiotic resistance, Nat. Rev. Microbiol. 9 (2011) 894–896. doi:10.1038/nrmicro2693.
[8] R.M. Tomb, T.A. White, J.E. Coia, J.G. Anderson, S.J. MacGregor, M. Maclean, Review of the Comparative Susceptibility of Microbial Species to Photoinactivation Using 380–480 nm Violet-Blue Light, Photochem. Photobiol. 94 (2018) 445–458. doi:10.1111/php.12883.
[9] Y. Wang, Y. Wang, Y. Wang, C.K. Murray, M.R. Hamblin, D.C. Hooper, T. Dai, Antimicrobial blue light inactivation of pathogenic microbes: State of the art, Drug Resist. Updat. 33–35 (2017) 1–22. doi:10.1016/j.drup.2017.10.002.
[10] F.D. Halstead, J.E. Thwaite, R. Burt, T.R. Laws, M. Raguse, R. Moeller, M.A. Webber, B.A. Oppenheim, Antibacterial activity of blue light against nosocomial wound pathogens growing planktonically and as mature biofilms, Appl. Environ. Microbiol. 82 (2016) 4006–4016. doi:10.1128/AEM.00756-16.
[11] R.M. Amin, B. Bhayana, M.R. Hamblin, T. Dai, Antimicrobial blue light inactivation of Pseudomonas aeruginosa by photo-excitation of endogenous porphyrins: In vitro and in vivo studies, Lasers Surg. Med. 48 (2016) 562–568. doi:10.1002/lsm.22474.
[12] A. Gupta, M.S. Vrahas, C.K. Murray, T. Dai, M.E. Sherwood, R. Yin, G.P. Tegos, Y.-Y. Huang, M.R. Hamblin, Blue Light Rescues Mice from Potentially Fatal Pseudomonas aeruginosa Burn Infection: Efficacy, Safety, and Mechanism of Action, Antimicrob. Agents Chemother. 57 (2012) 1238–1245. doi:10.1128/aac.01652-12.
[13] Y. Wang, X. Wu, J. Chen, R. Amin, M. Lu, B. Bhayana, J. Zhao, C.K. Murray, M.R. Hamblin, D.C. Hooper, T. Dai, Antimicrobial Blue Light Inactivation of Gram-Negative Pathogens in Biofilms: In Vitro and in Vivo Studies, J. Infect. Dis. 213 (2016) 1380–1387. doi:10.1093/infdis/jiw070.
[14] G. Fila, M. Krychowiak, M. Rychlowski, K. P. Bielawski, M. Grinholc, Antimicrobial blue light photoinactivation of Pseudomonas aeruginosa: Quorum sensing signaling molecules, biofilm formation and pathogenicity, J. Biophotonics. (2018). doi:10.1002/jbio.201800079.
[15] V.T. Orlandi, E. Martegani, F. Bolognese, Catalase A is involved in the response to photooxidative stress in Pseudomonas aeruginosa, Photodiagnosis Photodyn. Ther. 22 (2018) 233–240. doi:10.1016/j.pdpdt.2018.04.016.
[16] K. McKenzie, M. Maclean, I. V. Timoshkin, E. Endarko, S.J. Macgregor, J.G. Anderson, Photoinactivation of bacteria attached to glass and acrylic surfaces by 405 nm light: Potential application for biofilm decontamination, Photochem. Photobiol. 89 (2013) 927–935. doi:10.1111/php.12077.
[17] C.K. Stover, X.Q. Pham, A.L. Erwin, S.D. Mizoguchi, P. Warrener, M.J. Hickey, F.S. Brinkman, W.O. Hufnagle, D.J. Kowalik, M. Lagrou, R.L. Garber, L. Goltry, E. Tolentino, S. Westbrock-Wadman, Y. Yuan, L.L. Brody, S.N. Coulter, K.R. Folger, A. Kas, K. Larbig, R. Lim, K. Smith, D. Spencer, G.K. Wong, Z. Wu, I.T. Paulsen, J. Reizer, M.H. Saier, R.E. Hancock, S. Lory, M. V Olson, Complete genome sequence of {Pseudomonas} aeruginosa {PAO}1, an opportunistic pathogen, Nature. 406 (2000) 959–964. doi:10.1038/35023079.
[18] V.T. Orlandi, F. Bolognese, B. Rolando, S. Guglielmo, L. Lazzarato, R. Fruttero, Anti-pseudomonas activity of 3-nitro-4-phenylfuroxan, Microbiol. (United Kingdom). 164 (2018) 1557–1566. doi:10.1099/mic.0.000730.
[19] V.T. Orlandi, F. Villa, S. Cavallari, P. Barbieri, S. Banfi, E. Caruso, P. Clerici, Photodynamic therapy for the eradication of biofilms formed by catheter associated Pseudomonas aeruginosa strains, 26 (2011) 129–133.
[20] W.H. Poh, N. Barraud, S. Guglielmo, L. Lazzarato, B. Rolando, R. Fruttero, S.A. Rice, Furoxan Nitric Oxide Donors Disperse Pseudomonas aeruginosa Biofilms, Accelerate Growth, and Repress Pyoverdine Production, ACS Chem. Biol. 12 (2017) 2097–2106. doi:10.1021/acschembio.7b00256.

[21] F. Bolognese, M. Bistoletti, P. Barbieri, V.T. Orlandi, Honey-sensitive Pseudomonas aeruginosa mutants are impaired in catalase A, Microbiol. (United Kingdom). 162 (2016) 1554–1562. doi:10.1099/mic.0.000351.
[22] F. Bolognese, C. Scanferla, E. Caruso, T. Orlandi, PT, Int. J. Biol. Macromol. (2019). doi:10.1016/j.ijbiomac.2019.04.061.
[23] M. H. Hadwan, L. A. Almashhedy, A. R. S. Alsalman, Precise method fot the assessment of catalase-like activity in seminal fluids, International Journal of Pharma and Bio Sciences, 4 (2013) 949–954.
[24] M. Toyofuku, B. Roschitzki, K. Riedel, L. Eberl, Identification of proteins associated with the pseudomonas aeruginosa biofilm extracellular matrix, J. Proteome Res. 11 (2012) 4906–4915. doi:10.1021/pr300395j.
[25] E. Banin, K. M. Brady, E. P. Greenberg, Chelator-Induced Dispersal and Killing of Pseudomonas aeruginosa Cells in a Biofilm, Infect. Sci. 72 (2006) 2064–2069. doi:10.1128/AEM.72.3.2064.
[26] P. V. Gawande, K. Lovetri, N. Yakandawala, T. Romeo, G.G. Zhanel, D.G. Cvitkovitch, S. Madhyastha, Antibiofilm activity of sodium bicarbonate, sodium metaperiodate and SDS combination against dental unit waterline-associated bacteria and yeast, J. Appl. Microbiol. 105 (2008) 986–992. doi:10.1111/j.1365-2672.2008.03823.x.
[27] C.J. Sanchez, K.S. Akers, D.R. Romano, R.L. Woodbury, S.K. Hardy, C.K. Murray, J.C. Wenke, D-amino acids enhance the activity of antimicrobials against biofilms of clinical wound isolates of Staphylococcus aureus and Pseudomonas aeruginosa, Antimicrob. Agents Chemother. 58 (2014) 4353–4361. doi:10.1128/AAC.02468-14.
[28] M. Wainwright, T. Maisch, S. Nonell, K. Plaetzer, A. Almeida, G.P. Tegos, M.R. Hamblin, Photoantimicrobials—are we afraid of the light?, Lancet Infect. Dis. 17 (2017) e49–e55. doi:10.1016/S1473-3099(16)30268-7.
[29] G. Fila, A. Kawiak, Blue light treatment of Pseudomonas aeruginosa: Strong bactericidal activity, synergism with antibiotics and inactivation of virulence factors, 8 (2017) 938–958.
[30] D. Shin, Y. Choi, Y. Cho, Unusual Properties of Catalase A (KatA) of Pseudomonas aeruginosa PA14 Are Associated with Its Biofilm Peroxide Resistance, 190 (2008) 2663–2670. doi:10.1128/JB.01580-07.
[31] J.S. Lee, Y.J. Heo, J.K. Lee, Y.H. Cho, KatA, the major catalase, is critical for osmoprotection and virulence in Pseudomonas aeruginosa PA14, Infect. Immun. 73 (2005) 4399–4403. doi:10.1128/IAI.73.7.4399-4403.2005.
[32] C.W. Hall, T.F. Mah, Molecular mechanisms of biofilm-based antibiotic resistance and tolerance in pathogenic bacteria, FEMS Microbiol. Rev. 41 (2017) 276–301. doi:10.1093/femsre/fux010.
[33] C. Beloin, S. Renard, J.M. Ghigo, D. Lebeaux, Novel approaches to combat bacterial biofilms, Curr. Opin. Pharmacol. 18 (2014) 61–68. doi:10.1016/j.coph.2014.09.005.
[34] M. Hessling, B. Spellerberg, K. Hoenes, Photoinactivation of bacteria by endogenous photosensitizers and exposure to visible light of different wavelengths - a review on existing data. FEMS Microbiol Lett. 364 (2017). doi: 10.1093/femsle/fnw270.
[35] V. V. Bumah, D.S. Masson-Meyers, S.E. Cashin, C.S. Enwemeka, Wavelength and bacterial density influence the bactericidal effect of blue light on methicillin-resistant Staphylococcus aureus (MRSA), Photomed. Laser Surg. 31 (2013) 547–553. doi:10.1089/pho.2012.3461.
[36] E. Caruso, S. Banfi, P. Barbieri, B. Leva, V.T. Orlandi, Synthesis and antibacterial activity of novel cationic BODIPY photosensitizers, J. Photochem. Photobiol. B Biol. 114 (2012) 44–51. doi:10.1016/j.jphotobiol.2012.05.007.
[37] R. Lubart, A. Lipovski, Y. Nitzan, H. Friedmann, A possible mechanism for the bactericidal effect of visible light, Laser Ther. 20 (2011) 17–22. doi:10.5978/islsm.20.17.
[38] C.P. Sabino, M. Wainwright, C. Dos Anjos, F.P. Sellera, M.S. Baptista, N. Lincopan, M.S. Ribeiro, Inactivation kinetics and lethal dose analysis of antimicrobial blue light and photodynamic therapy, Photodiagnosis Photodyn Ther. 28 (2019)186-191. doi: 10.1016/j.pdpdt.2019.08.022.
[39] V.T. Orlandi, F. Bolognese, L. Chiodaroli, T. Tolker-Nielsen, P. Barbieri, Pigments influence the tolerance of Pseudomonas aeruginosa PAO1 to photodynamically induced oxidative stress. Microbiology. 161 (2015) 2298-309. doi:10.1099/mic.0.000193.
[40] A. Lipovsky, Y. Nitzan, R. Lubart. A possible mechanism for visible light-induced wound healing. Lasers Surg Med. 40 (2008) 509-14. doi: 10.1002/lsm.20668.

[41] K.J. Reszka, G.M. Denning, B.E. Britigan, Photosensitized oxidation and inactivation of pyocyanin, a virulence factor of *Pseudomonas aeruginosa*, Photochem Photobiol. 82 (2006) 466-73. PubMed PMID: 16613500.
[42] S. Hendiani, M. Pornour, N. Kashef, Quorum-sensing-regulated virulence factors in *Pseudomonas aeruginosa* are affected by sub-lethal photodynamic inactivation. Photodiagnosis Photodyn Ther. 26 (2019)8-12. doi: 10.1016/j.pdpdt.2019.02.010.
[43] M.R. Hamblin, G. Jori, Photodynamic Inactivation of Microbial Pathogens: Medical and Environmental, Royal Society of Chemistry, 2011.

Effect of blue light on *Pseudomonas aeruginosa* biofilms in central venous catheters

Preliminary study

Abstract

Background. *Pseudomonas aeruginosa* is an opportunistic pathogen, able to escape from antibiotic actions and to form biofilm on tissues and abiotic surfaces. The phenomenon of antibiotic resistance is a quickly growing and dangerous threat for human's health, encouraging the research of new non-antibiotic approaches against microbial pathogens. Among these approaches, antimicrobial Blue Light Therapy (aBLT) seem very promising.

Aim. In this preliminary study, aBLT was aimed at inhibiting and/or eradicating biofilm of *P. aeruginosa* grown on central venous catheters (CVC).

Material and methods. Traditional technique as viable count method was used to evaluate the effect of blue light on *P. aeruginosa* biofilms. ANOVA analysis highlighted the statistical significance of the obtained results.

Results. The formation of biofilm in the lumen of catheters was successfully prevented by 410 nm blue light. Furthermore, a significant eradication of adherent population viability was also achieved on CVC colonized by 24h *P. aeruginosa* biofilm.

Conclusions. Preliminary results highlight the great potential of aBLT in controlling catheter-associated infections.

1. Introduction

Pseudomonas aeruginosa is a bacterial opportunistic pathogen able to grow on biological tissues or inert surfaces, where it can form structured communities called biofilms (Moradali et al., 2017). In the clinical field, common examples are represented by the colonization of wounds or skin lesions or by the adhesion to the airways epithelia of Cystic Fibrosis patients, where conventional antibiotic therapies have no efficacy due to biofilm enhanced drug resistance (El Zowalaty et al., 2015).

Inert surfaces of medical devices, such as catheters, central lines, and prostheses, can support the adhesion of pathogen populations, with drastic reductions in patients' prognosis expectancies. Biofilm structure ensures a reservoir of cells to bacterial populations even in the presence of conventional antimicrobial therapies and a possible dissemination of cells to other body districts. As a result, resident biofilms not only impair the functionality of medical devices, but they could be the cause of general septicemias upon possible infiltration into the bloodstream (Rybtke et al., 2015). In this scenario, both inhibition and eradication of microbial biofilms require urgent strategies to be applied as alternative to or in conjunction with conventional therapies. This study was aimed at investigating the potential of antimicrobial Blue Light Therapy (aBLT) in inhibiting and/or eradicating the biofilms of *P. aeruginosa* formed in the lumen of central venous catheters (CVC) routinely used in clinical settings.

2. Materials and methods

2.1 Bacterial strain and culture conditions

Pseudomonas aeruginosa PAO1 was used as model microorganism to perform biofilm photoinactivation experiments. Bacterial cultures were grown in in Luria-Bertani (LB) medium in liquid or solid form (1,5% W/V agar).

1.2 Light source

The lighting unit for the antibiofilm tests was the LULab system with light emission at a wavelength of 410 nm. An irradiance of 100 mW/cm^2 was used and the samples were irradiated for 4500s, with a final fluence rate of 450 J/cm^2.

2.3 Biofilm photoinactivation assay on CVC

P. aeruginosa PAO1 were grown in LB medium at 37°C under agitation (200 rpm). Overnight cultures were diluted 200-fold in M9 minimal medium supplemented with 10 mM glucose and 0,2% W/V casamino acids, used as carbon and nitrogen sources. A volume of 150 µL of the diluted samples (approx. 10^7 CFU/mL) was added to sterile segments of central venous catheters of 3 cm, which were subsequently subjected to light irradiation. Unirradiated (dark) samples were always included as

controls. To investigate the effect of inhibition on biofilm formation, PAO1 cells were irradiated under blue light at 410 nm, reaching a final light dose of 450 J/cm^2. Upon irradiation, samples were incubated at 37°C for 24 hours in Petri dishes to allow biofilm formation. To assess the potential of aBLT in eradicating PAO1 biofilms, the same experimental setting was applied to PAO1 preformed biofilms obtained after growth of 24 hours at 37°C in static conditions (figure 1).

As for the previous experiments in multi-well plates, the viable count technique was adopted to quantify biofilm formation. After removal of the planktonic phases with the inoculated volume of growth medium, sessile populations were recovered by flowing fresh phosphate buffer solution (1X PBS) in the lumen of each catheter. Collected samples were submitted to the protocol of viable count by 10-fold serial dilutions of each sample and plating a volume (10 µl) of undiluted or diluted samples on LB agar. After incubation at 37°C for 24h, cell density was expressed as CFU/catheter in accordance with colony numbers on agar plates. All experiments were repeated independently for at least three times, and statistical analyses were performed by one-way ANOVA.

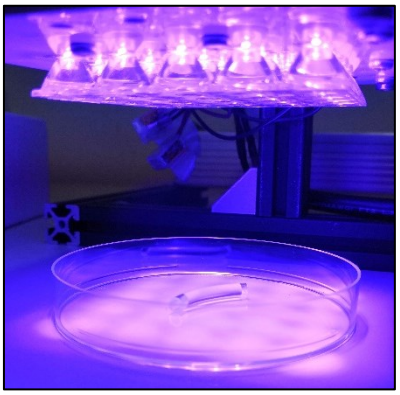

Figure 1. Representative image of the experimental setup used to evaluate the effect of 410 nm blue light irradiation on the eradication of *P. aeruginosa* PAO1 biofilm grown in the lumen of a central venous catheter.

3. Results and discussion

aBLT (antimicrobial Blue Light Therapy) is emerging as a promising strategy to contrast pathogens growth and spread, with multiple targets inside cells and a possible application both in inhibiting and, above all, eradicating pathogen biofilms. Among medical devices, catheters represent an important challenge since pathogen colonization could result in bloodstream contamination as a result of lesions generated, for example, during surgical device removal.

The efficacy of aBLT in inhibiting the biofilm formation by *P. aeruginosa* was evaluated by using an experimental model based on segments of central venous system catheters after inoculation with PAO1 cultures. Experimental setups were intended at irradiating preformed or growing biofilms with 410 nm LED devices and evaluating cell vitality as an indicator of antimicrobial and or/antibiofilm activity of blue light.

Figure 2A illustrates the experimental results both in terms of inhibition and eradication of PAO1 biofilms after irradiation with 410 nm blue light (panels A and B, respectively).

A dramatic decrease in cell vitality was observed when considering inhibition potential of blue light treatment, in comparison to dark controls. Notably, from a population with cell density of ~10^8 CFU/catheter, blue light delivered at a final light dose of 450 J/cm^2 reduced cell viability to a degree comparable to the lower detection limit of the system.

As mentioned above, the presence of mature biofilms on medical devices could contribute to increase the infection severity and spreading of pathogens in other body niches and the eradication potential of blue light treatment was evaluated accordingly. Light at410 nm was delivered to catheters contaminated with 24h old biofilms of *P. aeruginosa* PAO1 model strain (figure 2B). A 4 Log reduction was observed when comparing the experimental samples to unirradiated controls.

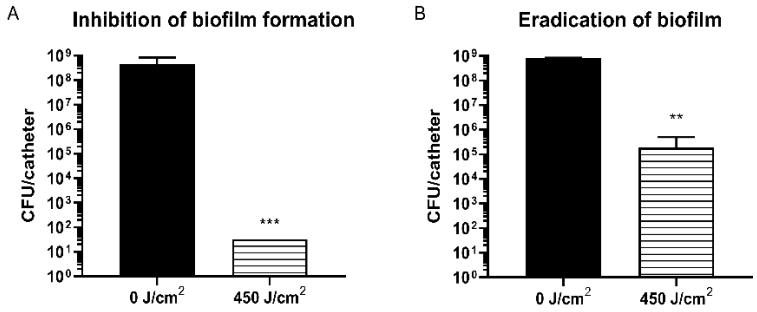

Figure 2. Effects of the treatment with blue light of *P. aeruginosa* biofilms grown in central venous system catheters. A) inhibition of biofilm formation with 410 nm blue light. B) eradication of preformed biofilms by 410 nm blue light. Blue light was delivered at 450 J/cm^2 fluence rate. Black bars represent control dark samples; striped bars represent irradiated samples. Data are the mean of three independent experiments ± standard deviation, and statistical analyses was performed by one-way ANOVA (**p < 0,01; ***p < 0,0001).

These preliminary results are a promising start for the use of blue light as an antimicrobial approach, where the absence of an external PS could avoid problems deriving from incorrect drug delivery to target cells. More details will be discussed in the following section.

References

El Zowalaty, M. E., Al Thani, A. A., Webster, T. J., El Zowalaty, A. E., Schweizer, H. P., Nasrallah, G. K., et al. (2015). Pseudomonas aeruginosa: Arsenal of resistance mechanisms, decades of changing resistance profiles, and future antimicrobial therapies. *Future Microbiol.* 10, 1683–1706. doi:10.2217/fmb.15.48.

Moradali, M. F., Ghods, S., and Rehm, B. H. A. (2017). Pseudomonas aeruginosa lifestyle: A paradigm for adaptation, survival, and persistence. *Front. Cell. Infect. Microbiol.*

Rybtke, M., Hultqvist, L. D., Givskov, M., and Tolker-Nielsen, T. (2015). Pseudomonas aeruginosa Biofilm Infections: Community Structure, Antimicrobial Tolerance and Immune Response. *J. Mol. Biol.* 427, 3628–3645. doi:10.1016/j.jmb.2015.08.016.

5. Discussion

In recent years, the rise and spread of drug resistant microbial infections have become main issues for the scientific community. As a possible result of massive antibiotic use, pathogens are becoming much more resistant to conventional antimicrobial treatments, with inherent reduction in life expectancy for infected patients. In particular, this alarming phenomenon, known as antimicrobial resistance (AMR), often involves nosocomial pathogens that affect the highly susceptible population of hospitalized patients, worsening their health conditions (Pendleton et al., 2013; Santajit and Indrawattana, 2016). Many virulence factors, such as proteases, pigments, quorum sensing signalling molecules, are produced and secreted by microbial pathogens and are effective in coping with host defence systems and facilitating the growth and establishment of sessile populations, called biofilms. The ability to grow in highly structured communities enables microbial cells to communicate with one another and to share public goods, resembling a pseudo-multicellular organism. As a whole, biofilm formation is a multistep process, that starts from provisional interactions between small populations of cells and suitable substrates and results in the formation of sessile communities of pathogens, which are protected from the external environment by the externally secreted matrix (Del Pozo and Patel, 2007). Spreading of microorganisms represents a common trait of biofilm lifestyle since clusters of cells usually detach from the adherent mass and colonize surrounding districts. As a result, biofilm-mediated infections are typically recalcitrant to antibiotic agents and become the cause of persistent infections (Percival et al., 2015; Jamal et al., 2018). For these reasons, big efforts are needed to find new therapeutic approaches against multidrug resistant pathogens, and to efficiently target microbial infections where biofilms are involved. Along with conventional antimicrobial therapies, new promising strategies are emerging, based on the combinatorial effect of visible light, oxygen, and particular chemicals, called photosensitizers, in damaging the overall structure of microbial cell and leading pathogens to death. These strategies were originally devoted to antitumoral applications, but promising outcomes characterized their subsequent application in antimicrobial field.

In this experimental thesis, photodynamic treatment was tested against the three model pathogens *Pseudomonas aeruginosa*, *Staphylococcus aureus* and *Candida albicans*, both in biofilm and planktonic lifestyles. Antimicrobial Photodynamic Therapy (aPDT) involves visible light in combination with a photosensitizing compound, which is able to absorb photons and undergo to chemico-physical transformation, causing the production of oxidising species ($^1O_2$, $O_2^{\cdot-}$, H_2O_2, and $\cdot OH$). When the photosensitizer is located in proximity of cell envelopes or in the cytoplasm of microbial cells, the oxidative stress generated upon light delivery causes the damage of cellular structures and macromolecules, leading microbial cell to death (St. Denis et al., 2011; Wainwright et al., 2017b). Other than aPDT, a very recent approach known as antimicrobial Blue Light Therapy (aBLT), exploits blue light alone to kill pathogens, probably through the photoexcitation of endogenous sensitizing compounds (e.g. porphyrins and/or flavins) that elicits an oxidative damage to microbial cells (Wang et al., 2016, 2017).

Light-based strategies presented many attractive features, especially their wide-spectrum activity against most classes of microbial pathogens, including Gram-positive bacteria, Gram-negative bacteria, and yeasts, due to the multitarget nature of photo-oxidative damage. Further, multidrug resistant strains are as sensitive as wild-type microorganisms to photoinactivation, and the selection of photo-resistant strains seemed to be improbable even after multiple cycles of photo-treatment. The use of visible light sources to activate endogenous or exogenous photosensitizing compounds makes the process cost efficient and safe for treated tissues. When applied to superficial lesions, light could be easily delivered, while, in the case of deep-seated infections, the use of optical fibre technology allows an effective tissues irradiation (Hamblin and Abrahamse, 2018).

We assayed two classes of PSs with the same experimental setup as potential candidates for microbial inactivation and especially for antibiofilm PDT. Though intriguing, this was a challenging effort, since we identified optimal *de novo* experimental conditions to get reproducible results in terms of biofilm growth, light delivery, total biomass measurement, and cell viability count for Gram-positive/Gram negative-bacteria and yeast (Cieplik et al., 2014). Together with microbial type

strains, clinical isolates were included in PDT experiments as they often display some genetic traits which confer increasing fitness in host tissue invasion and colonization. They were compared in terms of total biomass, cell viability and biofilm tolerance to PDT-induced oxidative stress conditions. The functional interaction between photosensitizing compounds and target microbial cells is certainly one of the main hotspots for efficient microbial photoinactivation, despite the variability in experimental outcomes that could be linked to unpredictable details, such as growth media composition, culture age, and biofilm manipulation. In a general and theoretical model, the activity of PSs should require an "intimate" distance between PS compounds and microbial cells since reactive oxygen species are characterized by short expiration rates. As a result, the qualities of a proficient PS should include a long-lived electronically excited triplet state, high photo-stability, high quantum yield of singlet oxygen production, suitable hydrophobic/hydrophilic character, high affinity for the desired microbial species, and low molecular weight to facilitate penetration in microbial biofilms. Such a great number of features results in expected variability in the efficacy of different PSs towards microbial pathogens, according to the chemical nature, structure, thickness of the cell wall and global charge of the surface layers. Still, a common requested feature of photo-activated molecules is a negligible level of toxicity out of light irradiation, together with the absence of mutagenicity for both eukaryotic cells and microorganisms (Soukos and Goodson, 2011; Cieplik et al., 2013, 2018b).

Among currently available synthetic photosensitizers we have taken into consideration the diaryl-porphyrins and the recently considered class of boron-dipyrromethens (BODIPYs). Diaryl-porphyrins (P1-P13) are characterised by a tetrapyrrolic macrocycle that bears two substituents in position 5 and 15 and have a maximum excitability peak in the range of blue light (~420 nm). While the BODIPY core is formed by a difluoro-boradiazaindacene, differently substituted in position 8, and BODIPYs (B1-B15) have an absorption peak in the green region of the visible spectrum (~540 nm). Therefore, two different light sources were used for their specific activation: a 410 nm blue LED and a 520 nm green LED, respectively.

The screening of both classes of PSs started with the study of binding between molecules and each microbial species since a certain interaction between cells and PSs is necessary for PDT efficacy (Sobotta et al., 2019). The interaction between PSs and microorganisms is strictly dependent to the chemical features of the outer envelopes of each species. It has been proved that the outer wall has a certain photo-inhibitory role, since non-walled microorganisms (e.g. mollicutes) are readily susceptible to photodynamic killing independently of the PS chemical structure (Bertoloni et al., 1985).

In the case of Gram-negative bacteria, the charge of PS compounds strongly influenced their binding to the cells. Non-ionic molecules, both diaryl-porphyrins and BODIPYs, poorly interact with *P. aeruginosa* cells, if compared to cationic PSs. This aspect could be explained by the negatively charged external envelope of *P. aeruginosa*, where electrostatic interactions could happen between cells and cationic molecules (Jori et al., 2006). Moreover, in the case of cationic compounds, the "self-promoted uptake" pathway allows the destabilization of the cell envelope, in which cracks appear, enabling the PS uptake (George et al., 2009; Sobotta et al., 2019). The envelope of Gram-positive bacteria is characterized by a porous peptidoglycan layer, whose permeability is higher than that of the outer membrane of Gram-negative bacteria. Indeed, the Gram-positive cell wall does not act as a permeability barrier, since macromolecules with large molecular weight (30-60 kDa) successfully reach the plasma membrane (Jori et al., 2006). This feature is also responsible for the observed differences in sensitivity between the two groups of bacteria when treated with different types of antimicrobial agents (Yin et al., 2013). Non-ionic BODIPYs showed good binding yields if compared to non-ionic diaryl-porphyrins, which showed a lower affinity in the interaction with *S. aureus.* Cationic PSs belonging to both classes displayed high binding yield with the Gram-positive pathogen, probably due to the presence of negatively charged teichuronic acids in the cell wall (Jori et al., 2006).

A possible involvement of surface total charge in the interaction between PSs and cell targets was found also in the yeast *C. albicans*, which is characterized by a negatively charged envelope made of β-glucan and chitin (Dai et al., 2009) and shows higher

affinity for cationic PSs than non-ionic ones for both diaryl-porphyrins and BODIPYs.

In literature, it was reported that a positive charge is required for an effective photodynamic inactivation (PDI) of microbial pathogens (Yin et al., 2013; Sobotta et al., 2019). However, despite the apparent poor yield of binding between non-ionic molecules and microorganisms, especially *P. aeruginosa* and *C. albicans*, good photoinactivation rates were observed also with some non-ionic PSs. These results could be the evidence of possible PDT activities which exclude chemical interactions between PSs and cellular targets, still requiring minimal distances to exert proficient effects. Notably, in *P. aeruginosa*, diaryl-porphyrins with two positive charges (P11) resulted in an efficient photoinactivation, while positively charged BODIPYs did not affect PAO1 viability, and the best photodynamic activity was unexpectedly obtained with the non-ionic BODIPY B9.

In the same experimental setups, an inhibitory PDT activity on *P. aeruginosa* PAO1 biofilms was observed with P11 (30 μM) and B9 (40 μM) after irradiation with 30 J/cm^2 of blue and green light, respectively. Even if the fluence rate emitted by the two light sources was comparable, Cieplik and colleagues suggested that comparisons can not be made between different PS-light systems without taking into consideration other irradiation parameters and absorption characteristics of each single PS. In particular, the number of photons absorbed per second by each PS allows the comparison of the antimicrobial photodynamic efficacy rates per excited PS molecule (Cieplik et al., 2015). In our case, two different PS concentrations were used, and a lower amount of porphyrin P11 showed to be sufficient to successfully inhibit the biofilm formation by *P. aeruginosa* if compared to the BODIPY B9. Interestingly, UR48 and BT1 strains of *P. aeruginosa* isolated in clinical settings resulted as susceptible as the wild-type PAO1 to biofilm inhibition by both P11 diaryl-porphyrin and B9 BODIPY, even if they are biofilm hyper-producers. This aspect could support the potential of aPDT in the management of clinical infections where pathogenic clinical strains are involved and could highlight the importance of repeated experimental trials to identify optimal and reproducible conditions to test PDT effectiveness on different microbial strains.

Concerning biofilm eradication, a certain photo-killing effect was observed with both P11 and B9 PSs on both free-living and sessile bacterial populations. However, the BODIPY compound (40 μM) showed a better anti-*Pseudomonas* effect than the porphyrin PS (30 μM). Confocal microscopy analyses of adherent populations of recombinant GFP-tagged PAO1 cells, showed a significand and reproducible decrease in fluorescence emission after PDT treatment with both PSs. This reduction was not observed in corresponding adherent biomasses exposed to PSs in the dark or irradiated without PS compounds. Importantly, GFP expression was induced after PDT treatment and this, together with control results, can rule out possible direct effects of radiation on fluorescent protein. Instead, cellular metabolism and/or overall viability could be impaired by PDT treatment, with inherent reduced emission of GFP fluorescence. In view of this promising explanation, suffering cells, could be more suitable targets for conventional antimicrobial treatments, inferring a possible functional synergy between PDT and conventional antibiotic therapies. This strategy could be applied not only for free-living cells but, especially, for sessile pathogen populations. However, more experimental trials are still needed to understand the effects of PDT on biofilm matrix production, since porphyrins and BODIPYs were non effective in lowering biofilm matrix in *P. aeruginosa* PAO1 biofilms.

The Gram-positive bacterium *S. aureus* was successfully inactivated by non-ionic photosensitizing compounds – P4, B2 and B5 – which showed better performances than cationic diaryl-porphyrins and BODIPYs. Thus, probably, a positive charge is not requested for *S. aureus* photoinactivation. In particular, non-ionic BODIPYs were active at very low concentrations (0,5 μM) if compared to porphyrin P4 (20 μM) in inhibiting biofilm development by this pathogen. Light parameters of irradiation devices were set at fluence rates of 20 J/cm^2 and 40 J/cm^2 for BODIPYs and porphyrins, respectively. The photodynamic efficacy was independent from the antibiotic-susceptibility features of *S. aureus* strains, since MSSA and MRSA strains showed similar sensitivity to aPDT with porphyrins and BODIPYs. This observation holds great promises for the future, since conventional antimicrobial therapies suffer of inefficacy when facing genetic mutations affecting specific drug targets. As mentioned before, PDT treatment directs toxic reactive oxygen species to different

cellular targets, lowering the frequency of possible resistance mutations. Photo-eradication of *S. aureus* biofilms was very efficient with B2 and B5 compounds at 0.5 μM concentration, where the viability of planktonic and sessile populations decreased at the lowest detectable limit of the experimental setup. In the case of porphyrin P4 (30 μM), a good rate of eradication was also obtained, despite no decrease of total adherent biomass was observed upon PDT treatment.

An effective photodynamic treatment of the pathogenic yeast *C. albicans* was observed with monocationic compounds: P10 and B13 showed the highest antifungal performances among diaryl-porphyrins and BODIPYs, respectively. P10 and B13 were able to inhibit the growth of a structured yeast biofilm after irradiation at fluence rates of 150 and 30 J/cm^2 of blue and green light, respectively. PDT treatment with these photosensitizing compounds revealed to be efficient also against biofilms of the pathogenic strains isolated in clinical context.

Both types of PSs showed low efficacy in the eradication of yeast mature biofilms, and only a slight decrease of cell viability was detected in adherent populations with P10 porphyrin photo-treatment. As detailed before, PDT applications are somehow limited by the need of efficient PS delivery to target cells. Experimental assays also showed unexpected results when considering the relationship between overall charges of microbial external structures compared to PS net charge. Still, short lived reactive species are responsible for pathogen photo-killing and a spatial proximity is always required between the chemicals and target cells. Notably, some PSs families, such as porphyrins or functionalized riboflavin, share chemical structure with cellular molecules which are present in microbial cells and could act as “trojan horses” in photodynamic treatment.

In recent years, blue light radiation (400 – 500 nm) showed very promising attitudes in killing microbial pathogens independently of PS administration (Wang et al., 2017). This application of blue light radiation was specifically named antimicrobial Blue Light therapy (aBLT) and, in this experimental work, was used against the microbial pathogen *Pseudomonas aeruginosa*, both for planktonic and biofilm lifestyles. Both 410 and 455 nm wavelengths were able to inhibit the formation of an adherent community, but 410 nm light had a greater effect than 455

nm blue light. Other than wild-type PAO1 strain, 15 clinical isolates of *P. aeruginosa* were sensitive to blue light treatment, that prevented the formation of adherent biomasses. *P. aeruginosa* PAO1 was also successfully inactivated in the lumen of central venous catheters (CVC) where it was not able to growth as organized biofilms upon photo-treatment with 410 nm blue light.

Blue light was also successful in eradicating preformed biofilms of PAO1 strain, suggesting its potential in the treatment of biofilm-mediated infections. Also in this case, 410 nm light showed a better antibiofilm performance as compared to 455 nm radiation, with a clear and reproducible antimicrobial activity on bacterial populations. Since medical devices are subjected to the development of microbial biofilm on their surfaces, blue light (410 nm) was applied on CVC colonized by biofilms of *P. aeruginosa*, showing its potential for the treatment of medical devices-associated infections.

Interestingly, blue light (410 and 455 nm) greatly reduced the amount of biofilm biomass, and this important observation is at odds with "classical" PDT treatments which showed frequent inefficacy against biofilm matrix structures. Further investigations are in progress to elucidate possible direct effects on preformed structures stability compared to cellular metabolism impairment and, as a consequence, reduced production of extracellular structures. A thorough investigation of blue light activity on the main components the biofilm matrix was performed. At first, blue light radiation proved to be efficient in killing PAO1 free-living cells where a direct involvement of oxidative stress was clearly assessed. When addressing blue light potential against biofilm matrix, we tentatively examined the direct effects of radiation on separate representative classes of matrix components, i.e. saccharides, proteins, nucleic acids. This simplified model had the possible advantage of detecting single interactions with matrix components, not necessarily detectable in the overall complex system. As representatives of saccharides, proteins/enzymes, and DNA we used ONPG, PAO1 recombinant catalase/ *Escherichia coli* recombinant β-galactosidase, and plasmid DNA, respectively. Importantly, PAO1 catalase is produced by the pathogen as a first-line defence against oxidative stress and is particularly useful in pathogen-host interaction when

coping with H_2O_2 burst of neutrophils during the development of infections. All these molecules were sensitive to blue light inactivation at 410 nm, and catalase A was susceptible to both wavelengths of radiation. However, the enzyme β-galactosidase and the plasmid DNA showed a certain sensitivity only when the photoinactivation was performed in culture media collected upon cell growth. These preliminary outcomes could be in agreement with the observed decrease of biofilm matrix reduction upon blue light irradiation and suggest that a possible endogenous photosensitizing compound could be released by the cells in the extracellular environment during their growth as planktonic cultures or in biofilm communities.

Conclusions

- In this thesis, a screening work allowed the identification of new promising photosensitizing compounds that should be taken into consideration in further studies with *in vivo* models.
- The screening of diaryl-porphyrins allowed to identify a dicationic PS active on *P. aeruginosa*, a non-ionic molecule active on *S. aureus* and a monocationic diaryl-porphyrin for the inactivation of *C. albicans*.
- Non-ionic BODIPYs showed antimicrobial activity especially on *S. aureus,* and unexpectedly on *P. aeruginosa*. While *C. albicans* was inactivated by a monocationic BODIPY.
- Diaryl-porphyrins and BODIPYs had an inhibitory effect on the biofilms of the model pathogens, and a certain activity in biofilm eradication was observed.
- Each pathogen was properly inactivated by PSs with peculiar chemical features and none of the PSs showed antimicrobial activity in common against the three pathogens.
- The application of aPDT in industrial, agricultural, environmental fields, or where more than one microbial species is involved, should consider a combination of two or more PSs.
- The possibility to conjugate these PSs to delivery systems like magnetic nanoparticles, peptides or encapsulation in biopolymers should be addressed since a PS efficient delivery in infected areas is an important issue to consider.

- An interesting antibiofilm activity on bacterial cells and biofilm matrix was observed against the pathogen *P. aeruginosa* by the irradiation with blue light alone. Blue light at 410 nm was more active than 455 nm light.
- aBLT showed its potential as disinfection system for medical devices such as central venous catheters.
- Future studies should address the specificity and the potential of blue light radiation against biofilm components, both at cellular and macromolecular matrix level. The occurrence of "failures" in PDT activity against biofilm structures could be ascribed, also, to defects in proper diffusion of PSs due to the external matrix barrier. Under this aspect, the potential of aBLT approach, with the possible effect of internal photosensitizers, could impair the formation of new biofilm structures and impair the organization of pre-existing ones.
- A complete exploitation of aPDT and aBLT emerging strategies should not exclude a complementary approach with conventional antibiotic therapies. Also, conjugation of PSs with nanoparticles and other technological devices should be addressed in the everlasting fight against antimicrobial resistant pathogens.

6. Summary

According to the World Health Organization (WHO), by 2050 drug-resistant bacteria will cause 10 million deaths per year if no action is taken. In addition, the treatment of recalcitrant infections is complicated by the ability of pathogens to form biofilms, the microbial communities in adhesion to tissues or inert surfaces that are tolerant to common antimicrobial agents. In this scenario, the interest in alternative and adjuvant approaches to target multidrug-resistant microorganisms, to prevent biofilm formation and/or to eradicate biofilms are compelling goals to address.

In this thesis, two light-based approaches were investigated as promising strategies against microbial pathogens: antimicrobial Photodynamic Therapy (aPDT) and antimicrobial Blue Light Therapy (aBLT).

Antimicrobial Photodynamic Therapy is based on the generation of photo-oxidative stress induced upon irradiation of drugs, known as photosensitizers (PSs), by a specific visible light wavelength. Microbial death occurs because of the photo-oxidation of macromolecules and/or cellular structures. The multi-target and rapid oxidative burst elicited during PDT seemed to prevent the selection of resistant mutants and showed its potential against microbial biofilms. In this thesis, a screening of PS compounds belonging to the families of diaryl-porphyrins and BODIPYs was performed in the photoinactivation of three microbial pathogens recently emerged for their increase resistance to antimicrobials: the Gram-negative *Pseudomonas aeruginosa*, the Gram-positive *Staphylococcus aureus*, and the yeast *Candida albicans*.

P. aeruginosa cells were successfully photoinactivated by a dicationic diaryl-porphyrin (P11) and, unexpectedly, by a non-ionic BODIPY (B9). Both compounds succeeded in preventing the biofilm formation of *P. aeruginosa* PAO1 and Cystic Fibrosis isolates.

The Gram-positive *S. aureus* was inactivated by non-ionic PSs belonging to both families: the diaryl-porphyrin P4 and BODIPYs B2 and B5. These compounds inhibited the formation of biofilms by MSSA and MRSA strains, independently from their antibiotic susceptibility profile, and eradicated adherent and planktonic populations of mature biofilms.

The eukaryotic yeast *C. albicans* was sensitive to aPDT with monocationic molecules – porphyrin P10 and BODIPY B13 – that showed activity on both type-strain and clinical isolates. *C. albicans* biofilm formation was inhibited by these compounds and a certain activity was observed also on mature adherent communities.

More recently, antimicrobial Blue Light Therapy (aBLT) emerged as another promising light-based strategy to be applied in antimicrobial field. Indeed, blue light was inferred to cause photo-oxidative stress by excitation of endogenous photoactive compounds that elicit an oxidative stress in microbial cells. Several microbial pathogens have been found to be sensitive to blue light irradiation, and herein, the effects of blue light at 410 and 455 nm on *P. aeruginosa* biofilm were investigated. Light at 410 nm was more active than 455 nm in inhibiting biofilm formation of the wild-type PAO1 and 15 clinical strains of *P. aeruginosa*. Moreover, antimicrobial effects of blue light were observed in biofilm eradication and a notable anti-matrix activity emerged. To thoroughly investigate the effect of blue light on extracellular matrix components, molecules representative of exopolysaccharides (*ortho*-nitrophenyl-β-D-galactopyranoside - ONPG), proteins (β-galactosidase), extracellular DNA (plasmid DNA), and virulence factors (catalase A) were analysed upon blue light treatment. Light at 410 nm caused detrimental effects on ONPG structure, on enzyme activity of β-galactosidase, and modified plasmid DNA conformation. Blue light at 410 and 455 nm were also efficient in inactivating catalase A, a virulence factor playing an important role in pathogenic mechanisms.

In this thesis, application of aPDT and aBLT demonstrated to be promising antimicrobial strategies that find application in many fields, including medical, industrial, environmental, and agricultural areas. In conclusion, the growing concern of infections caused by MDR pathogens and/or microbial biofilms could be managed by a combination of both visible-light based techniques, aPDT and aBL.

7. Bibliography

Agazzi, M. L., Ballatore, M. B., Durantini, A. M., Durantini, E. N., and Tomé, A. C. (2019). BODIPYs in antitumoral and antimicrobial photodynamic therapy: An integrating review. *J. Photochem. Photobiol. C Photochem. Rev.* 40, 21–48. doi:10.1016/j.jphotochemrev.2019.04.001.

Alangaden, G. J. (2011). Nosocomial Fungal Infections: Epidemiology, Infection Control, and Prevention. *Infect. Dis. Clin. North Am.* 25, 201–225. doi:10.1016/j.idc.2010.11.003.

Albertson, G. D., Niimi, M., Cannon, R. D., and Jenkinson, H. F. (1996). Multiple efflux mechanisms are involved in Candida albicans fluconazole resistance. *Antimicrob. Agents Chemother.* 40, 2835–2841. doi:10.1128/aac.40.12.2835.

Albuquerque, P., and Casadevall, A. (2012). Quorum sensing in fungi a review. *Med. Mycol.* 50, 337–345. doi:10.3109/13693786.2011.652201.

Allison, R. R., and Moghissi, K. (2013). Photodynamic therapy (PDT): PDT mechanisms. *Clin. Endosc.* 46, 24–29. doi:10.5946/ce.2013.46.1.24.

Allison, R. R., and Sibata, C. H. (2010). Oncologic photodynamic therapy photosensitizers: A clinical review. *Photodiagnosis Photodyn. Ther.* 7, 61–75. doi:10.1016/j.pdpdt.2010.02.001.

Amin, R. M., Bhayana, B., Hamblin, M. R., and Dai, T. (2016). Antimicrobial blue light inactivation of Pseudomonas aeruginosa by photo-excitation of endogenous porphyrins: In vitro and in vivo studies. *Lasers Surg. Med.* 48, 562–568. doi:10.1002/lsm.22474.

Amos-Tautua, B. M., Songca, S. P., and Oluwafemi, O. S. (2019). Application of porphyrins in antibacterial photodynamic therapy. *Molecules* 24. doi:10.3390/molecules24132456.

Assis, L. M., Nedeljković, M., and Dessen, A. (2017). New strategies for targeting and treatment of multi-drug resistant Staphylococcus aureus. *Drug Resist. Updat.* 31, 1–14. doi:10.1016/j.drup.2017.03.001.

Awuah, S. G., and You, Y. (2012). Boron dipyrromethene (BODIPY)-based photosensitizers for photodynamic therapy. *RSC Adv.* 2, 11169–11183. doi:10.1039/c2ra21404k.

Banfi, S., Caruso, E., Buccafurni, L., Battini, V., Zazzaron, S., Barbieri, P., et al. (2006a). Antibacterial activity of tetraaryl-porphyrin photosensitizers: An in vitro study on Gram negative and Gram positive bacteria. *J. Photochem. Photobiol. B Biol.* 85, 28–38. doi:10.1016/j.jphotobiol.2006.04.003.

Banfi, S., Caruso, E., Buccafurni, L., Murano, R., Monti, E., Gariboldi, M., et al. (2006b). Comparison between 5,10,15,20-tetraaryl- and 5,15-diarylporphyrins as photosensitizers: Synthesis, photodynamic activity, and quantitative structure-activity relationship modeling. *J. Med. Chem.* 49, 3293–3304. doi:10.1021/jm050997m.

Banfi, S., Nasini, G., Zaza, S., and Caruso, E. (2013). Synthesis and photo-physical properties of a series of BODIPY dyes. *Tetrahedron* 69, 4845–4856. doi:10.1016/j.tet.2013.04.064.

Bassetti, M., Vena, A., Croxatto, A., Righi, E., and Guery, B. (2018). How to manage Pseudomonas aeruginosa infections. *Drugs Context* 7, 1–18. doi:10.7573/dic.212527.

Beirao, S., Fernandes, S., Coelho, J., Faustino, M. A. F., Tom, P. C., Neves, M. G. P. M. S., et al. (2014). Photodynamic Inactivation of Bacterial and Yeast Biofilms With a Cationic Porphyrin. 1387–1396. doi:10.1111/php.12331.

Belanger, C. R., Mansour, S. C., Pletzer, D., and Hancock, R. E. W. (2017). Alternative strategies for the study and treatment of clinical bacterial biofilms. *Emerg. Top. Life Sci.* 1, 41–53. doi:10.1042/etls20160020.

Beloin, C., Renard, S., Ghigo, J. M., and Lebeaux, D. (2014). Novel approaches to combat bacterial biofilms. *Curr. Opin. Pharmacol.* 18, 61–68. doi:10.1016/j.coph.2014.09.005.

Benstead, M., Mehl, G. H., and Boyle, R. W. (2011). 4,4'-Difluoro-4-bora-3a,4a-diaza-s-indacenes (BODIPYs) as components of novel light active materials. *Tetrahedron* 67, 3573–3601. doi:10.1016/j.tet.2011.03.028.

Bertoloni, G., Viel, A., Grossato, A., and Jori, G. (1985). The photosensitizing activity of haematoporphyrin on mollicutes. *J. Gen. Microbiol.* 131, 2217–2223. doi:10.1099/00221287-131-9-2217.

Billings, N., Ramirez Millan, M., Caldara, M., Rusconi, R., Tarasova, Y., Stocker, R., et al. (2013). The Extracellular Matrix Component Psl Provides Fast-Acting Antibiotic Defense in Pseudomonas aeruginosa Biofilms. *PLoS Pathog.* 9. doi:10.1371/journal.ppat.1003526.

Blair, J. M. A., Webber, M. A., Baylay, A. J., Ogbolu, D. O., and Piddock, L. J. V. (2015). Molecular mechanisms of antibiotic resistance. *Nat. Rev. Microbiol.* 13, 42–51. doi:10.1038/nrmicro3380.

Bowler, L. L., Zhanel, G. G., Ball, T. B., and Saward, L. L. (2012). Mature Pseudomonas aeruginosa biofilms prevail compared to young biofilms in the presence of ceftazidime. *Antimicrob. Agents Chemother.* 56, 4976–4979. doi:10.1128/AAC.00650-12.

Brackman, G., Breyne, K., De Rycke, R., Vermote, A., Van Nieuwerburgh, F., Meyer, E., et al. (2016). The Quorum Sensing Inhibitor Hamamelitannin Increases Antibiotic Susceptibility of Staphylococcus aureus Biofilms by Affecting Peptidoglycan Biosynthesis and eDNA Release. *Sci. Rep.* 6, 1–14. doi:10.1038/srep20321.

Brackman, G., Cos, P., Maes, L., Nelis, H. J., and Coenye, T. (2011). Quorum sensing inhibitors increase the susceptibility of bacterial biofilms to antibiotics in vitro and in vivo. *Antimicrob. Agents Chemother.* 55, 2655–2661. doi:10.1128/AAC.00045-11.

Bragonzi, A., Wiehlmann, L., Klockgether, J., Cramer, N., Worlitzsch, D., Döning, G., et al. (2006). Sequence diversity of the mucABD locus in Pseudomonas aeruginosa isolates from patients with cystic fibrosis. *Microbiology* 152, 3261–3269. doi:10.1099/mic.0.29175-0.

Brannon, J. R., and Hadjifrangiskou, M. (2016). The arsenal of pathogens and antivirulence therapeutic strategies for disarming them. *Drug Des. Devel. Ther.* 10, 1795–1806. doi:10.2147/DDDT.S98939.

Breidenstein, E. B. M., de la Fuente-Núñez, C., and Hancock, R. E. W. (2011). Pseudomonas aeruginosa: All roads lead to resistance. *Trends Microbiol.* 19, 419–426. doi:10.1016/j.tim.2011.04.005.

Burda, W. N., Fields, K. B., Gill, J. B., Burt, R., Shepherd, M., Zhang, X. P., et al. (2012). Neutral metallated and meso-substituted porphyrins as antimicrobial agents against Gram-positive pathogens. *Eur. J. Clin. Microbiol. Infect. Dis.* 31, 327–335. doi:10.1007/s10096-011-1314-y.

Campoy, S., and Adrio, J. L. (2017). Antifungals. *Biochem. Pharmacol.* 133, 86–96. doi:10.1016/j.bcp.2016.11.019.

Carpenter, B. L., Situ, X., Scholle, F., Bartelmess, J., Weare, W. W., and Ghiladi, R. A. (2015). Antiviral, antifungal and antibacterial activities of a BODIPY-based photosensitizer. *Molecules* 20, 10604–10621. doi:10.3390/molecules200610604.

Caruso, E., Banfi, S., Barbieri, P., Leva, B., and Orlandi, V. T. (2012). Synthesis and antibacterial activity of novel cationic BODIPY photosensitizers. *J. Photochem. Photobiol. B Biol.* 114, 44–51. doi:10.1016/j.jphotobiol.2012.05.007.

Caruso, E., Cerbara, M., Malacarne, M. C., Marras, E., Monti, E., and Gariboldi, M. B. (2019a). Synthesis and photodynamic activity of novel non-symmetrical diaryl porphyrins against cancer cell lines. *J. Photochem. Photobiol. B Biol.* 195, 39–50. doi:10.1016/j.jphotobiol.2019.04.010.

Caruso, E., Gariboldi, M., Sangion, A., Gramatica, P., and Banfi, S. (2017). Synthesis, photodynamic activity, and quantitative structure-activity relationship modelling of a series of BODIPYs. *J. Photochem. Photobiol. B Biol.* 167, 269–281. doi:10.1016/j.jphotobiol.2017.01.012.

Caruso, E., Malacarne, M. C., Banfi, S., Gariboldi, M. B., and Orlandi, V. T. (2019b). Cationic diarylporphyrins: In vitro versatile anticancer and antibacterial photosensitizers. *J. Photochem. Photobiol. B Biol.* 197, 111548. doi:10.1016/j.jphotobiol.2019.111548.

Caruso, E., Malacarne, M. C., Marras, E., Papa, E., Bertato, L., Banfi, S., et al. (2020). New BODIPYs for photodynamic therapy (PDT): Synthesis and activity on human cancer cell lines. *Bioorganic Med. Chem.* 28, 115737. doi:10.1016/j.bmc.2020.115737.

Cavalheiro, M., and Teixeira, M. C. (2018). Candida Biofilms: Threats, challenges, and promising strategies. *Front. Med.* 5, 1–15. doi:10.3389/fmed.2018.00028.

Chanda, W., Joseph, T. P., Wang, W., Padhiar, A. A., and Zhong, M. (2017). The potential management of oral candidiasis using anti-biofilm therapies. *Med. Hypotheses* 106, 15–18. doi:10.1016/j.mehy.2017.06.029.

Chatterjee, M., Anju, C. P., Biswas, L., Anil Kumar, V., Gopi Mohan, C., and Biswas, R. (2016). Antibiotic resistance in Pseudomonas aeruginosa and alternative therapeutic options. *Int. J. Med. Microbiol.* 306, 48–58. doi:10.1016/j.ijmm.2015.11.004.

Chiang, W. C., Nilsson, M., Jensen, P. Ø., Høiby, N., Nielsen, T. E., Givskov, M., et al. (2013). Extracellular DNA shields against aminoglycosides in Pseudomonas aeruginosa biofilms. *Antimicrob. Agents Chemother.* 57, 2352–2361. doi:10.1128/AAC.00001-13.

Cieplik, F., Deng, D., Crielaard, W., Buchalla, W., Hellwig, E., Al-Ahmad, A., et al. (2018a). Antimicrobial photodynamic therapy – what we know and what we don't. *Crit. Rev. Microbiol.* 44, 571–589. doi:10.1080/1040841X.2018.1467876.

Cieplik, F., Deng, D., Crielaard, W., Buchalla, W., Hellwig, E., Al-Ahmad, A., et al. (2018b). Antimicrobial photodynamic therapy – what we know and what we don't. *Crit. Rev. Microbiol.* 44, 571–589. doi:10.1080/1040841X.2018.1467876.

Cieplik, F., Pummer, A., Regensburger, J., Hiller, K. A., Späth, A., Tabenski, L., et al. (2015). The impact of absorbed photons on antimicrobial photodynamic efficacy. *Front. Microbiol.* 6. doi:10.3389/fmicb.2015.00706.

Cieplik, F., Späth, A., Regensburger, J., Gollmer, A., Tabenski, L., Hiller, K., et al. (2013). Free Radical Biology and Medicine Photodynamic bio fi lm inactivation by SAPYR — An exclusive singlet oxygen photosensitizer. *Free Radic. Biol. Med.* 65, 477–487. doi:10.1016/j.freeradbiomed.2013.07.031.

Cieplik, F., Tabenski, L., Buchalla, W., Maisch, T., and Al-ahmad, A. (2014). Antimicrobial photodynamic therapy for inactivation of biofilms formed by oral key pathogens. 5, 1–17. doi:10.3389/fmicb.2014.00405.

Collins, T. L., Markus, E. A., Hassett, D. J., and Robinson, J. B. (2010). The Effect of a Cationic Porphyrin on Pseudomonas aeruginosa Biofilms. 411–416. doi:10.1007/s00284-010-9629-y.

Corbin, B. D., Seeley, E. H., Raab, A., Feldmann, J., Miller, M. R., Torres, V. J., Anderson, K. L., Dattilo, B. M., Anderson, K. L., Dunman, P. M., Gerads, R., Caprioli, R., Nacken, W., Chazin, W. J., and Skaar, E. P. (2008). Metal chelation and inhibition of Bacterial Growth in Tissue Abscesses. *Science (80-.).* 319, 962–966.

Cormick, M. P., Alvarez, M. G., Rovera, M., and Durantini, E. N. (2009). Photodynamic inactivation of Candida albicans sensitized by tri- and tetra-cationic porphyrin derivatives. *Eur. J. Med. Chem.* 44, 1592–1599. doi:10.1016/j.ejmech.2008.07.026.

Dadar, M., Tiwari, R., Karthik, K., Chakraborty, S., Shahali, Y., and Dhama, K. (2018). Candida albicans - Biology, molecular characterization, pathogenicity, and advances in diagnosis and control – An update. *Microb. Pathog.* 117, 128–138. doi:10.1016/j.micpath.2018.02.028.

Dai, T., and Hamblin, M. R. (2017). Visible Blue Light is Capable of Inactivating Candida albicans and Other Fungal Species. *Photomed. Laser Surg.* 35, 345–346. doi:10.1089/pho.2017.4318.

Dai, T., Huang, Y. Y., and Hamblin, M. R. (2009). Photodynamic therapy for localized infections-State of the art. *Photodiagnosis Photodyn. Ther.* 6, 170–188. doi:10.1016/j.pdpdt.2009.10.008.

Davis, J. S., Hal, S. Van, and Tong, S. Y. C. (2015). Combination antibiotic treatment of serious methicillin-resistant staphylococcus aureus infections. *Semin. Respir. Crit. Care Med.* 36, 3–16. doi:10.1055/s-0034-1396906.

Del Pozo, J. L., and Patel, R. (2007). The challenge of treating biofilm-associated bacterial infections. *Clin. Pharmacol. Ther.* 82, 204–209. doi:10.1038/sj.clpt.6100247.

Derbise, A., Pierre, F., Merchez, M., Pradel, E., Laouami, S., Ricard, I., et al. (2013). Inheritance of the lysozyme inhibitor Ivy was an important evolutionary step by Yersinia pestis to avoid the host innate immune response. *J. Infect. Dis.* 207, 1535–1543. doi:10.1093/infdis/jit057.

Donnelly, R. F., McCarron, P. A., and Tunney, M. M. (2008). Antifungal photodynamic therapy. *Microbiol. Res.* 163, 1–12. doi:10.1016/j.micres.2007.08.001.

Driscoll, J. A., Brody, S. L., and Kollef, M. H. (2007). The epidemiology, pathogenesis and treatment of Pseudomonas aeruginosa infections. *Drugs* 67, 351–368. doi:10.2165/00003495-200767030-00003.

Du, Q., Ren, B., He, J., Peng, X., Guo, Q., Zheng, L., et al. (2020). Candida albicans promotes tooth decay by inducing oral microbial dysbiosis. *ISME J.* doi:10.1038/s41396-020-00823-8.

Durantini, A. M., Heredia, D. A., Durantini, J. E., and Durantini, E. N. (2018). BODIPYs to the rescue: Potential applications in photodynamic inactivation. *Eur. J. Med. Chem.* 144, 651–661. doi:10.1016/j.ejmech.2017.12.068.

El Zowalaty, M. E., Al Thani, A. A., Webster, T. J., El Zowalaty, A. E., Schweizer, H. P., Nasrallah, G. K., et al. (2015). Pseudomonas aeruginosa: Arsenal of resistance mechanisms, decades of changing resistance profiles, and future antimicrobial therapies. *Future Microbiol.* 10, 1683–1706. doi:10.2217/fmb.15.48.

Ferrer-Espada, R., Wang, Y., Goh, X. S., and Dai, T. (2019). Antimicrobial Blue Light Inactivation of Microbial Isolates in Biofilms. *Lasers Surg. Med.*, 1–7. doi:10.1002/lsm.23159.

Fisher, R. A., Gollan, B., and Helaine, S. (2017). Persistent bacterial infections and persister cells. *Nat. Rev. Microbiol.* 15, 453–464. doi:10.1038/nrmicro.2017.42.

Foster, T. J. (2017). Antibiotic resistance in Staphylococcus aureus. Current status and future

prospects. *FEMS Microbiol. Rev.* 41, 430–449. doi:10.1093/femsre/fux007.
Freitas, M. A. A., Pereira, A. H. C., Pinto, J. G., Casas, A., and Ferreira-Strixino, J. (2019). Bacterial viability after antimicrobial photodynamic therapy with curcumin on multiresistant Staphylococcus aureus. *Future Microbiol.* 14, 739–748. doi:10.2217/fmb-2019-0042.
Frimannsson, D. O., Grossi, M., Murtagh, J., Paradisi, F., and Oshea, D. F. (2010). Light induced antimicrobial properties of a brominated boron difluoride (BF2) chelated tetraarylazadipyrromethene photosensitizer. *J. Med. Chem.* 53, 7337–7343. doi:10.1021/jm100585j.
Gallagher, W. M., Allen, L. T., O'Shea, C., Kenna, T., Hall, M., Gorman, A., et al. (2005). A potent nonporphyrin class of photodynamic therapeutic agent: Cellular localisation, cytotoxic potential and influence of hypoxia. *Br. J. Cancer* 92, 1702–1710. doi:10.1038/sj.bjc.6602527.
García, I., Ballesta, S., Gilaberte, Y., Rezusta, A., and Pascual, Á. (2015). Antimicrobial photodynamic activity of hypericin against methicillin-susceptible and resistant Staphylococcus aureus biofilms. *Future Microbiol.* 10, 347–356. doi:10.2217/FMB.14.114.
Gaspar, M. C., Couet, W., Olivier, J. C., Pais, A. A. C. C., and Sousa, J. J. S. (2013). Pseudomonas aeruginosa infection in cystic fibrosis lung disease and new perspectives of treatment: A review. *Eur. J. Clin. Microbiol. Infect. Dis.* 32, 1231–1252. doi:10.1007/s10096-013-1876-y.
Gayathri, T., Barui, A. K., Prashanthi, S., Patra, C. R., and Singh, S. P. (2014). Meso-Substituted BODIPY fluorescent probes for cellular bio-imaging and anticancer activity. *RSC Adv.* 4, 47409–47413. doi:10.1039/c4ra07424f.
George, S., Hamblin, M. R., and Kishen, A. (2009). Uptake pathways of anionic and cationic photosensitizers into bacteria. *Photochem. Photobiol. Sci.* 8, 788–795. doi:10.1039/b809624d.
Gonzales, F. P., Felgenträger, A., Bäumler, W., and Maisch, T. (2013). Fungicidal photodynamic effect of a twofold positively charged porphyrin against Candida albicans planktonic cells and biofilms. *Futur. Med.* 8, 785–797.
Gorman, A., Killoran, J., O'Shea, C., Kenna, T., Gallagher, W. M., and O'Shea, D. F. (2004). In vitro demonstration of the heavy-atom effect for photodynamic therapy. *J. Am. Chem. Soc.* 126, 10619–10631. doi:10.1021/ja047649e.
Gwynne, P. J., and Gallagher, M. P. (2018). Light as a broad-spectrum antimicrobial. *Front. Microbiol.* 9, 1–9. doi:10.3389/fmicb.2018.00119.
Hall, C. W., and Mah, T. F. (2017). Molecular mechanisms of biofilm-based antibiotic resistance and tolerance in pathogenic bacteria. *FEMS Microbiol. Rev.* 41, 276–301. doi:10.1093/femsre/fux010.
Hamblin, M. R. (2016). Antimicrobial photodynamic inactivation : a bright new technique to kill resistant microbes. *Curr. Opin. Microbiol.* 33, 67–73. doi:10.1016/j.mib.2016.06.008.
Hamblin, M. R., and Abrahamse, H. (2018). Can light-based approaches overcome antimicrobial resistance? *Drug Dev. Res.*, 1–20. doi:10.1002/ddr.21453.
Hancock, R. E. W., and Brinkman, F. S. L. (2002). Function of Pseudomonas porins in uptake and efflux. *Annu. Rev. Microbiol.* 56, 17–38. doi:10.1146/annurev.micro.56.012302.160310.
Holmes, A. H., Moore, L. S. P., Sundsfjord, A., Steinbakk, M., Regmi, S., Karkey, A., et al. (2016). Understanding the mechanisms and drivers of antimicrobial resistance. *Lancet* 387, 176–187. doi:10.1016/S0140-6736(15)00473-0.
Hooper, D. C. (2002). Fluoroquinolone resistance among Gram-positive cocci. *Lancet Infect. Dis.* 2, 530–538. doi:10.1016/S1473-3099(02)00369-9.
Hsieh, C. M., Huang, Y. H., Chen, C. P., Hsieh, B. C., and Tsai, T. (2014). 5-Aminolevulinic acid induced photodynamic inactivation on Staphylococcus aureus and Pseudomonas aeruginosa. *J. Food Drug Anal.* 22, 350–355. doi:10.1016/j.jfda.2013.09.051.
Hsieh, Y. H., Zhang, J. H., Chuang, W. C., Yu, K. H., Huang, X. Bin, Lee, Y. C., et al. (2018). An in vitro study on the effect of combined treatment with photodynamic and chemical therapies on Candida albicans. *Int. J. Mol. Sci.* 19. doi:10.3390/ijms19020337.
Hu, X., Huang, Y.-Y., Wang, Y., Wang, X., and Hamblin, M. R. (2018). Antimicrobial Photodynamic Therapy to Control Clinically Relevant Biofilm Infections. *Front. Microbiol.* 9, 1–24. doi:10.3389/fmicb.2018.01299.
Jamal, M., Ahmad, W., Andleeb, S., Jalil, F., Imran, M., Nawaz, M. A., et al. (2018). Bacterial biofilm and associated infections. *J. Chinese Med. Assoc.* 81, 7–11. doi:10.1016/j.jcma.2017.07.012.
Janoff, E. N., Rubins, J. B., Fasching, C., Charboneau, D., Rahkola, J. T., Plaut, A. G., et al. (2014).

Pneumococcal IgA1 protease subverts specific protection by human IgA1. *Mucosal Immunol.* 7, 249–256. doi:10.1038/mi.2013.41.
Jenul, C., and Horswill, A. R. (2018). Regulation of Staphylococcus aureus Virulence. *Microbiol. Spectr.* 6, 1–21. doi:10.1128/microbiolspec.gpp3-0031-2018.
Jori, G., Fabris, C., Soncin, M., Ferro, S., Coppellotti, O., Dei, D., et al. (2006). Photodynamic therapy in the treatment of microbial infections: Basic principles and perspective applications. *Lasers Surg. Med.* 38, 468–481. doi:10.1002/lsm.20361.
Kapteyn, J. C., Montijn, R. C., Dijkgraaf, G. J. P., Van den Ende, H., and Klis, F. M. (1995). Covalent association of β-1,3-glucan with β-1,6-glucosylated mannoproteins in cell walls of Candida albicans. *J. Bacteriol.* 177, 3788–3792. doi:10.1128/jb.177.13.3788-3792.1995.
Kelly, S. L., Lamb, D. C., Kelly, D. E., Manning, N. J., Loeffler, J., Hebart, H., et al. (1997). Resistance to fluconazole and cross-resistance to amphotericin B in Candida albicans from AIDS patients caused by defective sterol Δ5,6-desaturation. *FEBS Lett.* 400, 80–82. doi:10.1016/S0014-5793(96)01360-9.
Khan, H. A., Baig, F. K., and Mehboob, R. (2017). Nosocomial infections: Epidemiology, prevention, control and surveillance. *Asian Pac. J. Trop. Biomed.* 7, 478–482. doi:10.1016/j.apjtb.2017.01.019.
Kleinpenning, M. M., Smits, T., Frunt, M. H. A., van Erp, P. E. J., van de Kerkhof, P. C. M., and Gerritsen, R. M. J. P. (2010). Clinical and histological effects of blue light on normal skin. *Photodermatol. Photoimmunol. Photomed.* 26, 16–21. doi:10.1111/j.1600-0781.2009.00474.x.
Kluytmans, J., Van Belkum, A., and Verbrugh, H. (1997). Nasal carriage of Staphylococcus aureus: Epidemiology, underlying mechanisms, and associated risks. *Clin. Microbiol. Rev.* 10, 505–520. doi:10.1128/cmr.10.3.505-520.1997.
Koo, H., Allan, R. N., Howlin, R. P., Stoodley, P., and Hall-Stoodley, L. (2017). Targeting microbial biofilms: Current and prospective therapeutic strategies. *Nat. Rev. Microbiol.* 15, 740–755. doi:10.1038/nrmicro.2017.99.
Kruppa, M. (2009). Quorum sensing and Candida albicans. *Mycoses* 52, 1–10. doi:10.1111/j.1439-0507.2008.01626.x.
Kwiecinski, J. M., and Horswill, A. R. (2020). Staphylococcus aureus bloodstream infections: pathogenesis and regulatory mechanisms. *Curr. Opin. Microbiol.* 53, 51–60. doi:10.1016/j.mib.2020.02.005.
Le, K. Y., and Otto, M. (2015). Quorum-sensing regulation in staphylococci-an overview. *Front. Microbiol.* 6, 1–8. doi:10.3389/fmicb.2015.01174.
Le Negrate, G., Faustin, B., Welsh, K., Loeffler, M., Krajewska, M., Hasegawa, P., et al. (2008). Salmonella Secreted Factor L Deubiquitinase of Salmonella typhimurium Inhibits NF-κB, Suppresses IκBα Ubiquitination and Modulates Innate Immune Responses . *J. Immunol.* 180, 5045–5056. doi:10.4049/jimmunol.180.7.5045.
Li, X. Z., and Nikaido, H. (2009). Efflux-Mediated Drug Resistance in Bacteria. *Drugs* 64, 159–204. doi:10.2165/00003495-200464020-00004.
Lindsay, J. A., and Holden, M. T. G. (2004). Staphylococcus aureus: Superbug, super genome? *Trends Microbiol.* 12, 378–385. doi:10.1016/j.tim.2004.06.004.
Liu, X., Chang, Q., Ferrer-Espada, R., Leanse, L. G., Goh, X. S., Wang, X., et al. (2020). Photoinactivation of Moraxella catarrhalis Using 405-nm Blue Light: Implications for the Treatment of Otitis Media. *Photochem. Photobiol.* 96, 611–617. doi:10.1111/php.13241.
Lubart, R., Lipovski, A., Nitzan, Y., and Friedmann, H. (2011). A possible mechanism for the bactericidal effect of visible light. *Laser Ther.* 20, 17–22. doi:10.5978/islsm.20.17.
Magana, M., Pushpanathan, M., Santos, A. L., Leanse, L., Fernandez, M., Ioannidis, A., et al. (2020). The value of antimicrobial peptides in the age of resistance. *Lancet Infect. Dis.* 20, e216–e230. doi:10.1016/S1473-3099(20)30327-3.
Maisch, T. (2015). Resistance in antimicrobial photodynamic inactivation of bacteria. *Photochem. Photobiol. Sci.* 14, 1518–1526. doi:10.1039/c5pp00037h.
Maisch, T. (2020). Photoantimicrobials—An update. *Transl. Biophotonics* 2, 1–9. doi:10.1002/tbio.201900033.
Malatesti, N., Munitic, I., and Jurak, I. (2017). Porphyrin-based cationic amphiphilic photosensitisers as potential anticancer, antimicrobial and immunosuppressive agents. *Biophys. Rev.* 9, 149–168. doi:10.1007/s12551-017-0257-7.

Mamone, L., Ferreyra, D. D., Gándara, L., Di Venosa, G., Vallecorsa, P., Sáenz, D., et al. (2016). Photodynamic inactivation of planktonic and biofilm growing bacteria mediated by a meso-substituted porphyrin bearing four basic amino groups. *J. Photochem. Photobiol. B Biol.* 161, 222–229. doi:10.1016/j.jphotobiol.2016.05.026.

Marrie, T. J., Nelligan, J., and Costerton, W. J. (1982). A scanning and transmission electron microscopic study of human nodular goitre. *Circulation* 66, 1339–1341. doi:10.1111/j.1365-2559.1983.tb02216.x.

Mayer, F. L., Wilson, D., and Hube, B. (2013). Candida albicans pathogenicity mechanisms. *Virulence* 4, 119–128. doi:10.4161/viru.22913.

Mohammed, Y. H. E., Manukumar, H. M., Rakesh, K. P., Karthik, C. S., Mallu, P., and Qin, H. L. (2018). Vision for medicine: Staphylococcus aureus biofilm war and unlocking key's for anti-biofilm drug development. *Microb. Pathog.* 123, 339–347. doi:10.1016/j.micpath.2018.07.002.

Moormeier, D. E., and Bayles, K. W. (2017). Staphylococcus aureus biofilm: a complex developmental organism. *Mol. Microbiol.* 104, 365–376. doi:10.1111/mmi.13634.

Moradali, M. F., Ghods, S., and Rehm, B. H. A. (2017). Pseudomonas aeruginosa lifestyle: A paradigm for adaptation, survival, and persistence. *Front. Cell. Infect. Microbiol.*

Mukherjee, P. K., and Chandra, J. (2004). Candida biofilm resistance. *Drug Resist. Updat.* 7, 301–309. doi:10.1016/j.drup.2004.09.002.

Mulani, M. S., Kamble, E. E., Kumkar, S. N., Tawre, M. S., and Pardesi, K. R. (2019). Emerging strategies to combat ESKAPE pathogens in the era of antimicrobial resistance: A review. *Front. Microbiol.* 10. doi:10.3389/fmicb.2019.00539.

Nami, S., Aghebati-Maleki, A., Morovati, H., and Aghebati-Maleki, L. (2019). Current antifungal drugs and immunotherapeutic approaches as promising strategies to treatment of fungal diseases. *Biomed. Pharmacother.* 110, 857–868. doi:10.1016/j.biopha.2018.12.009.

Natan, M., and Banin, E. (2017). From Nano to Micro: Using nanotechnology to combat microorganisms and their multidrug resistance. *FEMS Microbiol. Rev.* 41, 302–322. doi:10.1093/femsre/fux003.

Nobile, C. J., and Johnson, A. D. (2015). Candida albicans Biofilms and Human Disease . *Annu. Rev. Microbiol.* 69, 71–92. doi:10.1146/annurev-micro-091014-104330.

Orlandi, V. T., Bolognese, F., Rolando, B., Guglielmo, S., Lazzarato, L., and Fruttero, R. (2018a). Anti-pseudomonas activity of 3-nitro-4-phenylfuroxan. *Microbiol. (United Kingdom)* 164, 1557–1566. doi:10.1099/mic.0.000730.

Orlandi, V. T., Caruso, E., Tettamanti, G., Banfi, S., and Barbieri, P. (2013). Photoinduced antibacterial activity of two dicationic 5,15-diarylporphyrins. *J. Photochem. Photobiol. B Biol.* 127, 123–132. doi:10.1016/j.jphotobiol.2013.08.011.

Orlandi, V. T., Martegani, E., and Bolognese, F. (2018b). Catalase A is involved in the response to photooxidative stress in Pseudomonas aeruginosa. *Photodiagnosis Photodyn. Ther.* 22, 233–240. doi:10.1016/j.pdpdt.2018.04.016.

Orlandi, V. T., Martegani, E., Bolognese, F., Trivellin, N., Maťátková, O., Paldrychová, M., et al. (2020). Photodynamic therapy by diaryl-porphyrins to control the growth of Candida albicans. *Cosmetics* 7, 1–19. doi:10.3390/COSMETICS7020031.

Orlandi, V. T., Rybtke, M., Caruso, E., Banfi, S., Tolker-Nielsen, T., and Barbieri, P. (2014). Antimicrobial and anti-biofilm effect of a novel BODIPY photosensitizer against Pseudomonas aeruginosa PAO1. *Biofouling* 30, 883–891. doi:10.1080/08927014.2014.940921.

Orlandi, V. T., Villa, F., Cavallari, S., Barbieri, P., Banfi, S., Caruso, E., et al. (2011). Photodynamic therapy for the eradication of biofilms formed by catheter associated Pseudomonas aeruginosa strains. 26, 129–133.

Pang, Z., Raudonis, R., Glick, B. R., Lin, T. J., and Cheng, Z. (2019). Antibiotic resistance in Pseudomonas aeruginosa: mechanisms and alternative therapeutic strategies. *Biotechnol. Adv.* 37, 177–192. doi:10.1016/j.biotechadv.2018.11.013.

Pantosti, A., Sanchini, A., and Monaco, M. (2007). Mechanisms of antibiotic resistance in Staphylococcus aureus. *Future Microbiol.* 2, 323–334. doi:10.2217/17460913.2.3.323.

Park, D., Choi, E. J., Weon, K. Y., Lee, W., Lee, S. H., Choi, J. S., et al. (2019). Non-Invasive Photodynamic Therapy against -Periodontitis-causing Bacteria. *Sci. Rep.* 9, 1–12. doi:10.1038/s41598-019-44498-4.

Pendleton, J. N., Gorman, S. P., and Gilmore, B. F. (2013). Clinical relevance of the ESKAPE

pathogens. 11, 297–308.
Percival, S. L., Suleman, L., Vuotto, C., and Donelli, G. (2015). Healthcare-Associated infections, medical devices and biofilms: Risk, tolerance and control. *J. Med. Microbiol.* 64, 323–334. doi:10.1099/jmm.0.000032.
Perumal, P., Mekala, S., and Chaffin, W. L. J. (2007). Role for cell density in antifungal drug resistance in Candida albicans biofilms. *Antimicrob. Agents Chemother.* 51, 2454–2463. doi:10.1128/AAC.01237-06.
Philippova, T. O., Galkin, B. N., Zinchenko, O. Y., Rusakova, M. Y., Ivanitsa, V. A., Zhilina, Z. I., et al. (2003). The antimicrobial properties of new synthetic porphyrins. *J. Porphyr. Phthalocyanines* 7, 755–760. doi:10.1142/s1088424603000926.
Phillips, P. L., and Schultz, G. S. (2012). Molecular Mechanisms of Biofilm Infection: Biofilm Virulence Factors. *Adv. Wound Care* 1, 109–114. doi:10.1089/wound.2011.0301.
Pires, D. P., Melo, L. D. R., Vilas Boas, D., Sillankorva, S., and Azeredo, J. (2017). Phage therapy as an alternative or complementary strategy to prevent and control biofilm-related infections. *Curr. Opin. Microbiol.* 39, 48–56. doi:10.1016/j.mib.2017.09.004.
Pithan, E., Righi, M., Bruno, C., Christ, R., Antonio, M., and Zanini, K. (2016). Photodiagnosis and Photodynamic Therapy Antimicrobial photodynamic effect of phenothiazinic photosensitizers in formulations with ethanol on Pseudomonas aeruginosa biofilms. *Photodiagnosis Photodyn. Ther.* 13, 291–296. doi:10.1016/j.pdpdt.2015.08.008.
Purrello, S. M., Garau, J., Giamarellos, E., Mazzei, T., Pea, F., Soriano, A., et al. (2016). Methicillin-resistant Staphylococcus aureus infections: A review of the currently available treatment options. *J. Glob. Antimicrob. Resist.* 7, 178–186. doi:10.1016/j.jgar.2016.07.010.
Ramage, G., Rajendran, R., Sherry, L., and Williams, C. (2012). Fungal biofilm resistance. *Int. J. Microbiol.* 2012. doi:10.1155/2012/528521.
Rapacka-Zdonczyk, A., Wozniak, A., Pieranski, M., Woziwodzka, A., Bielawski, K. P., and Grinholc, M. (2019). Development of Staphylococcus aureus tolerance to antimicrobial photodynamic inactivation and antimicrobial blue light upon sub-lethal treatment. *Sci. Rep.* 9, 1–18. doi:10.1038/s41598-019-45962-x.
Rasamiravaka, T., Labtani, Q., Duez, P., and El Jaziri, M. (2015). The formation of biofilms by pseudomonas aeruginosa: A review of the natural and synthetic compounds interfering with control mechanisms. *Biomed Res. Int.* 2015. doi:10.1155/2015/759348.
Rice, L. B., and Rice, L. B. (2014). Progress and Challenges in Implementing the Research on ESKAPE Pathogens. 31. doi:10.1086/655995.
Richter, K., Van Den Driessche, F., and Coenye, T. (2017). Innovative approaches to treat Staphylococcus aureus biofilm-related infections. *Essays Biochem.* 61, 61–70. doi:10.1042/EBC20160056.
Roca, I., Akova, M., Baquero, F., Carlet, J., Cavaleri, M., Coenen, S., et al. (2015). The global threat of antimicrobial resistance: Science for intervention. *New Microbes New Infect.* 6, 22–29. doi:10.1016/j.nmni.2015.02.007.
Römling, U., Kjelleberg, S., Normark, S., Nyman, L., Uhlin, B. E., and Åkerlund, B. (2014). Microbial biofilm formation: A need to act. *J. Intern. Med.* 276, 98–110. doi:10.1111/joim.12242.
Rugiero, M., Orlandi, V. T., and Caruso, E. (2019). Effetto di due nuovi BODIPY in terapia fotodinamica antimicrobica. doi:10.1017/CBO9781107415324.004.
Rybtke, M., Hultqvist, L. D., Givskov, M., and Tolker-Nielsen, T. (2015). Pseudomonas aeruginosa Biofilm Infections: Community Structure, Antimicrobial Tolerance and Immune Response. *J. Mol. Biol.* 427, 3628–3645. doi:10.1016/j.jmb.2015.08.016.
Sanguinetti, M., Posteraro, B., and Lass-Flörl, C. (2015). Antifungal drug resistance among Candida species: Mechanisms and clinical impact. *Mycoses* 58, 2–13. doi:10.1111/myc.12330.
Santajit, S., and Indrawattana, N. (2016). Mechanisms of Antimicrobial Resistance in ESKAPE Pathogens. 2016.
Sobotta, L., Skupin-Mrugalska, P., Piskorz, J., and Mielcarek, J. (2019). Porphyrinoid photosensitizers mediated photodynamic inactivation against bacteria. *Eur. J. Med. Chem.* 175, 72–106. doi:10.1016/j.ejmech.2019.04.057.
Soukos, N. S., and Goodson, M. (2011). Photodynamic therapy in the control of oral biofilms. 55, 143–166.
St. Denis, T. G., Dai, T., Izikson, L., Astrakas, C., Anderson, R. R., Hamblin, M. R., et al. (2011). All

you need is light, antimicrobial photoinactivation as an evolving and emerging discovery strategy against infectious disease. *Virulence* 2, 509–520. doi:10.4161/viru.2.6.17889.
Stover, C. K., Pham, X. Q., Erwin, A. L., Mizoguchi, S. D., Warrener, P., Hickey, M. J., et al. (2000). Complete genome sequence of {Pseudomonas} aeruginosa {PAO}1, an opportunistic pathogen. *Nature* 406, 959–964. doi:10.1038/35023079.
Sudbery, P. E. (2011). Growth of Candida albicans hyphae. *Nat. Rev. Microbiol.* 9, 737–748. doi:10.1038/nrmicro2636.
Sunahara, H., Urano, Y., Kojima, H., and Nagano, T. (2007). Design and synthesis of a library of BODIPY-based environmental polarity sensors utilizing photoinduced electron-transfer-controlled fluorescence ON/OFF switching. *J. Am. Chem. Soc.* 129, 5597–5604. doi:10.1021/ja068551y.
Taslı, H., Akbıyık, A., Topaloğlu, N., Alptüzün, V., and Parlar, S. (2018). Photodynamic antimicrobial activity of new porphyrin derivatives against methicillin resistant Staphylococcus aureus. *J. Microbiol.* 56, 828–837. doi:10.1007/s12275-018-8244-7.
Taylor, P. K., Yeung, A. T. Y., and Hancock, R. E. W. (2014). Antibiotic resistance in Pseudomonas aeruginosa biofilms: Towards the development of novel anti-biofilm therapies. *J. Biotechnol.* 191, 121–130. doi:10.1016/j.jbiotec.2014.09.003.
Tsolekile, N., Nelana, S., and Oluwafemi, O. S. (2019). Porphyrin as diagnostic and therapeutic agent. *Molecules* 24. doi:10.3390/molecules24142669.
Van Acker, H., Van Dijck, P., and Coenye, T. (2014). Molecular mechanisms of antimicrobial tolerance and resistance in bacterial and fungal biofilms. *Trends Microbiol.* 22, 326–333. doi:10.1016/j.tim.2014.02.001.
Verderosa, A. D., Totsika, M., and Fairfull-Smith, K. E. (2019). Bacterial Biofilm Eradication Agents: A Current Review. *Front. Chem.* 7, 1–17. doi:10.3389/fchem.2019.00824.
Wagner, S., Sommer, R., Hinsberger, S., Lu, C., Hartmann, R. W., Empting, M., et al. (2016). Novel Strategies for the Treatment of Pseudomonas aeruginosa Infections. *J. Med. Chem.* 59, 5929–5969. doi:10.1021/acs.jmedchem.5b01698.
Wainwright, M. (1998). Photodynamic Antimicrobial Chemotherapy. *J. Antimicrob. Chemother.* 42, 13–28. doi:10.1002/9783527676132.ch10.
Wainwright, M., and Giddens, R. M. (2003). Phenothiazinium photosensitisers: Choices in synthesis and application. *Dye. Pigment.* 57, 245–257. doi:10.1016/S0143-7208(03)00021-4.
Wainwright, M., Maisch, T., Nonell, S., Plaetzer, K., Almeida, A., Tegos, G. P., et al. (2017a). Photoantimicrobials—are we afraid of the light? *Lancet Infect. Dis.* 17, e49–e55. doi:10.1016/S1473-3099(16)30268-7.
Wainwright, M., Maisch, T., Nonell, S., Plaetzer, K., Almeida, A., Tegos, G. P., et al. (2017b). Photoantimicrobials—are we afraid of the light? *Lancet Infect. Dis.* 17, e49–e55. doi:10.1016/S1473-3099(16)30268-7.
Wang, Y., Wang, Y., Wang, Y., Murray, C. K., Hamblin, M. R., Hooper, D. C., et al. (2017). Antimicrobial blue light inactivation of pathogenic microbes: State of the art. *Drug Resist. Updat.* 33–35, 1–22. doi:10.1016/j.drup.2017.10.002.
Wang, Y., Wu, X., Chen, J., Amin, R., Lu, M., Bhayana, B., et al. (2016). Antimicrobial Blue Light Inactivation of Gram-Negative Pathogens in Biofilms: In Vitro and in Vivo Studies. *J. Infect. Dis.* 213, 1380–1387. doi:10.1093/infdis/jiw070.
Winstanley, C., O'Brien, S., and Brockhurst, M. A. (2016). Pseudomonas aeruginosa Evolutionary Adaptation and Diversification in Cystic Fibrosis Chronic Lung Infections. *Trends Microbiol.* 24, 327–337. doi:10.1016/j.tim.2016.01.008.
Wright, G. D. (2005). Bacterial resistance to antibiotics: Enzymatic degradation and modification. *Adv. Drug Deliv. Rev.* 57, 1451–1470. doi:10.1016/j.addr.2005.04.002.
Yin, R., Dai, T., Avci, P., Jorge, A. E. S., De Melo, W. C. M. A., Vecchio, D., et al. (2013). Light based anti-infectives: Ultraviolet C irradiation, photodynamic therapy, blue light, and beyond. *Curr. Opin. Pharmacol.* 13, 731–762. doi:10.1016/j.coph.2013.08.009.
Yogo, T., Urano, Y., Ishitsuka, Y., Maniwa, F., and Nagano, T. (2005). Highly efficient and photostable photosensitizer based on BODIPY chromophore. *J. Am. Chem. Soc.* 127, 12162–12163. doi:10.1021/ja0528533.
Zagami, R., Sortino, G., Caruso, E., Malacarne, M. C., Banfi, S., Patanè, S., et al. (2018). Tailored-BODIPY/Amphiphilic Cyclodextrin Nanoassemblies with PDT Effectiveness. *Langmuir* 34,

8639–8651. doi:10.1021/acs.langmuir.8b01049.
Zecconi, A., and Scali, F. (2013). Staphylococcus aureus virulence factors in evasion from innate immune defenses in human and animal diseases. *Immunol. Lett.* 150, 12–22. doi:10.1016/j.imlet.2013.01.004.
Zhang, Y., Zhu, Y., Chen, J., Wang, Y., Sherwood, M. E., Murray, C. K., et al. (2016). Antimicrobial blue light inactivation of Candida albicans : In vitro and in vivo studies. *Virulence* 7, 536–545. doi:10.1080/21505594.2016.1155015.
Zhang, Y., Zhu, Y., Gupta, A., Huang, Y., Murray, C. K., Vrahas, M. S., et al. (2014). Antimicrobial blue light therapy for multidrug-resistant Acinetobacter baumannii infection in a mouse burn model: Implications for prophylaxis and treatment of combat-related wound infections. *J. Infect. Dis.* 209, 1963–1971. doi:10.1093/infdis/jit842.

Publications

Caruso, E., Orlandi, V.T., Malacarne, M.C., Martegani, E., Scanferla, C., Pappalardo, D., … & Izzo, L. (2021). BODIPY-loaded micelles based on polylactide as surface coating for photodynamic control of *Staphylococcus aureus. Coatings,, 11(2), 223.*

Martegani, E., Bolognese, F., Trivellin, N., & Orlandi, V. T. (2020). Effect of blue light at 410 and 455 nm on Pseudomonas aeruginosa biofilm. *Journal of Photochemistry and Photobiology B: Biology*, *204*, 111790.

Orlandi, V. T., Martegani, E., Bolognese, F., Trivellin, N., Maťátková, O., Paldrychová, M., ... & Caruso, E. (2020). Photodynamic Therapy by Diaryl-Porphyrins to Control the Growth of Candida albicans. *Cosmetics*, *7*(2), 31.

Armenia, I., Marcone, G. L., Berini, F., Orlandi, V. T., Pirrone, C., Martegani, E., ... & Marinelli, F. (2018). Magnetic nanoconjugated teicoplanin: a novel tool for bacterial infection site targeting. *Frontiers in microbiology*, *9*, 2270.

Orlandi, V. T., Martegani, E., & Bolognese, F. (2018). Catalase A is involved in the response to photooxidative stress in Pseudomonas aeruginosa. *Photodiagnosis and photodynamic therapy*, *22*, 233-240.

Acknowledgments

I would like to kindly thank my tutor, Prof. Viviana Orlandi, and my supervisor, Prof. Flavia Marinelli, that gave me the opportunity to work and increase my scientific knowledge at the laboratory of Applied Microbiology at the University of Insubria. I am grateful for the high quality of scientific research and the serene and stimulating environment of the laboratory.

I sincerely thank Prof. Enrico Caruso and the laboratory of Organic Chemistry at the University of Insubria for the chemical synthesis of compounds used in this thesis and their support and suggestion in the discussion of results.

Many thanks to Dr Fabrizio Bolognese for its guidance in laboratory and to all my colleagues and students that worked with me during these years, especially Chiara, Martina, and Davide.

Special thanks to my parents, my sister Ilaria, Marco, and my nephews Lorenzo, Andrea, and Giorgia for the support and encouragement during these years. Without them, it would have been more difficult.

Last but not least, special thanks to my boyfriend Lorenzo and to my friends Cinzia, Elena, Giulia, Tecla, Gianmario and Alberto for their love and friendship in these years and hopefully for the rest of my life.